IDENTIFYING AND TARGETING IMMUNOGENIC MUTATIONS IN OVARIAN CANCER

by

Spencer David Martin

B.Sc. The University of Victoria, 2010

A THESIS SUBMITTED IN PARTIAL FULFILLMENT OF
THE REQUIREMENTS FOR THE DEGREE OF

DOCTOR OF PHILOSOPHY
in
THE FACULTY OF GRADUATE AND POSDOCTORAL STUDIES
(Interdisciplinary Oncology)

THE UNIVERSITY OF BRITISH COLUMBIA
(Vancouver)

June 2016

Abstract

A hallmark of cancer is the accumulation of mutations, and a small proportion of these give rise to mutant neoantigens – mutated peptides bound to Major Histocompatibility Complex (MHC) and recognized by T cells. Accumulating evidence suggests that mutant neoantigens (hereafter referred to as "neoantigens") underlie successful immune therapies in cancers with high mutation loads, such as melanoma. Moreover, neoantigen-specific vaccines have successfully targeted highly mutated murine tumor models. However, less is known about neoantigen-specific T cell responses in cancers with moderate mutation loads, such as ovarian cancer. I hypothesized that (1) modified peptide-based vaccination schedules can lead to enhanced antigen-specific T cell responses; (2) neoantigen-specific vaccines can elicit T cell responses that eradicate murine ovarian tumors; and (3) neoantigen-reactive T cells are detectable in human ovarian tumors and peripheral blood. To activate high frequencies of antigen-specific T cells, I developed a vaccination method involving repeated, daily immunizations with long peptides and adjuvant. This method elicited robust T cell responses that eliminated established murine tumors. I used these enhanced vaccination methods to target tumor-specific mutations identified by exome- and RNA-sequencing of the ovarian tumor model ID8-G7. Prophylactic and therapeutic vaccinations were performed targeting all expressed mutations that had a predicted MHCI binding affinity < 1500 nM (n=17 mutations). Though the vaccines elicited robust T cell responses to most mutations, activated T cells failed to recognize ID8-G7 tumors *in vitro* and failed to control tumor growth *in vivo*, indicating that none of the evaluated mutations represented authentic neoantigens. I also investigated the neoantigen-specific T cell repertoire in blood and tumor samples donated by an ovarian cancer patient. A neoantigen-specific T cell response was identified in the first recurrence tumor sample, and a derived T cell clone recognized tumor from each of three time points. Furthermore, peripheral blood samples donated prior disease recurrence harbored T cells recognizing the same mutation. The results presented here show that neoantigen-specific T cells can arise spontaneously in ovarian tumors and are detectable in peripheral blood; however, low mutation burdens in ovarian cancer may limit the utility of neoantigen-targeted vaccines to a minority of patients with this disease.

Preface

All of the work presented here was performed at the Trev and Joyce Deeley Research Centre (DRC) and the Michael Smith Genome Sciences Centre (GSC) at the British Columbia Cancer Agency. All methods involving humans were approved by the University of British Columbia's Research Ethics Board: H07-00463. All methods involving murine models were approved by the University of Victoria Research Ethics Board: 2011-032(4) (Analysis of the immune response to cancer in murine models. Principal investigator: Brad Nelson). Additional approval by University of British Columbia Animal Care and Biosafety Committee was not required. The use of The Cancer Genome Atlas (TCGA) data is exempt from ethics requirements as stated by the Tri-council policy statement article 2.2.

Portions of Chapter 1, including a version of Illustration 3, were modified from a published review article and used with permission: Martin SD, Coukos G, Holt RA, Nelson BH. (2015) Targeting the undruggable: immunotherapy meets personalized oncology in the genomic era. Ann Oncol. 26(12):2367-74. I was the first author and responsible for reviewing the literature, composing the manuscript, and editing the paper. G. Coukos, RA Holt, and BH Nelson contributed conceptually and edited versions of the manuscript. The version of record can be found at: http://annonc.oxfordjournals.org/content/26/12/2367.long

Figure 1 in Chapter 2 was used with permission from a manuscript that I co-authored: Wick DA, Martin SD, Nelson BH, Webb JR. (2011) Profound CD8+ T cell immunity elicited by sequential daily immunization with exogenous antigen plus the TLR3 agonist poly(I:C). Vaccine. 29(5):984-93. JR Webb and DA Wick conceived of the idea for this figure and conducted the experiment. For all other sections of Chapter 2, I performed data collection and analysis, interpretation of results, and concept formation under the supervision of BH Nelson BH and RA Holt.

A version of Chapter 3 is from a published manuscript: Martin SD, Brown SD, Wick DA, Nielsen JS, Kroeger DR, Twumasi-Boateng K, Holt RA, Nelson BH. (2016) Low mutation burden in ovarian cancer may limit the utility of neoantigen targeted vaccines. PLoS One. 11(5):e0155189. SD Brown contributed Figure 15, DA Wick, JS Nielsen, DR Kroeger, K Twumasi-Boateng, were involved with concept formation and editing the manuscript. RA Holt and BH Nelson were involved throughout the project with concept

formation and editing the manuscript. Exome and RNA-seq data were mapped to the reference genome by the GSC sequencing core. I performed all other bioinformatic analysis, constructed the sequencing library, and conceived and conducted all wet lab experiments.

Figures 4.1, 4.2, 4.3, and Table 2 are from a manuscript that I co-authored: Wick DA, Webb JR, Nielsen JS, Martin SD, Kroeger DR, Milne K, Castellarin M, Twumasi-Boateng K, Watson PH, Holt RA, Nelson BH. (2013) Surveillance of the tumor mutanome by T cells during progression from primary to recurrent ovarian cancer. Clin Cancer Res. 20(5):1125-34. I was involved with concept formation and editing the manuscript. DA Wick was involved in concept formation, data collection and analysis of results, and composing and editing the manuscript. JS Nielsen, DR Kroeger, K Milne, M Castallarin, K Twumasi-Boateng, and PH Watson were involved with concept formation and editing the manuscript. RA Holt and BH Nelson were lead investigators and involved with concept formation and composing and editing the manuscript. Figures 4.4 – 4.13 are from a manuscript in preparation. I was involved with concept formation, data collection, analysis of results, and composing and editing the manuscript. BH Nelson and RA Holt were involved with concept design and editing the manuscript.

Table of contents

List of tables

List of figures

List of illustrations

List of abbreviations

ACT	Adoptive Cell Therapy
AIRE	Autoimmune Regulator
APC	Antigen Presenting Cells
ATP	Adenosine Triphosphate
AUC	Area Under the Curve
B2M	Beta-2 Microglobulin
BMT	Bone Marrow Transfer
CAF	Cancer Associated Fibroblasts
CAR	Chimeric Antigen Receptor
CCL	Chemokine Ligand
CCR	Chemokine Receptor
CTL	Cytotoxic T Lymphocytes
CTLA4	Cytotoxic T lymphocyte antigen 4
CXCL	Chemokine Ligand
CXCR	Chemokine receptor
DAMP	Danger Associated Molecular Patterns
DC	Dendritic Cell
DNMT	DNA Methyl Transferase
ECM	Extracellular Matrix
ER	Endoplasmic Reticulum
GM-CSF	Granulocyte Macrophage Colony-Stimulating Factor
GMP	Good Manufacturing Practices
GVHD	Graft Versus Host Disease
GVL	Graft Versus Leukemia
HLA	Human Leukocyte Antigen
HMGB1	High Mobility Group Box 1
HPV	Human Papillomavirus
HSP	Heat Shock Proteins
HSDL1	Hydroxysteroid Dehydrogenase-Like protein 1
IC50	Inhibitory Concentration that displaces 50% of a standard
ICOS	Costimulatory receptor
ICS	Intracellular Cytokine Staining
IDO	Indoleamine 2,3-dioxygenase
IFA	Incomplete Freunds Adjuvant
IFN	Interferon
IL	Interleukin
LAG3	Lymphocyte Activating Gene 3
LCMV	Lymphocytic Choriomeningitis Virus
MHCII	Major Histocompatibility Complex Class II
MDSC	Myeloid Derived Suppressor Cells
MHC	Major Histocompatibility Complex
MHCI	Major Histocompatibility Complex Class I
MMP	Matrix Metalloproteinase

MS	Mass Spectrometry
mTEC	medullary Thymic Epithelial Cell
NGS	Next Generation Sequencing
OTI	Ovalbumin specific T cells
OVA	Chicken ovalbumin
PADRE	Pan DR Epitope
PAMP	Pathogen Associated Molecular Patterns
PBMC	Peripheral Blood Mononuclear Cells
PD-1	Programmed cell Death 1
PD-L1/2	Programmed cell Death Ligand 1/2
PHA	Phytohaemaglutanin
PRR	Pattern Recognition Receptors
PSGL1	P Selectin Glycoprotein 1
REP	Rapid Expansion Protocol
SNP	Single Nucleotide Polymorphisms
TAL	Tumor Associated Lymphocytes
TAM	Tumor Associated Macrophages
TAP	Transporter associated with Antigen Processing
TCGA	The Cancer Genome Atlas
TCR	T Cell Receptor
TIL	Tumor Infiltrating Lymphocytes
TIM3	T cell Immunoglobulin and Mucin domain containing 3
TLR	Toll-Like Receptor
VEGF	Vascular Endothelial Growth Factor
Vβ	Variable segment of the TCR-beta gene

Acknowledgements

I will remember my time at the Deeley Research Centre and Genome Sciences Centre as some of the best years of my life, and I would like to thank several people, without whom, I could not have completed this PhD project.

First, I would like to thank my supervisor Dr. Brad Nelson and my co-supervisor Dr. Robert Holt. The wisdom, guidance, and patience that they provided me were critical for accomplishing the goals of this project. Their faith in me helped me to persevere through several months of frustration, when project completion seemed unfathomably distant. Furthermore, their timely edits and thoughtful critiques of this thesis were fundamental to its completion.

I would also like to thank my graduate committee members Drs. John Webb and Angela Brooks-Wilson for their sound advice that helped to avoid pitfalls and false leads that would have sunk this project. I could not have hoped for a better graduate committee.

I owe a special thanks to Darin Wick. The fascinating scientific conversations that we shared are among my best memories of my graduate years. His mentorship and technical expertise was the foundation on which I built each chapter of this project. Moreover, our enjoyable intellectual battles over different scientific hypotheses built my confidence and helped polish my arguments for defending each scientific stance that I took. It is fair to say that I would not have completed this project without his guidance and friendship.

In addition, I thank my colleagues at the Deeley Research Centre and Genome Sciences Centre for making both labs such enjoyable places in which to work. In particular, I thank Dr. Julie Nielson for her insight and wisdom she shared with me. Our many discussions about navigating through the sometimes treacherous waters of a PhD project helped keep me on track and focused. Further, I thank Drs. David Kroeger, Kwame Twumasi-Boateng, Nathan West, and Julian Lum for their assistance editing papers and helping me understand the intricacies of writing to an audience, and I thank Jessica Pettigrew for her fine work managing the mouse colony.

Finally, I would like to thank my family and friends for supporting me through these years, and I look forward to spending more time with each of them in the coming months.

Chapter One: Introduction

Anti-tumor immunity can have profound impacts on cancer patient survival, and decades of research have revealed the targets that underlie the anti-tumor immune response. Over 100 years ago, physicians observed that tumors would occasionally spontaneously regress when cancer patients experienced infections, leading some to hypothesize that stimulating the immune system could activate anti-tumor immunity. Later, it was found that T cells recognized and killed tumor cells expressing target "antigens" on the cell surface [1]. Decades of research into the source of these tumor antigens resulted in a relatively short list of proteins [2]. Occasionally, the identified antigens were shared among cancer patients, and therapeutic anti-cancer vaccines were developed to elicit immune responses directed towards these shared antigens [3]. However, research also showed that mutated proteins gave rise to mutated tumor antigens, or so called "neoantigens", unique to individual tumors, and these personal neoantigens represented a major challenge for anti-cancer vaccine development [2]. How can one identify a mutation that gives rise to a neoantigen from among the three billion nucleotides in the human genome? Historically, highly technical, time-consuming methods were required to identify each antigen, thereby limiting neoantigen discovery to case reports. Thus, it remained infeasible to scale-up neoantigen discovery to guide clinical vaccine development. However, improvements in DNA sequencing technologies, or "Next-Generation Sequencing" (NGS), have made identifying tumor mutations relatively routine [4], thereby opening a new avenue for discovering neoantigen targets for vaccines.

Sequencing tumors provides a list of mutations that can potentially give rise to neoantigens; however, this wealth of information also brings several questions about targeting neoantigens with vaccines. For example, how can we identify authentic neoantigens from among all tumor mutations? How can vaccines effectively target neoantigens once they are identified? What proportion of mutations is recognized by the immune system? Which tumor types are susceptible to neoantigen targeted immunotherapy?

Some studies have been published that investigate these questions in the settings of melanoma and highly mutated murine tumor models, but studies investigating neoantigens in tumor types with moderate mutation burdens are lacking. One example of a moderately mutated tumor type is ovarian cancer, which in theory might be susceptible to personalized

neoantigen-specific vaccines since improved patient survival is associated with higher immune responses [5,6]. As described in this thesis, I investigated methods to activate immune responses to mutations in murine ovarian tumors, and I assessed the theoretical feasibility of vaccinating human ovarian cancer patients with neoantigen-targeted vaccines. Specifically, I hypothesized that (1) modified vaccination schedules can lead to improved T cell responses to peptide vaccines, (2) neoantigen-specific peptide vaccines can elicit therapeutic T cell responses towards murine ovarian cancer, and (3) naive or activated neoantigen-reactive T cells are present in ovarian cancer patient tumors and blood.

Here in Chapter 1, I review the basic interactions between the immune system and tumor cells, and I provide a background on the biology of the most critical anti-tumor immune cell: the T cell. Further, I discuss clinical uses of immune therapy, with particular attention to anti-cancer vaccines. Subsequently, I discuss NGS technology, and I review the studies that have used NGS to identify neoantigens. Finally, I provide a brief background on ovarian cancer and give rationale for targeting this disease with neoantigen-specific vaccines.

1.1 T cell biology and activation

Overview

The goal of most contemporary anti-cancer immune therapies is to activate anti-tumor CD4 and CD8 T cells. To understand how the immune system recognizes tumor cells, one needs to consider the basic biology of T cells and the mechanisms used by T cells to recognize their targets. The T Cell Receptors (TCR) on T cells recognize short peptides (called epitopes) bound to the Major Histocompatibility Complex (MHC) on the target cell surface. These peptides are derived from digested intracellular and membrane bound proteins. A few peptides are proteolytically cleaved from the parent protein, bound to MHC, and shuttled to the cell surface as a peptide/MHC complex. When T cells are activated by peptide/MHC, the protein from which the epitope was derived is called an antigen. There are two types of MHC molecules encoded by Human Leukocyte Antigen (*HLA*) genes: MHC class I (MHCI) and MHC class II (MHCII). Almost all nucleated cells express MHCI, which presents peptides to CD8 T cells. CD8 T cells can directly kill cells that display epitopes on MHCI. Professional Antigen Presenting Cells (APCs) additionally express MHCII, which presents peptides to CD4 T cells. Most commonly, T cells recognize peptides derived from

pathogens; however, T cells can also recognize epitopes on tumors if the epitopes are sufficiently different from peptide/MHC found in healthy tissue. Furthermore, T cells may also recognize self antigens, occasionally resulting in autoimmunity

In the following sections, I will first describe the antigen side of the T cell/target cell interaction. I discuss antigen processing, peptide/MHC interactions, and software to predict peptide affinity for MHC. Subsequently, I deconstruct the T cell side of the T cell/target cell interaction. I review T cell development in the thymus, APC activation of naive T cells, T cell activation *in vivo* and *in vitro,* and functions of activated T cells. Finally, I review mechanisms that tumors employ to evade the anti-cancer immune response.

Antigen processing

The production and presentation of peptides by target cells is a fundamental step for activating T cells and killing target cells (Illustration 1). Within the cytosol, cellular and viral (if the cell is infected) proteins are regularly degraded into short peptides by the proteasome, which is primarily responsible for generating the C-terminus of MHCI bound peptides [7]. A subset of these peptides is translocated into the Endoplasmic Reticulum (ER) via the Transporter associated with Antigen Processing (TAP). Empty MHCI molecules bound to β-2 Microglobulin (B2M) are stabilized in the ER by the chaperone proteins calreticulin and ERp57, and they are coupled to TAP via the chaperone protein tapasin [8]. Thus, as peptides enter the ER, empty MHCI molecules are immediately available to bind. Peptides unable to bind MHCI are trimmed on the N-termini by ER amino peptidases into 8 – 10mers, potentially increasing their ability to bind MHCI [9]. Peptides that fail to bind MHCI are transported back into the cytosol to be processed into monomer amino acids for recycling [10]. Once a peptide binds the peptide-binding groove of MHCI with sufficient affinity (peptide/MHC binding is described in the next section), the peptide/MHCI/B2M complex becomes stable and is released from the chaperone proteins, transported through the Golgi apparatus, glycosylated, and shuttled to the surface of the cell [11]. There, the peptide/MHCI complex is presented for interrogation by the T Cell Receptor (TCR) on T cells. This process is called the endogenous antigen presentation pathway, and it is the primary mechanism that allows tumor cells to be recognized and killed by T cells (Illustration 1). Cancer cells may have aberrant protein production (i.e. overexpressed oncoproteins, mutant proteins, viral

oncogenes) that can lead to unique peptide presentation patterns, which may be recognized by T cells and result in tumor cell destruction.

Professional antigen presenting cells (APCs) are primarily responsible for activating naive T cells that recognize antigens. Similar to most nucleated cells, APCs present peptides derived from intracellular proteins (or pathogens) via the endogenous antigen presentation pathway. However, APCs express additional cellular machinery, evolved to ingest, process, and present extracellular antigens (for example tumor antigens). The process of extracellular antigen presentation on MHCI molecules is called cross-presentation [12]. In this mechanism, APCs endocytose extracellular antigens and translocate the antigens from endosomes into the cytosol. There, antigens enter the endogenous antigen presentation pathway explained above, and peptides derived from the antigens are presented on MHCI [13]. In addition to presenting peptides on MHCI to CD8 T cells, APC present peptides derived from extracellular antigens on MHCII to CD4 T cells. Within endosomes, the peptide binding groove of MHCII is occupied by the Class II-associated Ii Peptide (CLIP). Cathepsins within endosomes digest endocytosed antigens into short peptides, and some of these peptides bind to MHCII with sufficient affinity to displace CLIP in the MHCII peptide binding groove. The peptide/MHCII complex is then shuttled to the cell surface where it can be interrogated by CD4 T cells (Illustration 1) [8]. The antigen processing pathway generates only a few peptides from each protein. For example, a study of viral epitopes found that only 16% of peptides capable of binding to MHCI with high affinity (IC50 < 100 nM, described below) were naturally processed, highlighting antigen processing as a major limiting step in the generation of antigenic peptides [14]. The net effect of antigen processing is the generation of a set of peptides suitable to bind MHC molecules (described next).

Peptide/MHC interaction

The amino acid sequence of a peptide determines its binding affinity for a given MHC molecule, and consequently, whether the peptide/MHC can be found on the cell surface. The affinity of a specific peptide for a specific MHC can be measured empirically as the peptide concentration that displaces 50% of a benchmark peptide from cell-free MHC molecules, and the inhibitory concentration is measured as IC50 values. A peptide/MHCI binding affinity of IC50 < 500 nM was empirically found to identify most authentic antigenic

peptides [15]. MHCI binding peptides are usually between 8 to 11 amino acids long, most often 9mers, and MHCII binding peptides are usually between 13 to18 amino acids long, as the open ends of the MHCII peptide binding groove allow extended peptides to bind [8]. Peptide binding to the MHC is the single most limiting factor determining which peptides are presented [16]. For example, *in silico* analysis of all possible 9mer peptides from a set of viral proteomes revealed a median of 2% of peptides (range of .07% to 10.4%) bind to a given MHCI with a predicted IC50 < 500 nM [17].

HLA loci (encoding MHC proteins) are the most polymorphic sites in the genome, which increases the complexity of identifying MHC-binding peptides [18]. The human population contains thousands of different *HLA* alleles, and the peptide binding groove is the most polymorphic site on the protein [19]. This results in each *HLA* allele product having a different peptide binding preference. Each person has three MHCI-encoding genes (*HLA-A, -B, -C*) and up to six different *HLA* class I alleles (one paternal and one maternal for each locus). Also, each person has three MHCII encoding loci (*HLA-DP, -DQ, -DR*). Expression of multiple, highly-polymorphic *HLA* alleles results in a large variety of peptides presented on each person's set of MHC molecules [19]. Additionally, because very few people have perfectly matching sets of *HLA* alleles, the set of peptides presented from any given antigen is unique for each person. While the extreme level of *HLA* allele polymorphism is advantageous for protection against viral and bacterial pathogens, it makes identification of antigenic epitopes highly challenging. The identification of immunogenic cancer epitopes is an area of intense investigation and is at the foundation of my search for cancer neoantigens.

The affinity with which a peptide binds to an MHC allele is a critical parameter that determines whether a tumor antigen will mediate tumor rejection. Studies show that T cell recognition of peptides with high MHCI binding affinity led to tumor rejection, whereas T cell recognition of peptides with lower MHCI binding affinity led to tumor relapse [20,21]. Higher binding affinity of a peptide to MHC generally leads to longer time of peptide presentation, thereby increasing the time that a TCR may contact the peptide/MHC [22,23]. The model epitope SIINFEKL is an example of a high affinity epitope used extensively in murine models to assess tumor immunity (and used in studies in Chapter 2). This peptide binds MHCI (H-2Kb) with an IC50 = 1.4 nM [24], and targeting this antigen has led to tumor eradication in several mouse tumor models [25-27]. As a comparison, the epitope

AAGIGILTV from a tumor antigen (MART1) commonly targeted in human melanoma has an MHCI binding affinity of IC50 = 6955 nM [28], and targeting this antigen has led to few clinical responses [28,29]. Thus, the binding affinity of a peptide to MHCI is an important factor in evaluating cancer antigens, and many antigens targeted in human cancers to date have low MHCI binding affinities.

Epitope prediction

Epitope prediction algorithms can predict, with high accuracy, the binding affinity of a peptide for a given MHCI. The algorithm NetMHC performed the best in a competition to determine the best epitope prediction algorithm of the many available [30]. This algorithm uses machine learning based on measured, validated epitopes for each *HLA* allele to refine epitope predictions [31], and prediction accuracy is highest for common *HLA* alleles, for which more training data are available [30]. Another algorithm, called NetMHCpan (developed by the same group) can be used for *HLA* alleles with less training data [32]. This algorithm uses the primary genetic sequence of the queried *HLA* allele to identify biochemical characteristics of peptides likely to bind to the MHC binding groove. The program then assesses queried peptides to determine whether they have the characteristics necessary for MHC binding [32]. These epitope prediction algorithms achieved a Pearson correlation coefficient of 0.912 of predicted versus measured IC50 scores [33] and an Area Under the Curve (AUC) of 0.957 for true positives versus false positive epitopes [34]. Additionally, studies investigating viral epitopes showed that 94.8% of T cells activated by a virus recognized epitopes within the top 1% of predictions [35]. However, determining cutoffs for identifying antigens has been challenging as each *HLA* allele has different levels of peptide promiscuity [17]. For example, the percentage of peptides that bind MHCI with IC50 < 500 nM can range from 0.07% to 10% among different *HLA* allele products [17]. While some studies use a binding affinity cutoff of 500 nM for every *HLA* allele [14], others use a cutoff of the top 1% of binding peptides for each *HLA* allele, thereby generating an equal sized list of potential epitopes for each *HLA* allele [17]. Using higher cutoffs results in reduced probability that an authentic epitope is overlooked, but it increases the number of epitopes that require investigation. In my assessment of neoantigen peptide binding predictions in Chapter 3, I used a relaxed cutoff of IC50 < 1500 nM to reduce the probability

of missing authentic epitopes. Notably, epitope predictions determine only whether minimal-epitope peptides are likely to bind to a given MHC allele; however, cellular antigen processing machinery can generate only 16% of peptides that are capable of surface binding to a given MHC [14]. Thus, most predicted MHCI binding peptides will not be authentic antigens because target cells will not produce them.

Although antigen processing prediction and MHCII epitope binding prediction algorithms have been designed, accuracy is not reliable enough for applications in vaccine design [36,37]. For example, the best MHCII epitope prediction algorithms have an AUC of only 0.8 for true positive versus false positive predictions [38]. Processing algorithms are quite accurate for the proteasome when tested in cell free proteasome assays; however, the large number of different proteases in cells and the effects of highly-polymorphic MHC make processing predictions of whole cells less accurate than for cell free assays [38]. Recent improvements in the processing prediction algorithm NetChop3.0 Cterm resulted in correct identification of 95% of authentic processed antigens within the top 50% of predictions, but this level of accuracy is substantially lower than that for MHCI binding predictions [38]. Additionally, MHCII epitope prediction algorithms are not yet accurate enough for designing vaccines [39-41]. The best MHCII prediction algorithms predict the core sequence of MHCII binding peptides with an AUC of 0.85 for true positive versus false positives, but accuracy diminishes when flanking amino acid sequences are included [42]. Improvements to both antigen processing algorithms and MHCII epitope prediction algorithms would benefit cancer vaccine design.

Thus far, I have reviewed the antigen side of the T cell/antigen interaction. In the next sections I will review the T cell side of this fundamental reaction in anti-tumor immunity.

The TCR and T cell development in the thymus

The role of the TCR is to distinguish “foreign” from “self” peptides presented by MHC molecules on the cell surface. The TCR for each T cell is generated through somatic rearrangement of the variable (V), diversity (D), and joining (J) gene segments, found within the TCR loci [43], and addition and/or removal of nucleotides at the splice sites [44]. The result is the expression of a unique TCR on each T cell. Theoretically, the rearrangements could result in a near limitless diversity of TCR sequences. However, sequencing TCRs in

healthy donors reveals that about 3 million to 25 million unique TCR sequences are expressed among the 10^{11} to 10^{12} mature T cells found in the body [45,46]. T cell selection within the thymus limits the number of different TCRs found among mature T cells within the body.

The purpose of thymic selection is to generate a T cell repertoire that is capable of recognizing and killing pathogen infected cells but not healthy cells. Pre-T cells are generated in the bone marrow and migrate to the thymus, where the TCR is rearranged and T cell maturation takes place. Thymic selection of T cells is based on the differential avidity of the TCRs for self-peptide/MHC complexes presented by thymic epithelial and dendritic cells. Only 10% of T cells that enter the thymus will express a TCR that, by chance, binds to self-peptide/MHC on thymic cortical epithelial cells with enough avidity to be positively selected; the other 90% of unselected T cells undergo apoptosis at this stage of development [47]. Positive selection of T cells induces upregulation of anti-apoptosis molecules like BCL-2 [48], the cytokine receptor IL-7Rα, and the chemokines receptor CCR7. Upregulation of these molecules promotes T cell survival and migration to the thymic medulla [48-50]. Medullary Thymic Epithelial Cells (mTECs) express the promiscuous transcription factor AutoImmune REgulator (AIRE) resulting in transcription of almost all proteins encoded in the genome, and by extension, almost all possible self peptide/MHC [51,52]. Of the T cells that enter the medulla, 50% are potentially autoreactive, as they express TCRs that bind with high avidity to self-peptide/MHC on medullary thymic epithelial cells or thymic dendritic cells [47]. T cells expressing the highest affinity TCRs undergo rapid apoptosis (negative selection), and T cells with slightly less high affinity TCRs convert to regulatory T cells (immune inhibitory cells discussed later). The result of thymic selection is a mature T cell repertoire with limited reactivity to self (i.e., central tolerance) but potentially strong reactivity to foreign antigens [48]. The T cells that survive thymic selection and enter the periphery are called “naive” T cells, as they have yet to encounter antigen and become activated.

While important for a well-tuned immune system, central tolerance is not absolute. Because the avidity of TCR binding to self-peptide/MHC dictates T cell survival, T cells with TCR that bind to peptides presented at low levels in the thymus may survive central tolerance [53,54]. An elegant study using mice that expressed Cre as a self-antigen in distinct

tissues demonstrated the “leakiness” of central tolerance [55]. The study showed that mice expressing Cre under control of a ubiquitously expressed gene promoter generated almost no Cre-specific T cells, meaning Cre-specific T cells died due to thymic negative selection. However, mice expressing Cre under control of lungs or gut specific promoters generated Cre-specific T cells that escaped negative selection, and a large proportion of these T cells were regulatory T cells. Further, mice expressing Cre under control of a pancreas specific promoter generated Cre-specific T cells that escaped negative selection, and these T cells were not regulatory T cells [55]. Intriguingly, in all cases, spontaneous Cre specific autoimmunity was not observed, highlighting the multiple overlapping mechanisms that maintain self-tolerance beyond thymic selection [56]. These nuances of self-tolerance provide opportunities for targeting tumor antigens with limited expression on normal cells. For example, if the self-peptides are expressed at low levels in the thymus and high levels on tumors, T cells recognizing these peptides could escape thymic selection, become activated, and recognize and kill tumor cells. I will further discuss the implications of incomplete central tolerance on tumor immunity in a future section on classes of antigen.

Activation of APC for antigen presentation

Naive T cells that survive thymic selection and enter the periphery must become activated to carry out their functions of defending against pathogens or cancer. Dendritic cells (DCs) are specialized antigen presenting cells (APC) that are primarily responsible for activating naive T cells; indeed, depletion of all DCs prevents naive T cell activation [57]. Within peripheral tissues, DCs may be infected with viruses or bacteria. Alternatively, DCs may ingest bacteria, viruses, tumor cells, or foreign proteins through phagocytosis, macropinocytosis or endocytosis. Molecules on viruses and bacteria that contain Pathogen Associated Molecular Patterns (PAMPs), and molecules released from necrotic cells – including tumor cells – that contain Danger Associated Molecular Patterns (DAMPs), serve as danger signals that bind to Pattern Recognition Receptors (PRR) and alert DCs to pathogens or damage (Illustration 2). Specific PRR called Toll-Like Receptors (TLR) bind DAMPs (e.g., heat shock proteins (HSP), galactin-3 and High Mobility Group Box 1 (HMGB1)) and PAMPs (e.g., peptidoglycan (TLR2), LPS (TLR4), flagellin (TLR5), dsRNA (TLR3), ssRNA (TLR8), and non-methylated CpG (TLR9)) [58]. When PRR on DCs bind

to their respective ligands, DCs undergo phenotypic changes resulting in DC maturation [59]. They upregulate antigen presenting molecules like MHCI, MHCII; co-stimulatory molecules like CD80 and 86, 41BBL, OX40L, and CD70 [60]; and immunostimulatory cytokines like IL-12 and IFN-γ [61]. Once matured, DCs stop further ingestion of antigens, process and present epitopes derived from pathogens or tumors, and migrate to the nearest draining lymph node so that processed antigens can be efficiently interrogated by T cells (Illustration 2). Matured DCs are capable of potently stimulating T cells that recognize antigens presented on the DC surface. Thus, DCs initiate the T cell response towards potentially dangerous antigens, including cancer antigens.

Activation of naive T cells

T cells that have yet to be exposed to their cognate antigen are defined as naive, and these cells can be activated through interactions with antigen-presenting DCs. In mice, naive T cells express low levels of CD44 and high levels of CD62L and CCR7, thereby decreasing rates of extravasation into tissue and increasing the rate of entry into lymph nodes [62]. Lymph nodes are specialized compartments evolved to efficiently facilitate T cell encounters with antigen presenting dendritic cells. Within a lymph node, intra-vital 2-photon microscopy showed that each T cell interacts with up to 320 dendritic cells per hour, and each dendritic cell interacts with 500 T cells per hour [63]. The result is extremely efficient recruitment of naive T cells into antigen driven responses. Studies using DNA barcoding of naive antigen-specific T cells showed that a 72 hour bacterial infection recruited 95% of all naive T cells capable of recognizing a bacterial antigen [64].

For a naive T cell to become activated, the TCR on the T cell must recognize peptide epitopes bound to MHC molecules. The strength of the TCR-peptide/MHC binding is a key factor in determining the activation and expansion of naive T cells [65]. T cells with high avidity TCR require binding to very few (less than 10) peptide/MHC complexes, whereas T cells with low avidity TCR may require binding of thousands of cognate peptide/MHC complexes [66,67]. TCR binding to peptide/MHC results in phosphorylation of the closely associated CD3 complex, which initiates a signalling cascade that leads to T cell activation [68]. In addition to the signal received by TCR binding to peptide/MHC, T cells require appropriate costimulatory signals to become fully activated. Naive T cells constitutively

express CD28 on the surface, which binds to upregulated CD80 or CD86 on mature DCs. When CD28 on a T cell binds to upregulated CD80/86 on DCs concurrently with TCR stimulation, naive T cells become activated, produce Interleukin (IL)-2, and up-regulate other co-stimulatory receptor molecules like ICOS, 41BB, and OX40 [69]. When these molecules bind their cognate ligands on mature DCs, T cell proliferation is enhanced and T cell maturation can be modulated [68]. T cell activation is also enhanced by cytokines like IL-12, Interferon (IFN)-α, and IFN-β secreted by activated DCs [70]. The amount of antigen, avidity of the TCR for the antigen, appropriate costimulation, and cytokine milieu all work to coordinate the quality and size of the T cell activation. Once activated, T cells proliferate rapidly and can expand up to 10^5-fold in a week [71].

Activated CD4 T cells can provide further maturation signals that allow DCs to become fully matured or "licensed" [72]. When mature DCs present an antigen that is recognized by a CD4 T cell, the naive CD4 T cell becomes activated, as described above. Activated CD4 T cells upregulate CD40L, which binds to CD40 on DCs and licenses the DC [73]. Thus, CD4 T cells "help" DC activation and are often referred to as "helper T cells". DCs that receive activation signals from CD4 T cells increase secretion of cytokines like IL-12, which further enhance activation of naive CD8 T cells. In virus infected mouse models, CD4 help was necessary for full CD8 T cell activation and memory formation (described below) [74]. Additionally, CD4 T cell interactions with DCs can induce production of the chemokines CCL3 and CCL4 (MIP-1α and MIP-1β), which attract antigen specific CD8 T cells to the licensed DCs and increase the efficiency of CD8 T cell activation [75].

TCR stimulation in the absence of co-stimulatory signals may lead to T cell death, anergy, tolerance, or conversion to regulatory cells, and this process is necessary to avoid T cell mediated autoimmunity to self-antigens [76]. Cell apoptosis occurs often during normal physiological processes, and to avoid autoimmunity, it is crucial that T cell responses are not initiated towards this normal cell death. Thus APCs phagocytose apoptotic blebs and present processed peptides in a non-stimulatory context, often while secreting T cell inhibiting molecules like TGF-β and IL-10 [77]. When the TCR is engaged at the same time as the T cell is stimulated by these cytokines, T cells become inactivated [76]. Though these mechanisms reduce the incidence of autoimmunity, tumors often utilize these processes to deactivate tumor-specific T cells (discussed below) [78].

In vitro *T cell activation*

The pathways and processes described above relate to T cell activation *in vivo*; however, *in vitro* T cell activation is often required to study human tumor-reactive T cells. Several protocols have been developed for *in vitro* T cell activation using both antigen-specific activation and non-antigen-specific activation. For example, mitogens like phytohaemaglutanin (PHA) and concanavalin A bind to sugars and cause T cell receptor oligomerization, resulting in polyclonal, non-antigen specific T cell activation and expansion [79]. Alternatively, agonist anti-CD3 antibodies can polyclonally activate T cells in a non-antigen specific manner. The antibodies must bind to CD3 in a focused signal to result in T cell activation; therefore, anti-CD3 coated beads or plate bound anti-CD3 are often used to drive T cell activation [80]. Another method called the Rapid Expansion Protocol (REP) uses agonist CD3 antibodies, IL-2, and allogeneic feeder cells to polyclonally expand T cells [80]. Furthermore, cells transfected with DC derived co-stimulatory molecules have been used as artificial APCs [81,82]. For each of the above methods, T cell growth cytokines like IL-2, IL-7, IL-15 or IL-21 must be provided [83]. In addition to polyclonal, non-antigen-specific T cell expansion methods outlined above, antigen-specific T cell activation protocols have been developed. One method uses DCs harvested from peripheral blood that are subsequently pulsed with antigenic peptide or transfected with RNA or DNA encoding antigen. The DCs are then matured using TLR agonists and co-cultured with T cells [84]. This method results in selective expansion of antigen-specific T cells compared to bystander T cells, thereby increasing the frequency of the cells of interest in the resultant T cell cultures.

Effector cells

CD8 T cells

Once naive CD8 T cells have been activated, they proliferate and differentiate into effector Cytotoxic T Lymphocytes (CTL) or long-lived memory CD8 T cells. Several factors determine the peak number of activated antigen-specific T cells and their differentiation status. These factors include the precursor frequency of naive CD8 T cells that can recognize the antigen [85], the affinity of the antigenic peptide for MHCI [85], the affinity of the TCR for peptide/MHCI [65], the duration of the TCR-peptide/MHCI interaction [86], the type of co-stimulation received from the APC [87,88], the duration of antigen exposure [89], and the

cytokine milieu in which the T cell was activated. When appropriately stimulated, a CD8 T cell can undergo more than 15 rounds of cell division, resulting in > 50,000-fold expansion [90]. Once activated, CD8 T cells differentiate into cytotoxic T cells (CTL) and express effector molecules regulated by the master CTL transcription factor Tbet [91]. Tbet induces expression of cytotoxic molecules like granzymes, and perforin, inflammatory cytokines like IFN-γ and TNF-α [92] and chemotactic molecules like P selectin glycoprotein 1 (PSGL1) and CCR5 [92]. When a CTL recognizes cognate peptide/MHC on a cell in the periphery, the T cell forms an immunological synapse that intimately binds the T cell to the target cell. The T cell then releases perforin, which forms a pore in the target cell, and granzyme, which enters the target cell and initiates caspase mediated cell apoptosis [93]. Additionally, CTL express FAS, which binds to FASL on the target cell and induces target cell apoptosis [93]. Furthermore, peptide/MHCI stimulated CTL release inflammatory cytokines that inhibit cell growth and cause upregulation of antigen presenting molecules on the target cell, thereby making the target more amenable to T cell mediated killing. Most cancer immunotherapies have attempted to activate CTL because of their ability to directly recognize and kill tumor cells that express cognate peptide/MHCI.

After T cell expansion in response to infection, 90% of the T cells present at the peak undergo apoptosis, and the surviving T cells form long-lived memory T cells [61]. These memory T cells have frequencies that are greatly increased compared to the original naive repertoire for the same antigen. They have a reduced threshold for activation compared to naive T cells, and they can survive for decades [61]. Memory cells can be described in two main categories: central memory cells (T_{CM}), which express high levels of CD62L and CD44 and reside primarily in lymph nodes; and effector memory cells (T_{EM}), which express low levels of CD62L but high levels of CD44 and are found in circulation and in tissues [61]. Memory T cells upregulate Foxo1, which represses T-bet expression and decreases effector functions [94]. Memory T cells may be formed from two main mechanisms: they may differentiate from former CTL and undergo a phenotypic change into memory T cells, and/or they may be formed during the original antigenic encounter, whereby a small subset of the activated T cells immediately forms memory cells [95,96].

When CTL are chronically exposed to antigen, they undergo a phenotypic transformation into a hyporesponsive state called exhaustion. Exhausted T cells express

immune checkpoint molecules like cytotoxic T lymphocyte antigen-4 (CTLA-4), which binds to CD80/86 on APC; programmed cell death-1 (PD-1), which binds to PD-L1 and PD-L2 on APC and target cells; and lymphocyte activating gene (LAG3), which binds to MHCII [97]. When these molecules bind their respective ligands, T cells are inhibited from killing. Moreover, exhausted T cells lose the ability to secrete inflammatory cytokines, proliferate, and kill target cells [98]. Intratumoral T cells often express markers of exhaustion. Moreover, blocking exhaustion pathways has led to improved anti-tumor immunity and increased survival in several tumor types. This therapeutic concept is called "immune checkpoint blockade" and is discussed in more detail later.

CD4 T cells

Once activated by APCs presenting antigenic peptides on MHCII, CD4 T cells can function as helper T cells (Th). Activated CD4 T cells have several functions that help to orchestrate immune responses. Depending on the context of the activating signal, they can differentiate into several different "T helper" subtypes, including Th1, Th2, Th17, regulatory T cells and more. They can also switch subtypes in certain situations. Th1 CD4 T cells are thought to be the most critical for activating robust anti-tumor immunity; therefore, I will focus discussion on this T helper subtype. As mentioned previously, Th1 cells license DCs, endowing DCs with the ability to more fully activate CD8 T cells. Additionally, Th1 cells secrete cytokines like INF-γ in the tumor microenvironment, leading to increased expression of the chemokines CXCL9 and CXCL10 and increased CTL recruitment [99]. Moreover, the cytokines secreted by Th1 CD4 T cells can cause a phenotypic switch of innate cells, leading to enhanced anti-tumor immunity. For example, M2 (wound healing) macrophages can be transformed into anti-tumor M1 (pathogen defense) macrophages [100]. Th1 cells can also kill tumor cells directly via TCR recognition of MHC on the tumor cell surface [101]. Finally, Th1 cells may recognize tumor cells or APC within the tumor microenvironment and produce inflammatory cytokines that lead to retarded tumor growth [102]. Similar to CD8 T cells, CD4 T cells form long-lived memory cells able to respond more quickly than naive cells, thereby providing additional protection from recurrent infection.

Regulatory T cells

Regulatory T cells (Tregs) are critical regulators of the immune system. Tregs express the transcription factor FoxP3, and mutations causing defects in FoxP3 lead to fatal

autoimmunity in both mice and humans [103,104]. Tregs can develop in the thymus when they bind to self peptide/MHC with high affinity, or they can differentiate from naive CD4 T cells in the periphery due to TCR stimulation coupled with TGF-β signalling [105]. Tregs inhibit effector T cell responses through several mechanisms: they secrete immune inhibiting cytokines like TGF-β [106] and IL-10 [107] to dampen T cell activation and convert APCs to a tolerogenic phenotype; they express CTLA-4, which can lead to deactivation of CD8 T cells [108]; they express CD39 and CD73, which convert the DC-maturing molecule ATP into immune dampening adenosine [109,110]; they can act as IL-2 sponges, thereby reducing IL-2 availability for other T cells and inhibiting growth of effector T cells [111]; and they can directly kill effector T cells, through granzyme and perforin mediated pathways [112]. Though Tregs play a crucial role in maintaining immune homeostasis, preventing autoimmunity, and inducing tolerance to commensal bacteria, they also play an important role in inhibiting the immune response to cancer (described below).

Immunodominance

When the immune system responds to a specific pathogen, multiple T cell clones that recognize different epitopes become activated and proliferate, and they may inhibit one another. After expansion, the relative frequencies of CTL that recognize each epitope form a highly-reproducible hierarchy referred to as the "immunodominance" hierarchy [113]. The T cells that expand to the highest numbers are called immunodominant T cells, and those that expand to lower numbers are called subdominant T cells. The immunodominance hierarchy may be caused by various overlapping factors. For example, one group found that all of the immunodominant T cell responses to a murine infection with LCMV were towards epitopes that bound to MHCI with an IC50 < 25 nM [85], indicating that peptide/MHCI affinity was an important determinant of immunodominance. Another group found that the naive T cell precursor frequency was highly correlated with the peak T cell frequency, indicating that the immunodominance hierarchy may be imprinted in the naive repertoire [114]. When responding to a complex antigen with multiple T cell epitopes, immunodominant T cells can inhibit proliferation of subdominant T cells, a phenomenon called immunodomination [16]. The abrogated expansion of the subdominant T cell only becomes apparent after five days [115], and the effect is only observed when both antigens are presented on the same APC.

When activated by DCs, immunodominant T cells secrete IFN-γ, which causes the DC to secrete the immune inhibiting molecule IDO and abrogate subdominant T cell expansion [115-117]. Furthermore, direct competition for available antigen on APCs also leads to immunodomination [118]. Immunodomination has been observed among both CD8 T cells [119] and CD4 T cells [115]. In the anti-cancer vaccine setting, immunodominance is an important factor when considering the number of antigens to use in a vaccination regimen. For example if a highly immunogenic antigen and a weakly immunogenic antigen are coupled in a vaccine, the T cell response to the highly immunogenic epitope may dominate the T cell response; thus, immunodomination by T cells recognizing one epitope may inhibit the anti-tumor T cell response to another epitope.

Spontaneous anti-tumor immunity

Though many of the mechanisms of T cell immunity described in previous sections were elucidated using viral and bacterial infection models, they apply to the spontaneous T cell response to tumors as well. As tumors grow, a proportion of the tumor cells undergo apoptosis or necrosis. Necrotic tumor cells release both tumor antigens and immune stimulating DAMPs into the tumor microenvironment. Subsequently, tumor antigens can be endocytosed by APCs and processed and presented on MHC molecules. Additionally, DAMPs like ATP and HMGB1 bind to PRR on DCs, inducing DC maturation [58]. The matured DCs migrate to the draining lymph node and activate tumor antigen-specific naive CD4 and CD8 T cells. Once a T cell is activated, it proliferates and differentiates to express effector molecules like IFN-γ, TNF-α, granzyme, perforin, and chemotactic molecules like PSGL1 and CXCR3. The activated T cells then migrate out of the lymph node and into circulation. Tumor inflammation can cause selectins (for example P-selectin) to be expressed on tumor vascular endothelial cells and chemokines (for example CXCL9/10) to be present in the vascular lumen ExtraCellular Matrix (ECM). When selectin ligands on activated T cells encounter selectins on activated vasculature (i.e. PSGL1 on T cells binds P-selectin on vascular cells), T cells roll along the vascular wall and interact with chemokines found in the vascular ECM (for example CXCR3 on T cells binds CXCL9/10 on the ECM) [120]. Ligation of chemokine receptors can induce T cells to express integrins and lead to T cell extravasation into the tumor tissue [120]. Once in the tumor, TCR on T cells may bind to

cognate peptide/MHC expressed on the tumor surface and kill the tumor via FAS or granzyme/perforin mediated pathways. Debris from tumor cells killed by T cells can serve as additional antigens and DAMPs, providing a positive feedback loop and leading to increased inflammation and further T cell mediated tumor killing (Illustration 2) [121].

Immune evasion by cancer

Under selective pressure from anti-tumor immunity, the tumor cell population evolves mechanisms to evade the immune system [122]. Some of these mechanisms include attracting Tregs, attracting innate suppressive cells, inhibiting antigen presentation, and expressing immune inhibiting molecules. Cancer cells and Tumor-Associated Macrophages (TAM) secrete cytokines like CCL22 that recruit Tregs to the tumor microenvironment [123]. Tregs dampen anti-tumor immunity and promote tumor progression. They can convert anti-tumor CD4 T cells into Tregs, and they inhibit anti-tumor CTL. Moreover, increased ratios of Tregs to CD8 T cells are associated with poor overall survival in several tumor types [124-126]. Tumors also attract immature monocytes and induce their conversion into suppressive cells like TAMs and Myeloid Derived Suppressor Cells (MDSC) [127-129]. TAMs express immune inhibiting molecules like arginase-1, IL-10 and TGF-β, and they secrete wound healing molecules like Vascular Endothelial Growth Factor (VEGF) and Matrix Metalloproteinase (MMP)9, which prevent extravasation of anti-tumor T cells [112,127]. MDSCs are a heterogeneous mixture of cell types that inhibit T cell responses through expression of arginase-1 and suppressive cytokines [130].

In addition to recruiting immune suppressive cells, tumor clones may be selected that have impaired antigen presentation, enabling evasion of the anti-tumor immune response. If an immune response is directed towards non-essential tumor proteins, the tumor may evolve to prevent expression of those antigens [131,132]. In this case, the immune system removes tumor subclones that express highly immunogenic epitopes, a process called “immune editing” [122]. Additionally, tumors may down-regulate or mutate genes involved in antigen presentation, thereby eliminating antigenic peptide/MHC expression [131,133]. Furthermore, tumor cells can express, or induce expression of, molecules like PD-L1/PD-L2, Galectin 9, and CD80/86, which bind to the T cell inhibiting molecules PD-1, TIM-3 and CTLA-4, respectively [134]. Through combinations of these various mechanisms, tumors evolve to

evade anti-tumor immunity. Intense investigation is focused on developing cancer treatments that reverse these immune evasion pathways [133].

Having introduced the basics of T cell biology and the mechanisms by which T cells target and kill tumor cells, I will next discuss how modulating anti-tumor T cell responses can lead to improved cancer patient survival.

1.2 Clinical advances in T cell mediated cancer immunotherapy

For over 100 years, researchers have attempted to harness the immune system to induce anti-tumor immunity and improve cancer patient survival. Multiple treatments have been investigated in the clinic, some of which have led to dramatic successes. Most trials have targeted metastatic melanoma, a highly immunogenic and deadly type of cancer. However, immunotherapies have also begun to improve patient survival in other tumor types. In this section, I describe some historical cancer immunotherapy trials and provide an overview of the recent clinical successes leading to increased interest in this field.

Early immunotherapies – bacteria and IL-2

In the 1890's, William Coley pioneered the earliest use of immunotherapy to treat human cancers. He injected the bacteria *Streptococcus pyogenes* and *Serratia marcescens* into tumors, which stimulated an anti-bacterial immune response that would occasionally spread to the tumor [135]. These treatments – known as "Coley's toxins" – did not become widely adopted for cancer treatment, as only sporadic successes were achieved. However, a similar treatment has found a place in modern cancer therapy: intravesical administration of bacteria (Bacillus Calmette-Guerin (BCG)) is used as an adjuvant after surgical resection in non-muscle invasive bladder cancers. Maintenance treatment with BCG reduces the risk of recurrence and progression in patients with superficial bladder cancer [136]. Successful BCG treatment is dependent on several factors including adhesion of the BCG bacteria to the bladder wall, internalization of the bacteria by cancer cells, induction of T cell stimulating cytokines, and induction of a secondary immune response that attacks tumor cells [137]. However, 20% of patients treated with BCG stop treatment due to severe side effects such as cystitis, fever, or systemic infection [138], which are not associated with dose or duration of BCG administration [139].

Cytokine therapy is another early cancer immunotherapy that has shown efficacy in some cancer types. IFN-α treatment induced the first-ever survival benefit in a randomized controlled phase III clinical trial of metastatic melanoma, leading to FDA approval of this therapy in some settings [140]. Unfortunately, the treatment was highly toxic and led to reduced treatment doses in most patients [140]. Interestingly, T cell mediated autoimmunity was highly correlated with better overall, and relapse-free, survival [141], suggesting that direct stimulation of T cells accounted for the successes. Clinical trials of systemic therapy with another T cell stimulating cytokine, IL-2, resulted in partial response rate of 10% in metastatic melanoma, leading to FDA approval of IL-2 for metastatic melanoma [142,143]. In one trial, 6% of patients observed complete responses but 2% of patients died due to adverse events, highlighting the severe toxicity of this cytokine and the need for careful patient selection based on overall health [142,144]. Both IFN-α and IL-2 therapies provide non-specific T cell stimulation in cancer patients, which in some cases leads to anti-tumor T cell activation. However, IL-2 also stimulates Tregs, which can inhibit anti-tumor immunity [145,146].

Adoptive T cell therapies

Adoptive cell therapy (ACT) includes multiple techniques that use modified or expanded immune cells harvested from patients or healthy donors to treat tumors. Here, I focus on Tumor Infiltrating Lymphocyte (TIL), Bone Marrow Transfer (BMT), and Chimeric Antigen Receptor (CAR) ACT, and I discuss dendritic cell transfer in later chapters on vaccines. The earliest form of ACT utilized BMT for treatment of leukemias. Originally, patients received myeloablative chemotherapy and radiation to kill proliferating leukocytes including leukemia cells. Subsequently, patients received BMT to reconstitute the hematopoietic system, thereby rescuing the patient from hematopoietic failure and death. Further analysis revealed that patients who experienced graft versus host disease (GVHD) experienced a reduced likelihood of tumor relapse [147-149]. Further, one study found that leukemia patients treated with T cell depleted BMT or bone marrow from an identical twin observed higher relapse rates than patients treated with BMT containing T cells or non-identical twin BMT [149]. This study indicated that successful BMT treatments of leukemia were mediated by donor T cells killing leukemia cells rather than myeloablative

chemotherapy killing the tumor cells. The observation of the Graft Versus Leukemia (GVL) effect of donor T cells spurred development of non-myeloablative chemotherapy to precondition patients for BMT, thereby reducing morbidity of this treatment [150-152]. Subsequent studies determined that T cells often recognized minor histocompatibility antigens – antigens derived from single nucleotide polymorphisms (SNPs) that differ between donor and host – which mediated the graft versus leukemia effect [153,154].

Several centres conduct ACT using *ex vivo* expanded TIL for cancer treatment. Tumor reactive T cells are enriched in the tumor compared to peripheral blood, but they often exhibit an exhausted phenotype [155]. Thus, to reinvigorate tumor reactive T cells, tumors are surgically resected, and TIL are expanded *ex vivo* using high doses of IL-2 and a subsequent REP [80]. Billions of expanded T cells are then transferred back to the cancer patient after the patients are preconditioned with lymphodepleting chemotherapy [156]. Finally, patients are treated with maintenance doses of IL-2 to promote T cell survival [156]. Phase I and II clinical trials using ACT have resulted in response rates of over 50% in metastatic melanoma patients [157-159], and responses to TIL-ACT treatment in other tumor types have been observed in phase I trials [160,161]. However, due to the highly technical protocols and specific infrastructure necessary for this treatment, no phase III randomized controlled trials have been reported to date.

A third type of ACT treatment uses engineered T cells that express Chimeric Antigen Receptors (CARs). For these treatments, autologous T cells are transfected with a construct containing the antigen binding domain of an antibody fused to the intracellular signaling domains of the TCR subunit CD3 and one or more T cell co-stimulatory molecules [162]. Thus, CAR T cells are not MHC restricted; they can bind antigens in native form on the target cell surface. CARs directed towards the B cell marker CD19 (CD19-CARs) have yielded complete response rates of 80 – 90% in acute lymphocytic leukemia [163,164]. The majority of CAR therapies have targeted CD19 or CD20 on hematologic malignancies, but CAR therapies targeting other tumor associated cell surface markers are in development [165,166]

Together, ACT clinical trials provide unequivocal evidence of the profound anti-tumor effects of T cells under specific circumstances. However, with the exception of a few lineage specific targets like CD19, the antigens that underlie many successful anti-tumor

immune responses have remained largely unknown due the diversity of tumor antigens and the technical challenges associated with identifying T cell antigens (as discussed below).

Antibodies to activate T cells

The stunning clinical success of immune checkpoint blockade antibodies has elevated the field of cancer immunotherapy over the last five years [167]. Recently, the immune modulatory antibodies Ipilimumab (Yervoy) and Pembrolizumab (Keytruda) received FDA approval for treatment of metastatic melanoma [168,169], and Nivolumab received FDA approval for melanoma and Non Small Cell Lung Carcinoma (NSCLC) [170,171]. These antibodies bind to T cells and block signalling of inhibitory T cell surface receptors CTLA-4 (for Ipilimumab) and PD-1 (for Pembrolizumab and Nivolumab) [172,173]. The net effect is to enhance T cell reactivity toward tumors. Phase III clinical trials of Nivolumab demonstrated a remarkable objective response rate of 40% in highly pretreated metastatic melanoma patients [170], and it improved survival compared to standard of care in renal cell [174] and lung carcinomas [175,176] . Furthermore, while ACT therapy requires expert manipulation of T cells *ex vivo* and requires a unique product for every patient, checkpoint blockade therapy is an off-the-shelf treatment that can be administered in most hospitals. Thus, these therapies are becoming quickly adopted for treatment of some malignancies.

Numerous other T cell activating antibodies are in various stages of development for cancer treatment. For example, Blinatumomab has been FDA approved for treatment of a subset of acute lymphoblastic leukemia patients, based on a single-arm trial that induced complete response in 43% of patients [177,178]. This bi-specific antibody binds to both CD19 on malignant cells and to CD3 on T cells, thereby re-directing T cell killing to malignant cells expressing CD19 [177]. Additionally, T cell modifying antibodies that block immune checkpoint molecules like TIM3 and LAG3 are in development, and clinical trials have been initiated [179]. Furthermore, antibodies that activate T cell co-stimulatory molecules such as OX40 (CD134) [180], CD27 [181], GITR [181] and 41BB (CD137) [182] are in development and some have entered clinical trials. Finally, combinations of T cell activating antibodies induce improved responses compared to single antibody treatments [183-185]. With the vast array of T cell modifying antibodies in the drug development pipeline, large numbers of clinical trials will be required to identify optimal combinations.

Vaccines

In the next section, I discuss various vaccination strategies, and I examine the mechanisms of immune activation by therapeutic anti-cancer vaccines.

1.3 Therapeutic, T cell mediated anti-cancer vaccines

Tremendous efforts have been focussed on developing therapeutic vaccines to activate anti-tumor T cells that recognize specific tumor antigens. Prophylactic vaccines have enjoyed a great deal of success targeting tumors with a viral etiology. For example prophylactic vaccination against Human Papillomavirus (HPV) has been approved in several countries, leading to reduced incidence of cervical cancer [186]. Unfortunately, to date therapeutic anti-cancer vaccines have demonstrated fewer successes [187], but improvements are ongoing. The goal of therapeutic vaccines is to activate T cells that recognize antigens enriched on – or specifically expressed by – tumor cells. To maximize effectiveness, therapeutic cancer vaccines should be designed to achieve the following: delivery of antigen to DCs, presentation of peptides on DCs, induction of DC maturation, and activation of large numbers of T cells with high affinity TCRs. Multiple formulations of cancer vaccines have yielded increased patient survival in phase II trials in prostate, breast, lung, and other cancers [188-190], and some have entered phase III clinical trials [191,192]. Moreover, a prostate cancer vaccine that uses autologous DCs pulsed with the tumor associated antigen Prostatic Acid Phosphatase (PAP) was the first therapeutic anti-cancer vaccine approved by the FDA [193]. In this section on therapeutic cancer vaccines, I first discuss antigen identification methods and different classes of antigens that have been targeted with anti-cancer vaccines. Subsequently, I review various vaccination strategies, with a focus on peptide based vaccines as these were used in studies in Chapter 2 and 3.

Methods of tumor antigen discovery

The first step towards developing a tumor antigen targeted vaccine is to identify suitable tumor antigens. The search for antigens responsible for tumor rejection has been an active area of research for decades [194]. This search led to the first identification of a mouse tumor CTL antigen, in 1988 [195], and the first identification of a human tumor CTL antigen, in 1991 [196]. Since then, numerous tumor antigens recognized by tumor specific T

cells have been identified [1]. Four methods have been used to identify the majority of tumor antigens: 1) cDNA library screens, 2) reverse immunology approaches, 3) SERological analysis of recombinant cDNA EXpression libraries (SEREX), and 4) proteomic analysis of peptides eluted from MHC.

cDNA library screens assess tumor reactive T cells against cDNA libraries generated from the autologous tumor. The method first requires the identification and isolation of tumor reactive T cell clones. Next, the *HLA* restriction of the clone is determined. Subsequently, a tumor cDNA library is constructed and small pools containing 50 – 100 cDNAs are transfected into host cells that express the restricting *HLA* allele. Clonal tumor reactive T cells are then stimulated with transfected host cells, and transfected cultures that elicit T cell activation are identified. Each cDNA within the pool that stimulated the T cell clone is individually transfected into additional host cells to determine the single cDNA that the T cell recognizes. Finally, the single T cell-stimulating cDNA is sequenced to identify the gene containing the T cell antigen [197]. A benefit of this method is that it assesses a T cell clone already known to be tumor reactive, and it is largely unbiased towards expected antigens. A drawback of this method is that it is labor and resource intensive.

In contrast to cDNA library screens that start with a tumor reactive T cell clone, reverse immunology approaches for tumor antigen discovery starts with identification of a suspected tumor antigen based on tumor-restricted expression. Once a suspected tumor antigen is identified, epitope prediction software can be used to select potential minimal epitopes that bind to a given MHC. Alternatively, APC can be transfected with the gene encoding the suspected antigen. Next, the minimal peptides or transfected APC are co-incubated with T cells, *in vitro,* to activate and expand antigen-specific T cells. Finally, tumor reactivity of the expanded cells is assessed using *in vitro* killing assays or T cell recognition assays [198]. A drawback to this method is that many T cell responses that recognize minimal peptides fail to recognize tumor cells due to lack of antigen processing [14]. Additionally, because high densities of antigen are presented by DCs, low avidity T cells may expand which may not be therapeutically beneficial. The current project uses reverse immunology approaches with tumor specific mutations as suspected antigens.

Another method, called SEREX, uses components of both of the above techniques to identify tumor antigens [199]. The SEREX technique uses phage expression libraries of

tumor cDNA to screen autologous patient serum and identify antibody responses to tumor-antigen. Once an antibody response is identified, indicating an immune response to an antigen, the cDNA is sequenced to identify the gene recognized by patient antibodies. Finally, reverse immunology approaches are used to detect T cell responses to the identified antigen [200]. A drawback of this method is that only antigens that elicit antibody responses are identified.

T cell epitopes can also be discovered using mass spectrometry (MS) analysis of peptides eluted from MHC molecules. In this method, tumor cells are lysed and MHC proteins are isolated using immunoprecipitation. Epitopes are then eluted using acids, and the peptides are analyzed by MS [201]. A major benefit of this technique is that it identifies only authentic epitopes (i.e. epitopes that are naturally processed and presented by the analyzed cell). Therefore, MS has high selectivity since it avoids cryptic epitopes that would not be processed by antigen processing machinery. However, MS is technically challenging, requires large numbers of input cells, and has low sensitivity [1]. Another challenge for tumor antigen discovery using MS is that the data are usually interrogated using human peptidome databases, and so tumor mutations may be overlooked [1]. However, these challenges are being addressed by improving MS technologies to increase sensitivities and by using patient-specific DNA sequencing to build peptidome databases that includes tumor mutations [202].

The approaches above have identified several tumor antigens [2]. I will next discuss the classes of tumor antigens that have been targeted with vaccines.

Classes of tumor antigens for vaccines

"Cancer antigen" is a broad term that includes protein-derived epitopes presented in MHCI and MHCII, tumor-associated post-translationally modified peptide epitopes, surface expressed proteins recognized by antibodies or CARs, and lipid antigens presented on CD1d. Here, I limit discussion to conventional peptide epitopes derived from tumor proteins and presented on MHC. For a tumor antigen to be an effective vaccine target, the antigenic epitope must be presented at higher levels on tumor cells than normal cells. As I discuss below, tumor antigens fall into several major groups, each with distinct advantages and disadvantages as targets for cancer immunotherapy.

Viral antigens

Cancers of viral origin express virus-derived proteins that can be recognized by the immune system. For example, the E6 and E7 proteins from Human PapillomaVirus (HPV) make ideal therapeutic vaccine targets [203]. These antigens are tumor restricted, and proteins derived from the virus are implicated in tumorigenesis of cervical cancer, head and neck cancers and others [204,205]. Additionally, viral antigens are completely foreign, meaning that T cells bearing high affinity TCR recognizing viral antigens are not subject to central tolerance. Interestingly, patients with HPV positive oropharyngeal tumors are at a 58% reduced risk of death compared to HPV negative tumors, perhaps indicative of anti-HPV immunity [206]. However, only about 15% of cancers worldwide [207] have a viral etiology, limiting the broader applicability of targeting viral antigens with vaccines [205].

Differentiation/overexpressed

Genes with increased expression due to amplification or other mechanisms can give rise to "overexpressed" T cell antigens. Examples include Human Epidermal growth factor Receptor 2 (HER2) on breast and ovarian carcinomas [208-210], and Mouse Double Minute 2 homolog (MDM2) in multiple cancers [211]. Also, proteins that are differentially expressed in the tissue of origin of the tumor can give rise to "differentiation" antigens. For example, melanomas often express the differentiation antigens MART1, gp100 and Tyrosinase [212,213]. T cells recognizing overexpressed and differentiation antigens have been identified in several tumor types [1]. However, since differentiation and overexpressed antigens are also present in healthy tissue, T cells recognizing these classes of antigens are often low affinity as a result of thymic negative-selection [211,214,215]. Moreover, targeting such antigens with immunotherapy brings the risk of autoimmune toxicity [216]. Additionally, as part of normal peripheral tolerance mechanisms, Tregs may recognize overexpressed and differentiation antigens, thereby limiting the effectiveness of these vaccine targets [55].

CT antigens

Many human cancers express cancer-testis (CT) antigens [1]. These proteins are normally expressed only in adult gametes, but can be aberrantly expressed in tumors due to DNA hypomethylation and gene dysregulation [217]. While the tumor-restricted expression pattern of CT antigens makes them attractive targets for immunotherapy, typically they are

expressed by only a portion of tumor cells and are dispensable for tumor cell survival [218]. Thus, tumor sub-clones that do not express the antigen are likely to evade CT-antigen directed immunity. Furthermore, though expression of CT antigens is mostly limited to adult gametes, studies of CT antigen knock-out mice suggest that thymic negative selection may eliminate some T cells that express the highest affinity TCRs for CT antigens [219].

Mutated antigens

Finally, as discussed in detail in sections below, mutations represent a unique class of tumor antigen that has recently become experimentally accessible as a result of NGS advances. These antigens are tumor-restricted, which limits the potential for on-target/off-tumor toxicity. Additionally, by definition, tumor mutations are not coded in the germ line; thus, T cells with high affinity TCR recognizing tumor mutations survive thymic selection. However, each tumor harbors a unique set of mutations with few mutations shared among patients, meaning targeting tumor mutations typically requires personalized strategies.

Anti-tumor vaccination strategies

The goal of anti-cancer vaccines is to induce high-frequencies of potent T cells capable of recognizing and killing tumor cells while avoiding non-tumor tissues. Several strategies have been developed to accomplish this goal, including use of irradiated tumor cells, antigen pulsed DCs, antigenic DNA, antigenic RNA, recombinant viruses and bacteria, and protein and peptide antigens. In the following paragraphs, I will discuss the theory behind each of these strategies and the benefits and drawbacks of each.

Tumor cell/ lysate vaccines

Whole tumor cell vaccines stimulate oligoclonal anti-cancer T cell responses towards tumor associated antigens expressed within the inoculated cell. The most clinically advanced vaccine candidate is called GVAX, which targets prostate cancer. This vaccine contains a mixture of two prostate cancer cell lines that are transfected to express Granulocyte Macrophage Colony Stimulating Factor (GM-CSF) [220], a cytokine that induces production of monocytes and their differentiation into DCs [221,222]. Unfortunately, phase III clinical trials with GVAX failed due to lack of efficacy [223]. Tumor lysates have also been used as vaccine reagents. Lysed cancer cells release immune stimulating agents like HMGB1, ATP, and heat shock proteins, which promote maturation of DCs and increased cross-presentation

of antigens. Vaccinations with lysates combined with various adjuvants have led to improved survival of tumor bearing mice [224,225]. A major benefit of lysate/cell based vaccines is that prior knowledge of specific tumor antigens is not necessary, as in theory, these techniques induce T cell responses towards any antigens present in the tumor. Moreover, these vaccines may elicit oligoclonal T cell responses to multiple tumor antigens. However, monitoring T cell responses to the vaccine is challenging since the tumor antigens remain unknown [220]. Furthermore, most of the vaccine is composed of normal cellular components; thus, self-peptides may outcompete immunogenic tumor epitopes for binding to MHC and may induce tolerance [226].

DC vaccines

Vaccines involving live, modified DCs are under intense investigation and have resulted in some clinical successes. As mentioned above, Sipuleucel-T – the first FDA approved therapeutic vaccine – is comprised of patient DCs pulsed with the prostate tumor associated antigen PAP [193]. DC vaccines involve collecting monocytes from patient PBMC, and inducing DC differentiation using cytokines like GM-CSF and IL-4 [227]. DCs are then induced to present tumor antigens using various methods: (1) Co-incubation with tumor cell lysate [228], (2) fusion to tumor cells [229], (3) co-incubation with peptide or protein tumor antigens [230], or (4) transfection with RNA or DNA encoding tumor antigens [227]. Various methods are in development to induce DC maturation prior to adoptive transfer. Though tumor-lysate-pulsed DC vaccines can induce maturation via DAMPs released by the dying cells, others have endeavoured to optimize DC stimulation [231]. For example DC maturation cocktails have incorporated cytokines and TLR agonists including TNF-α, IL-1β, IFN-γ, IFN-α, and poly(I:C) [232,233]. Benefits of DC vaccines include providing high concentrations of epitope on the APC surface, and ensuring DCs are in a matured state prior to inoculations. However, the highly specialized expertise necessary to generate these vaccines and substantial infrastructure for DC adoptive therapy limit clinical application of this technique.

DNA and RNA vaccines

Bacterial plasmids encoding tumor antigens have been developed to elicit anti-tumor immunity. Encoded within the DNA itself are unmethylated CpG, which are PAMPs that bind to TLR9 and induce DC maturation [234]. Thus, a benefit of DNA vaccines is that they

are self-adjuvanted. Once DNA gains entry into a DC, the antigenic sequence is transcribed and translated, and the encoded protein is digested and enters the endogenous antigen presenting pathway. Only a small fraction of the injected DNA reaches DC nuclei and is translated [234], meaning immune responses generated by most DNA vaccines are often weak. However, new technologies for efficient delivery of DNA to DCs are improving host antigen presentation and T cell activation [235,236].

In vitro transcription of tumor-antigen-encoding DNA produces RNA that can be used in vaccines to target antigens, including neoantigens [237,238]. mRNA is harvested from expression vectors, purified, and administered to patients. Some of the vaccine accesses the cytosol of DCs, and the mRNA is translated. Encoded proteins enter the endogenous antigen processing pathway, and epitopes are presented on MHCI and MHCII [239]. Similar to DNA vaccines, RNA binds to TLRs on DC and induces maturation; thus, RNA vaccines are self adjuvanting. A drawback of these vaccines is that free, naked RNA is unstable *in vivo,* as RNases quickly digest them [240]. However, strategies are being developed to increase uptake of RNA by DCs and increase stability *in vivo.* For example, repeated intra-lymph node injections dramatically improve RNA-encoded-antigen presentation by DCs and enhance activation of antigen specific T cells in mice [237]. Moreover, RNA can be stabilized with proteins like protamine [241], or encapsulated in liposomes [242].

Viral and bacterial vector vaccines

Viral and bacterial vectors manipulated to express tumor antigens elicit robust anti-tumor T cell responses in mice and in humans. Natural TLR agonists on these vectors induce DC maturation. Furthermore, the vectors can be designed to encode T cell stimulating molecules like CD80, ICAM-1 and LFA-3 [188]. Viral vector anti-cancer vaccines have resulted in positive responses in the clinic and phase III trials are underway in prostate cancer [243]. One limitation of these vaccines is that GMP quality is difficult to achieve for each vaccine formulation, thereby limiting these vaccines to shared tumor antigens [244]. Additionally, the multitude of vector antigens present induces vector-specific T cells that can inhibit tumor-antigen-specific T cells. This problem is being addressed using heterologous priming and boosting vectors with only the tumor antigens shared among inoculums [245,246]. While this ensures that only the tumor-specific T cells are boosted, it also increases the complexity of delivering the vector based vaccines.

Protein and peptide vaccines

Proteins and peptides are the most common antigen formulations used in anti-cancer vaccines, but vaccine formulae require optimization. Several groups have developed anti-cancer vaccines using peptides encoding minimal epitopes of known cancer antigens, often admixed in an oil emulsion called Montanide [247,248]. This vaccination strategy occasionally elicits robust T cell responses in humans [249]; however, clinical responses have so far been rare [247-249]. The main explanations for poor clinical efficacy of minimal peptides in oil emulsions are (1) weak adjuvants [250], (2) Montanide-induced mis-localization of T cells to the injection site [251], and (3) inappropriate presentation of the antigen by non-APC [252].

Inclusion of weak adjuvants may partially explain the poor clinical activity of minimal peptide vaccines to date. For example, in many peptide vaccine formulations, Montanide is the sole adjuvant. Though Montanide induces some level of DC maturation, the T cell responses elicited are generally weak, and antigen specific T cells can become tolerized [253,254]. Another adjuvant that has been used in several trials is GM-CSF [255,256]. GM-CSF induces generation and differentiation of monocyte derived DCs and macrophages [257,258]; however, the unanticipated effects of increasing MDSCs, TAMs, and tolerizing DCs may result in reduced clinical efficacy of vaccines that use GM-CSF [259,260]. Indeed, a multi-center clinical trial of peptide vaccines in Montanide with or without GM-CSF found that T cell responses were elicited in 34% of patients that received GM-CSF compared to 73% of patients who received peptide in Montanide alone [261]. Indeed, the majority of peptide-based anti-cancer vaccines to date may have been hindered by these suboptimal adjuvants.

In contrast to Montanide and GM-CSF, TLR agonists are powerful DC maturation agents [262,263]. Some of the most common TLR agonists in use are LPS, a bacterial outer membrane component that stimulates TLR4 [264]; poly(I:C), a double stranded viral RNA mimic that stimulates TLR3 [265]; CpG, a bacterial DNA mimic that stimulates TLR9 [266]; and Imiquimod, a small molecule that stimulates TLR7 [267,268]. Studies in mice show that vaccines with TLR agonists induce dramatically increased T cell activation compared to vaccines using oil emulsions alone [252,268]. In mice, CpG and poly(I:C) have shown

superior adjuvant effects compared to LPS [269], and hence many contemporary clinical anti-cancer vaccines have incorporated these TLR agonists in vaccine formulae [270].

In addition to its suboptimal adjuvant effects, oil emulsions may have unanticipated effects on T cell localization and tolerization. A study in mouse models showed that the slow releases of minimal-epitope peptides from oil emulsion depots (incomplete Freunds adjuvant (IFA)) allowed direct surface binding and presentation of peptides on non-professional APC. Peptide presentation by non-APCs in a non-inflammatory environment induced T cell tolerance and death [251,253]. Moreover, antigen presentation on cells surrounding the antigen depot led to mis-localization of activated, antigen-specific T cells to the injection site rather than the tumor. Thus, the antigen injection site became a "T cell graveyard" [271]. T cell mis-localization may induce severe injection site swelling often observed with vaccines using minimal peptides in Montanide [247,248]. To overcome the limitations of minimal peptide vaccines, synthetic long peptides (SLP) are increasingly used in vaccine formulae [272].

Synthetic long peptide vaccines

Synthetic Long Peptides (SLP) greater than 20 amino acids long have many advantages over minimal peptide vaccines. For example, MHCI molecules cannot accommodate peptides longer than 15 amino acids, so SLPs are unable to surface bind to non-professional APC at the vaccine injection site. Therefore, SLP are targeted to professional APC, which process and cross-present epitopes and activate antigen specific T cells [252]. One study found that SLP vaccines and the TLR9 agonist CpG induced antigen presentation only on draining lymph node DCs, which led to superior T cell activation compared to minimal peptide vaccines [252]. Furthermore, they found that SLP in PBS elicited more robust T cell responses than SLP in Montanide [269]. An additional benefit of SLP vaccines is that they often encode both MHCI and MHCII epitopes, thereby improving CD8 T cell memory formation [272]. Furthermore, since DC antigen processing and presentation machinery dictates the identity of the presented epitope, predefining the minimal epitope within the SLP is not required. Finally, DCs process and present SLP more quickly and efficiently than protein antigens, resulting in improved T cell activation towards SLP vaccines [273]. When combined with TLR agonists, SLP vaccines activate potent anti-tumor T cell responses that have cured tumor-bearing mice in several disease settings [274-276]

and led to clinical responses in patients [277]. For example, long peptide vaccines targeting E6 and E7 induced complete responses in 9 of 19 patients with grade-three vulvar intraepithelial neoplasias [278]. However, the paucity of strong antigens – with HPV proteins a notable exception – has been a major hurdle limiting the effectiveness of SLP vaccines in the clinic [278]. Using next-generation sequencing (NGS) to identify neoantigens (described below) may surmount this hurdle and provide ideal antigens for use in SLP vaccines.

Many of the benefits described above make SLP a highly attractive antigen formulation for use in neoantigen targeted vaccines. First, the simplicity of generating Good Manufacturing Practices (GMP) quality SLP for any antigen makes them convenient for designing personalized vaccines [279]. Second, previous knowledge of the minimal mutant epitope is not necessary as SLP encompass all possible mutant epitopes for a given mutation. Third, the ease of adding appropriate DC maturation signals like TLR agonists to a SLP vaccine adds to the attractiveness of this technique. However, improved methods are still required to maximize anti-tumor T cell responses to SLP vaccines. Our group has extensive experience using protein vaccines to target tumor antigens [203,280]. However, to target tumor neoantigens, generating a full-length protein for each mutation would be too cumbersome. I reasoned that our expertise in protein vaccination could be applied to SLP vaccines for use in targeting tumor neoantigen studies.

In a subsequent section, I will further discuss the concept of targeting neoantigens; but first, I will review the advances in sequencing technology that make targeting neoantigens possible.

1.4 Next generation sequencing

History and platform

Sequencing the entire human genome was a landmark achievement of mankind. In 1977, Frederick Sanger first developed a method to sequence DNA using di-deoxynucleotides (ddNTPs) to prematurely terminate DNA polymerization [281]. Over the next decades, improvements to this technique were developed, including incorporation and detection of fluorescently labeled ddNTPs [282,283], PCR [284], and the introduction of capillary sequencing [285]. These technologies led to the successful sequencing of the first human genome in 2001 [286,287]. However, using Sanger sequencing based methods to

determine the sequence of an entire genome was feasible for only the largest sequencing centers.

The advent of Next Generation Sequencing (NGS) has distributed the ability to sequence genomes to much smaller labs. The technique – dubbed "massively parallel sequencing" – involves sequencing millions of overlapping, very short fragments (typically 100 to 1000 bp) of source DNA. Several NGS platforms have been developed, but the most common – and the platform that I employed – is the Solexa/Illumina suite of sequencers. The source DNA is fragmented into short pieces, size selected, amplified, and fused to adapter sequences that are complementary to sequences found on the solid glass flow cell. The processed DNA fragments are added to the flow cell and anneal to the complementary sequences. Bridge amplification results in clusters of DNA fragments bound to the flow cell, with each cluster containing multiple copies of one fragment of DNA [288]. The sequencing chemistry can then proceed. The system uses four nucleotides (ATCG) that are each bound to a different colored fluorophore and blocked at the 3'-OH position to prevent more than one nucleotide being added in each step. After the sequencing primers are added, nucleotides are added, and the following sequence occurs for each DNA strand: (1) A single complementary nucleotide extends the primer; (2) non-integrated nucleotides are washed away; (3) a laser excites the fluorophore and the color of each fragment cluster is recorded; (4) the fluorophores are cleaved from the nucleotides; and (5) the 3'-OH is de-blocked and the newly synthesized strand is ready for the next nucleotide addition. This process is repeated 100 times (for my 100 bp sequencing runs), and the sequence of the colors emitted after each cycle are processed to determine the sequence of each fragment of DNA. This 100 bp of DNA sequence is called a "read".

Massively parallel DNA sequencing can introduce errors that may be mistaken for real variants. For example, DNA is amplified prior to sequencing; therefore, PCR errors can be incorporated into some of the PCR product DNA. Since each product DNA strand is individually sequenced, strands with incorrect bases incorporated will be assessed as containing the different nucleotide [289]. Furthermore, problems with the sequencing chemistry can result in loss of signal and increased error towards the end of each read due to increased probability of failed or mis-incorporated bases. Moreover, clusters that overlap can lead to merged fluorescence emissions and low quality base-calls. To measure some of these

effects, phred base-quality scores can be used to assign the probability of an incorrect base call for each position [290]. These scores allow error recognition, which assists analysis and filtering and helps identify true variation [290]. However, template construction errors (like PCR error) have high base-quality scores, so these metrics cannot eliminate these errors. Because many base-call errors are largely sporadic, they can be overcome by "deeper" sequencing (i.e., obtaining more sequencing reads from the same input DNA). When each base is sequenced multiple times within multiple reads, many of the errors are drowned out by multiple correct sequences. The depth of sequencing is given as fold coverage of the target DNA and typically ranges from 30-fold to thousands-fold, depending on the assay design.

In addition to base-calling errors, the highly repetitive nature of mammalian reference genomes can lead to mapping errors [291]. Often the sequence of a read is similar to several different loci within the reference genome, making determination of the true location of the sequencing read, and any variants within it, challenging [291]. Therefore, validation of identified variants is generally performed using a different assay design. For example, as described in Chapter 3, I used whole exome sequencing to identify variants, and I used RNA-sequencing to confirm the variants. Alternatively, Sanger sequencing, or targeted re-sequencing, of PCR amplified loci can validate variants. Despite the challenges of determining true variation within NGS data, sequencing technologies have shed light on the molecular lesions that lead to cancer.

Genome, exome and transcriptome sequencing

The three main classes of NGS used to identify tumor-specific coding mutations are whole genome sequencing (WGS), whole exome sequencing (WES), and whole transcriptome sequencing (RNA-seq) [292]. WGS, as the name implies, determines the sequence of the entire genome, approximately 98% of which is not protein-coding. This method can help to identify point mutations, as well as large structural rearrangements and gene amplifications/deletions. However, the majority of the sequencing data are intronic or intergenic and not useful for identifying epitopes, the vast majority of which are derived from translated proteins. This makes WGS inefficient for identifying immunogenic epitopes compared to the next two methods. WES is a method to enrich for DNA encoding exonic

sequences [293]. The method employs biotinylated RNA baits that are complementary – and hybridize – to exonic sequences. The method makes sequencing far more efficient for identifying epitopes, as only the protein-coding portion of the genome (approximately 2%) is sequenced. However, since each exon is sequenced as an island, and most fusion breakpoints are within non-captured introns, WES cannot be used to identify most gene fusions. RNA-seq, as the name implies, assesses RNA that is processed into DNA for sequencing. For mRNA-seq, sample RNA is harvested and the mRNA is enriched and converted into double stranded DNA prior to shearing and sequencing. Thus, the method specifically sequences only transcribed genes [294]. RNA-seq can identify fusions, point mutations, and alternative splicing variants [295-297]. In addition, expression levels can be inferred from the proportion of RNA-seq reads that map to a given gene [298]. However, RNA-seq is inherently noisy due to infidelity of transcription and splicing within the source cells and degradation during processing [299]. For the most robust identification of potential epitopes, RNA-seq can be coupled with WES or WGS.

NGS in cancer

NGS has dramatically expanded our understanding of cancer. Sequencing both tumor tissue and matched normal tissue can identify tumor-specific alterations in the genome and transcriptome that influence cancer development, progression, and response to treatment. Initially, it was hoped that sequencing tumors would reveal a circumscribed set of druggable, recurrently-mutated genes responsible for the malignant phenotype (i.e., driver mutations). However, sequencing of thousands of tumor genomes has dampened these hopes. The majority of driver genes identified to date are mutated in at most a few percent of patients [300]. Indeed, large-scale sequencing projects like The Cancer Genome Atlas (TCGA) continue to identify new oncogenes as more tumors are sequenced [301,302]. Moreover, most somatic tumor-mutations are thought to be passengers and not implicated in tumorigenesis [300,303,304]. Furthermore, the mutational load differs by over three orders of magnitude within and between cancer types [300,303,304]. Collectively, the mutational diversity revealed by NGS highlights the need for personalized treatments that exploit the unique mutation profile of each tumor.

Personalized oncology

Several centers are developing pipelines for administering personalized cancer treatments targeting NGS-identified molecular lesions. The first genomics-guided personalized cancer treatment was administered to a patient with metastatic adenocarcinoma of the tongue [305]. Integrated analysis of genome and transcriptome data revealed a putative driver mutation in the PTEN gene, as well as overexpression of the RET gene. Although this tumor type is not normally treated with RET inhibitors, on the basis of the NGS data, the patient was given the RET inhibitor Sunitinib, which led to temporary disease stabilization. In another study, NGS of a thyroid cancer identified a personal point mutation in mTOR that conferred resistance to the mTOR inhibitor Everolimus [306]. Based on early case reports such as these, several centres have initiated personalized cancer therapy trials [307-309]. One group sequenced a panel of 182 – 236 known driver genes in highly aggressive tumors from 34 patients [307]. Patients received one or more drugs tailored to their mutation profile. Of eleven evaluable patients, three achieved a partial response and four achieved stable disease. While these results are encouraging, the majority of mutant gene products are not targetable with the current armamentarium of pharmaceuticals, thereby limiting the efficacy and broader applicability of personalized cancer therapy [310,311]. Furthermore, there is limited financial incentive for pharmaceutical companies to develop drugs for rare driver mutations with niche markets. These factors severely limit pharmacological approaches to personalized cancer therapy. However, personalized cancer immunotherapy may overcome some of these limitations.

1.5 Neoantigens

Tumors develop tens to thousands of coding mutations during the process of tumorigenesis, and by random chance, a small proportion of these can give rise to new T cell epitopes or “neoantigens”. While some mutations are within proteins on the cell surface and potentially targetable with monoclonal antibodies [312] or CAR T cells [313], the majority of mutations are intracellular, and therefore, antigen presentation on MHC is necessary. Neoantigens can arise when mutations affect either TCR contact residues [314] or anchor residues in peptide epitopes with affinity for MHC I or II [315]. Even a single amino acid substitution can yield an epitope that is sufficiently different from self to mark tumor cells

for T cell mediated destruction. Here, I discuss the benefits of neoantigens compared to other antigens, and I review strategies to identify and target neoantigens.

Historical identification of neoantigens

The concept of neoantigens is not new. By screening tumor-derived cDNA libraries with tumor-reactive T cell clones, several early studies provided anecdotal examples of immune system recognition of neoantigens [197,316,317]. Such studies demonstrated that neoantigens can be derived from both driver [318-320] and passenger genes [321,322] and are present in many different types of tumors, including melanoma [323], renal cell carcinoma [324], oral squamous cell carcinoma [318], colorectal carcinoma [325], lung carcinoma [326], and chronic myelogenous leukemia [327]. Some studies have indicated that neoantigens can be the predominant class of antigen recognized by TIL [1,328]. Moreover, some clinical responses to anti-cancer vaccines targeting self-antigens may be attributable to neoantigen specific T cells activated through "antigen spreading". This phenomenon was observed in a patient who responded to a pox virus vaccine expressing the CT antigen MAGE. When the patient's TIL were analyzed, few T cells recognized the vaccine antigen; however, a robust neoantigen specific T cell response was detectable after vaccination, which was absent prior to vaccination [329]. Furthermore, neoantigen-specific T cell responses have been associated with complete or partial tumor regression either spontaneously or after therapy [330-332]. About half of all tumor antigens discovered to date are neoantigens [2]. Most of these antigens were discovered using cDNA libraries or reverse immunology techniques described above; however, advances in NGS technology provide new strategies for identifying neoantigens and have expanded the number of potentially targetable neoantigens in each tumor.

Advantages of neoantigens

As therapeutic targets, neoantigens have several advantages over other classes of tumor antigen. First, neoantigen-specific T cells are not subject to thymic tolerance; therefore, high-affinity T cell clones may be available for immunotherapy [333]. Notably, T cells bearing TCRs with high affinity for their cognate antigens have greater cytotoxic capacity, longer persistence in the tumor environment, and decreased susceptibility to

immune suppression [67,334]. Second, while differentiation and overexpressed antigens are expressed by non-tumor tissues, neoantigens are exclusively expressed by tumor cells, reducing the potential for off-target toxicity [216]. Third, while viral and CT antigens may be expressed in only a limited number of tumors, NGS has revealed that a large proportion of tumors express multiple mutant gene products that could potentially serve as T cell targets [300]. However, as discussed next, it remains a major technical challenge to identify *bona fide* neoantigens from the tens to thousands of tumor mutations identified by NGS.

Frequency and computational identification of neoantigens

For a mutation to give rise to a neoantigen, several criteria must be met: a) the mutation must be present within a peptide that is processed from the parent protein by intracellular antigen processing machinery; b) the mutant peptide must bind with sufficient affinity to MHC; and c) the patient's immune repertoire must contain T cells with sufficient affinity and specificity for the mutant epitope. As a result of these criteria, only a small percentage of mutations give rise to authentic T cell epitopes. For example, only 2% of peptides bind to a given HLA allele with an IC50 < 500 nM [17], and only 8% of peptides capable of binding MHCI are processed, presented, and recognized by host T cells [14]. From these data, one would predict that only a small proportion of mutations give rise to authentic neoantigens. Moreover, since the number of somatic point mutations in human tumors can vary by five orders of magnitude within and between tumor types [300,303], from the perspective of neoantigen load, some cancers are intrinsically more immunogenic than others.

Until recently, the identification of personal neoantigens required highly labour-intensive techniques that precluded routine use in the clinic; however, advances in NGS and epitope prediction are starting to address this feasibility issue. In addition to mutation profiles, a patient's *HLA* type can be extracted from NGS data with high accuracy [335], thereby enabling epitope prediction to identify candidate neoantigens in large patient cohorts. For example, in a study analyzing data from The Cancer Genome Atlas (TCGA), the potential immunogenicity of 22,758 missense mutations from 515 tumors across six cancer types was assessed *in silico* [336]. The study found that the number of predicted neoantigens was positively associated with CD8 T cell infiltration and patient survival. Moreover, a study

of endometrial cancers found that high numbers of predicted neoantigens, caused by dysfunctional DNA proofreading, was associated with an increased cytotoxic immune signature and improved survival [337]. These results were corroborated and extended by a study that revealed a positive relationship between mutational load and cytotoxic immune cell signatures within tumors [338]. Interestingly, the authors also found that the frequency of predicted highly immunogenic mutations was lower than expected in some tumor types, raising the possibility that T cells may have exerted selective pressure against tumor cells expressing neoantigens. Furthermore, two complementary retrospective analyses have highlighted the ability of NGS and epitope prediction algorithms to identify validated targets of spontaneously-activated neoantigen-reactive T cells. One study found that epitope prediction correctly identified 87% of published neoantigens [330] (using an IC50 < 500 nM [15]). The second study found that exome sequencing and epitope prediction correctly identified 76 – 82% of published neoantigens [339], demonstrating the high sensitivity of these techniques. However, to identify tumor neoantigens prospectively, predicted neoantigens must still undergo empirical validation.

NGS to identify neoantigens

Despite current limitations of epitope prediction and processing algorithms, studies have used NGS to identify neoantigens in several tumor types, and increasing evidence points to neoantigens underlying the success of several immunotherapies.

Neoantigen and checkpoint blockade therapy

Several lines of evidence suggest that neoantigens are the targets underlying effective anti-tumor T cell responses induced by immune checkpoint blockade. For example, patients with tumor types that harbour large mutational burdens, such as melanoma and NSCLC, experience the highest response rates to PD-1 blocking antibodies [331,340]. Moreover, patients with colorectal cancers harboring mismatch repair defects and correspondingly large mutation burdens responded more favorably to immune checkpoint blockade than patients with fewer tumor mutations [341]. Additionally, patients with melanoma with high mutational loads respond more favorably to Ipilimumab [332] and PD-1 blocking therapies than patients with melanomas harboring fewer mutations [331]. These results were extended in a study demonstrating that an increased number of “clonal

neoantigens" (i.e. neoantigens present within all cells in a tumor) was associated with clinical response to checkpoint blockade, whereas a high subclonal-mutation count was associated with poor survival [342]. Further evidence for the role of neoantigen-specific T cells in checkpoint blockade therapy was provided by a study of a murine sarcoma model [343]. After treating tumor-bearing mice with either PD1 or CTLA4 blocking antibodies, NGS was used to identify two neoantigen-specific T cell responses in TIL. The neoantigen-specific T cells were activated strongly by checkpoint blockade and mediated a potent anti-tumor effect *in vivo* [343]. Finally, in a case report of a melanoma patient who responded well to Ipilimumab, T cell responses against two neoantigens expanded five-fold during Ipilimumab treatment in step with the clinical response to therapy [344]. These studies support the hypothesis that neoantigens are key T cell targets underlying effective checkpoint blockade. Potentially, the number of mutations within a tumor could stratify patients and identify who would respond best to these treatments, though defining cutoffs would be challenging (Illustration 3).

Neoantigens in adoptive cell therapy (ACT)

Several studies suggest neoantigens are critical targets of successful TIL-ACT trials in melanoma patients. These studies involved whole exome sequencing of tumor samples and screening of *ex vivo* expanded TIL for recognition of tumor specific mutant peptides or minigenes. In a study of three melanoma patients who responded favorably to ACT [345], NGS identified 264 to 574 non-synonymous mutations per case, and TIL were found to recognize two to three neoantigens in each patient. For one patient, neoantigens accounted for the majority of the tumor-specific T cell response, suggesting that neoantigen-specific T cells may have been responsible for the clinical response. In another study by the same group, NGS was used to identify neoantigen-specific T cell responses in two patients who had achieved durable responses to ACT [346]. Previously, conventional cDNA screening methods on the same TIL product had overlooked these neoantigens, indicating that NGS methodologies may be more sensitive for identifying neoantigens than other methods. Moreover, another study interrogated CD4 T cells from two patients who responded favorably to ACT [347] and found that neoantigen-specific CD4 T cell responses comprised a substantial proportion of the ACT product. Furthermore, two studies have identified expanded, neoantigen-reactive T cells within melanoma patient peripheral blood using

tandem minigenes [348] or neoantigen specific tetramers [349]. Together, these findings suggest that neoantigen-specific T cells are often present in melanoma patients and may be important mediators of successful ACT in this disease.

Similar approaches have been applied to identify and target neoantigens in other types of cancer with varying levels of success. In one study, neoantigen-specific CD8 T cell responses were detected in peripheral blood from two Chronic Lymphocytic Leukemia (CLL) patients who achieved long-term remission following allogeneic hematopoietic stem cell transplantation [350]. Other studies have directly targeted neoantigens with ACT (Illustration 3), as illustrated by a case report involving a patient with metastatic cholangiocarcinoma [101]. The patient received ACT and experienced tumor stabilization for 13 months. NGS revealed that approximately 25% of the TIL product used for ACT was comprised of a neoantigen-specific CD4 T cell clone recognizing a point mutation in the putative driver gene ERBB2IP. Once the tumor progressed, a near clonal population of mutation-specific T cells was selected for infusion. Subsequently, the patient experienced tumor regression without new tumor growth for at least 6 months after ACT. In contrast to this successful case study, an expanded study by the same group targeted 10 gastrointestinal tumors and identified 18 neoantigen-specific CD4 or CD8 TIL (range = 0 - 3 per case) [351]; however, treatment with TIL products enriched for mutation reactive T cells failed to prolong progression-free survival for most patients [351]. While the cholangiocarcinoma patient was successfully treated with neoantigen-specific T cell clones that recognized a driver mutation (in ERBB2IP), the patients in the follow-up study were treated with neoantigen clones that recognized mostly passenger mutations, indicating that neoantigen-based immunotherapies may be most successful when targeting driver mutations. Notably, the follow-up study did not assess neoantigen-specific T cells recognition of tumor cells; therefore, lack of tumor cell recognition is an alternative explanation for the failure of neoantigen-specific T cells to mediate tumor control [351].

Pre-clinical and clinical neoantigen-targeted vaccines

For mutations to be of general utility as vaccine targets, a reasonable proportion must give rise to *bona fide* MHCI or MHCII binding epitopes. However, at present there is very little information regarding the proportion of mutations that meet this criterion. In the

aforementioned studies involving TIL, ≤ 1% of tumor mutations elicited T cell responses [344,345,347,350]. However, these studies were designed to detect only pre-existing T cell responses. What has yet to be quantified systematically is the proportion of mutant peptides that are presented by MHCI or MHCII but ignored by the immune system. Immune monitoring in clinical trials has shown that vaccination can induce *de novo* T cell responses to mutations in genes such as BCR-ABL, P53, and RAS [327,352-357], lending support to the notion that neoantigens can be ignored by the immune system in the absence of intervention. Thus, an important area for research is to develop methods to predict, quantify, and therapeutically target neoantigens that evade spontaneous immune recognition.

With NGS, one can expand the number of targets for vaccines beyond shared mutations such as mutant RAS or BCR-ABL to the entire complement of somatic mutations in an individual's tumor. Thus, a compelling use of NGS is to guide the design of personalized, neoantigen-specific therapeutic cancer vaccines. This approach has been applied in preclinical settings. In one such study, NGS of the melanoma murine model B16 identified 962 mutations, of which 50 with favorable epitope prediction and expression levels were targeted with peptide vaccines [358]. Two of these peptide vaccines extended the survival of mice bearing established B16 tumors. The authors subsequently extended these results and found that neoantigen specific CD4 helper T cells were important mediators of the anti-tumor responses, and combining several mutant targets in a single vaccine improved survival of tumor-bearing mice [238]. Additional studies have demonstrated the efficacy of mutation-specific peptide vaccines in mouse models of colon cancer and carcinogen-induced sarcoma [314,315,343].

Based on these pre-clinical successes, at least two personalized neoantigen-targeted trials using either mutant RNA or mutant peptides as antigens are currently recruiting patients with melanoma, a highly mutated cancer type [359,360]. Additionally, the first NGS-based neoantigen vaccine trial was recently published and involved three metastatic melanoma patients [354]. Nine mutated peptides were found to induce activation of neoantigen-specific CD8 T cells. These T cell responses fell into three categories: (1) those detected prior to vaccination and subsequently expanded, (2) those detected only after vaccination, and (3) those activated towards mutations that were not naturally processed and, therefore, not useful for immunotherapy. These data demonstrate that neoantigen-specific T

cells can be activated by vaccination in cancer patients [354]; however, no data on patient outcomes has yet been published.

Concluding remarks about neoantigens

As NGS plays an increasing role in the care of cancer patients, opportunities will arise for the rational design of targeted immunotherapies (Illustration 3). Already, NGS has helped researchers discover that neoantigen-specific T cell responses are implicated in the efficacy of checkpoint blockade and ACT. Building on these early findings, one can envision several clinical applications in the near term, including (1) stratifying patients for checkpoint blockade based on the number of predicted neoantigens in tumors; (2) determining the effective dose and duration of checkpoint blockade by tracking neoantigen-specific T cell responses over time; (3) generating neoantigen-specific T cell products for ACT [101]; and (4) designing personalized vaccines encoding predicted neoantigens [354] (Illustration 3). Of these, neoantigen-specific vaccines seem poised to be the most feasible in the immediate future due to the simplicity of generating GMP quality reagents. However, the paucity of studies investigating human cancers with fewer mutations than highly mutated melanoma is a major impediment for the broad implementation of this type of therapy. Moreover, the pre-clinical neoantigen-specific vaccines studies to date have targeted tumors containing anywhere from 949 to 4285 nonsynonymous mutations [238,314,343,358]. In contrast, human tumors contain a median of only 44 non-synonymous mutations [303], raising the question of whether tumors with intermediate to low mutation burdens are amenable to neoantigen-targeted vaccination. As discussed next, ovarian cancer is a common, clinically challenging malignancy that may illustrate both opportunities and challenges associated with targeting neoantigens.

1.6 Ovarian cancer

High grade serous ovarian carcinoma (HGSC) is the most common histological subtype of ovarian cancer, and long-term survival rates have not improved beyond 30-40% for the last 30 years [5]. Thus, HGSC is a disease in dire need of new therapeutic options. It has an intermediate mutation burden, and extended patient survival is strongly associated

with TIL [6]; thus, HGSC is a compelling disease for testing the applicability of neoantigen-targeted vaccines in malignancies with intermediate mutation loads.

HGSC incidence and treatment

Of all ovarian cancers, HGSC is the most common subtype. Worldwide, the incidence of HGSC is 190,000 per year, and it accounts for 114,000 deaths annually [361]. The disease is usually diagnosed as a stage III or IV malignancy, resulting in high mortality rates. Several lines of evidence point to the distal fallopian tubes as the cellular source of most HGSC cases [279,362], though genetic mutations in cells of the ovary can also lead to malignancy [363]. At diagnosis, about a third of HGSC patients present with ascites, a peritoneal fluid accumulation that often contains tumor cells, Cancer Associated Fibroblasts (CAFs) and immune cells [364]. Ascites samples are often drained by paracentesis to improve patient comfort. Treatment typically involves surgical debulking and platinum based chemotherapy in either the adjuvant or neoadjuvant setting, to which most HGSC tumors are highly responsive. Unfortunately, 80 – 90% of HGSC recur and eventually develop chemotherapy resistance [5].

Genetics of HGSC

In contrast to highly mutated malignancies such as melanoma, HGSC harbors a median of only 40 missense mutations per tumor [365], placing it very near the median for human cancers [303]. P53 is nearly ubiquitously mutated among HGSC cases, but no other gene is mutated in > 15% of HGSC cases [366]. Rather than point mutations, it is a disease that is associated with chromosomal instability, with DNA losses and gains a common characteristic [367]. In 50% of HGSC patients, this phenotype is due to disruption of homologous recombination DNA repair proteins – most often BRCA1 or BRCA2 – through mutations or transcriptional silencing [368]. HGSC is characterized by a high degree of intratumoral heterogeneity, which arises early during disease progression [369]. Using micro-arrays, two separate groups have identified four molecular subtypes of HGSC: C1/mesenchymal, C2/immune, C4/differentiated, and C5/proliferative [366,370]. When assessed by IHC, it was shown that C2/immune and C4/differentiated tumors contained a large proportion of intraepithelial TIL, and patients with the C2/immune subtype experienced

extended survival [370]. The inter- and intra-tumoral heterogeneity of HGSC make this disease a particularly attractive target for personalized oncology, including immunotherapy.

Immune responses to ovarian cancer

Several studies have implicated immunity as an important factor in HGSC, and further studies attempted to harness the immune system to fight this disease. Similar to other cancers, in HGSC, the presence of tumor-infiltrating CD3 T cells and CD8 T cells is associated with survival [6,371], which has inspired efforts to develop immune-based treatments [372]. A phase II clinical trial of a PD-1 blocking antibody for platinum resistant HGSC patients resulted in a modest objective response rate of 15% and a disease control rate of 45% [373]. These response rates are substantially lower than rates seen in melanoma and lung cancers [176,374], indicating that other treatment modalities are needed. Additional PD-1 and PD-L1 blocking antibody trials are ongoing [375]. Several candidate target antigens have been identified, including p53 [376], WT-1 [377], NY-ESO-1 [378,379], mesothelin [380], and folate receptor [381]. Unfortunately, clinical anti-cancer vaccines targeting HGSC have shown limited benefits.

Probably the most highly investigated target in HGSC is the CT antigen NY-ESO-1. When assessed by IHC, NY-ESO-1 protein was present in 43% of HGSC tumors [382]. Further, 30% of HGSC patients generated an antibody response to NY-ESO-1, indicating immune activation towards this antigen [382]. Based on these findings, several different vaccination strategies targeting NY-ESO-1 have been tested. One group used heterologous prime/boost with viral vectors, which activated CD8 and CD4 T cells in 46% and 91% of patients respectively. T cell responses associated with improved overall survival compared with patients who failed to mount NY-ESO-1 specific T cell activation [378]. Furthermore, vaccines with overlapping SLP encompassing most of the NY-ESO-1 protein mixed with poly(I:C) in Montanide elicited robust T cell responses capable of recognizing APCs pulsed with NY-ESO-1 protein [378]. One challenge with targeting this antigen has been that 66% of NY-ESO-1 expressing tumors displayed a heterogeneous, mosaic expression pattern [382], which led to outgrowths of antigen loss variants [383]. To overcome this, one group used DNA methyl transferase (DNMT) inhibitors to promote expression of NY-ESO-1 on

the tumor. When DNMT was used in conjunction with a vaccine comprised of NY-ESO-1 protein, Montanide, and GM-CSF, disease stability was achieved in 50% of patients [384].

To date, each of the antigens targeted in ovarian cancer vaccines represents a self-antigen, which suffers from issues of immunological tolerance, autoreactivity, or heterogeneous expression. Treating HGSC with neoantigen-specific vaccines potentially surmounts these obstacles and may result in beneficial outcomes.

1.7 Thesis objectives

Neoantigens are attractive targets for rationally designed anti-tumor vaccines for several reasons: (1) Neoantigens are tumor-restricted and may be recognized by high-affinity T cells; (2) neoantigen-targeted vaccines have successfully extended the survival of mice bearing highly mutated tumor models [314,343,358]; and (3) several studies indicate that neoantigens may underlie successful immunotherapy in humans with highly mutated tumor types [331,332,385]. However, it is unknown whether neoantigen-targeted anti-tumor vaccines can effectively treat ovarian cancers, which have lower mutation burdens and are thought to be less immunogenic than melanoma.

The overall goal of my research was to investigate the concept of treating ovarian cancer using therapeutic vaccines targeting neoantigens. My thesis has three aims. **Aim 1**: To develop potent SLP vaccination methods for use in neoantigen-targeted vaccines. **Aim 2**: To identify immunogenic mutations in a mouse model of ovarian cancer, and use mutated SLP vaccines to treat tumor-bearing mice. **Aim 3**: To determine the proportion of somatic mutations that give rise to neoantigens in human HGSC.

Demonstrating that neoantigen-targeted vaccines can eradicate murine ovarian tumors and that neoantigens are present in human HGSC tumors would support further development of neoantigen-targeted vaccines for this cancer type.

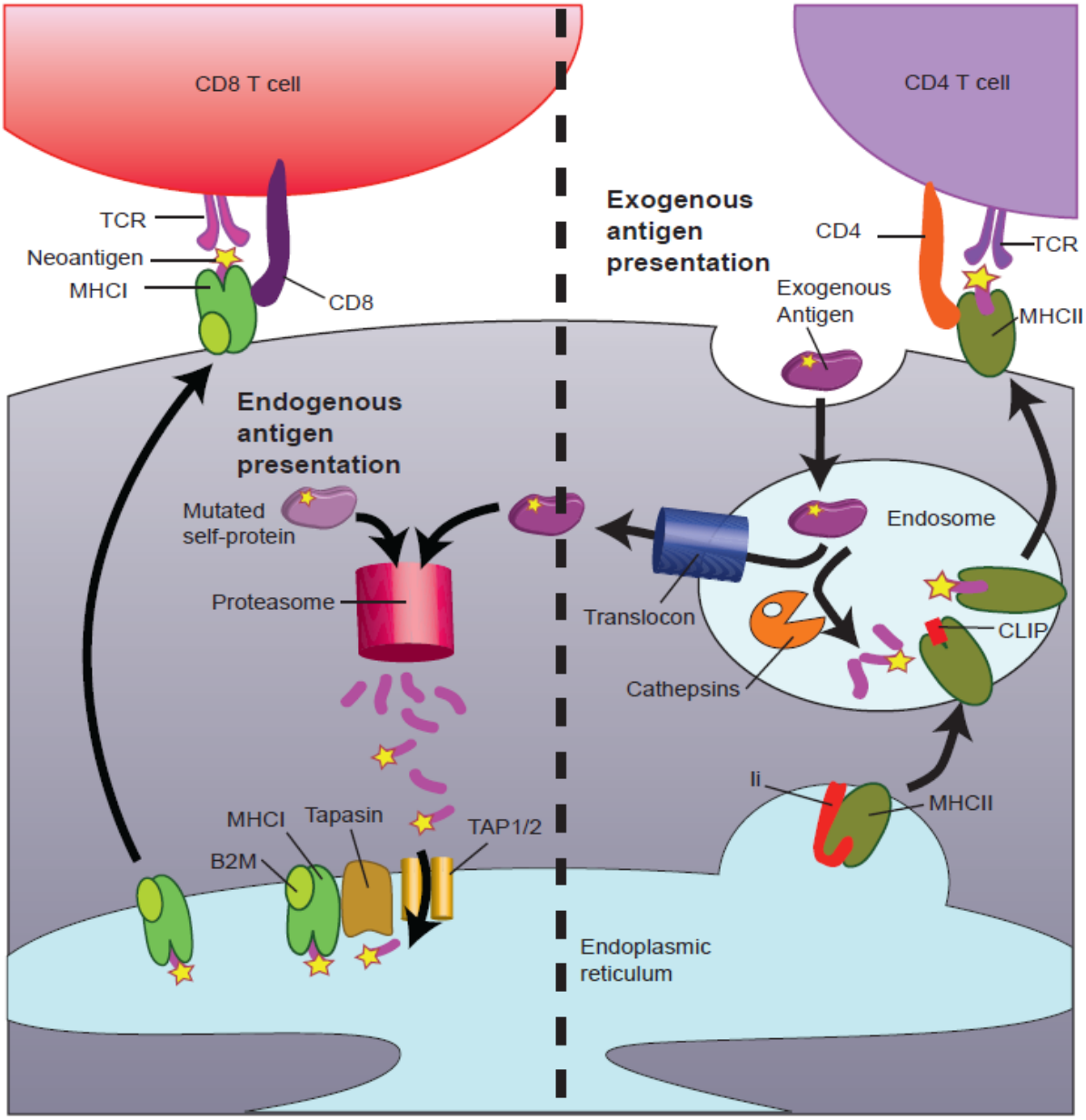

Illustration 1. Endogenous and exogenous antigen presentation.
Endogenous, mutated self-proteins are digested by the proteasome into short peptides. A subset of these peptides is transported into the ER by TAP1 and 2. Tapasin assists loading of appropriate peptides into MHCI. The loaded MHCI/peptide/B2M complex is shuttled to the cell surface where it can be interrogated by the TCR on CD8 T cells. APCs can endocytose exogenous antigens, which enter endosomes. The antigen can be retrotranslocated into the cytosol by translocons, enter the endogenous antigen presentation pathway, and be cross-presented to CD8 T cells. Alternatively, the antigen can be digested in the endosome by cathepsins into short peptides. Peptides that bind to MHCII with sufficient affinity can replace CLIP in the MHCII peptide binding groove. The MHCII/peptide complex is transported to the cell surface for interrogation by TCR on CD4 T cells.

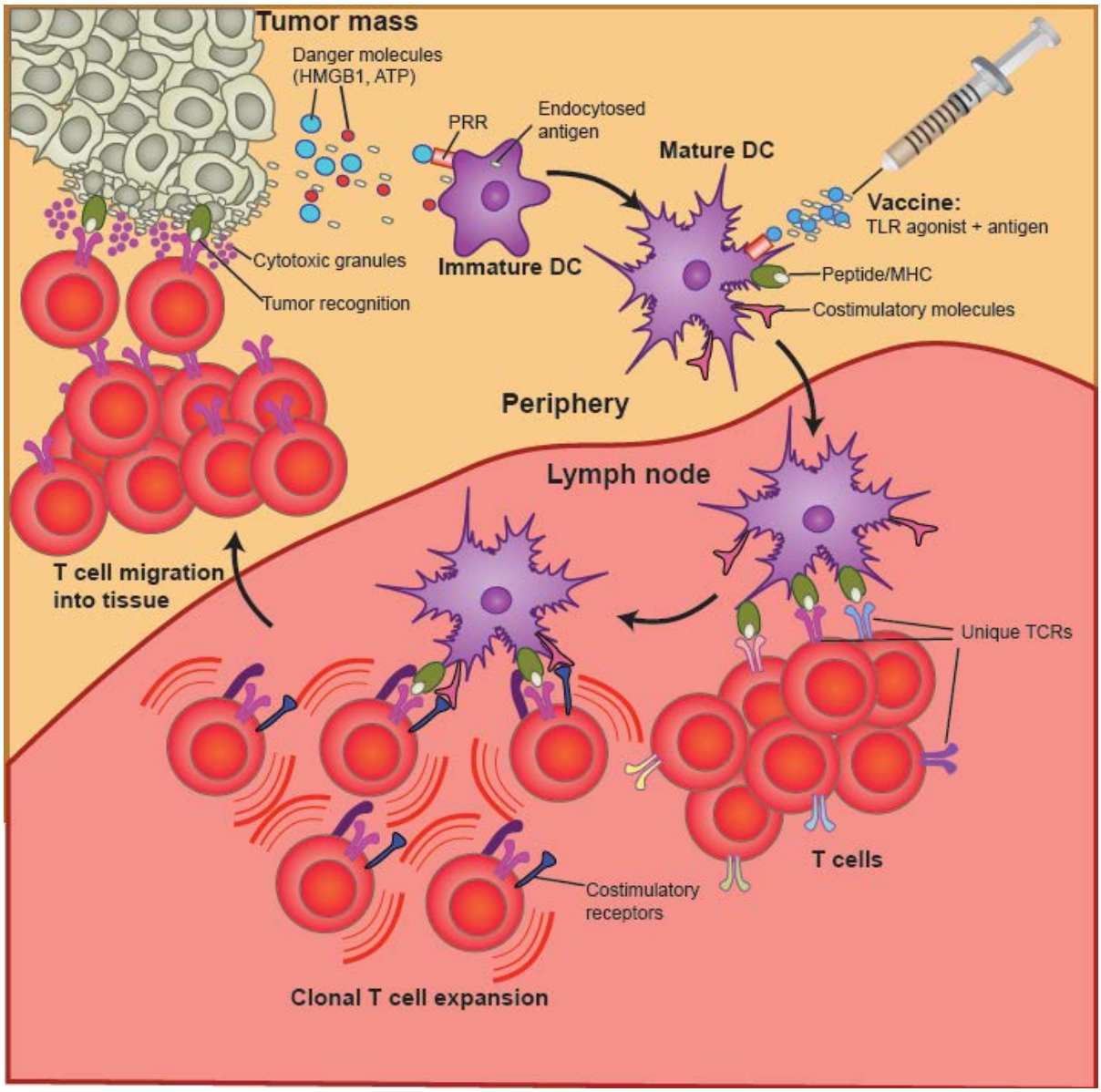

Illustration 2. Tumor antigen-specific T cell activation and tumor killing.
Necrotic tumor cells release DAMPs and tumor antigens into the extracellular milieu. Tumor antigens are endocytosed by immature DCs, and DAMPS bind to PRR on the DC, causing DC maturation. Alternatively, tumor antigens and danger signals (often TLR agonists) are delivered in a vaccine to cause DC maturation and antigen presentation. Mature DCs upregulate T cell costimulatory molecules, process endocytosed antigen, present processed peptide/MHC on the cell surface, and migrate to the draining lymph node. Naive T cells, each with a unique TCR, scan the DC with the TCR receptor. Once a TCR binds peptide/MHCI with high enough avidity, the T cell becomes activated. It clonally proliferates, differentiates into CTL, and migrates out of the lymph node and into inflamed tissue (towards the tumor). In the tumor microenvironment, each T cell scans tumor cells and once the TCR binds cognate peptide/MHC, the T cell releases cytotoxic granules and kills the tumor.

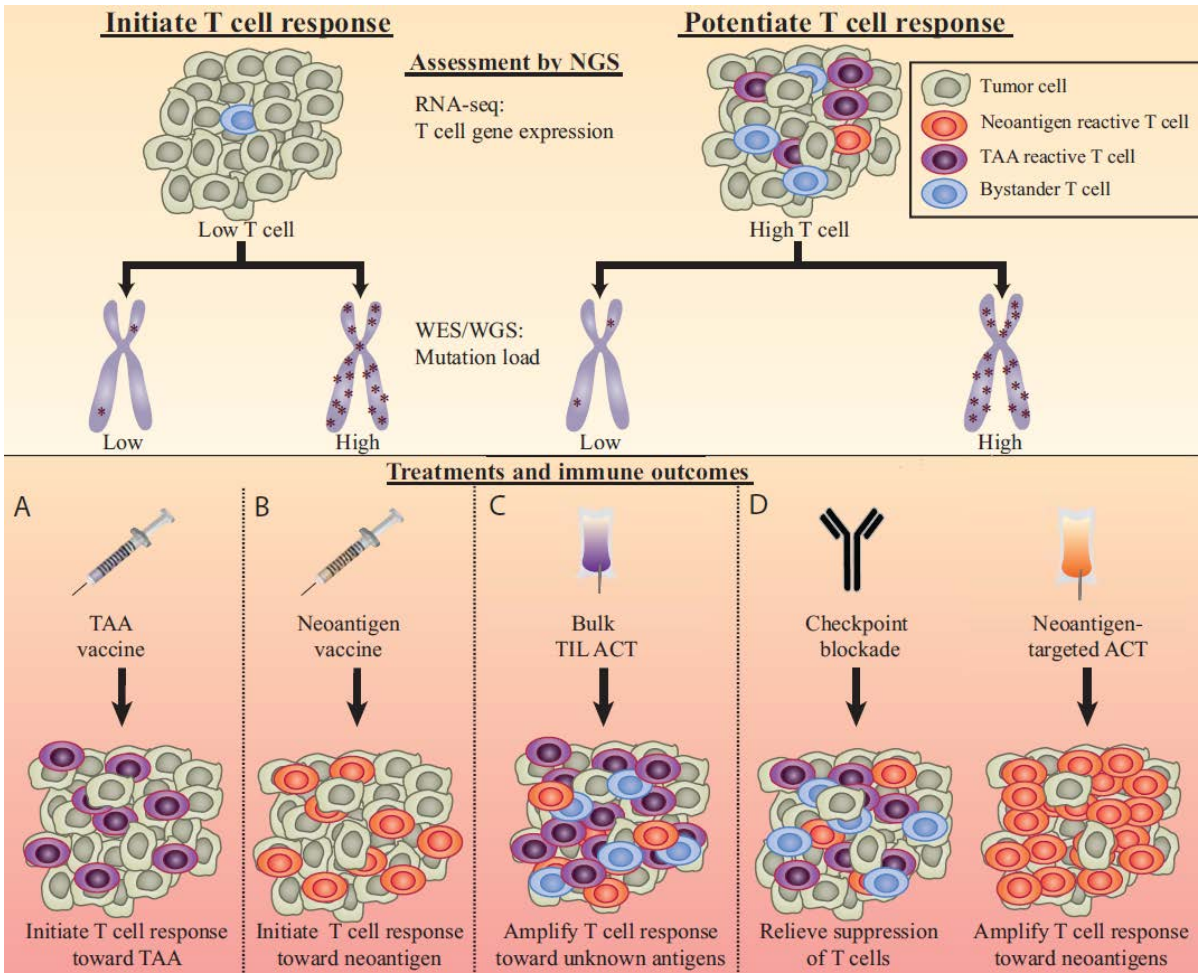

Illustration 3. Proposed use of NGS data to personalize immunotherapy.
(This is a pre-copyedited, author-produced PDF of an article accepted for publication in *Annals of Oncology* following peer review. The version of record [386] is available online at: **http://annonc.oxfordjournals.org/content/26/12/2367.long**) The goals of immunotherapy are to either potentiate pre-existing anti-tumor T cell responses or initiate anti-tumor T cell responses, if anti-tumor immunity is low. The level of pre-existing tumor immunity can be assessed by measuring the level of T cell markers in RNA-seq data [338]. The total mutation load can be determined using whole genome or whole exome sequencing (WGS/WES). A) Patients with low T cells and low mutation load may benefit most from personalized tumor associated antigen (TAA) specific vaccines to activate T cells towards highly expressed TAA, which can be identified using RNA-seq data. B) Patients with low T cells and a high mutation load may benefit most from neoantigen-specific vaccines. C) Patients with high T cells but a low mutation load may benefit most from standard ACT, to amplify intratumoral T cells against undefined antigens. D) Patients with high T cells and high mutation load may benefit most from either checkpoint blockade, to relieve T cell suppression, or neoantigen-targeted ACT, to amplify the mutation reactive T cell response. Combination therapies can also be used.

Chapter Two: Improving long-peptide vaccines for cancer therapy

2.1 Introduction

Although Synthetic Long Peptides (SLP) have proved superior to minimal peptides as vaccine antigens, SLP vaccination rarely achieves rapid and robust antigen-specific T cell activation. SLP have many favorable characteristics for targeting tumor-specific mutations: (1) SLP can be produced to very high purity; (2) SLP pools can be generated quickly to make personalized vaccines; (3) they may contain CD4 and CD8 T cell epitopes; and (4) they effectively target dendritic cells for cross-presentation. However, SLP vaccines often elicit weak primary T cell responses (responses to the first vaccination) compared those elicited by viral and bacterial infections, demonstrating that current SLP vaccines are suboptimal. Adding Toll-Like Receptor (TLR) agonists to peptide vaccines improved T cell activation, and "prime-boost" strategies (first a "prime" immunization followed by one or more "boost" immunizations at later time points) dramatically increase peak secondary T cell responses [252,387]. However, the responses often take weeks to evolve [269] and tumors may progress during that time. Moreover, a slowly evolving T cell response can cause tumors to upregulate immune suppressive molecules [388]. In contrast a potent primary T cell response can overwhelm the tumor and induce tumor rejection [388]. Thus, optimizing SLP vaccination methods to elicit potent primary T cell responses could lead to improved anti-tumor efficacy.

One of the variables leading to lower primary T cell responses to peptides compared to viral infection could be the time that the antigen and adjuvant are present *in vivo.* In the work described here, I examined T cell responses to modified vaccination schedules. I hypothesized that shortening the intervals between prime and boost could mimic a viral infection and lead to improved T cell responses to soluble SLP and protein vaccines.

Most SLP vaccine protocols have used long interval prime-boost schedules and were mixed in oil emulsions that release antigen slowly [389,390]. However, as described extensively in Chapter 1, vaccines delivered in oil emulsions led to T cell anergy, T cell mislocalization [251], and sub-optimal anti-tumor effects [187]. This motivated investigation of prime-boost vaccines that incorporated SLP and the TLR agonist poly(I:C) in PBS.

Studies showed that SLP plus poly(I:C) vaccines solubilised in PBS activated more antigen specific T cells compared to SLP plus poly(I:C) in oil emulsions [269]. However, vaccinations in PBS increased T cell responses only after boosting [269]; T cell responses were undetectable after the prime and prior to the boost [269]. Unlike oil emulsions, PBS does not act as an antigen depot. Therefore, peptide and poly(I:C) in PBS were quickly eliminated from the vaccine site, thereby reducing the primary T cell expansion to soluble vaccines. Potentially, vaccines delivered in PBS could elicit superior T cell responses if the antigen and adjuvant persisted at the site of injection.

Murine studies provide numerous lines of evidence indicating that the duration of antigen presentation by mature APCs is a critical factor for generating robust primary T cell expansion. For example, *in vitro* studies showed that optimal T cell expansion occurred when T cells were exposed to antigen and co-stimulation for at least 2 days and received stimulating cytokines for three days [391]. Furthermore, in a study that used ampicillin to limit the duration of a *L. monocytogenes* infection to 24, 48, or 60 hours, significantly fewer antigen specific CD8 T cells were activated in mice experiencing abbreviated infections [392]. Mechanistically, the studies showed that elimination of the bacterial infection decreased the expression of the costimulatory molecules CD80 and CD86 on DCs, causing reduced activation of T cells [392]. Furthermore, antibodies blocking the interaction between TCR and peptide/MHC at either one, two, or three days post infection led to significantly fewer antigen-specific CD4 and CD8 T cells in the primary expansion, indicating that antigen presentation for at least three days was required to fully activate T cells [393]. Moreover, a study that investigated *in vitro* primed OTI T cells (from transgenic mice that express a single TCR recognizing the model antigen ovalbumin (OVA)) transferred into naive recipient mice found that continued exposure to antigen and inflammatory signals (provided by a model virus Lymphocytic Choriomeningitis (LCMV) expressing OVA) was necessary for full T cell expansion [394]. However, in mice vaccinated with soluble peptide and the TLR agonist CpG, antigen presentation and upregulation of CD80, CD86 and CD40 on DCs was significantly reduced two days after vaccination [395]. Together, these studies indicate that antigen presentation on activated DCs for at least three to four days is necessary for optimal primary T cell expansion, yet soluble peptide and TLR agonist vaccines provide antigen and DC stimulation for two days or less.

Another consideration when developing peptide vaccines is whether CD4 help is necessary for CD8 T cell expansion. As discussed in Chapter 1, CD4 T cells can licence dendritic cells and cause them to continue to express co-stimulatory molecules, and CD4 T cells are required to establish long lived memory CD8 T cells [396]. To induce a CD4 T cell response that augments CD8 T cell expansion and memory formation, some vaccine studies have added the PAn DR Epitope (PADRE), which binds to many human and mouse MHCII alleles. One study showed that inclusion of the PADRE epitope in a SLP plus CpG vaccine caused a slight increase in responding T cells and a modest, non-significant improvement in survival after tumor challenge [397]. Another study found that mixing the E7-epitope (from HPV) and PADRE peptides resulted in slightly improved survival of tumor bearing mice compared to E7 peptide vaccination alone [398]. A third study added the PADRE antigen to a virus like particle encoding the E7 epitope to treat tumor bearing mice and found a slightly increased survival compared to mice that received the vaccine without the PADRE epitope [399]. Each of the above studies showed only a modest improvement in responses when a CD4 helper epitope was included in the vaccination, and it was unclear whether CD4 help was required for robust CD8 T cell proliferation in response to long peptides and TLR agonist vaccination.

Here, I tested multiple variations of SLP and protein vaccines for activating large numbers of antigen-specific T cells and inducing tumor regression. First, repeated close-interval vaccinations were compared to fewer inoculations for activating large numbers of CD8 T cells. Second, the optimal time period between prime and boost was assessed for inducing secondary expansion of CD8 T cells. Third, a vaccine combining a CD4 targeted- and a CD8 targeted-SLP was compared to vaccinating with a CD8 SLP alone. Daily vaccinations on four consecutive days led to significantly increased numbers of antigen specific CD8 T cells compared to fewer inoculations. Also, a second round of vaccinations 21 days after the initial four inoculations boosted the T cell responses. Additionally, I found that T cell responses to an SLP vaccine encompassing a CD8 T cell epitope were not enhanced when co-administered with an SLP encompassing a CD4 T cell epitope. Furthermore, co-administration of the two SLP vaccines failed to augment clearance of antigen expressing tumor cells. The results presented here provide a framework for

developing high potency SLP vaccines to target tumor specific mutations discussed in Chapter 3.

2.2 Methods

Mice and E.G7 cell line

C57BL/6 mice were purchased from Jackson Labs and maintained under specific pathogen-free conditions. All mouse protocols were approved by the Animal Care Advisory Committee at the University of Victoria, following Canadian Council for Animal Care guidelines. All experiments involved six to 12 week old mice. E.G7 tumor cells were grown in complete RPMI + HEPES (Gibco: 22400-089) supplemented with 10% FBS (Gibco: 12483-020), 2mM L-glutamine (Hyclone: SH30034.01), 100U/ml Penicillin and 100µg/ml Streptomycin (Hyclone: SV30010), 50 µm β-mercaptoethanol (Sigma: M6250), and sodium pyruvate (Hyclone: SH30239.01).

Peptides and Vaccinations

Six to twelve week old C57BL/6 mice were anesthetized and subcutaneously inoculated in the flank using a 27 gauge needle. Each inoculation was composed of 50 µg of SLP (ProImmune) (long-SIINFEKL: PDEVSGLEQLESIINFEKLTEWTSSNVME, long-OT-II: SAESLKISQAVHAAHAEINEAGREVVGSA, or long-Spas1-mut: VTRLLLEGISSTHVNHLHCLHEFVKSQTT) or 100 µg of chicken ovalbumin (OVA) (Sigma: cat# A5503) and 10 µg poly(I:C) (Amersham: 27-4732) admixed to a total of 300 µl in sterile PBS (Gibco: 20012-027). When two peptides were inoculated together, 50 µg of each peptide was added to 10 µg of poly(I:C) in sterile PBS to a total of 300 µl. For therapeutic vaccination experiments, mice received daily vaccinations for four consecutive days once the E.G7 tumors reached 36 mm^2 as measured by caliper.

IFN-γ ELISPOT

In accord with MIATA guidelines [400], ELISPOT assays were performed using validated, standard operating protocols. Mice were euthanized using isofluorane, and spleens were immediately processed into single cell suspensions by pressing through 100 µm screens in complete RPMI (RPMI + HEPES supplemented with L-glutamine, β-mercaptoethanol,

penicillin and streptomycin, sodium pyruvate and 10% FBS). Red blood cells were lysed using ACK lysis buffer, and fresh splenocytes were counted on a Guava cytometer using Viacount (Cat#: 4000-0130). Splenocytes were diluted to 9 x 10^6 live cells/ml (usually between 75 – 85% of splenocytes were viable) in complete RPMI. ELISPOT plates (MSIP, Millipore: MSIPS4W10) were coated with 10 µg/ml of anti-mouse IFN-γ (mAb AN18, Mabtech: 3321-3-1000) capture antibody and incubated overnight at 4°C. Plates were washed and blocked for 2 hours at 37°C, 5% CO_2 with complete RPMI. Within 2 hours of sacrificing mice, 9 x 10^5 live, processed splenocytes were added to each well and stimulated with 5 µg of the minimal peptide epitopes (for long-SIINFEKL, minimal peptide SIINFEKL was used, for the long OT-II, minimal peptide ISQAVHAAHAEINEAGR was used, and for long-Spas1-mut, minimal peptide STHVNHLHC was used), media alone, or 5 µg/ml Concanavalin A (Sigma: C5275) as positive control. Cultures were incubated for 20 hours at 37°C and 5% CO_2. Plates were washed, 1 µg/ml of secondary antibody (biotinylated anti-IFN-γ: mAbR4-6A2, Mabtech: 3321-6-250 was added, and plates were incubated for 2 hours at 37°C. Plates were developed using Vector Labs' Vectastain ABC Elite kit (Cat#: PK-6100) and Vectastain AEC substrate reagent (Cat#: SK-4200) according to manufacturer's protocol and scored with an automated plate reader (AID) using preset parameters that have been validated over several experiments.

Flow cytometry

Blood was harvested from the saphenous vein and processed within two hours. Red blood cells were lysed using ACK lysis buffer (Lonza: 10-548E), washed two times and incubated for 30 minutes at 4°C with fixable viability dye-EF780 (0.5 µl/1 ml suspension, eBioscience: 65-0865-18). After 30 minutes, cells were washed and incubated for 30 minutes at room temperature with anti-MHCII-FITC (1/200, eBiosciences: 1250166) and anti-CD8-APC (1/500, eBioscience: 17-0081-83) antibodies and a Kb-SIINFEKL tetramer-PE conjugate (1/40, Beckman Coulter: T03000). Cells were washed two times and analysed on a FacsCalibur flow cytometer. At least 10^5 events were collected and analyzed using FlowJo V7.6.5.

Tumor regression experiments

E.G7 tumor cells were grown in complete RPMI, harvested, and washed three times in sterile PBS. Eight to 12 week old female C57BL/6 mice were inoculated in the right flank with 2 x 10^5 E.G7 tumor cells in 200 µl of PBS. Once tumors reached 36 mm^2 as measured by electronic digital caliper (Fowler Sylvac Ultra-Cal Mark III), mice were vaccinated with SLP and poly(I:C). Tumors were measured daily, and mice were sacrificed once tumors reached 400 mm^2.

2.3 Results

Repeated vaccinations induced robust T cell responses

In an effort to generate T cell responses to protein and peptide vaccines similar in magnitude to acute viral infections, vaccination schedules were modified to mimic the duration of acute viral infection (typically less than six days). To test this concept and empirically determine the optimal number of vaccinations to deliver, mice were vaccinated with poly(I:C) and the model antigen chicken ovalbumin (OVA) protein, an antigen that has been used extensively to examine immunity. Mice were vaccinated on day 0; days 0 and 1; days 0, 1, and 2; or days 0, 1, 2, and 3. For all groups, IFN-γ ELISPOT assays were performed on splenocytes on day 7. Mice that received four consecutive immunizations with OVA protein and poly(I:C) exhibited significantly higher frequencies of antigen-specific T cells (minimal epitope SIINFEKL) compared to mice vaccinated fewer times (Figure 1). The total amount of vaccine delivered did not account for this effect, as mice vaccinated with a single dose of four times the amount of OVA and poly(I:C) elicited smaller T cell responses (Figure 1). This vaccination schedule was dubbed “cluster vaccination”, as it involved a “cluster” of daily “vaccinations” on four consecutive days.

Cluster vaccination using SLP targeting CD8 and CD4 T cells

Cluster vaccination with the protein OVA proved effective for activating large numbers of antigen-specific T cells, but SLP peptides vaccines offer many advantages for targeting neoantigens compared to proteins (as discussed above and in Chapter 1). Therefore, I tested whether cluster vaccination using SLP antigens could activate large numbers of

antigen-specific T cells. Three main questions were critical for translating the cluster vaccination protocol to SLP vaccines: (1) Does cluster vaccination activate more T cells than a conventional single-dose prime/boost vaccination schedule? (2) Can cluster vaccination using SLP activate both CD8 and CD4 T cells? (3) Does co-vaccination with a SLP spanning a known CD4 epitope augment the CD8 T cell response? To assess each of these questions, cluster vaccination was performed using poly(I:C) and different combinations of two 29mer SLP: one SLP ($OVA_{246-274}$: "long-SIINFEKL") spanned a known CD8 T cell epitope (SIINFEKL), and a second SLP ($OVA_{318-346}$: "long-OT-II") spanned a known CD4 T cell epitope (ISQAVHAAHAEINEAGR). As a comparator, control mice were vaccinated with whole OVA protein and poly(I:C), as in Figure 1. Additionally, mice were vaccinated with long-SIINFEKL peptide on days 0 and 7 to assess the magnitude of T cell expansion induced by a conventional prime-boost vaccination schedule. Blood was harvested from mice every two to three days and stained with Kb-SIINFEKL tetramers to assess antigen-specific T cell expansion. A schematic of the vaccination and tissue harvesting schedules is shown in Figure 2a, and an example of tetramer staining is shown in Figure 2b.

Cluster vaccination elicited robust T cell responses to SLP antigens. For example, cluster vaccination with long-SIINFEKL SLP activated antigen-specific T cells to a similar extent as cluster vaccination with OVA protein (Figure 2c). Further, while cluster vaccination with long-SIINFEKL SLP massively expanded antigen-specific T cells, single vaccination with the same peptide resulted in almost no measurable response. However, when the single vaccination was boosted seven days later (single prime/boost), the peak T cell responses on day 15 were similar to those seen with cluster vaccinated mice on day 7 (Figure 2c). To assess whether cluster vaccination could activate CD4 T cells, mice were vaccinated with poly(I:C) and long-OT-II peptide or OVA protein. On day eight after vaccination, splenocytes were harvested and ELISPOT assays were performed using the OT-II epitope ($OVA_{323-339}$) as recall antigen. Cluster vaccination with the long-OT-II peptide activated more $OVA_{323-339}$-specific T cells than vaccination with OVA protein (Figure 2d). Finally, co-immunization with long-SIINFEKL peptide and long-OT-II peptide was tested to determine whether the SIINFEKL specific response would be augmented by a CD4 T cell response. Surprisingly, co-immunization failed to increase the number of SIINFEKL-specific T cells compared to vaccination with long-SIINFEKL peptide alone (Figure 2c). Further,

cluster vaccination with long-OT-II alone activated $OVA_{323-339}$-specific T cells to a greater extent than mice co-vaccinated with long-OT-II and long-SIINFEKL (Figure 2d). In summary, cluster vaccination was effective for activating both CD8 and CD4 T cells towards MHCI and MHCII epitopes, respectively. Moreover, cluster vaccination with SLP elicited T cell responses that were similar in magnitude, but accumulated more rapidly, than single prime/boost regimens. Finally, co-immunization with two SLP (encompassing a CD4 and CD8 T cell epitope) did not improve epitope-specific T cell responses to either peptide; rather, a trend toward lower T cell expansion was observed.

E.G7 tumor treatment with peptide-based cluster vaccination

To determine whether T cell responses activated by SLP cluster vaccination could induce tumor regression, mice harbouring established, OVA-expressing tumors (E.G7) were therapeutically vaccinated with various SLP regimens. Mice bearing subcutaneous E.G7 tumors (approximately 36 mm^2) were subjected to (1) cluster vaccination with long-SIINFEKL SLP alone, (2) cluster vaccination with long-SIINFEKL SLP and long-OT-II SLP, (3) cluster vaccination with long-OT-II SLP alone, or (4) single dose priming/boost vaccination with long-SIINFEKL SLP. Poly(I:C) was included in all inoculation. Tumors in mice that received single prime-boost with long-SIINFEKL or cluster vaccination with long-OT-II alone responded with a short period of disease stabilization followed by tumor progression (Figure 3). Tumors in mice that received cluster vaccination with long-SIINFEKL SLP and long-OT-II SLP responded with an acute tumor regression followed by tumor progression (Figure 3). However, whereas complete responses were not observed in any other group, cluster vaccination with long-SIINFEL SLP alone caused complete regression of E.G7 tumors in 3/5 mice (Figure 3). Thus, in contrast to a conventional prime-boost strategy, cluster vaccination with long-SIINFEKL SLP activated CD8 T cell responses of sufficient magnitude and immediacy to eradicate established E.G7 tumors. This response was not enhanced – and may have been hindered – by the addition of a long peptide (long-OT-II) encompassing a known, tumor specific CD4 helper epitope.

Timing of cluster boosting

In preparation for therapeutic vaccinations using mutant epitopes of potentially weak immunogenicity, the feasibility of boosting cluster vaccinated T cells using a second round of inoculations was assessed. Accordingly, mice that had been vaccinated with poly(I:C) and (1) long-SIINFEKL SLP, (2) OVA protein, or (3) long-SIINFEKL SLP and long-OT-II SLP were boosted on days 21 – 23 after the first immunization with a second cluster vaccination involving the same antigens. CD8 T cell responses were measured in peripheral blood using a Kb-SIINFEKL-tetramer. Strikingly, a substantial secondary expansion of antigen specific T cells was observed in mice cluster-primed and cluster-boosted with long-SIINFEKL SLP (Figure 4a). In contrast, the primary and secondary expansions of antigen-specific T cells were similar when mice were cluster-prime and cluster-boosted with OVA protein or with a combination of long-SIINFEKL and long-OT-II SLPs (Figure 4).

To determine the optimal time interval between cluster-prime and cluster-boost, mice were cluster-primed with long-SIINFEKL on days 0 – 3 and cluster-boosted on either days 4 – 7, 7 – 10, 14 – 17, or 21 – 23. Peripheral blood was harvested from mice every two days and assessed by Kb-SIINFEKL tetramer. The cluster boosts increased the frequency of antigen-specific T cell above the cluster-prime only when the boost was initiated on day 21 (Figure 5a). Furthermore, cluster boosting at early time points (e.g. days 4 – 7) caused a highly significant decrease in the number of antigen-specific T cells at day 7 compared to mice that did not receive a cluster boost (Figure 5b). These data suggest that vaccine activated T cells require at least 21 days after the cluster prime to form memory T cells capable of a secondary expansion, and continuous daily vaccinations beyond four days leads to blunted peak T cell responses.

Cluster-prime/cluster-boost with a neoantigen-encoding peptide

Cluster-prime and cluster-boost activated large numbers of SIINFEKL-specific T cells. However, SIINFEKL is an uncommonly high affinity epitope that may not be representative of cancer antigens in general. Thus, it was unknown whether this regimen would be broadly applicable to other antigens, in particular neoantigens. Therefore, I assessed the T cell response to cluster-prime/cluster-boost with an SLP encompassing a known neoantigen from the Spas1 protein (found in the TRAMP-C2 mouse prostate tumor

model [401]) (long-Spas1-mut). Male mice were vaccinated on either (1) days 0 - 3 and days 21 – 23 (cluster-prime/cluster-boost), or (2) days 21 – 23 only (cluster-prime). Mice were sacrificed on day 28, and IFN-γ ELISPOT assays were performed on splenocytes. Cluster-prime and cluster-boost activated significantly more neoantigen-specific T cells compared to cluster-prime alone (Figure 6). Though the cluster-prime/cluster-boost vaccination schedule was not used to assess tumor control, the technique was effective for activating large numbers of T cells towards SLPs encompassing both a model antigen (SIINFEKL) and a tumor neoantigen (mutated Spas1).

2.4 Discussion

To induce regression of established mouse tumors using neoantigen-targeted SLP, vaccinations strategies should elicit immediate, robust, antigen-specific T cell responses, typically observed in response to viral or bacterial infections. As described here, repeated, daily inoculations of SLP and poly(I:C) may have mimicked a viral infection and elicited immediate and potent anti-tumor T cell responses. Repeated, close interval vaccinations for four days resulted in increased numbers of antigen activated CD8 T cells compared to fewer vaccinations. Further, a second round of SLP vaccinations boosted the T cell response when the delay between cluster prime and cluster boost was 21 days, and this timing was adequate for boosting both model antigen (SIINFEKL) and neoantigen specific CD8 T cells. Additionally, inclusion of an SLP encompassing a known CD4 epitope failed to augment the primary activation of CD8 T cells, secondary boost of CD8 T cells, or tumor control. The results here corroborate several studies showing that full activation of antigen specific T cells requires *in vivo* antigen and adjuvant exposure for at least four days [392-394]. However, most peptide vaccination schedules do not account for this requirement, which may explain why SLP vaccines to date have shown limited efficacy against human tumors [3]. Though statistical analyses were not performed due to the low number of mice in each group, the data shown here were representative of several experiments with various antigens. Moreover, they demonstrate improved SLP vaccination protocols for targeting cancer antigens, including neoantigens.

Although daily vaccinations for four days induced improved T cell responses, continued vaccinations beyond four days led to a blunted peak T cell response and may have

induced T cell exhaustion (Figure 5). In a microarray analysis, one study found that when mice were exposed to chronic infections for more than six days, antigen-specific T cells increased expression of T cell exhaustion markers like PD-1, 2B4, and CTLA-4 and reduced expression of effector molecules like IFN-γ, TNF-α, and perforin [402]. Interestingly, oil emulsions used in many vaccine formulae slowly release antigen over weeks or months [251], and though they occasionally induce large numbers of T cells, only a small percentage of the T cells secrete effector cytokines [403]. Thus, SLP vaccines in oil emulsions may cause T cell exhaustion due to prolonged antigen exposure, similar to chronic viral infections. Similarly, I observed blunted T cell expansion when mice were vaccinated on eight consecutive days (Figure 5b), which may have mimicked a chronic viral infection and induced T cell exhaustion [402]. My results demonstrate a discrete time window that antigen and adjuvant should be present in a mouse for peak T cell activation and avoidance of exhaustion: three or fewer days is too short, whereas eight days is too long.

Other groups have also modified the timing of administering soluble antigen in vaccines. One group assessed daily vaccinations of minimal peptides and CpG, and though the T cell responses were small, they also found that daily vaccinations led to increased T cell activation [404]. Furthermore, another group developed implantable micro-needles that release antigen over four days. When OVA and poly(I:C) were added to these needles, SIINFEKL specific T cells expanded to over 10% of the total CD8 T cell repertoire [405]. Continued development of these methods to deliver antigen for a discrete length of time will likely lead to improved T cell expansion, and potentially, improved clinical responses to vaccines.

The optimal time between cluster priming and cluster boosting may be unique for each antigen and may depend on the amount of inflammation induced by the prime. For example, one study showed that vaccination with *L. monocytogenes* led to impressive T cell expansion; however, the responding T cells had effector memory phenotype, and a booster vaccination was unable to increase the T cell frequency [406]. In contrast, vaccination with peptide-pulsed dendritic cells led to weak primary T cell expansion; however, the responding T cells had central memory phenotype, and a booster vaccination resulted in a massive increase in the frequency of antigen-specific T cells [406]. The study found that IFN-γ signalling from the highly immunogenic prime inhibited formation of central memory T cells

and prevented early boosting of the T cell response. The authors concluded that minimally inflammatory priming vaccinations activated T cells that could be boosted within a short time [407]. These studies may provide insight for understanding the differences between Spas1 neoantigen SLP and long-SIINFEKL SLP in the cluster-prime/cluster-boost setting. The cluster-prime with long-Spas1 SLP elicited a relatively weak T cell response of about 600 antigen specific T cells per million splenocytes, but the cluster-boost 21 days later elicited a further ten-fold expansion. In contrast, long-SIINFEKL SLP cluster-prime elicited robust T cell expansion of two percent of all circulating CD8 T cells, but the cluster-boost elicited only a further two-fold expansion. Timing of boosts may also be altered by inflammation. For example, single-dose prime using long-SIINFEKL SLP led to an almost undetectable primary T cell response, but the single-dose boost seven days later led to a huge amplification of antigen specific T cells (Figure 2c). In contrast, cluster-prime with long-SIINFEKL SLP elicited a robust primary T cell response, but cluster-boost amplified T cell responses only when initiated 21 days later (Figure 5a). Thus, similar to the published studies above, I found that weak primary T cell responses to peptide vaccinations could be boosted more quickly and to a greater extent than strong primary T cell responses. For neoantigen discovery in Chapter 3, these data implied that weakly immunogenic neoantigens may be potently boosted, and the resultant T cells may expand beyond the detection threshold for ELISPOT assays; whereas highly immunogenic neoantigens may be poorly boosted, but resultant T cells may have already expanded beyond the detection threshold for ELISPOT assays.

CD4 T cell responses are often found to be important for optimal tumor clearance [408,409]; however, addition of a CD4 antigen was dispensable for tumor rejection in the cluster vaccination setting. As discussed in Chapter 1, CD4 T cells can have multiple roles in cancer immunity. They can licence DCs to improve T cell activation, and they are critical for formation of memory CD8 T cells. However, CD4 T cells can also form Tregs that inhibit anti-tumor immunity. Others have shown that single prime-boost vaccinations combining SLP encompassing CD4 and CD8 epitopes led to improved survival of tumor bearing mice compared to vaccinating with SLP encompassing CD8 epitopes alone [25]. In contrast, I found that addition of long-OT-II SLP to the vaccine failed to enhance regression of E.G7 tumors compared to vaccination with long-SIINFEKL SLP alone (Figure 3). It is possible

that cluster vaccination sufficiently activated dendritic cells so that CD4 help was no longer necessary to elicit a curative antigen-specific CD8 T cell response. In support of this, one study showed that MHCII-negative mice (which lack CD4 T cells) mounted a CD8 T cell response that cleared *L. monocytogenes* equally well as mice fully constituted with CD4 T cells [410]. However, the study also showed that CD4 help was necessary for CD8 T cell memory formation and for CD8 T cells to respond to re-challenge [410]. I did not assess whether memory CD8 T cells were formed after tumors were cleared, but this could be assessed with a second tumor challenge at later time points. Some clinical trials have shown detrimental effects of including tumor specific CD4 T cell antigens in vaccines. For example, one trial found that 78% of patients observed CD8 T cell responses to melanoma-specific epitopes peptides when combined with peptides activating tetanus toxoid specific CD4 T cells (non-tumor associated antigen). However, only 19% of patients observed a CD8 T cell response when the vaccine was combined peptides activating melanoma associated antigens specific CD4 T cells. The authors speculated that Tregs may have reduced the CD8 T cell responses [411]. The same group also found that repeated weekly immunizations resulted in increased FoxP3 T cell accumulation at the vaccination site [412], indicating that Tregs may have become activated. Thus, the overall effects of co-administration of CD4 and CD8 T cell targeted peptides has yet to be elucidated, but the work presented here indicates that additional CD4 targeted peptides are not required for effective tumor clearance.

In conclusion, I showed that cluster vaccination activated both CD8 and CD4 T cells, and it was effective for activating both model- and neoantigen-specific T cells. Furthermore, cluster vaccination with a long peptide encompassing a CD8 T cell epitope led to curative responses in mice harbouring established E.G7 tumors. Moreover, CD8 T cells could be boosted to large numbers by a second round of cluster vaccination. Thus, the studies in Chapter 2 provide a platform for delivering therapeutic SLP vaccines targeting neoantigen-specific T cells. In Chapter 3, I applied these methods to target neoantigen-specific T cells in the ID8-G7 ovarian tumor model.

2.5 Figures

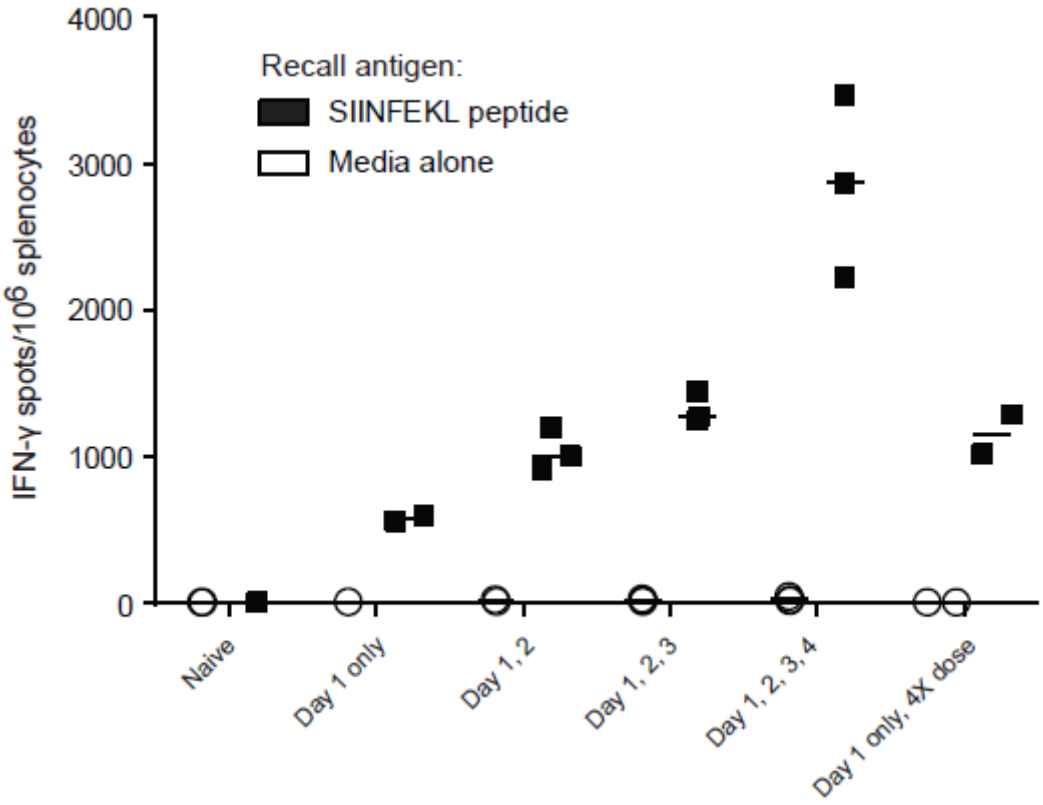

Figure 1. Consecutive daily immunizations to activate antigen specific T cells. (Figure modified and reproduced with permission from CCC [280]) Mice (n = 3 per group) were immunized subcutaneously with OVA protein (100 μg) and poly(I:C) (10 μg) on the days indicated. One group of mice was vaccinated on a single day with a four-fold larger dose of vaccine (400 μg OVA and 40 μg poly(I:C)). Mice were sacrificed seven days after the first vaccination, and IFN-γ ELISPOT assays were performed on splenocytes. Each point represents the number of T cells responding to minimal SIINFEKL peptide or media alone in a single mouse.

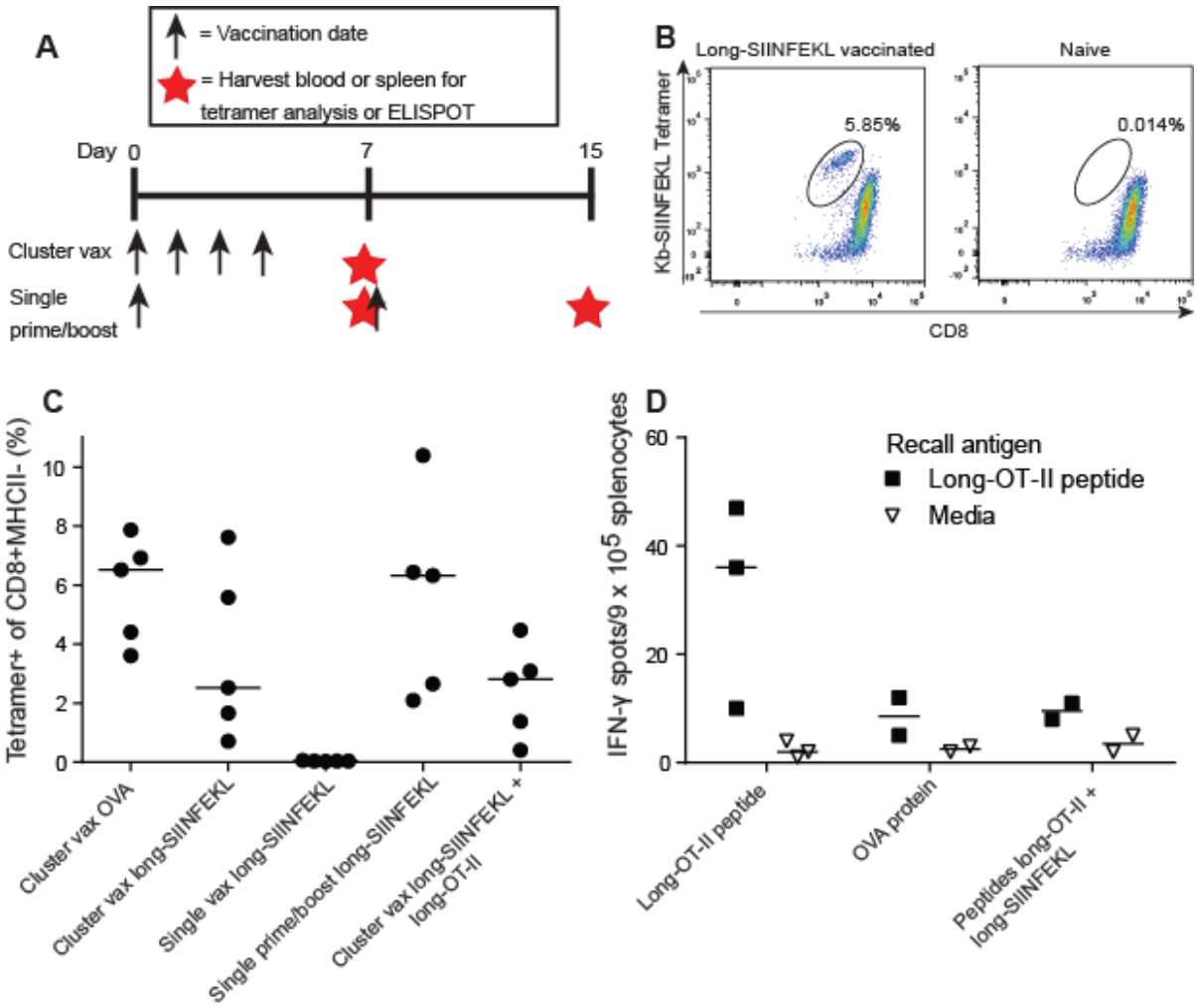

Figure 2. T cell responses to cluster vaccination with long peptides.
A. Schematic of vaccination and bleed tissue harvest for ELISPOT and tetramer analysis. Mice were vaccinated with poly(I:C) and various peptides, and PBMC or splenocytes were harvested at the peak of the T cell responses. **B.** Example tetramer staining on PBMC from a mouse that had been cluster vaccinated with long-SIINFEKL peptide (50 μg) and poly(I:C) (10 μg) and a naive mouse. Plots shown were gated on lymphocytes, then on CD8+,MHCII-. **C**. Summary data of tetramer positive CD8 T cells from mouse PBMC (n = 5 per group) vaccinated with the following schedules: Cluster vaccination with OVA protein (100 μg) and poly(I:C) (10 μg), cluster vaccination with long-SIINFEKL peptide (50 μg) and poly(I:C) (10 μg), single dose vaccination of long-SIINFEKL (100 μg) and poly(I:C) (50 μg) (day 7 bleed), single dose prime and single dose boost on day 7 with long-SIINFEKL (100 μg) and poly(I:C) (50 μg) (day 15 bleed), or cluster vaccination with long-SIINFEKL and long-OT-II peptides (50 μg each) and poly(I:C) (10 μg). **D**. IFN-γ ELISPOT assays on splenocytes from mice cluster vaccinated with poly(I:C) (10 μg) and either long-OT-II peptide (50 μg), OVA protein (100 μg) or long-OT-II (50 μg) and long-SIINFEKL (50 μg) peptides. Splenocytes were stimulated in ELISPOT wells with the minimal OT-II peptide (10 μg) or media alone. Each point represents the T cell response from a single mouse.

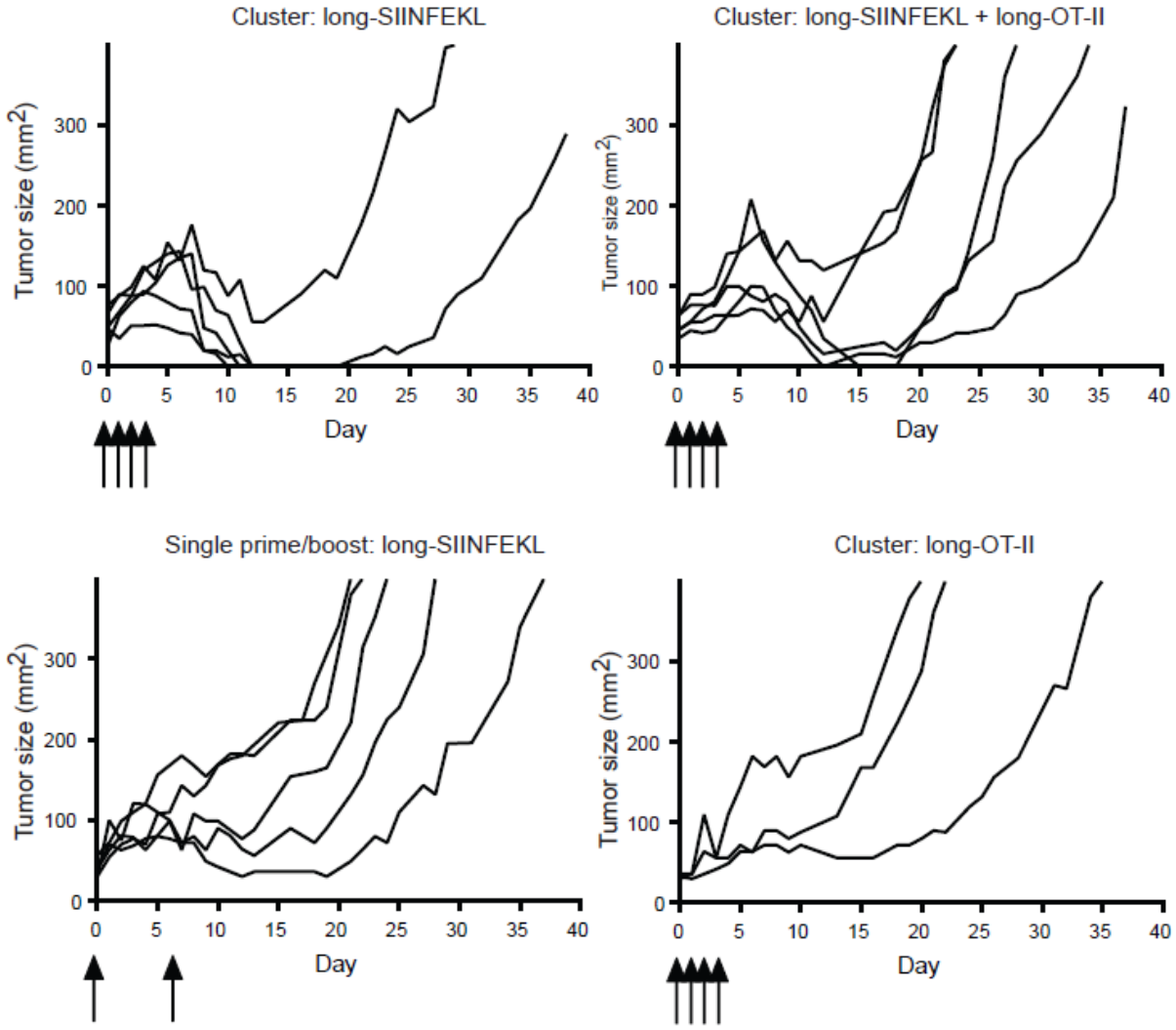

Figure 3. Vaccination to treat established E.G7 tumor cells.
Mice were inoculated with E.G7 tumor cells (2 x 10^5/mouse) and tumors were measured daily. Once tumors reached approximately 36 mm^2, mice (n = 5 per group) were vaccinated with one of the following reagent schedules: Cluster vaccination with long-SIINFEKL peptide (50 μg) and poly(I:C) (10 μg), cluster vaccination with long-SIINFEKL and long-OT-II peptides (50 μg each) and poly(I:C) (10 μg), single vaccination prime and day 7 boost with long-SIINFEKL (100 μg) and poly(I:C) (50 μg), or cluster vaccination with long-OT-II peptide alone. Arrows represent days that vaccinations were administered. Each line represents the tumor sizes of a single mouse. Mice were sacrificed once tumors reached 400 mm^2).

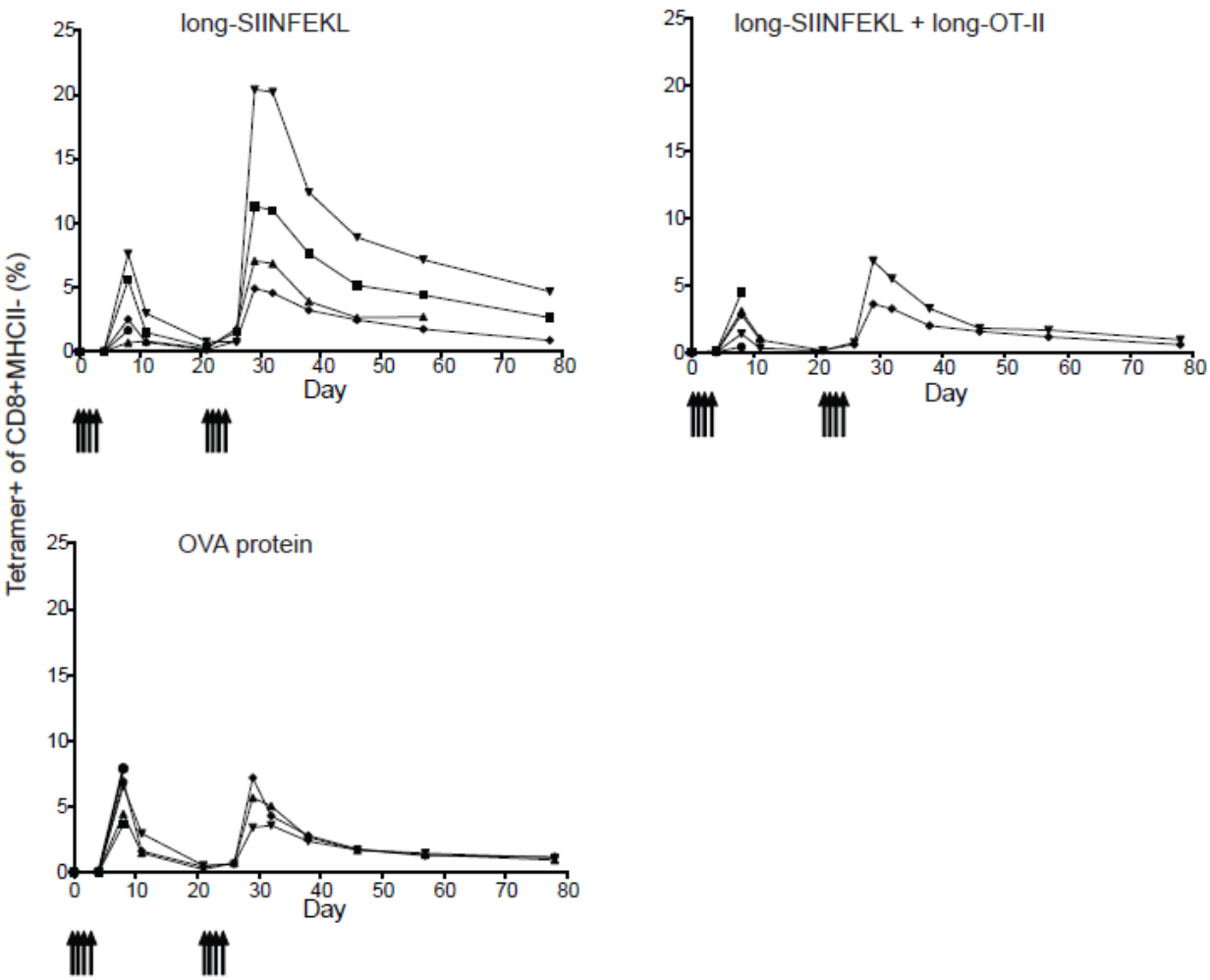

Figure 4. Effects of cluster boosting on CD8 T cell responses.
Mice were cluster vaccinated as in Figure 2 with poly(I:C) (10 μg) and either long-SIINFEKL peptide (50 μg), long-SIINFEKL and long-OT-II peptides (50 μg each), or OVA protein (100 μg). PBMC were harvested and stained with Kb-SIINFEKL tetramers as in Figure 2. Each line represents in a single mouse and the frequency of tetramer positive cells out of all CD8 T cells. Dates of vaccinations are represented with arrows.

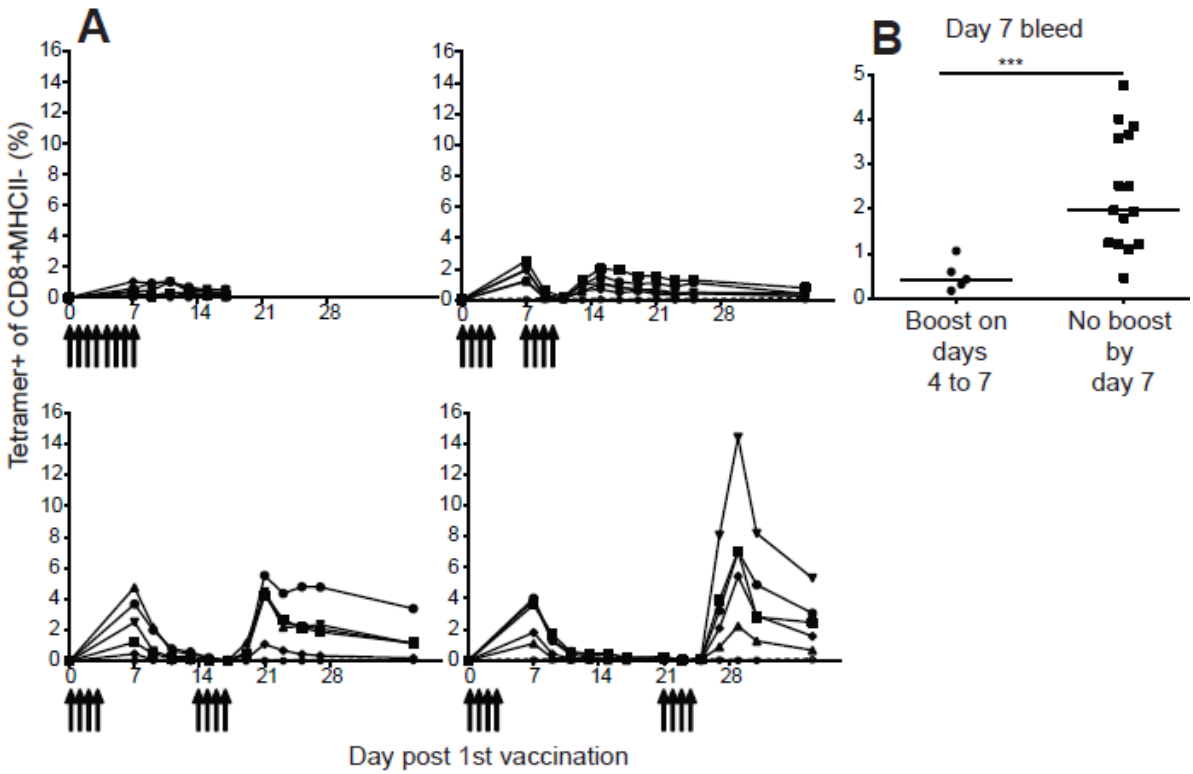

Figure 5. Effect of cluster boost timing on SIINFEKL specific T cell expansion. Mice (n = 5 per group) were vaccinated with long-SIINFEKL peptide (50 µg) and poly(I:C) (10 µg) on the days indicated with arrows. PBMC were harvested on day 0 and every 2 days starting on day 7 and stained as in Figure 2 with Kb-SIINFEKL specific tetramers. **A**. Each line represents the frequency of tetramer positive T cells in a single mouse over time. **B**. Frequencies of tetramer positive T cells on day 7 from mice vaccinated on days 0-3 and days 4-7 versus mice that had received vaccinations on days 0 – 3 and received the boosts after the day 7 blood draw. (Mann-Whitney test using Graphpad-Prism 6).

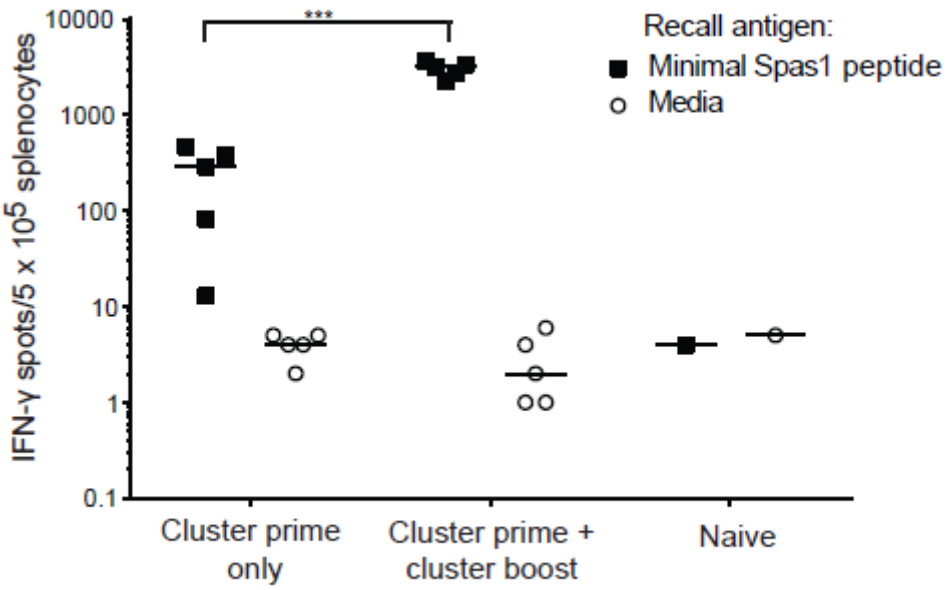

Figure 6. Cluster prime and cluster boost to activate neoantigen specific T cells. Mice (n = 5 per experimental group) were vaccinated with long-Spas1-mut peptide (50 μg) and poly(I:C) (10 μg) on days 21 – 24 (cluster prime) or days 0 – 3 and 21 – 24 (cluster prime + cluster boost). One mouse was not vaccinated and served as a negative control. Mice were sacrificed on day 28 and splenocytes were harvested. Splenocytes (5 x 10^5 cells/well) were added to ELISPOT wells and stimulated with minimal Spas1 mutant epitope or media alone. Spots represent the number of IFN-γ secreting cells per 5 x 10^5 splenocytes in a single mouse. Due to the extremely high number of antigen specific T cells, splenocytes from vaccinated mice were diluted 1/10 in splenocytes from naive mice.

Chapter Three: Targeting ID8-G7 tumor specific mutations with peptide vaccines

3.1 Introduction

As outlined in the previous chapter, I developed an effective protocol for activating neoantigen- and model antigen-specific T cells using cluster vaccination with SLP and poly(I:C). Here in Chapter 3, I apply this peptide vaccination protocol to target neoantigens in a mouse model of ovarian cancer (ID8-G7).

As discussed in Chapter 1, others have successfully targeted various highly-mutated mouse models with neoantigen-specific vaccines. However, the studies published to date have targeted tumors harboring extremely high mutation burdens, with between 949 and 4285 nonsynonymous mutations in each case [238,314,343,358]. Since human tumors contain a median of only 44 non-synonymous mutations [303], the question remains open as to whether these pre-clinical successes are relevant to human tumors with average mutation burdens. To predict the broader utility of neoantigen vaccines targeting human tumors with moderate mutation burdens, I first investigated neoantigen specific vaccines in a tumor model (ID8-G7) expected to harbour few mutations, and then I applied the results from the mouse model directly to human cancers using epitope prediction of TCGA mutations in HGSC.

The ID8 tumor line has been used extensively to study the biological and immunological characteristics of ovarian cancer [413-415]. After intraperitoneal implantation, the ID8 line gives rise to aggressive, widely disseminated cancers along with extensive ascites, similar to human HGSC pathology. These tumors are sensitive to immune checkpoint blockade [415] and adoptive T cell therapy [27]. Moreover, they can be therapeutically treated using protein vaccines targeting the CT antigen Sp17 [416], or using ID8 tumor lysate pulsed dendritic cell vaccines [231], making the ID8 model an attractive system to assess new T cell-based immunotherapies for ovarian cancer.

In contrast to mutagen induced murine models investigated previously, the ID8 tumor line arose by spontaneous transformation of normal murine ovarian surface epithelial cells during serial *in vitro* passage [417]; therefore, I hypothesized it would harbour a similar mutation burden to human ovarian cancers. On the other hand, since the transformation

process occurred entirely *in vitro*, in the absence of any immunological pressure, it might have given rise to neoantigens with unnaturally high MHC affinities. To mitigate this risk, I used a derivative of the ID8 line (ID8-G7), which underwent one round of *in vivo* passage in a syngeneic (C57Bl/6), immunocompetent mouse [27]. I anticipated this would result in a repertoire of neoantigens that more closely resembles tumors from immunocompetent ovarian cancer patients. While this may have eliminated expression of some immunogenic, dispensable mutations (i.e., passenger mutations), any essential driver mutations should have been retained. An added benefit of the ID8-G7 line was that it expresses the CD8 T cell epitope SIINFEKL, and near-complete regression of advanced disease can be achieved by adoptive transfer of SIINFEKL-specific CD8 T cells (OT-I T cells) [27], demonstrating the sensitivity of ID8-G7 tumors to immunological control. Thus, the ID8-G7 model provided a well-controlled system for evaluating neoantigens as targets for immunotherapy of human ovarian cancer.

To this end, I performed preclinical vaccine studies targeting tumor-specific mutations in ID8-G7. After performing whole exome and transcriptome sequencing of the tumor line, all identified nonsynonymous mutations were systematically evaluated as targets for prophylactic and therapeutic vaccination. Using data from The Cancer Genome Atlas (TCGA), I compared my findings to 220 human HGSC cases. Collectively, my findings from these murine and human studies indicate that the relatively low mutation load in ovarian cancer presents a major challenge for neoantigen-based vaccines.

3.2 Methods

Exome and RNA sequencing

Library construction, sequencing, and bioinformatic analysis were performed at Michael Smith's Genome Sciences Centre. Genomic DNA was extracted from cultured ID8-G7 tumor cells and normal C57Bl/6 splenocytes. DNA was prepared for exome selection according to the manufacturer's protocol using Agilent SureSelectXT Reagent kit HSQ (Cat# G9611A), and DNA was enriched for exomes using Agilent SureSelectXT All Mouse Exon Kit (Cat# 5190-4641). 100bp, paired-end sequencing was performed using the Illumina HiSeq2000 platform. After RNA extraction, mRNA was enriched using Miltenyi Biotec µMACS mRNA Isolation Kit (Cat# 130-090-276) and converted to cDNA using Invitrogen

Superscript Double-Stranded cDNA Synthesis Kit (Cat# 11917-010). cDNA was sheared, end polished, and ligated to adapters followed by 100bp paired-end sequencing on the Illumina HiSeq2000 platform.

Bioinformatic analysis

100bp paired-end reads from exome sequencing were mapped to the murine reference genome (mm9) using Burrows-Wheeler Aligner (BWA)[418]. Duplicates were flagged using Picard MarkDuplicates (version 1.102), and SNV and indels were identified using Samtools (version 0.1.18) pileup and VarFilter [419]. Variants were annotated using Annovar [420], and visually inspected using Integrated Genomics Viewer (IGV) (version 2.3.32) [421]. All variants found in dbSNP138 were removed. RNA-seq reads were aligned to a genome-plus-junctions reference (mm9) using BWA, and reads that mapped to junctions were repositioned as large-gapped genomic alignments. Reads were visualized using IGV to determine whether RNA sequencing reads contained mutated alleles identified in the exome sequencing data. If both RNA and exome sequencing data contained a variant that was not present in the C57BL/6 exome sequencing data, the variant was deemed a tumor-specific mutation. The predicted binding affinity to H-2Kb and H-2Db of mutated peptides was determined using NetMHCpan2.4 [32].

Mice and tumor cell lines

C57BL/6 mice were purchased from Jackson Labs and maintained under specific pathogen-free conditions. All mouse protocols were approved by the Animal Care Advisory Committee at the University of Victoria, following Canadian Council for Animal Care guidelines. Adoptive cell transfer of splenocytes from female OT-I transgenic mice (Jackson Labs) containing T cells recognizing the chicken ovalbumin $(OVA)_{257-264}$ epitope SIINFEKL were used as positive controls for tumor bearing experiments [422]. Mouse mammary tumor virus MMTV/$neu^{OT\text{-}I/OT\text{-}II}$ transgenic mice were used as hosts in tumor-bearing experiments [26]. These mice are tolerant to the SIINFEKL epitope due to expression of the OT-I epitope (SIINFEKL) tagged onto the rat *neu* gene in mammary epithelial tissue. ID8-G7 [27] tumor cells were grown in High Glucose DMEM (Hyclone: SH30022.01) supplemented with 5% FBS (Gibco: 12483-020), 2mM L-glutamine (Hyclone: SH30034.01), 100U/ml Penicillin

and 100µg/ml Streptomycin (Hyclone: SV30010), and 1X Insulin Transferrin Selenium (ITS) (Corning: 354351). 600µg/mL G418 (Corning: 30-234-CR) was added to maintain expression of the transgene MMTV/*neu*$^{OTI/OTI}$ on a cassette containing a neomycin resistance gene.

Vaccinations

Six to twelve week old female wild type (WT) or MMTV/*neu*$^{OT\text{-}I/OT\text{-}II}$ mice were anesthetized and subcutaneously inoculated in the flank using a 27 gauge needle. Each inoculation was composed of 25 – 50 µg of peptide (ProImmune) or 100 µg of chicken ovalbumin (OVA) (Sigma: cat# A5503) and 10 µg poly(I:C) (Amersham: 27-4732) admixed to a total of 300 µl in sterile PBS (Gibco: 20012-027). For therapeutic vaccination experiments, mice received daily vaccinations on days 3-6 after tumor inoculation. For all other vaccination experiments, mice received daily vaccinations on days -28 to -25 and -7 to -4 with either tumor implantation or sacrifice of mice on day 0. For vaccinations using tumor lysates as antigens, ID8-G7 tumor cells were grown as above. However, to eliminate FBS contamination in the tumor lysate inoculum, ID8-G7 tumor cells were maintained in FBS-free media composed of High Glucose DMEM supplemented with 2mM L-glutamine, 100U/ml Penicillin and 100µg/ml Streptomycin, and 1X Insulin Transferrin Selenium (ITS). After 48 hours in FBS-free media, cells were harvested, washed 3 times in sterile PBS and re-suspended to 10^7 cells/ml in PBS. Cells underwent seven freeze/thaw cycles and were sonicated to ensure complete lysis. Cell lysate suspension was assessed by trypan blue staining to ensure all cells were dead. WT or MMTV/*neu*-$^{OTI/OTII}$ transgenic mice were vaccinated on days 0 – 3 and days 21 – 24 with ID8-G7 lysate equivalent to 4 x 10^5 tumor cells and poly(I:C) (10 µg) admixed to 300 µl in PBS.

Tumor-bearing mouse experiments

ID8-G7 tumor cells were detached from plates using trypsin, washed 3 times in sterile PBS, and re-suspended in sterile PBS at 10^7 cells/ml. The cell suspension (10^6 cells in 100µl) was injected into the peritoneal cavity of each mouse. Mice were monitored and euthanized at the first sign of abdominal distension due to ascites accumulation. On necropsy, all mice with abdominal distension contained highly disseminated tumors. For adoptive transfer

experiments, OT-I transgenic mice were euthanized, and splenocytes were processed by pressing splenocytes through a 100µm nylon filter, lysing red blood cells with ACK lysis buffer (Lonza: 10-548E), and counting live splenocytes by trypan blue staining. OT-I splenocytes (10^5 cells in 100 µl) were injected into the tail vein of recipient mice, followed by vaccination with 100 µg of OVA and 10µg of poly(I:C) on four consecutive days.

IFN-γ and IL-2 ELISPOT assays

In accord with MIATA guidelines [400], ELISPOT assays were performed using validated, standard operating protocols. Vaccinated female mice were euthanized using isofluorane, and spleens were immediately processed into single cell suspensions by pressing through 100 µm screens in complete RPMI (RPMI + HEPES (Gibco: 22400-089) supplemented with L-glutamine, 50 µm β-mercaptoethanol (Sigma: M6250), penicillin and streptomycin, sodium pyruvate (Hyclone: SH30239.01) and 10% FBS). Red blood cells were lysed using ACK lysis buffer, and fresh splenocytes were counted on a Guava cytometer using Viacount (Cat#: 4000-0130). Splenocytes were diluted to 5 x 10^6 or 10^7 live cells/ml (usually between 75 – 85% of splenocytes were viable) in complete RPMI. ELISPOT plates (MSIP, Millipore: MSIPS4W10) were coated with 10 µg/ml of anti-mouse IFN-γ (mAb AN18, Mabtech: 3321-3-1000) or IL-2 (Mabtech: 3441-2H) capture antibody and incubated overnight at 4°C. Plates were washed and blocked for 2 hours at 37°C, 5% CO_2 with complete RPMI. Within 2 hours of mice being sacrificed, 5 x 10^5 to 10^6 live, processed splenocytes were added to each well and stimulated with 0.002 - 20 µg/ml of the indicated peptides, media alone, 5 µg/ml Concanavalin A (Sigma: C5275) as positive control, or suspensions of 10^5 tumor cells/well. Cultures were incubated for 20 hours at 37°C and 5% CO_2. Plates were washed, 1 µg/ml of secondary antibody (biotinylated anti-IFN-γ: mAbR4-6A2, Mabtech: 3321-6-250, or biotinylated anti-IL-2: Mabtech: 3441-2H) was added, and plates were incubated for 2 hours at 37°C. Plates were developed using Vector Labs' Vectastain ABC Elite kit (Cat#: PK-6100) and Vectastain AEC substrate reagent (Cat#: SK-4200) according to manufacturer's protocol and scored with an automated plate reader (AID) using preset parameters that have been validated over several experiments.

Intracellular cytokine staining (ICS) and cell sorting

Mice were vaccinated and euthanized as described above. Fresh splenocytes (2 x 10^6 cells/1ml/well) were incubated with 20 µg/ml of cognate mutant peptide, or media alone, in 24 well plates. For ICS, splenocytes were incubated for 2 hours at 37°C and 5% CO_2. GolgiPlug (BD: 51-2301KZ) was added, and the cells incubated for an additional 11 hours. Cells were then processed according to the manufacturer's protocol using the FoxP3/Transcription Factor Staining Set (eBioscience, Cat#: 00-5523). Briefly, cells were harvested and stained for 30 minutes with fixable viability dye (eF780, eBioscience: 65-0865-18), washed and stained for 30 minutes with surface antibodies (CD4-V450 BD: 560468; CD8-PE, TONBO Biosciences: 50-0081-U100; MHCII-FITC, eBiosciences: 1250166), fixed and permeabilized, and stained for 30 minutes with IFN-γ antibodies (IFN-γ-APC, eBiosciences: 17-5743). Analytical flow cytometry was performed on a BD FACSCalibur flow cytometer and analyzed using FlowJo (vX.07). For cell sorting, cells were harvested from 24 well plates after 24 hours of stimulation with peptide. Cells were filtered through a 40µm nylon filter, stained with viability dye-eFluor780, washed, and stained with surface antibodies (CD4-V450; CD8-V500, BD: 560776; MHCII-FITC; 41BB-PE, BioLegend:107105; OX40-APC, BioLegend: 119409). Cells were sorted using BD Influx cell sorter, and sorted cells were expanded in 100U/ml IL-2 (eBiosciences: 34-8021) in complete RPMI.

Neoantigen prediction in the TCGA lung cancer and HGSC datasets

TCGA mutation annotation files were parsed and HLA alleles predicted from RNA-seq data for HGSC, lung adenocarcinoma (LUAD), and lung squamous cell carcinoma (LUSC) tumors as previously described [336]. SNVs were further filtered by requiring at least one read in the RNA-seq bam file to have the mutated base. Samtools v0.1.17 was used to extract reads covering the mutation site from the indexed bam files, and a custom python script checked for the mutated base. Epitope predictions were performed for all 8-11mer peptides relative to autologous *HLA-A* allele(s) using NetMHCpan v2.8 [32]. An IC50 value of < 100 nM was used as the threshold for calling high affinity epitopes [14]. Since only *HLA-A* alleles were called due to challenges in calling unambiguous *HLA-B* and *C* alleles from 50bp sequencing data provided by TCGA, values were multiplied by 3 to account for 3

HLA loci (*HLA-A, B, C*). To estimate the likelihood of a patient with a given number of predicted neoantigens containing at least one authentic neoantigen, we applied the findings of a study showing that only 8% of peptides that bind MHCI with IC50 < 100 nM proved to be authentic (ie. 92% were not authentic) [14]. We calculated the chance of a patient containing 0 immunogenic mutations using the equation 0.92^N, where "N" equals the number of predicted neoantigens. Subtracting from one, we arrived at the percent likelihood of a patient with N predicted neoantigens containing at least one authentic neoantigen.

3.3 Results

Identification of mutations in the ID8-G7 tumor line

Exome sequencing was performed on genomic DNA from both the ID8-G7 tumor cell line and MMTV/*neu*$^{OTI/OTII}$ murine splenocytes. In addition, RNA-seq was performed on the ID8-G7 tumor line. Exome sequencing generated 127 million reads that mapped to the reference mouse genome, resulting in an average of 89-fold coverage. Paired-end RNA-seq generated 158 million mapped reads. After removing variants present in either the control mouse genome or dbSNP138, 92 non-synonymous tumor-specific coding variants were identified (Figure 7). Of these, 42 variants were present in at least 1 read within the RNA-seq data, indicating that they were transcribed. Non-sense mutations were excluded from analysis, as these were not expected to give rise to T cell epitopes. This left 39 non-synonymous, transcribed, missense or insertion/deletion (Indel) variants (Figure 7). The amino acid sequences encompassing the mutations were queried using epitope prediction software (NetMHCpan2.4 [32]). Using a relaxed cutoff of IC50 < 1500 nM, I identified 17 mutations predicted to give rise to at least one MHCI binding epitope, and these were advanced to vaccination experiments (Table 1). One additional predicted MHCI binding mutation (in the gene 1110021LRik) could not be assessed due to difficulties synthesizing the corresponding peptide. All of the targeted mutations qualified as intermediate affinity binders, as their predicted IC50 scores ranged from 103 – 1160 nM (Table 1).

Induction of mutation-reactive T cells by peptide vaccination

To determine whether any of the 17 predicted neoantigens were immunogenic, naive C57/Bl6 mice were vaccinated with 29mer peptides with the mutated residue in the central

position. By using 29mer peptides, intracellular antigen processing could potentially produce any mutation-bearing epitope of 15 amino acids or less. Each group of mice was vaccinated with 1 of the 17 mutant peptides and poly(I:C) on four consecutive days as previously described [280], followed by four additional daily inoculations three weeks later. T cell responses were assessed by IFN-γ ELISPOT. As described in Chapter 2, this vaccination schedule elicited robust T cell responses to 29mer peptides encoding SIINFEKL and mutant Spas1 (Figure 5 and 6). When used to target ID8-G7 tumor-specific mutations, vaccination elicited T cell responses to 11/17 mutant peptides (Figure 8). For these 11 responses, cross-reactivity to the wild type (WT) version of the peptide was assessed by titrating the WT and mutant peptides in IFN-γ ELISPOT assays. For 4/11 mutations, T cells responded to the mutant and WT peptides at similar concentrations, indicating a high degree of cross-reactivity (Figure 9). For the remaining 7/11 mutations, T cells showed > 100-fold higher sensitivity to the mutant peptide compared to the WT peptide (Figure 9). Intracellular cytokine staining revealed that 5/7 of these responses involved both CD4 and CD8 T cells (Figure 10), with CD4 T cells dominating the responses in 4/5 cases. The remaining 2/7 responses were mediated by CD4 T cells alone. Thus, 7/17 (41%) of mutant peptides elicited a mutation-specific T cell response after vaccination, and most responses were dominated by CD4 T cells.

Therapeutic vaccinations targeting ID8-G7 mutations

To test whether vaccine-activated mutation-specific T cells would eliminate ID8-G7 cells, mice that had been implanted three days earlier with ID8-G7 tumor cells were vaccinated on four consecutive days with individual mutant peptides and poly(I:C). As expected, 9/10 positive control mice that underwent ACT with OT-I followed by vaccination with OVA and poly(I:C) remained tumor free 80 days post tumor implantation (Figure 11). In contrast, none of the seven mutant peptide vaccines increased survival of mice beyond that seen with non-vaccinated control mice (Figure 11). Additionally, I performed similar therapeutic vaccinations using peptides that were either minimally immunogenic (Celsr, GM608, Mterfd1, Pla2g4a), or elicited cross-reactive T cells (Bat1a, D6ertd527a, Plcxd2, Tle1). These eight additional vaccines each failed to increase survival of tumor-bearing mice (Figure 11).

Prophylactic vaccinations of mice

Recognizing that cancer vaccines are not always effective for treating established tumors, I also tested mutant peptides in a prophylactic vaccination setting. Mice were vaccinated with mutant peptides on days -28 to -25 and -7 to -4, followed by intraperitoneal injection of ID8-G7 tumor cells on day 0. One animal per group was euthanized on day 0, and T cell activation was confirmed in all cases by IFN-γ ELISPOT. Mice that received adoptive transfer of OT-I and vaccination with OVA remained tumor free for > 300 days, confirming that ID8-G7 tumor cells were susceptible to T cell-mediated rejection. However, none of the mice vaccinated with mutant peptides showed a significant difference in survival compared to mice that received an irrelevant peptide or no vaccination (Figure 12). Thus, despite eliciting robust T cell responses, none of the mutant peptide vaccines demonstrated a significant anti-tumor effect in either the prophylactic or therapeutic settings.

In vitro tumor recognition experiments

To investigate why mutant peptide vaccines failed to provide tumor control *in vivo*, I assessed whether vaccine-induced T cells recognized ID8-G7 tumor cells *in vitro.* As before, mice were vaccinated with mutant peptides, and splenocytes were harvested on day 28. In IFN-γ (Figure 13a) and IL-2 (Figure 13b) ELISPOT assays, splenocytes from immunized mice responded strongly to corresponding mutant 29mer peptides but showed no response to ID8-G7 tumor cells. As a positive control, SIINFEKL-specific T cells responded to both peptide and ID8-G7 tumor cells (Figure 13a and 13b). To further assess CD4 T cell responses, splenocytes from vaccinated mice were stimulated *in vitro* with cognate peptides, sorted based on upregulation of 41BB and OX40 (Figure 13c), and expanded with IL-2. ID8-G7 tumor cells were pre-treated with IFN-γ, which resulted in up-regulation of MHCII (Figure 13c). Tumor cells and T cell lines were co-incubated overnight and assessed by IL-2 ELISPOT assay. None of the mutation-reactive CD4 T cells demonstrated recognition of ID8-G7 cells (Figure 13d). Collectively, the results of these tumor recognition experiments suggest that none of the assessed mutations gave rise to epitopes that were naturally presented by MHCI or MHCII on ID8-G7 tumor cells in sufficient quantity to stimulate T cells.

Vaccination with ID8-G7 tumor lysate and recall with mutant peptides

As an additional assay to determine whether ID8-G7 tumor specific mutations gave rise to authentic mutant epitopes, T cell responses to mutations were assessed from mice vaccinated with ID8-G7 tumor lysate and poly(I:C). My first attempt to vaccinate mice with an ID8-G7 tumor lysate resulted in overwhelming background in the ELISPOT assays (data not shown). I hypothesized that the source of the background was contaminating FBS from the media in which the ID8-G7 were grown. Thus, in the subsequent experiment, all FBS was removed from the media 48 hours prior to harvesting ID8-G7 tumor cells for use as lysate. The resultant FBS-free ID8-G7 tumor lysates were used as antigen in cluster vaccination prime and boost on WT and MMTV/neu-$^{OTI/OTII}$ transgenic mice. Splenocytes were harvested and incubated with each of the mutated peptides and ID8-G7 tumor cells in IFN-γ ELISPOT assays. Mutated peptides, long-SIINFEKL peptide, and ID8-G7 tumor cells each failed to induce responses by T cells from vaccinated MMTV/*neu*$^{OTI/OTII}$ transgenic mice (which are tolerant to SIINFEKL), indicating that the lysate vaccine did not activate mutation reactive T cells (Figure 14). In contrast, stimulation in the ELISPOT assay with both long-SIINFEKL peptide and ID8-G7 tumor cells activated robust T cell responses in vaccinated WT mice, indicating that the lysate vaccination was capable of eliciting tumor reactive T cells (Figure 14). These data provided further evidence that the ID8-G7 tumor line contained no neoantigens.

Predicted immunogenic mutations in human HGSC versus lung cancer

The findings in the ID8-G7 tumor model suggested that mutations with intermediate affinity for MHCI (with predicted IC50 scores from 103 - 1160 nM) have a low probability of giving rise to authentic, therapeutically relevant epitopes. Instead, high affinity epitopes may be required, as supported by numerous murine and human studies [20,21,330,339,423]. To explore the implications of this for human HGSC, the TCGA HGSC dataset (TCGA-OV) was interrogated to determine the proportion of tumors with somatic point mutations predicted to give rise to high affinity MHCI binding peptides (IC50 < 100 nM). For comparison, the lung carcinoma datasets were used as examples of tumor types with high mutation burdens. Candidate neoantigens were identified based on the following criteria: (1) The mutation presence in the tumor but not in matched normal tissue (Figure 15a); (2) at

least one read from RNA-seq data supporting expression of the mutated allele (Figure 15b); and (3) a predicted MHCI binding score of IC50 < 100 nM for at least one of the autologous *HLA-A* alleles (Figure 15c). Only samples with unambiguous *HLA-A* allele calls were analyzed for immunogenicity due to challenges in calling unambiguous *HLA-B* and *C* alleles from 50 bp sequencing data. Since only *HLA-A* alleles were assessed, the results were multiplied by three to account for the three MHCI loci in humans (*HLA-A*, *-B,* and *–C*). Using these parameters, the median number of predicted MHCI neoantigens was 6 for HGSC compared to 27 for lung cancer. Empirical studies of viral epitopes indicate that only 8% of peptides that bind MHCI with IC50 < 100 nM prove to be authentic epitopes (i.e., are naturally processed and presented by MHCI) [14]. Therefore, after multiplying by 0.08, we estimated that the expected number of authentic MHCI neoantigens in a tumor with median number of predicted epitopes was 0.48 for HGSC compared to 2.16 for lung cancer. Based on these assumptions, a patient with the median number of mutations would have only a 39% chance of containing one or more authentic MHCI-binding neoantigens in HGSC compared to an 89% chance in lung cancer. Put another way, 12% of HGSC cases versus 51% of lung cancers would have $\geq$ 90% likelihood of containing at least 1 neoantigen. Thus, results from both the ID8-G7 tumor model and TCGA data reveal the potential limitations of targeting neoantigens in HGSC.

3.4 Discussion

I investigated the concept of using neoantigen-specific vaccines to target ovarian cancer using a murine tumor model and *in silico* analysis of human HGSC data from TCGA. The ID8-G7 tumor line was analyzed by whole exome sequencing, RNA-seq, and epitope prediction, and 92 mutations were identified, 39 of which resulted in amino acid substitutions and were transcribed according to RNA-seq data. By *in silico* analysis, none of the transcribed mutations gave rise to neoepitopes predicted to bind MHCI with high affinity (IC50 < 100 nM); therefore, mice were vaccinated with mutant peptides containing MHCI epitopes with intermediate predicted affinity (IC50 scores of 103 - 1160 nM). Although 7/17 peptide vaccines elicited robust, mutation-specific CD4 and CD8 T cell responses, the mutation-reactive T cells failed to recognize ID8-G7 tumor cells *in vitro*. Moreover, neither

prophylactic nor therapeutic vaccination resulted in effective anti-tumor activity *in vivo*. When combined with published results [20,314,343], my findings indicate that high affinity, MHCI binding epitopes (IC50 < 100 nM) may be required to elicit neoantigen-reactive CD8 T cell responses capable of mediating tumor regression. Yet bioinformatic analysis of TCGA data revealed that only 12% of HGSC cases had $\geq$ 90% likelihood of harboring at least one neoantigen. Thus, this study highlights a major challenge associated with neoantigen-specific vaccines in HGSC and potentially other malignancies with intermediate to low mutation loads.

Although I used an established approach to predict CD8 T cell neoantigens, it is possible that relevant MHCI-binding neoantigens may have been overlooked. For example, using an MCA-induced mouse fibrosarcoma model, one group reported that therapeutically relevant neoantigens did not necessarily have the highest predicted MHCI binding affinity but rather the greatest difference of MHCI binding affinity between the mutant and wild type peptide [315]. However, two studies have shown that the majority of published human CD8 T cell neoantigens identified by non-biased cDNA library screens could be predicted based on the binding affinity of the mutant peptide alone [330,339]. In one of these studies, 22/31 (71%) of validated neoepitopes were predicted to bind autologous HLA with IC50 <100 nM, while most of the remaining neoepitopes (5/31, 16%) had predicted IC50 scores between 100 and 500 nM [330]. Furthermore, authentic CD8 T cell neoantigens identified in all other NGS-guided preclinical studies could be identified using high predicted binding scores (IC50 < 100 nM) [314,343,424]. Thus, since every predicted epitope with an IC50 score < 1500 nM was evaluated, it seems unlikely that authentic MHCI-binding neoantigens were missed by our analysis.

Recently, several groups have highlighted the importance of CD4 T cell responses to neoantigens. In one study, a neoantigen-targeted vaccine induced activation of CD4 T cells that mediated rejection of B16F10 melanoma [238]. Moreover, neoantigen-specific CD4 T cells are commonly found among tumor-infiltrating lymphocytes in melanoma patients [347]. Furthermore, adoptive transfer of a near-clonal population of neoantigen-reactive CD4 T cells resulted in regression of a human metastatic cholangiocarcinoma [101]. My neoantigen-specific vaccines were designed to allow processing of MHCII epitopes and activation of CD4 T cells, since all possible mutant epitopes up to 15 residues in length could

be processed from a mutant 29mer peptide. Indeed, CD4 T cells were the dominant component in 6/7 mutation-specific T cell responses, yet none of these responses translated to anti-tumor efficacy *in vivo.* It is possible that I overlooked therapeutically relevant CD4 T cell neoantigens that were > 15 residues in length or present among the 22 expressed mutations not assessed. Unfortunately, MHCII epitope prediction algorithms are not yet sufficiently accurate for efficient vaccine design [39-41]; however, the need for such tools is becoming increasingly evident for cancer immunotherapy.

Two important and related limitations of the ID8-G7 project were the effects of immune editing and the lack of strong MHCI binding peptides. Since the ID8-G7 tumor line had been passaged in an immunocompetent mouse, highly immunogenic neoantigens present in the parental ID8 line may have been lost or silenced due to the act of injecting an immunocompetent mouse with 10^6 tumor cells [122]. Immune editing of neoantigens was demonstrated in an MCA-induced sarcoma model, where a tumor that arose in an immune deficient mouse was found to carry a mutation which was lost upon transplantation of the tumor into an immunocompetent mouse [424]. Thus, immunogenic mutations may have been lost from the ID8-G7 tumor that grafted and eventually grew in the immunocompetent mouse. Supporting this hypothesis, I found that the ID8-G7 tumor genome contained four mutations within epitopes predicted to bind MHCI with IC50 < 100 nM that were not transcribed. It is possible that these may have been silenced due to immune editing. However, given the higher tumorigenic capacity of the ID8-G7 line compared to the parental ID8 line [27], it would appear that expression of these mutations is not required for tumor cell proliferation, viability or metastatic spread. Thus, at best, they may represent passenger mutations with questionable value as therapeutic targets. Despite these theoretical considerations, one must concede that murine tumor models inevitably have caveats with respect to immune editing. Ultimately, estimates of neoantigen load are best made in human cancers, where tumors develop under natural physiological conditions that include immune editing.

To this end, TCGA data were used to estimate the prevalence of neoantigens in HGSC and, as a comparator, lung cancer. It was calculated that a tumor with the median number of predicted neoantigens would likely contain 2.16 authentic neoantigens in lung cancer versus 0.48 in HGSC, meaning that many HGSC tumors may be devoid of authentic

neoantigens. Thus, in identifying patients likely to respond to neoantigen vaccines, it may be important to focus on the most highly mutated cases.

From my studies on the immune response to the mutated ID8-G7 genome, I determined that repeated vaccinations successfully activated T cells towards the majority of mutations tested. However, T cell activation towards mutations was only a first step to identifying therapeutically useful vaccine targets. Since only 8% of all peptides with a MHCI binding affinity < 100 nM are naturally processed and presented authentic antigens [14], few T cell responses induced by peptide vaccination were expected to recognize tumor cells. Indeed, none of the induced T cells recognized tumor, nor did they improve survival of tumor bearing mice. Furthermore, the analysis of TCGA data revealed that most human HGSC cases were expected to harbour no immunogenic mutations. With this in mind, in the studies described in Chapter 4, I identified a HGSC patient with a high predicted neoantigen load, and I searched for neoantigen reactive T cells within this patient's ascites and peripheral blood.

3.5 Figures

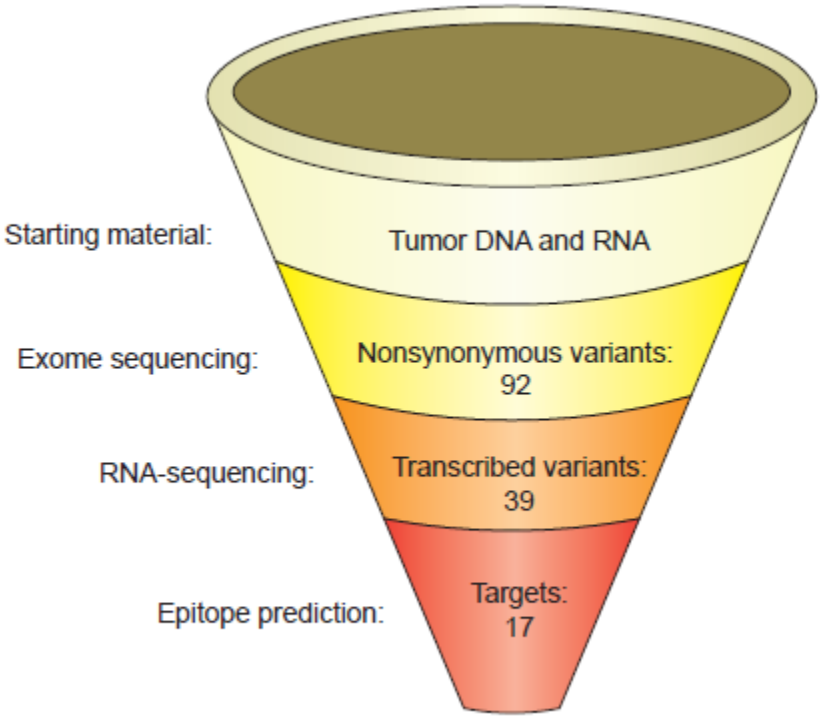

Figure 7. Identification of potentially immunogenic mutations.
Mutations were identified by whole exome sequencing, and expression was assessed using RNA-seq. Epitope prediction was performed using NetMHCpan2.4 [32]. Starting with 92 mutations in genomic DNA, 17 mutations within peptides predicted to bind MHCI (IC50 < 1500 nM) were advanced to subsequent experiments.

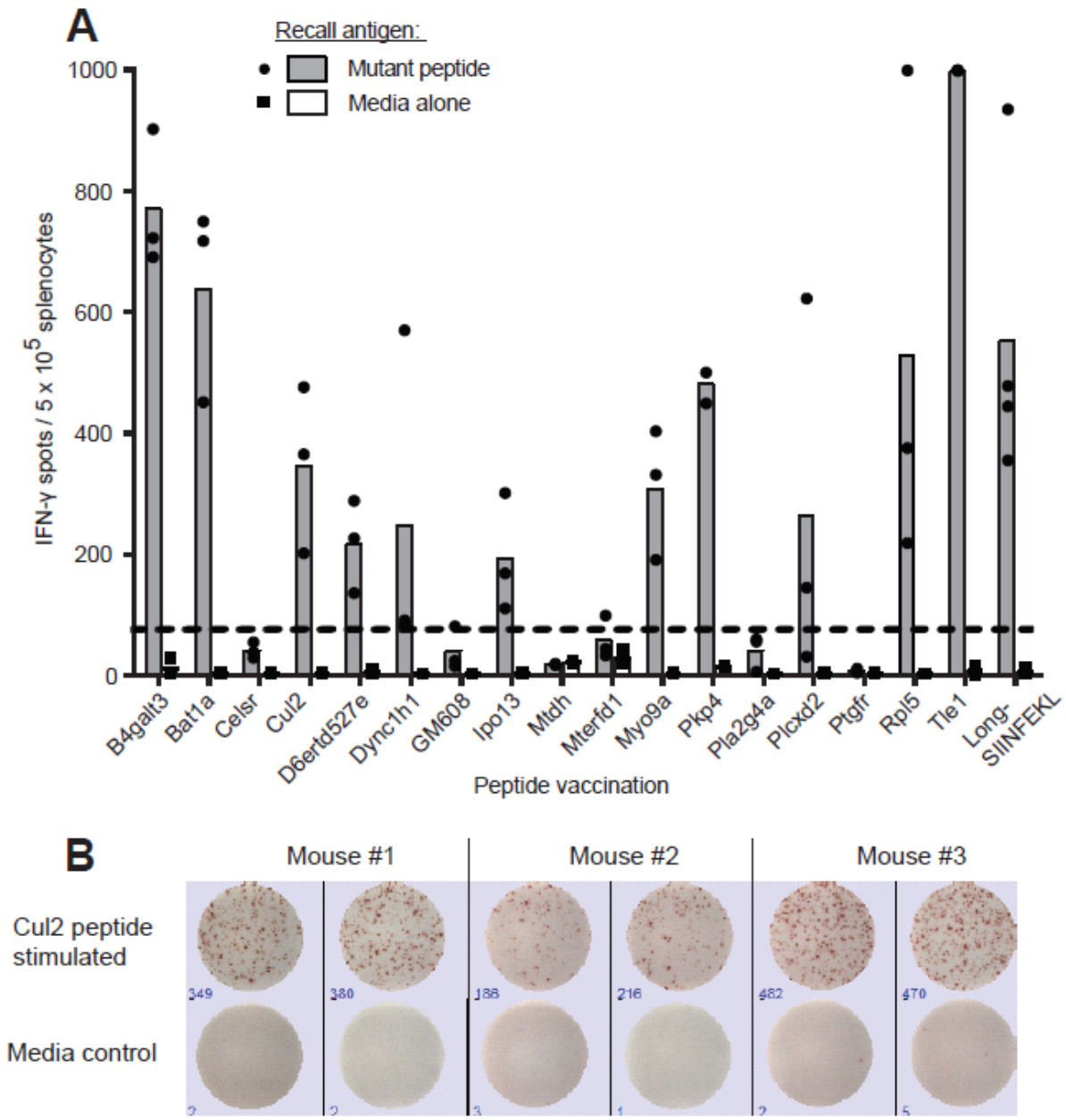

Figure 8. Immunogenicity of mutant peptides.
Mice (n = 3 per group) were vaccinated daily on days 0 - 3 and 21 - 24 with mutant 29mer peptides (50 µg, one peptide per group) and poly(I:C) (10 µg). On day 28, mice were euthanized, and splenocytes (10^6 cells/well) were stimulated in duplicate with mutant 29mer peptides (20 µg/ml) or media, and assessed by IFN-γ ELISPOT. Positive control mice were vaccinated with a 29mer peptide (long-SIINFEKL) encompassing the known $OVA_{257-264}$ epitope. **A.** Eleven of 17 mutant peptides elicited robust T cell responses. Dots represent responses in individual mice, and bars represent the mean for three mice. The dashed line shows the threshold for positivity (3 x maximum background for splenocytes in media alone determined post-hoc). **B.** Representative ELISPOT wells from 3 mice vaccinated with mutant Cul2 peptide and stimulated in duplicate with mutant Cul2 peptide or media alone.

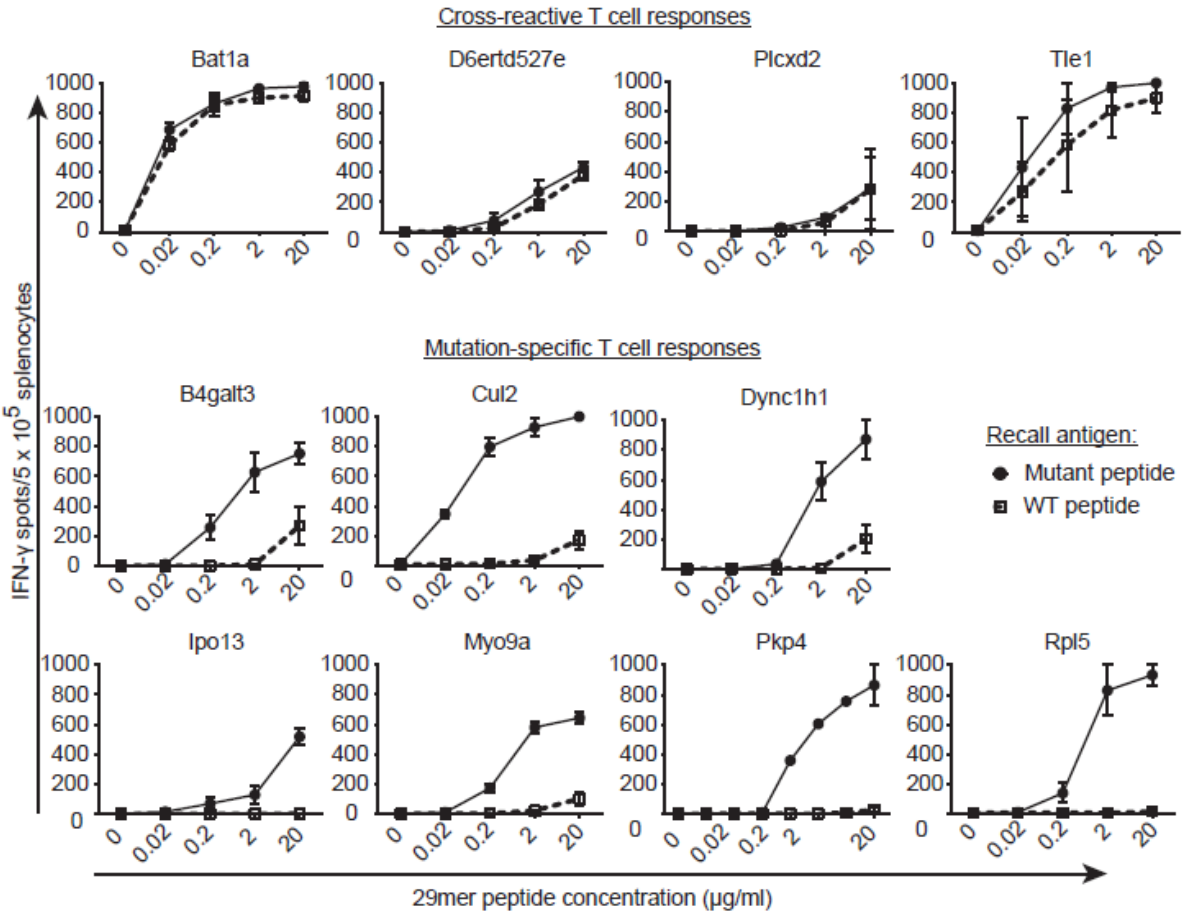

Figure 9. T cell specificity for mutant versus wild type peptides.
Mice (n = 2 per group) were vaccinated as in Figure 2. On day 28, mice were euthanized, and splenocytes (5 x 10^5 cells/well) were stimulated in duplicate with titrated concentrations of mutant or wild type 29mer peptides in IFN-γ ELISPOT wells. Dots and bars represent the mean and range of responses, respectively.

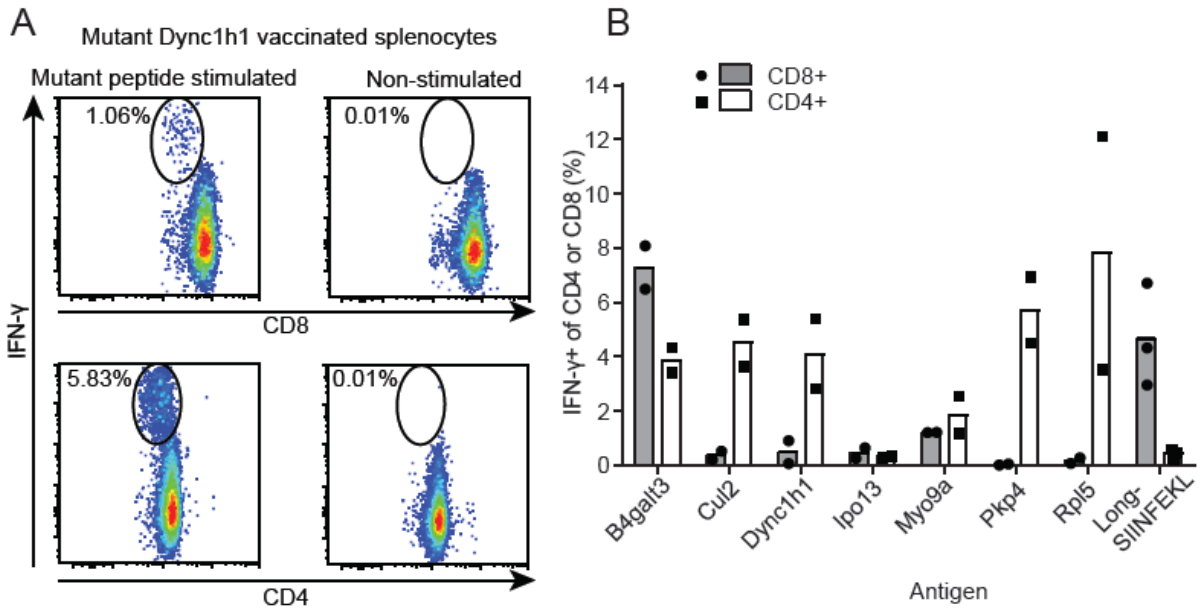

Figure 10. CD4 versus CD8 T cell responses to mutant peptide vaccines.
Mice (n = 2 per group) were vaccinated as in Figure 2. On day 28, splenocytes were harvested from vaccinated mice, incubated overnight in media containing the indicated mutant peptides or media alone, and analyzed by flow cytometry. Cells were gated on viability and lack of MHCII expression (activated murine T cells are MHCII negative). The percentage of IFN-γ-secreting CD8 and CD4 T cells was determined. **A.** Example of a mixed T cell response (CD8 *top* and CD4 *bottom*) to mutant Dync1h1 29mer peptide versus media alone. **B.** Summary of data for 7 mutant peptides and the positive control peptide long-SIINFEKL. Bars and dots represent mean and individual responses, respectively.

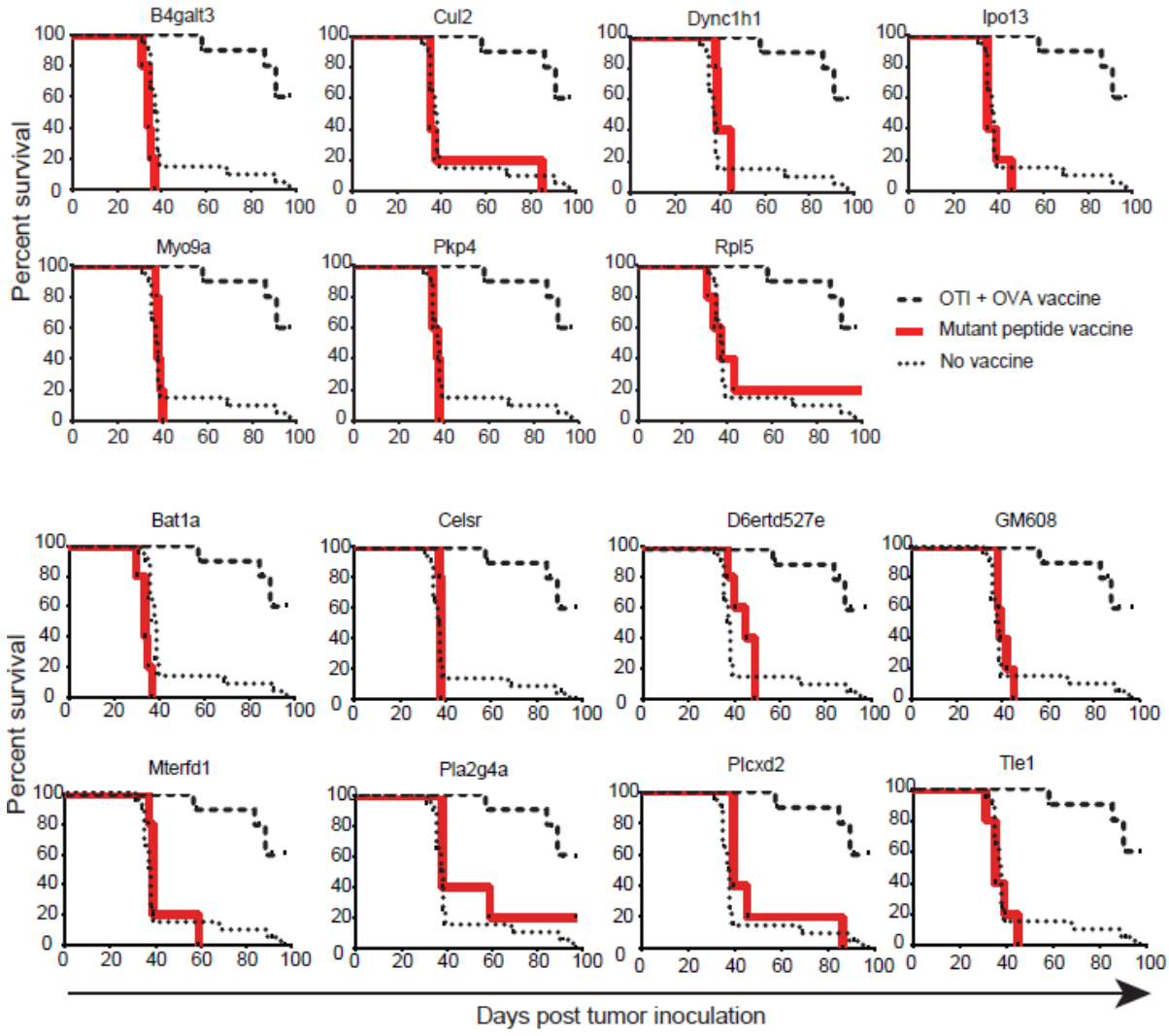

Figure 11. Therapeutic vaccination with mutant peptides.
Mice (n = 5 per group) received ID8-G7 tumor cells (10^6 cells) on day 0 and were therapeutically vaccinated on days 3 - 6 with individual mutant peptides (50µg) and poly(I:C) (10µg). As a positive control, one group was adoptively transferred OT-I splenocytes (10^5 cells) on day 2, followed by vaccination on days 3-6 with OVA protein (100 µg) and poly(I:C) (10 µg). Non-vaccinated mice served as negative controls. Each graph shows the survival of mice vaccinated with a single mutant peptide versus controls. Mice were euthanized once they displayed abdominal distension due to ascites.

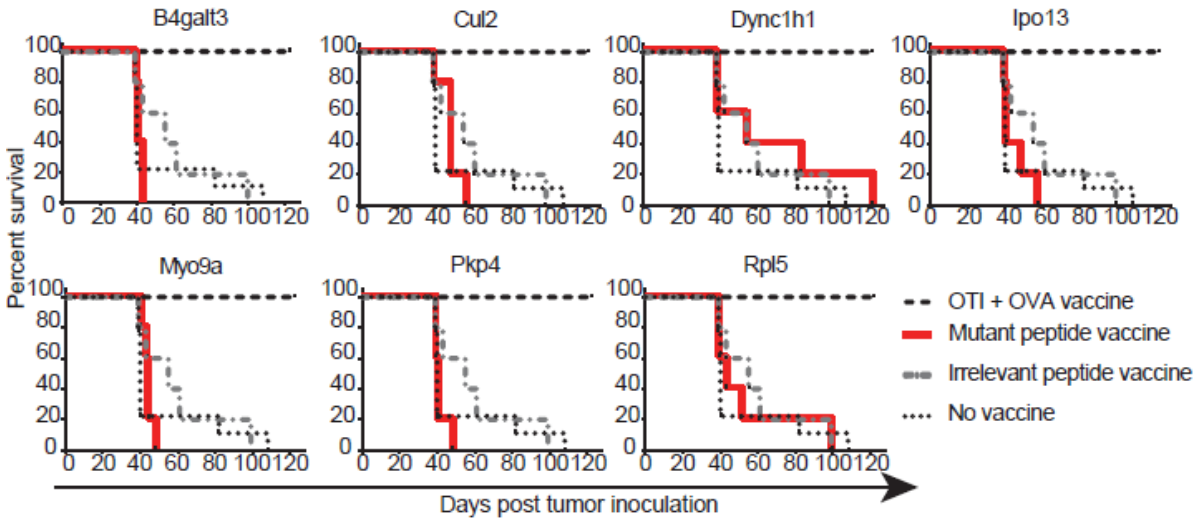

Figure 12. Prophylactic vaccinations with mutant peptides.
Mice (n = 5 per group) were vaccinated on days -28 to -25 and -7 to -4 with individual mutant peptides (25 µg) and poly(I:C) (10 µg). As in Figure 11, mice that received OTI and vaccination served as positive controls. As negative controls, one group was vaccinated with an irrelevant peptide, and a second group received no vaccination. On day 0, mice received ID8-G7 tumor cells (10^6). Mice were euthanized once abdominal distension due to ascites was observed.

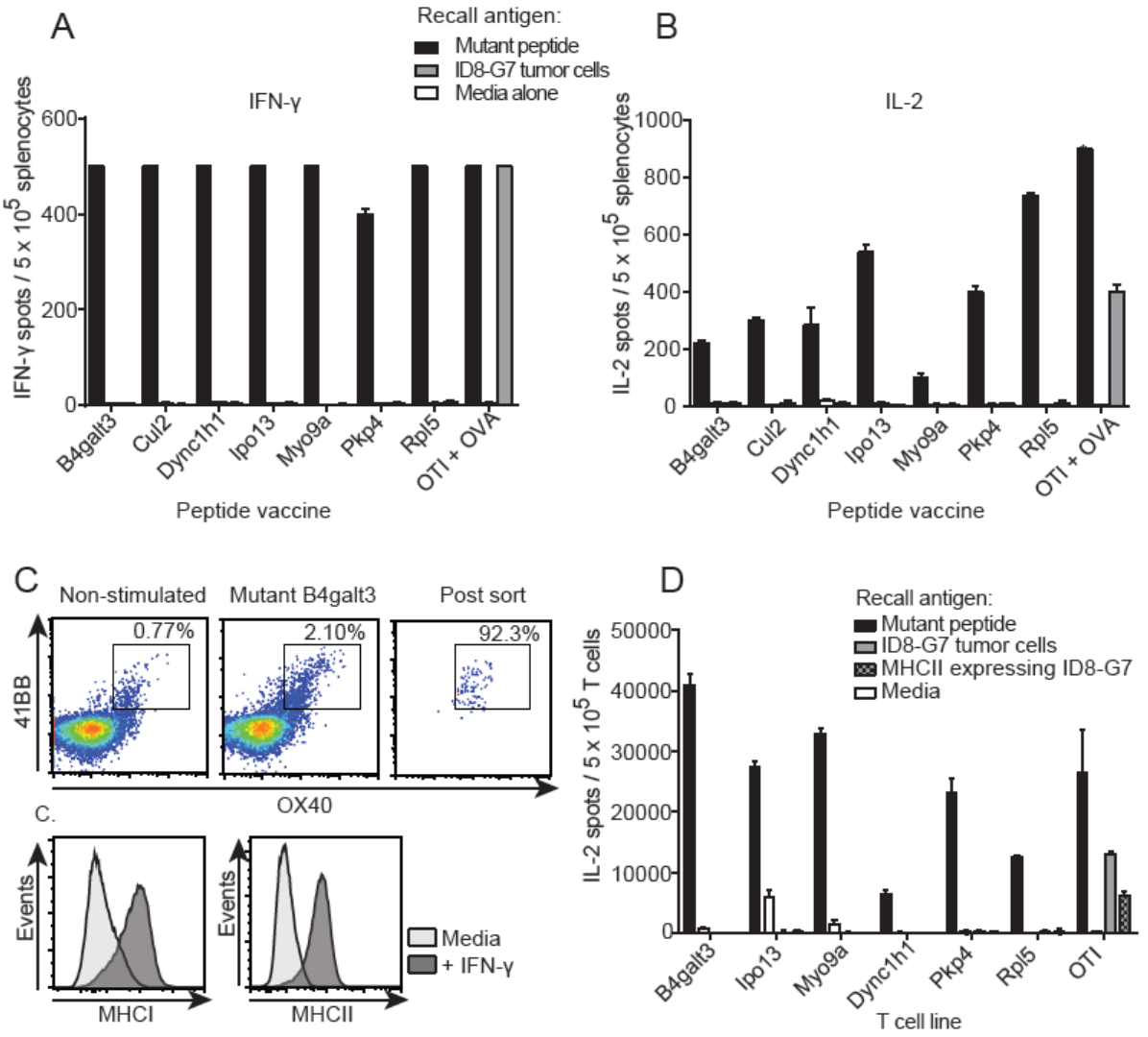

Figure 13. *In vitro* assessment of T cell reactivity to ID8-G7 tumor cells.
Mice were vaccinated as in Figure 2, and splenocytes were harvested on day 28. OT-I splenocytes were used as positive controls. Splenocytes (5×10^5 per well) were stimulated in duplicate with cognate mutant peptide (20 µg/ml), media alone, or ID8-G7 tumor cells (10^5 cells per well) and assessed by **A.** IFN-γ ELISPOT, or **B.** IL-2 ELISPOT. **C.** To assess tumor recognition by mutation-reactive CD4 T cells, 4-1BB$^+$OX40$^+$ CD4 T cells from the above mice were FACS purified and cultured in recombinant murine IL-2 (100 U/ml). ID8-G7 tumor cells were incubated in IFN-γ (100 U/ml) for 72 hours to cause up-regulation of MHCI and MHCII. Sorted and expanded CD4 T cells (10^4 per well) were stimulated in duplicate with cognate mutant peptide (20 µg/ml), media, ID8-G7 tumor cells or ID8-G7 tumor cells incubated in IFN-γ for 72 hours. OT-I T cells were used as a positive control for tumor cell recognition. Bars and lines represent mean and standard deviation of duplicate wells, respectively.

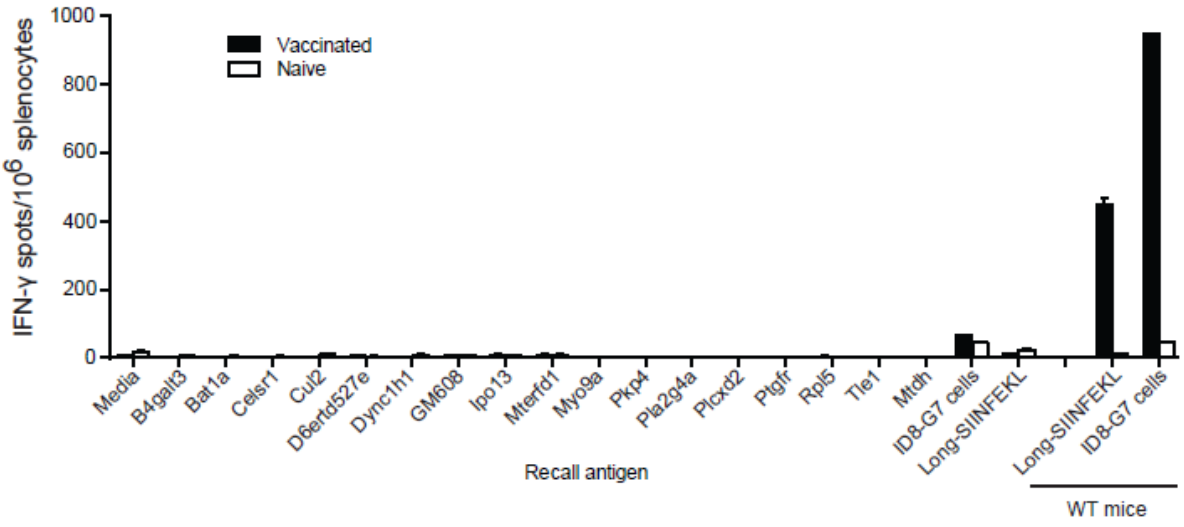

Figure 14. Tumor cell suspension vaccine and recall with mutant peptides. MMTV/neu-$^{OTI/OTII}$ mice (n = 3) were vaccinated with ID8-G7 tumor cell lysates (4 x 10^5 cell equivalents) and poly(I:C) on days 0 – 3 and days 21 – 24. On day 28, splenocytes were harvested and splenocytes of each group were pooled. Splenocytes (10^6/well were incubated with individual mutated peptides (20 μg/ml) or ID8-G7 tumor cells (10^5 cells/well) in ELISPOT assays. Lysate vaccinated wild type mice (n = 3) were used as positive controls as they are not tolerant to the SIINFEKL epitope nor to rat *neu.*

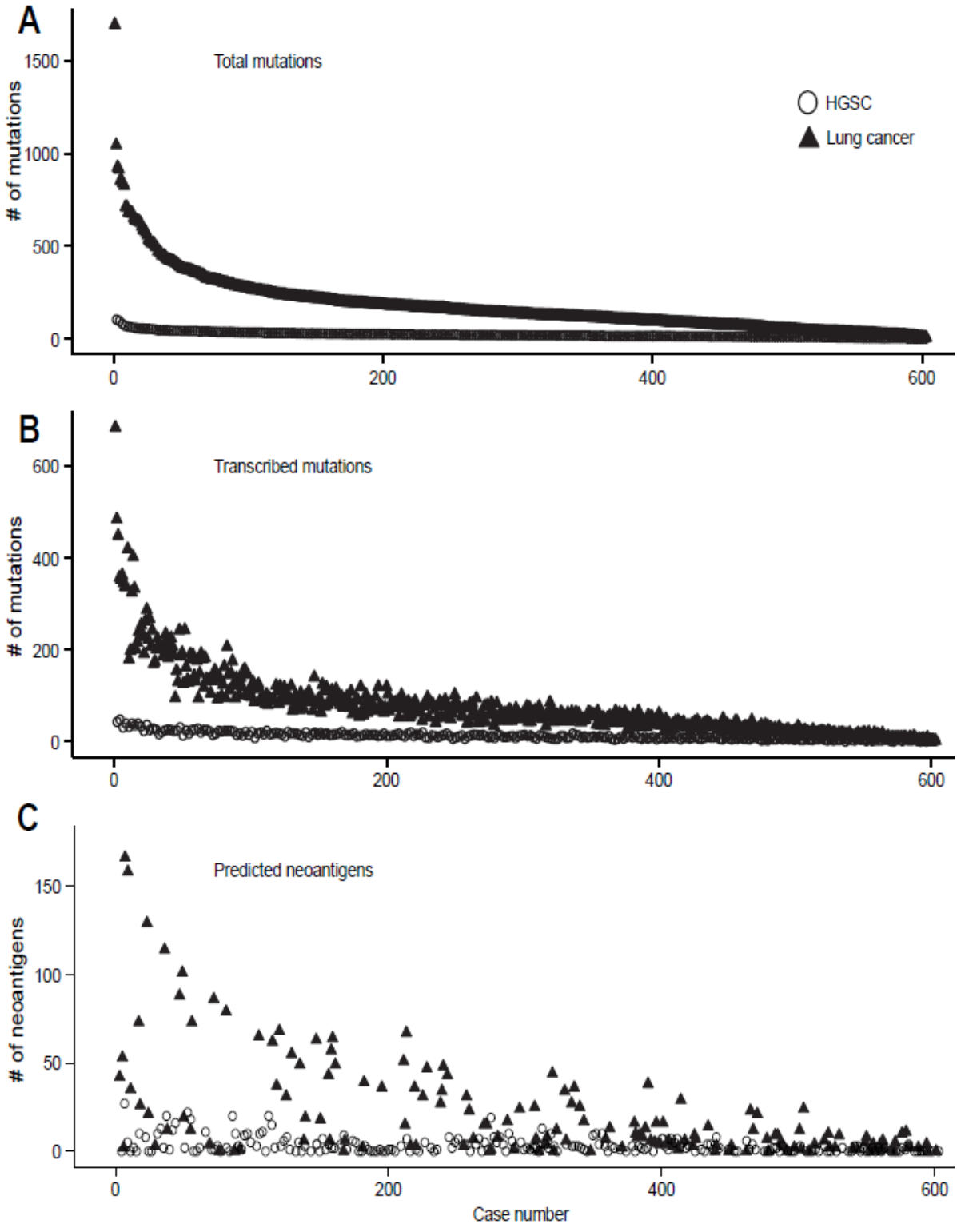

Figure 15. Mutation and neoantigen loads in human HGSC and lung cancer.

Figure 15. Mutation and neoantigen loads in human HGSC and lung cancer. Individual cases are aligned on the X axes in rank order according to the total number of mutations identified by whole exome sequencing (panel A); the same order of cases was used in panels B and C. Y axes indicate the number of mutations meeting the indicated criteria for each panel. Lung cancer cases (n = 603) are shown as solid black triangles, whereas HGSC cases (n = 274) are shown as hollow circles. **A.** Somatic, non-synonymous mutations identified by whole exome sequencing (total mutations). **B.** Somatic, non-synonymous mutations with at least one corresponding read in the RNA-seq data (transcribed mutations). **C.** Peptides predicted to bind autologous HLA-A with an IC50 < 100nM and containing somatic, non-synonymous, transcribed mutations. Only samples with unambiguous HLA-A allele calls are shown (lung n = 158, HGSC n = 220).

3.6 Tables

Table 3.1. Predicted epitopes and 29mer peptides selected for vaccination study							
Gene	aa substution	Predicted epitope	Score	H-2	¶Reads WT	¶Reads Mut	29mer peptide
1110021L09Rik	Y284S	LSLS**S**AISSPL	668	Kb	38	8	TGYVGLVFLGLSLS**S**AISSPLFGLLSDKM*
B4galt3	A21P	**P**VMMYLSLGGF	738	Kb	53	10	ERPCTLALLVGSQL**P**VMMYLSLGGFRSLS
Bat1a	S4P	MSF**P**GFFVV	699	Kb	79	15	MSF**P**GFFVVPSPSSSVGN**
Celsr1	P1063A	LNFTGAQV**A**RF	1100	Kb	33	33	VDIFDKLNFTGAQV**A**RFEDIQEELPRELE
Cul2	E222G	EYYKQ**G**ASNLL	1160	Kb	63	120	VSPFLTETGEYYKQ**G**ASNLLQESNCSQYM
D6Ertd527e	P233L	SS**L**RPSNRGSI	609	Db	2	1	SNTTTSSNSQSNSS**L**RPSNRGSISNYSNS
Dync1h1	V3088E	TSPALFNRC**E**L	434	Kb	208	114	KDRAATSPALFNRC**E**LNWFGDWSTEALYQ
Gm608	P947S	S**S**IESQSL	674	Kb	0	18	DMKSCTSANVLTPS**S**IESQSLVSQVSGLS
Ipo13	A165S	**S**LLELLTVL	1033	Db	1	176	QAEDSPVDSQGRCL**S**LLELLTVLPEEFQT
Mtdh	532_535del	**VTRHRQAQV**	614	Kb	0	60	SITLSKGDSDNSSS**HVTRHRQAQVKC*****
Mterfd1	K184T	I**T**QILLFL	1060	Kb	211	56	AANLLLRLDFEKHI**T**QILLFLKDLGLEDN
Myo9a	M2394V	VIVRLPS**V**	187	Kb	14	9	YPSPSSPVIVRLPS**V**SDVPEETLSSETAM
Pkp4	T1012I	FI**I**PVSTL	1119	Kb	212	93	SIYKKDGWNQNHFI**I**PVSTLERDRFKSHP
Pla2g4a	M234I	STWY**I**STL	352	Kb	204	88	CATYIAGLSGSTWY**I**STLYSHPDFPEKGP
Plcxd2	G280A	**A**GLKNTLV	634	Db	0	9	ILTPRVKTIARGLV**A**GLKNTLVHRNLPAI
Ptgfr	C121W	ISMVFSGL**W**PL	103	Kb	9	18	LCSIFGISMVFSGL**W**PLFLGSAMAIERCI
Rpl5	V159F	TGNK**F**FGAL	499	Kb	687	1753	YLDAGLARTTTGNK**F**FGALKGAVDGGLSI
Tle1	H393Y	AAYAGL**Y**SM	179	Db	0	39	NGELTSPGAAYAGL**Y**SMSPQMSAAAAAAA
OVA	N/A	**SIINFEKL**	392	Kb	N/A	N/A	**PDEVSGLEQLESIINFEKLTEWTSSNVME****
¶ Number of reads in RNA-seq data with the wild type (WT) or mutant (Mut) nucleotide							
* Peptide not tested due to inability to synthesize							
** Mutation occured in the 4th residue so 18mer peptide was assessed to ensure coverage of all possible mutated 15mers							
*** Frameshift deletion							
**** Model antigen used as positive control							

Table 1. Predicted epitopes and 29mer selected for vaccination

Chapter Four: Detection of neoantigen-specific T cells in human HGSC

4.1 Introduction

In the previous chapter, I showed in a murine model that vaccinations can activate T cells towards tumor-specific mutations; however, the activated T cells had no effect on survival of tumor bearing mice. Furthermore, by in silico analysis, I showed that just over half of human HGSC cases harbored no predicted high-affinity MHCI-binding neoantigens. On the other hand, these data also show that just under half of HGSC tumors *should* harbor predicted high-affinity MHCI-binding neoantigens. However, it is unknown how efficiently naive, neoantigen-reactive T cells get recruited into the anti-tumor immune response. For example, do HGSC tumors spontaneously activate neoantigen reactive T cells? If they do, are all possible neoantigen-reactive T cells found within the tumor, or does HGSC patient blood harbor activated or naive, neoantigen-reactive T cells that are prevented from infiltrating the tumor?

As discussed in Chapter 1, several studies have identified activated, neoantigen-reactive T cells within the TIL compartment [319,345,346,349]. However, T cells capable of reacting to authentic neoantigens may be prevented from entering – or they may be deactivated by – the hostile tumor microenvironment due to several reasons: (1) Tumor vasculature may downregulate expression of adhesion molecules, thereby preventing T cell extravasation [425]; (2) neoantigens may be presented in a non-inflammatory context, causing neoantigen-reactive T cell anergy [78]; (3) the tumor may recruit regulatory T cells, MDSCs, or TAM, leading to inhibited T cell response to stimuli [426]; and (4) the tumor and stroma may secrete anti-inflammatory cytokines, preventing activation of naive, neoantigen-reactive T cells [427]. For these reasons, patient peripheral blood may be an untapped reservoir of neoantigen-reactive T cells undetectable in the TIL compartment. Therefore, I hypothesized that (a) HGSC patients harbor activated, neoantigen-reactive T cells within both the TAL and peripheral blood compartments, and (b) peripheral blood contains additional naive neoantigen-specific T cells that are absent from the TAL compartment.

To test these hypotheses, a HGSC case was identified that had previously undergone whole exome sequencing and was found to harbor multiple mutations [428]. Aliquots of this

patient's live, Tumor Associated Lymphocytes (TAL) and peripheral blood mononuclear cells (PBMC) were available; thus, it was possible to assess this patient's activated and naive, neoantigen-reactive T cell repertoire within both the TIL and PBMC compartments. However, three interrelated challenges made identifying *naive*, neoantigen-reactive T cell particularly difficult: (1) Naive antigen-specific T cells exist in extremely low frequencies ($1/10^4$ to $1/10^7$) in peripheral blood [71,429,430]; (2) both TCR binding to cognate peptide/MHC, and T cell co-stimulation, are required to activate and expand naive T cells; (3) only two vials of this patient's PBMC were available from each of four blood draws. Since the detection threshold for immunological assays like ELISPOT and tetramer-based flow cytometry is about $1/10^4$ but naive T cell frequencies can be $1/10^7$, a method was required to both activate and enrich naive mutation-reactive T cells. As described in Chapters 2 and 3, vaccines can expand antigen-specific T cells *in vivo* to levels that are well within detection thresholds; however, the patient was not enrolled in a neoantigen-targeted vaccine clinical trial. Peptide-loaded, matured, autologous dendritic cells (DCs) can be used to selectively activate and expand antigen-reactive T cells *in vitro* [431]; however, DCs are rare in peripheral blood (< 1% DCs [432]), and insufficient patient PBMCs were available to stimulate T cells in this manner. FACS sorting using tetramers can be used to enrich for naive, antigen-reactive T cells [430]; however, tetramers for many HLA alleles are not yet available, and even if they were, limited amounts of patient blood precluded use of this method. The paucity of blood samples meant that a method was required to interrogate the complete repertoire of CD8 T cells within each vial of blood with minimal waste.

A promising alternative method had been published for identifying naive, neoantigen-specific CD4 T cells [433]. In this study, hundreds of parallel T cell cultures were polyclonally expanded, generating libraries of small-scale T cell cultures. Each culture was initially seeded with 2000 naive T cells, and these T cell cultures were expanded 1000- to 5000-fold. Therefore, after expansion, the frequency of each T cell clone in each culture theoretically remained at 1/2000, which is within immunological assay detection thresholds of $1/10^4$. Moreover, the total number of T cells in each culture was 5×10^6, a sufficient number of T cells for testing multiple antigens at 5×10^5 T cells/well in ELISPOT assays [433]. By assaying a library of 192 expanded T cell cultures, the study describing this technique assessed antigen reactivity of $2000 \times 192 = 3.8 \times 10^5$ initially naive T cells [433].

Thus, this study demonstrated a method to identify naive, antigen-reactive T cells within PBMC without requiring autologous stimulating cells, and this method was modified and applied to the current study.

In the current study, CD8 T cells – and not CD4 T cells – were assessed due to the following reasons: (1) CD8 T cells have direct cytotoxic effects on tumor cells and are thought to underlie many successful immunotherapies, whereas CD4 T cells can have both pro- and anti-tumor effects; (2) tumor recognition by CD8 T cells can be easily assessed using autologous tumor, whereas tumor recognition by CD4 T cells is more difficult to assess due to lack of MHCII expression on many tumors; and (3) epitope prediction algorithms are much more accurate for MHCI binding peptides compared to MHCII binding peptides. Therefore, CD8 T cells from three time points of *ex vivo* expanded TAL were assessed for recognition of patient tumor-specific mutations. A single mutated peptide (encoding a mutation in HSDL1) elicited a T cell response in the first ascites TAL, and this T cell clone recognized tumors from all three time points. However, this T cell clone was absent in all other TAL samples. Using the methods outlined by Geiger et al. [433], several additional mutation-specific T cells were detected in patient peripheral blood, including T cells that recognized mutant HSDL1. The T cells that recognized additional tumor mutations each failed to recognize tumor from any time point. In contrast, the blood derived mutant HSDL1 specific T cells recognized tumor from all three time points, and these T cells were identified in PBMC samples donated prior to tumor recurrence. This study indicates that tumors efficiently recruit and activate naive T cells capable of recognizing authentic neoantigens. Furthermore, the method presented here provides a framework for assessing and expanding neoantigen-reactive T cells from small quantities of peripheral blood and could be used to generate neoantigen-reactive T cell clones suitable for ACT.

4.2 Methods

Biospecimens and clinical data

The participant (IROC024) was enrolled with informed written consent in the BC Cancer Agency/Tumor Tissue Repository's "Immune Response to Ovarian Cancer" (IROC) study, which was approved by the Research Ethics Board of the BC Cancer Agency/University of British Columbia. Ascites samples were collected at primary surgery

and during palliative paracentesis. Ascites cells were separated from supernatant by centrifugation (300g x 10 min), and cryopreserved in 10% DMSO (Sigma: D2650), 50% FBS (Gibco: 12483-020), 40% complete RPMI + HEPES (Gibco: 22400-089) (supplemented with 10% FBS), 50 μmol β-mercaptoethanol (Sigma: M6250), 2 mmol L-glutamine (Hyclone: SH30034.01), and 1 mmol sodium pyruvate (Hyclone: SH30239.01). PBMC from IROC024 and healthy donors were isolated using density centrifugation with Ficoll (GE Healthcare: 17-1440-03) as previously described [434]. Cells were frozen first at -80°C in Mr. Frosty cases, then at -180°C in vapor phase liquid nitrogen. Patient HLA alleles were typed from exome sequencing data using published methods [335].

Epitope prediction and construction of peptide pools

NetMHCpan2.4 [32] was used to predict the binding affinity of mutated peptides to IROC024 *HLA* allele products. All possible mutated 8, 9, 10, and 11mers sequences spanning each mutation were assessed. All peptides that were predicted to bind the patient's MHCI with an IC50 < 50nM were purchased (crude, Genscript). In addition, for each mutation without a peptide predicted to bind with IC50 < 50 nM, the best predicted binding peptide (IC50 > 50 nM) was purchased. Thus every mutation was represented by at least one predicted MHCI-binding mutant peptide (Table 2). Peptides were solubilised in DMSO at 10 mg/ml. All peptides that encompassed the same IROC024 mutation were pooled into a single mutation-specific peptide pool. This resulted in 37 mutant peptide pools, each containing 1 to 13 peptides. Finally, aliquots of the 37 mutant peptide pools were pooled into a master peptide pool containing every predicted mutant-epitope (76 peptides in total). Pools of mutant 15mer peptides were also generated. Three 15mer peptides that overlapped by 11 amino acids were purchased for each mutation. This ensured that every mutant epitope 11 amino acids or smaller would be represented within at least one mutant 15mer peptide (Table 4-supplementary), allowing neoantigens that were not predicted to bind MHCI to be identified. For each mutation, the three mutant 15mers were pooled together resulting in 37 mutant 15mer pools. Finally, aliquots of each of the 37 pools were pooled together to make a master pool of 111 mutant 15mer peptides.

Generation of TAL lines from ascites

TAL were generated using a previously described protocol [80]. Briefly, bulk ascites were thawed in complete RPMI, washed, and re-suspended to 10^6 cells/ml in complete RPMI supplemented with 6000 U/ml of human IL-2 (generously provided by the National Cancer Institute, USA). Three ml of cell suspension was added to each well of a 6 well plate. Media was changed every two to three days, and cells were split as necessary to maintain concentration at approximately 10^6 cells/ml. After 2 weeks of T cell expansion in high dose IL-2, a modified rapid expansion protocol (REP) [80] was performed using irradiated (50 Gy) PBMCs from healthy donors (PBMC: T cell ratio = 100:1), IL-2 (300 U/ml [349]), and CD3 agonist antibody (30 ng/ml, eBioscience: 16-0037-85). T cells were expanded for two weeks and split to maintain concentration of 10^6 cells/ml. After two weeks, T cells were rested in low dose IL-2 (1 U/ml), to eliminate background IFN-γ secretion, and IL-7 (10 ng/ml (Peprotech: 200-07), to prevent T cell apoptosis.

Peripheral blood CD8 T cell expansion

Cryopreserved PBMC were thawed, washed, and resuspended in 3% FBS in PBS (Gibco: 20012-027). CD8 T cells were enriched by magnetic negative depletion using the CD8+ T Cell Isolation Kit (Miltenyi: 130-096-495) according to the manufacturer's protocol. Enriched cells were stained with viability-dye-EF780 (0.5 µl dye/2 ml cell suspension) (eBioscience: 65-0865-18), CD8-FITC (1/100, BioLegend: 300906) and CD4-PE (1/100, BioLegend: 357404) and assessed on a FacsCalibur flow cytometer using FlowJo analysis software (VX.07). Cells were counted using Viacount (Cat#: 4000-0130) on a Guava cell cytometer, and 2000 cells were added to each well of a round bottom 96 well plate. To serve as feeder cells, healthy donor PBMC were thawed, washed, irradiated (50 Gy), counted, and 2×10^5 cells were added to each well. Complete RPMI media was supplemented with human IL-2 (300 U/ml) and agonist CD3 antibody (30 ng/ml). Half of the media was removed and replaced with fresh media including additives on day 5 and every two days afterwards. Cells were split into replicate plates when cell pellets exceeded approximately 3 mm in diameter. After two weeks of expansion, one replicate plate was kept in reserve for future studies, and seven replicate plates were pooled using 96 well deep well tubes (Corning: 4408), keeping each original culture separate from all others. Pooled cultures were washed in complete

RPMI, re-suspended in resting media containing IL-2 (1 U/ml) and IL-7 (10 ng/ml), and distributed to 96 well flat bottom plates to rest. After 48 hours rest, replicate wells were pooled and washed in preparation for ELISPOT screens (described below). We dubbed this method "miniline" T cell expansion as it resulted in hundreds of T cell "lines" each derived from a "mini" aliquot of 2000 cells.

After the miniline ELISPOT screens, cultures that were mutation reactive were bulk-REP expanded. Wells from the reserve plate that corresponded to the mutation reactive wells in the ELISPOT were harvested. All of the T cells from each identified well were added to T25 flasks (Falcon: CA29185-300) and stimulated with IL-2 (300 U/ml), agonist CD3 antibody (30 ng/ml) and feeder cells (2 x 10^7 irradiated (50 Gy) PBMC from healthy donors) in 10 ml of complete RPMI. Cells were counted every two to three days and split as necessary to maintain cell concentration of 10^6/ml. After two weeks of expansion, cells were rested for two days in 1 U/ml of IL-2 and 10 ng/ml of IL-7. Aliquots of each bulk-REP expanded T cell culture were frozen at 2 to 20 million T cells/vial in 10% DMSO and 90% FBS.

IFN-γ ELISPOT assays

IFN-γ ELISPOT assays were performed according to the manufacturer's protocol (Mabtech). Briefly, nitrocellulose plates (MSIP, Millipore: MSIPS4W10) were incubated with 1/100 diluted IFN-γ capture antibody (mAb 1-D1K) (Mabtech: 3420-3-1000) in PBS overnight. Plates were washed with PBS and blocked for two hours with complete RPMI. Plates were washed again, and T cells were added to each well and stimulated with peptides or tumor cells as indicated in each section. After 20 hours of incubation at 37°C and 5% CO_2, cells were removed from ELISPOT plates using a multichannel pipette, and plates were washed with PBS containing 0.05% Tween20. Diluted secondary IFN-γ antibody (1/1000, Mabtech: 3420-6-1000) was added and incubated at 37°C and 5% CO_2 for two hours. Plates were washed again with PBS containing 0.05% Tween20, and developed with Vectastain Elite ABC kit (Vector Labs: PK-6100) and Vectastain AEC substrate reagent (Vector Labs: SK-4200). After 10 minutes, plates were rinsed with tap water, dried, and analyzed on an ELISPOT automatic plate reader (AID).

Miniline ELISPOT screens

The published study [433] demonstrating the utility of generating libraries of activated T cells to assess the naive repertoire used monocytes pulsed with protein antigens to stimulate T cell cultures, and it assessed reactivity based on [^{3}H]Thymidine incorporation [433]. However, for the current study, the lack of PBMC resources meant that monocytes were not available for stimulating T cell cultures. Since large peptides pools have been previously shown effective for identifying antigen-specific T cells [435], mutated-peptide pools were used as stimuli to identify mutation-reactive T cells in the current study. For each plate of miniline expanded T cell cultures, five replicate ELISPOT plates were used to assess reactivity to peptides. Five random cultures from each miniline plate were counted using Viacount on a Guava cytometer, and between 4 x 10^5 and 10^6 T cells were added to each ELISPOT well. One of the replicate ELISPOT plates was incubated with media alone as a negative control; one plate was stimulated with the minimal peptide pool (50 µg/ml); one plate was incubated with the 15mer mutated peptide pool (50 µg/ml); one plate was incubated with the MART1 minimal peptide (ELAGIGILTV) (Genscript) (5 µg/ml), and one plate was incubated with the CEF11 peptide (from EBV, GLCTLVAML) (5 µg/ml). Post hoc analysis of the pre-surgery ELISPOT screen indicated that a cutoff of > 13 spots and > 3-fold over background eliminated almost all false positive calls (positive in media wells). For example, miniline culture A1 would be considered mutation reactive if the A1 well on the mutant-peptide-stimulated ELISPOT plate contained > 13 spots and more than three-fold more spots than the average spot counts in well A1 on the media-stimulated ELISPOT plate and the A1 on the MART1 stimulated plate.

ELISPOT to identify specific mutation reactivity

The T cell response to the large peptide pool with all 37 mutations was deconvoluted to identify the single mutation that each bulk-REP expanded T cell line recognized. One million bulk-REP expanded T cells were added to each well of an ELISPOT plate. Duplicate wells were each stimulated with one of 37 minimal peptide pools comprised of all mutant peptides encompassing a single mutation (10 µg/ml). Alternatively, if a culture was identified as positive in the miniline screen in only the 15mer peptide stimulated well, the deconvolution ELISPOT assay was incubated with 37 mutant15mer pools, each comprised of three mutant 15mers encompassing a single mutation. Negative control wells were incubated

with media alone. Quadruplicate wells were incubated with either the full minimal mutant pool or the full 15mer mutant pool.

Tumor recognition ELISPOT

ELISPOT assays were used to assess whether sorted T cell lines recognized autologous ascites tumor cells. To enrich for tumor cells within bulk ascites samples, CD45 positive leukocytes were removed by magnetic separation with CD45 MicroBeads (Miltenyi: 130-045-801) according to the manufacturer's protocol. T cells (10^5) from each sorted T cell line were incubated with the cognate mutant peptide (5μg/ml), CD45 depleted ascites cells (2 x 10^4), and bulk ascites cells (10^5) from each time point. MART1 peptide was used as a negative control for each T cell line. Additionally, autologous CD40L activated B cells were used as negative control target cells, and CD40L activated B cells pulsed with cognate peptide were used as positive control target cells.

Generation of autologous CD40L activated B cells

Autologous B cells were generated as previously described [431]. Briefly, IROC024 PBMC (10^6 cells/well) were added to lethally irradiated (75 Gy) CD40-L cells (2.5 x 10^5 cells/well) (kindly provided by Dr. John Gordon) and cultured in Iscove's Modified Dulbecco's Medium (IMDM) with HEPES (HyClone: SH30228.01) supplemented with 10% heat inactivated human AB serum (Sigma: H4522-100ML), 1X Insulin Transferrin Selenium (ITS) (Corning: 354351), 2 mM L-glutamine, 50 μM β-mercaptoethanol, 100 U/ml Penicillin and 100 μg/ml Streptomycin (Hyclone: SV30010), 2 ng/ml human IL-4 (Peprotech: 200-04), and 1 μg/ml cyclosporine A (Sigma: C3662-5MG). Media was changed every 2 – 3 days as needed, and cells were split to maintain cell concentration of approximately 10^6/ml. Every 6 days, new CD40L cells were added to the cultures. Cultures were assessed by flow cytometry to determine the percentage of live cells that were CD19 positive (1/100, eBioscience: 11-0199-42).

Flow cytometry and FACS sorting

To sort mutation reactive T cells from frozen bulk-REP expanded T cell lines, the optimal resting conditions after thawing were determined empirically (Figure 30-supplementary). To isolate mutation reactive T cells, vials of bulk-REP expanded T cell lines

were thawed, allowed to recover for 24 hours in IL-2 (300 U/ml), and incubated with cognate peptide (10 µg/ml) for 24 hours. Cells were then washed in complete RPMI, and stained with fixable viability dye-V450 (1 µl/0.5 ml suspension, eBioscience: 65-0863-18). Cells were washed again and incubated with the surface staining antibodies CD8-FITC and 41BB-APC (1/100, BioLegend: 309810). Cells were assessed on an Influx cell sorter, and live, 41BB+CD8+ T cells were sorted into 200 µl of complete RPMI. FACS data were analyzed using FlowJo VX.07.

For Vβ spectratyping, sorted T cell lines were stimulated with cognate peptide for 24 hours, washed, and stained with viability dye-EF780. After 30 minutes incubation, cells were washed, and stained with surface antibodies for CD8-BV421 (1/200, BioLegend: 301036) and 41BB-APC. They were then divided into eight aliquots, each of which was stained with a different Vβ antibody cocktail (1/10, Beckman Coulter: IM3497) according to the manufacturer's protocol. The eight Vβ cocktails cover 70% of the Vβ repertoire. Cells were detected on a FacsCalibur flow cytometer and analyzed using FlowJo VX.07.

4.3 Results

IROC024 clinical course

IROC024 was considered a good candidate for studying neoantigen-reactive T cells due to five important characteristics: (1) The tumor and ascites were MHCI positive, allowing direct assessment of tumor recognition by T cells; (2) the tumor samples were previously shown by IHC to contain TIL, allowing interrogation of TIL specificity; (3) ascites had been donated at three time points, allowing assessment of the evolution of mutation reactive TIL over time; (4) blood had been donated at four time points, allowing investigation of T cell responses in peripheral blood over time; and (5) the tumor had been shown to harbour 37 missense mutations by whole exome sequencing [428], providing a target list of potential neoantigens.

The patient's clinical course is shown in Figure 16. The patient was initially treated with debulking surgery followed by chemotherapy with carboplatin and paclitaxel. Subsequently, the patient achieved biochemical remission for several months. However, the CA-125 level (a marker of tumor burden [436]) became elevated nine months post-surgery, indicating tumor recurrence. Another round of chemotherapy consisting of carboplatin and

gemcitabine was administered, and the disease went into a second remission. However, six months later, the CA-125 level rose again, indicating a second tumor recurrence. The patient received pegylated liposomal doxorubicin, but this proved ineffective. The patient succumbed to her disease 18 months after surgery (Figure 16).

The patient donated blood at the following time points: pre-surgery, three months post-surgery, six months post-surgery, and one year post-surgery. Ascites samples were collected at the time of primary surgery and each of the two recurrences (Figure 16). Whole exome sequencing had been performed previously on purified ascites-derived tumor cells from three ascites donation time points [428], and a total of 40 mutations were identified. Of these, 29 were stable over time, whereas the remainder disappeared (n = 7) or emerged (n = 4) over time. Three of these mutations resulted in premature stop codons that were not expected to give rise to T cell epitopes, leaving 37 potential neoantigens [428].

Identification of neoantigen-specific T cells in TAL

To determine whether IROC024 ascites harbored mutation-reactive T cells, TAL lines were generated from each of the three time points and assessed for mutation recognition. For each of the 37 patient mutations, epitope prediction was used to identify a set of potentially immunogenic mutated antigens. All mutant epitopes predicted to bind to autologous *HLA* allele products with an IC50 < 50 nM were assessed. For mutations without an epitope predicted to bind with IC50 < 50 nM, the best predicted MHCI binding mutant peptide was used (Table 2). Additionally, for each mutation, three overlapping 15mer peptides were used to provide an unbiased assessment of T cell reactivity, independent of epitope predictions. For each of the three ascites draws, TAL lines were generated using high dose IL-2 expansion followed by a REP, as previously described [80]. Peptides encompassing each mutation were used to stimulate expanded TAL lines in IFN-γ ELISPOT assays. Previously, the patient had been assessed for recognition of the CEF peptide pool (containing established minimal peptides from Cytomegalovirus (CMV), Epstein-Barr Virus (EBV), and Influenza Virus (IV)) and found to be highly reactive towards the CEF11 peptide. Therefore, CEF11 peptide and the CEF peptide pool were used as positive control stimulations. Of all the mutations and time points evaluated, we observed only one positive T cell response. Specifically, the TAL line from the first recurrent ascites sample recognized

both the predicted minimal epitope and the 15mer peptide pools encoding a point mutation (L25V) in HydroxySteroid Dehydrogenase-Like protein 1 ($HSDL1^{L25V}$) (Figure 17). There was no recognition of mutant HSDL1 in the primary or second recurrence TAL samples. Furthermore, no reactivity was found towards any of the other mutated peptides. Thus, of the 37 mutations in this patient's tumor, only one appeared to induce a T cell response identified in TAL, and only at one time point.

Although a T cell response was identified that recognized mutated peptides, to be an authentic neoantigen, the mutation-reactive T cells must also recognize tumor cells. Therefore, a mutant HSDL1-reactive T cell clone was generated by limiting dilution cloning. The clone was found to be highly reactive to the minimal epitope CYMEA**V**AL, and did not react to the wild type version of the peptide CYMEA**L**AL (Figure 18a). The HSDL1 mutant specific T cell clone was then assessed for recognition of autologous ascites tumor cells from each of the three time points. The T cell clone was slightly reactive to tumor cells from the primary time point and highly reactive to tumor cells from the first and second recurrence time points (Figure 18b). In an attempt to explain the variable reactivity to the tumor, the sequencing data were analyzed to determine the Variant Allele Frequency (VAF) of the HSDL1 mutation. The VAF was only 3.5% in the primary sample and > 50% in the first and second recurrences, which corresponded to the levels of tumor reactivity of the HSDL1 mutation-specific T cell clone (Figure 18c). Thus, the HSDL1 mutation was present in a minor subclone of the primary ascites tumor and became predominant in the first and second recurrence. Conceivably, the rapid expansion of this antigenic tumor clone may have triggered the HSDL1-specific T cell response observed at first recurrence. However, the T cell response was undetectable by second recurrence, despite continued expression of the mutant epitope.

Two explanations that most likely explained the apparent loss of the HSDL1 response at second recurrence were that the HSDL1 mutation-specific T cells became dysfunctional and unable to secrete IFN-γ, or they were physically absent from the ascites. Therefore, we sequenced the CDR3 region of the TCR-β chain on the HSDL1 mutation-specific clone, and performed CDR3 specific PCR amplification of ascites samples directly *ex vivo*. As expected, PCR successfully amplified the relevant CDR3 region from the first recurrence ascites. However, no PCR product was produced from the primary or second recurrence

samples. The limit of detection for this assay was estimated at $1/10^5$. Thus, the HSDL1 specific clone that was isolated was either absent or at exceedingly low frequencies in the primary and second recurrence samples.

Minilines to identify rare, antigen-specific T cells from peripheral blood

Despite the presence of mutant HSDL1 epitope on the primary and second recurrence ascites, the HSDL1 specific clone was absent from both of these samples. Therefore, I reasoned that other neoantigens could also be present on this tumor, despite a lack of corresponding T cells in TAL. I assessed PBMC from four blood donation time points to identify mutation-reactive T cells that were absent from TAL. The blood supply for IROC024 was very limited, so a method developed by Geiger et al. [433] was adapted for interrogating antigen specificity of peripheral blood CD8 T cells. The protocol was first piloted using *HLA-A2+* healthy donor PBMCs. CD8 T cells from a healthy donor were purified by negative magnetic depletion, and 2000 cells were seeded into each well of two 96 well plates (4×10^5 cells among 192 wells). Each miniline culture was REP expanded 1000- to 5000-fold into replicate plates, keeping each culture segregated. After expansion, cells were rested, and each of the 192 cultures was stimulated with the following antigens in IFN-γ ELISPOT assays: media as a negative control, CEF11 peptide as a positive control, MART1 peptide (to test for responses of high-frequency, naive T cells), and the IROC024 mutant peptide pool (work flow is shown in Figure 19a). For example the miniline culture in well A1 of plate 1 was distributed among five A1 wells in five ELISPOT plates, and each full ELISPOT plate was incubated with one of the antigens. Among 192 miniline cultures, five were MART1-reactive. Since MART1 T cells are naive in most healthy donors [437], the method was deemed effective for expanding and identifying naive, antigen specific T cells (Figure 19b). Additionally, 19 wells were CEF11 reactive, indicating that activated or memory cells could also be expanded and detected using this method (Figure 19b). Thus, the miniline approach proved effective for identifying both naive and activated antigen-specific T cells.

Identification of mutation-reactive CD8 T cells from PBMC

The miniline method was next used to interrogate IROC024 peripheral blood for mutation-specific CD8 T cells. Patient PBMC from each of four time points were thawed and enriched for CD8 T cells. Purity was $\geq$ 80% for each of the cultures, as assessed by flow cytometry (Figure 20a), and a total of 2.7 x 10^6 CD8 T cells among the four time points were seeded into 96 well plates as described above (2000 cells/culture, 1344 separate cultures). Each miniline was expanded into replicate plates, and one of each of the replicate plates was retained in reserve for future studies. Each miniline was stimulated with five antigens in IFN-γ ELISPOT assays: media alone, CEF11 peptide as a positive control, MART1 peptide, a pool of all predicted minimal binding mutant peptides, and a pool of overlapping 15mer mutant peptides. All wells were positive for CEF11 responses, indicating a high frequency of T cells in this patient that recognized this antigen. Furthermore, I identified 23 MART1 reactive wells from 8 x 10^5 CD8 T cells in the pre-surgery time point (Supplementary 29a) for a frequency of 1/~35,000, which is within the range for *HLA-A2+* healthy donors [433]. Since MART1 is a melanoma differentiation antigen and unlikely to be expressed on HGSC, this provided further evidence that the miniline approach could activate and identify naive T cells in patient PBMC. As for the peptide pools encoding the 37 mutations, a total of 27 positive T cell minilines were identified across the four time points and advanced to further analysis below (Figure 21, Figure 29-supplementary, and Table 3).

Identification of the specific mutations recognized by T cells

The miniline ELISPOT screens were performed in singlicate, so additional assays with increased numbers of cells were necessary to confirm mutation-reactivity and identify which specific mutation elicited the T cell response in each positive culture. Therefore, for each positive miniline culture, T cells from the corresponding well of the reserve plate were harvested and bulk-REP expanded. The cells expanded several hundred-fold over the course of two weeks, and aliquots of expanded T cells were frozen.

To confirm mutation reactivity and identify the specific mutation recognized by each of the 27 T cell lines, each bulk-REP expanded T cell line was assessed by IFN-γ ELISPOT for recognition of each of the 37 minimal epitope pools, each corresponding to all peptides encompassing the individual mutation. Three examples are shown in Figure 22. T cell line

4H2 recognized the NOX4-mutant peptide pool. T cell line 4C5 recognized the HSDL1-mutant peptide pool. T cell line 4D12 proved to be non-reactive. In total, 15 of the 27 bulk-REP expanded T cell lines responded to individual mutant peptide pools, whereas the remaining 12 lines were unresponsive to any of the mutations (Table 3). These unconfirmed T cell responses may have been false positives, or the antigen reactive T cells may have failed to expand in culture to reach detectable levels. In summary, 15 cultures were confirmed to react to a specific mutant peptide pool. In total, seven mutations were recognized and involved the genes KIAA1467 (n = 2 T cell lines), NOX4 (n = 2), CAPN7 (n = 1), ZNF41 (n = 1), MARK2 (n = 1), OR4C11 (n = 1), and HSDL1 (n = 7). As for the HSDL1 mutation specific T cell response in blood, one clone was identified in the pre-surgery sample, one in the three month sample, five in the 6 month sample (immediately prior to the first recurrence), and none in the one year sample.

Isolation of mutation-reactive T cells

To determine whether any of the 15 mutation-reactive T cell lines recognized autologous tumor, highly enriched T cell cultures of each mutation reactive T cell clone were required. Therefore, each bulk-REP expanded T cell line was FACS-purified based on peptide-induced CD137 expression and expanded to sufficient numbers for IFN-γ ELISPOT assays against tumor samples. An example FACS plot of CD137 upregulation is shown for the T cell line 4H2 stimulated with the mutant NOX4 peptide pool (Figure 23). After expansion, 11 of 15 sorted T cell lines were highly reactive to cognate peptides, and four of the sorted T cell lines were not reactive, indicating the original responding T cell clone had been lost during expansion. Examples of a reactive T cell line (4H2) and non-reactive T cell line (1D4) are shown in Figure 24a. Of the 11 successfully expanded T cell lines, seven recognized mutant HSDL1, and the four remaining lines recognized mutations in NOX4, CAPN7, ZNF41, and OR4C11 (Table 3).

To assess the frequency of each mutation reactive T cell clone within each sorted T cell line, cultures were analyzed by flow cytometry using a set of antibodies designed to discern the Vβ gene usage by T cells. Since a given T cell clone expresses only one of 47 functional Vβ genes [438], the frequency of T cells that express a specific Vβ can be used as a proxy to estimate the clonality of T cell cultures. An example of Vβ staining is shown in

Figure 26b for sorted T cell line 4H2. For each sorted T cell culture, 40% – 94% of the T cells expressed the same Vβ, indicating that these T cell lines were highly enriched for a single T cell clonotype (Table 3). Vβ combined with 41BB staining performed on peptide-stimulated cultures confirmed that T cells expressing the dominant Vβ were antigen specific. Four different Vβ were identified among the seven HSDL1-reactive T cell clones, indicating this mutant antigen was recognized by at least four distinct T cell clones. Figure 26c shows an example of sorted T cell line 4H2 stimulated with peptide and stained with Vβ and 41BB antibodies. In summary, I successfully generated 11 T cell lines containing mutation-reactive T cells at frequencies adequate for assessing tumor reactivity.

Identification of the minimal epitope recognized by each T cell line

Since each sorted T cell line had been stimulated with pools of all predicted minimal epitopes encompassing a single mutation, I next determined the minimal epitope recognized by each T cell line using IFN-γ ELISPOT assays. Each of the 11 sorted T cell lines was stimulated with individual minimal and 15mer mutant peptides that comprised the individual mutation peptide pool. The minimal epitope was operationally defined as the shortest peptide that elicited a response. Two examples (4H2 and 4C5) of minimal epitope identification are shown in Figure 25, and the epitope recognized by each T cell culture is listed in Table 3. Mistakenly, a typo meant that the peptide **R**SRSSSLGNK was ordered and used in addition to the true mutation **C**SRSSSLGNK found within the WNK1 gene. A sorted T cell line (1A10) was generated using the above methodology, but it recognized the typo and not the mutant or wild type version of the peptide. In subsequent experiments, this WNK1 typo-specific sorted T cell line was used as a negative control for tumor recognition experiments, since it would not be expected to recognize tumor.

T cell recognition of ascites tumor cells

To determine whether the sorted T cell lines recognized autologous tumor cells, I first assessed each of the HSDL1 reactive sorted T cell lines for reactivity to each time point of ascites in IFN-γ ELISPOT assays. As a positive control, I used the T cell clone (clone 1) that was derived from the first recurrent ascites sample and was previously shown to be tumor reactive (Figure 17). Similar to clone 1, each of the HSDL1 mutation-reactive sorted T cell

lines responded weakly to the primary ascites sample, highly to the first recurrent ascites sample, and variably to the second recurrent ascites sample (Figure 26). Thus, all seven HSDL1-specific T cell clones recognized autologous tumor cells with similar intensity and temporal dynamics.

Next, I assessed the tumor-reactivity of the four T cell lines that recognized mutations other than HSDL1. To increase confidence that any reactivity observed would be due to recognition of tumor rather than contaminating leukocytes, CD45 positive cells were magnetically depleted from ascites. For each ascites sample, CD45 contamination was reduced from 85% pre-depletion to less than 10% post-depletion (Figure 27). In IFN-γ ELISPOT assays, mutation-specific sorted T cell lines were stimulated with CD45 depleted ascites cells (2×10^4) and bulk ascites cells (10^5) from each time point. Minimal cognate peptide and minimal peptide-pulsed autologous B cells were used as positive control targets, and MART1 peptide and non-peptide pulsed B cells were used as negative control targets. A MART1 specific sorted T cell line and the WNK1-typo-specific (1A10) T cell line were used as negative controls, and an HSDL1-specific line (2D1) that proved tumor reactive in the previous experiment was used as a positive control. As expected, the negative control sorted T cell lines recognizing MART1 and WNK1-typo failed to recognize ascites from any time point. Also as expected, the positive control HSDL1-specific sorted T cell line (2D1) was weakly reactive to the primary ascites and highly reactive towards the first and second recurrent ascites samples (Figure 28). In contrast, each of the sorted T cell lines specific for mutations other than HSDL1 failed to recognize ascites cells from any time point (Figure 28). Thus, is appears that the HSDL1 mutation gave rise to the only bonafide MHCI epitope expressed by tumor cells and recognized by autologous T cells.

4.4 Discussion

To identify and assess T cell responses to the evolving mutation landscape in an ovarian cancer patient, I examined the naive and activated T cell responses to tumor-specific-mutations in patient IROC024 ascites and blood samples. A single T cell reactivity towards a mutant epitope (mutant HSDL1) was discovered in TAL from the first recurrent ascites, and a mutant HSDL1 T cell clone was derived that recognized tumor from each of the three ascites time points [439]. I adapted a published protocol [433] for activating and assessing

naive T cells and generated seven mutant-HSDL1 reactive T cell lines from peripheral blood: one from pre-surgery, one from three months post-surgery, and five from six months post-surgery. Further, I generated eight additional T cell lines that recognized six other mutations. High purity sorted T cell lines that recognized mutations in HSDL1, NOX4, CAPN7, ZNF41, and OR4C11 were assessed for tumor recognition. While each of the HSDL1-reactive T cell lines recognized all ascites tumor samples, all of the other mutation-reactive T cell lines failed to recognize any tumor sample. These data show that only the HSDL1 mutation gave rise to an authentic neoantigen, and this neoantigen induced a spontaneous T cell response that was detectable in both ascites and PBMC. This study provides the first assessment of both the activated and naive neoantigen-reactive T cell repertoire in HGSC. Further, this study indicates that spontaneous T cell activation towards authentic neoantigens is efficient, as the only authentic neoantigen elicited T cells detected in blood and in the ascites.

In this study, all mutant peptides were found to be cryptic when the corresponding T cells were undetectable in the ascites. This indicates that immunotherapies designed to activate naive neoantigen-reactive T cells may result in immune responses unable to recognize tumors. In contrast, studies to further expand or maintain activated neoantigen-reactive T cells may promote anti-tumor immunity by targeting only authentic neoantigens. One method to potentiate activated T cells is with PD-1 blockade [170], and studies have shown that responses to this therapy are associated with increased mutation load [331]. My data suggest that the success of this therapy may be due to neoantigen-specific T cell potentiation, rather than activation of *de novo* T cell responses. An example of this was seen in a case report of a patient who responded to Ipilimumab. It was found that the neoantigen-reactive T cell response identified in TIL after treatment was also present in PBMC prior to treatment (at a frequency of 0.08%) [344], indicating that these T cells had been activated spontaneously and prior to checkpoint blockade therapy [344]. My data show that the spontaneous HSDL1-mutation specific T cell responses ultimately failed to control tumor growth, as it was absent in the ascites from the second time point. One can speculate that checkpoint blockade therapy may have helped this patient by improving persistence of these T cells.

The current study highlights patient peripheral blood as an alternative source for tumor neoantigen reactive T cells, which may be utilized for ACT clinical trials. Many patients are deemed ineligible for TIL-ACT trials because TIL cannot be acquired. For example, surgical resection may be contraindicated due to the anatomical location of the tumor [440] or morbidity associated with tumor resection [441]. However, cancer patient peripheral blood is easily accessible and could be used as an alternative source of tumor reactive T cells. One group stimulated patient PBMCs *in vitro* with irradiated autologous tumor cells and generated T cell products for ACT [442]. A subset of patients treated with these T cells experienced clinical responses, demonstrating that peripheral blood can be used as a source of therapeutic T cells [442]. Clinical response can be elicited by adoptive transfer of near-clonal populations of neoantigen reactive T cells [101], and my study expands the number of potential patients eligible for such treatments by generating neoantigen-reactive T cell lines from small quantities of peripheral blood.

In addition to generating T cell clones from peripheral blood for ACT, neoantigen-reactive T cells could be monitored in peripheral blood to assess tumor burden. I found that the HSDL1 reactive T cell response was amplified at the six month blood draw ($5{:}10^6$ at six months versus $1{:}8x10^5$ at both pre and three months). Intriguingly, the six month blood draw was three months prior to detecting increased CA-125 levels and tumor recurrence (Figure 16); thus, the expansion of HSDL1 reactive T cells foreshadowed tumor recurrence and could have served as an early warning that the tumor was growing. With the ever decreasing cost of NGS and the ever improving technologies for identifying antigen specific T cells [433,443], identifying a *de novo* T cell response to a tumor mutation could augment current biochemical and imaging strategies to warn of impending tumor recurrence.

It is notable that the HSDL1 T cell expansion in peripheral blood coincided with an increase in the frequency of mutant HSDL1 positive tumor cells in IROC024, from 3.5% in the primary to 60% in the first recurrence (Figure 18). The sudden appearance of a large quantity of antigen may have sparked the HSDL1-specific T cell expansion. Ultimately, the T cell response failed to persist, demonstrating the anti-immune effects tumors may exert. In Chapter 5 (Conclusions), I will further discuss the evolution of T cell responses to the changing mutation landscape of tumors.

Due the limited number of PBMC samples for IROC024, we assessed peripheral blood CD8 T cells by adapting a published protocol for interrogating naive CD4 T cells [433]. In contrast to strategies that require large amounts of blood to generate autologous dendritic cells [431], the miniline approach maximized the proportion of CD8 T cells that could be interrogated for antigen reactivity. Thus, this method could be useful in situations where blood volumes are limiting. For example, patients with autoimmune diseases, or highly advanced tumors often become lymphopenic [444]. Moreover, patients involved in clinical trials are often capable of donating only small amounts of blood. The miniline approach could be applied to these patients to identify rare, antigen-specific T cells.

Despite the benefits of minilines for identifying rare, antigen-specific T cells from small quantities of peripheral blood, there are drawbacks to this approach for detecting the full complement of naive neoantigen-reactive T cells. For example, the low throughput of this method (i.e., 100 ELISPOT plates to analyze 4 x 10^6 originally naive cells) compared to high throughput techniques that use large quantities of blood meant that several mutation-reactive T cells were probably overlooked due to the small sample size analyzed. Indeed for most mutations recognized by T cells, only one mutation-specific T cell clone from one time point was identified, but these T cells were probably circulating at all time points. Another drawback of the miniline approach was a lack of antigen-specific T cell enrichment during expansion, which probably led to some mutation-reactive T cells becoming undetectable. For example, methods using antigen pulsed dendritic cells specifically expand T cells of interest, resulting in high frequencies of antigen-specific T cells in positive cultures [431]. In contrast, the miniline approach polyclonally activates all T cells [433]; thus, mutation-reactive T cells had no competitive growth advantage over irrelevant T cells. Moreover, during miniline expansion, anergic/exhausted tumor-reactive T cells would have a competitive growth disadvantage compared to non-anergic T cells [78]. Indeed, proliferation of each T cell was highly variable: even when investigating a single antigen – MART1 – the frequency of antigen-reactive T cells in positive cultures ranged from 14 to more than 800. Moreover, since some of the confirmed mutation-reactive T cell responses were right on the threshold of positivity in the ELISPOT screen (for example miniline culture 2G2 had only 14 spots/well), some mutation-reactive T cells were likely overlooked as they were just under the detection threshold. Expanding antigen-reactive T cells using dendritic cells overcomes many of the

challenges associated with miniline T cell expansion [431]. Alternatively, sorting tetramer positive CD8 T cells and cloning them directly from PBMC removes differential T cell expansion from the calculus [430]. Unfortunately, these techniques require large quantities of peripheral blood. Nonetheless, future efforts to interrogate the proportion of mutations that give rise to neoantigens should focus on patients with sufficient quantities of PBMC to make use of these superior techniques. On the other hand, the miniline approach provides a feasible means to identify antigen-specific T cells when blood samples are limited.

Authentic neoantigen-reactive T cells recognizing mutant HSDL1 were identified in the ascites and peripheral blood of a HGSC patient. However, the other evaluated mutations failed to give rise to authentic neoepitopes expressed by tumor cells. The reasons for the lack of tumor recognition are being investigated. To determine whether the mutated genes were expressed by the tumor, I will perform qPCR on ascites to determine the level of RNA expression of each mutant gene. To determine whether putative mutant epitopes were generated by antigen processing machinery, I will transfect autologous B cells with IVT-RNA encoding each mutation and test for T cell recognition of a non-malignant cell. Finally, to determine whether antigen processing defects within the tumor cell may prevent antigen processing of the mutant epitope, I will transfect autologous ascites cells with IVT-RNA of each mutation and test for recognition by T cells.

In summary, the data from this study indicate that spontaneous activation of authentic neoantigen-reactive T cells is efficient. Moreover, our findings suggest that the most useful immunotherapies will be those that potentiate spontaneously-activated neoantigen-reactive T cells. Finally, the miniline method proved effective for identifying rare, activated neoantigen-reactive T cells from small quantities of blood and may represent a viable alternative for generating neoantigen-reactive T cell clones for ACT in cases where blood volume is limiting.

4.5 Figures

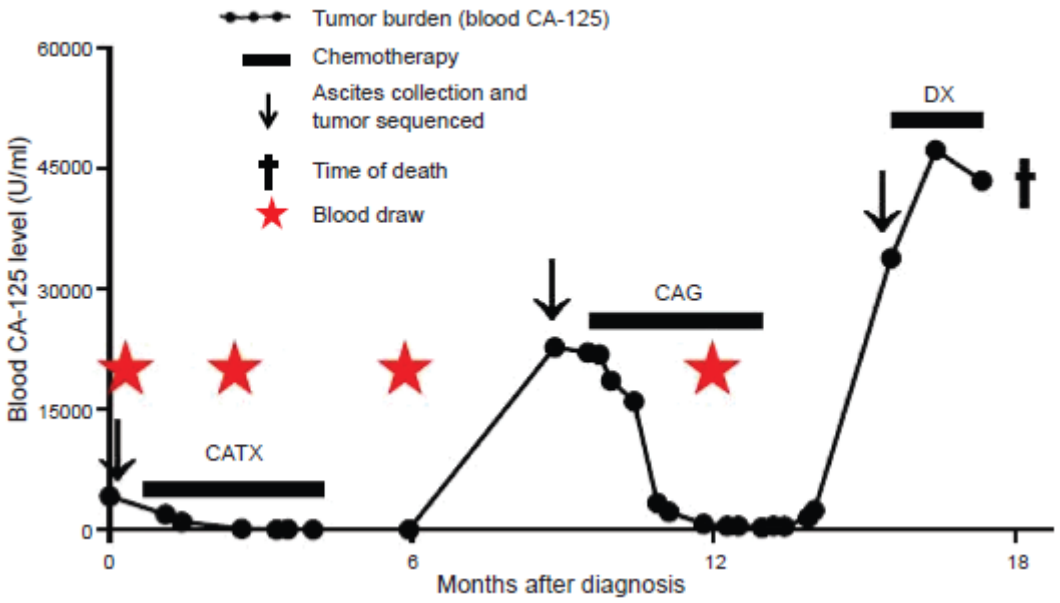

Figure 16. IROC024 clinical course.
(Figure modified and reproduced with permission from CCC [439]) Patient was enrolled in our centre's study on the Immune Response to Ovarian Cancer (IROC) at time point 0 and assigned a de-identification number (IROC024). The line and dots represent the measured blood CA-125 levels as a surrogate for tumor burden. Horizontal lines indicate the time of chemotherapy treatment. Arrows represent time points when ascites samples were donated, the cross represents time of death, and the red stars represent blood donations.

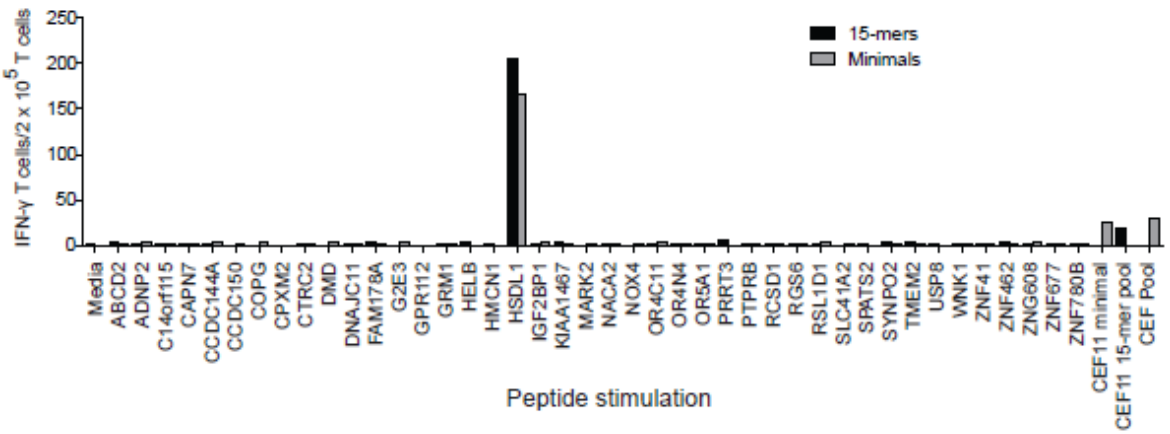

Figure 17. Mutation-specific T cell responses in the first recurrent ascites.
(Figure modified and reproduced with permission from CCC [439]) IROC024 ascites cells were incubated with 6000 U/ml of IL-2 to expand TAL and subsequently REP expanded. Resultant T cells (2 x 10^5/well) were stimulated with predicted MHCI binding peptides and overlapping 15mer peptides encompassing each mutation in an IFN-γ ELISPOT assay. The CEF peptide pool, the CEF11 minimal peptide, and a 15mer encompassing the CEF11 epitope were used as positive controls.

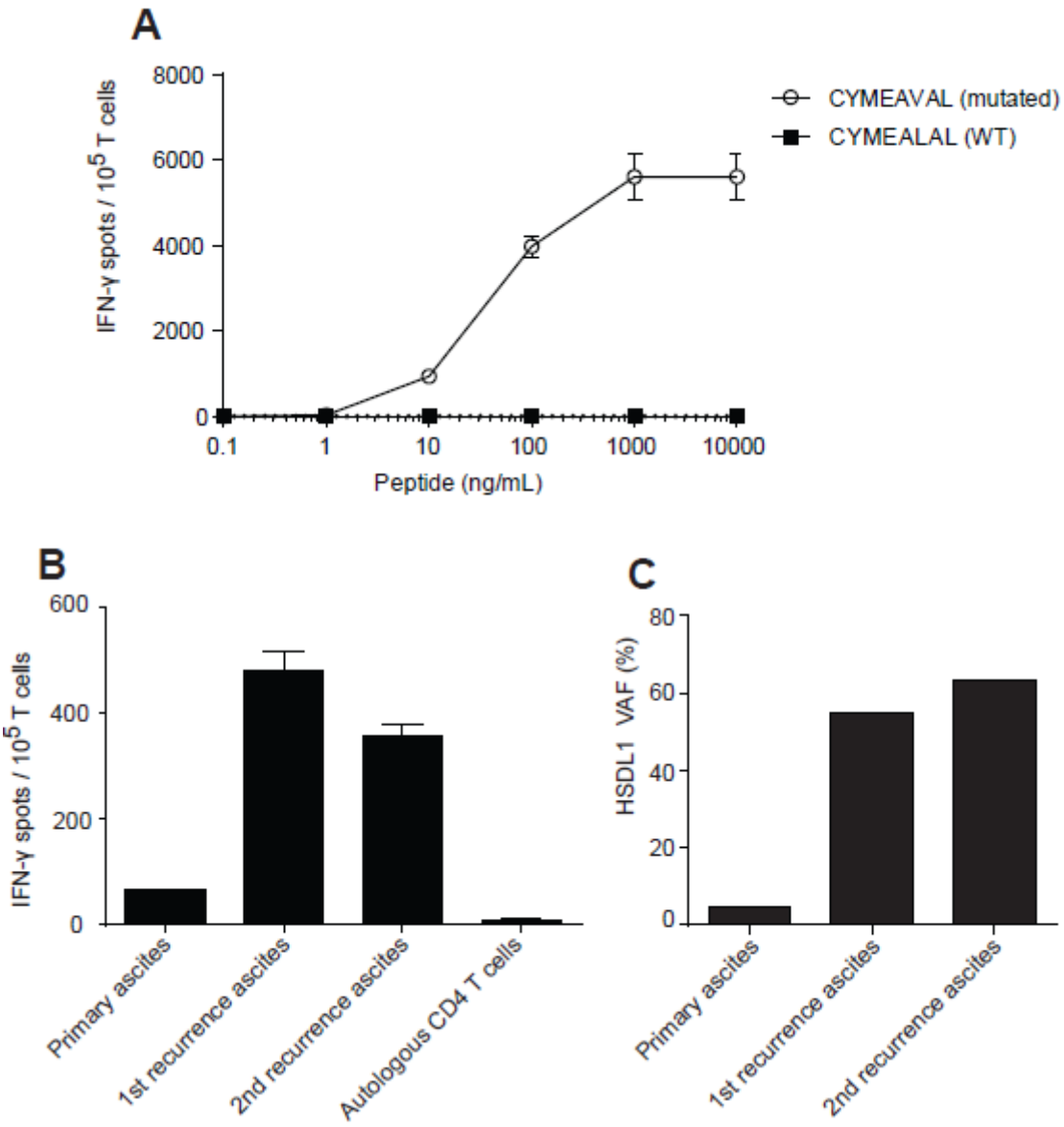

Figure 18. T cell reactivity to WT peptide and tumor, and VAF of HSDL1 mutation. **(**Figure modified and reproduced with permission from CCC [439]) **A**. A T cell clone that recognized mutant HSDL1 was stimulated in an ELISPOT assay with decreasing concentrations of the mutant (CYMEA**V**AL) and wild type (CYMEA**L**AL) peptides. **B**. The HSDL1 mutation-reactive T cell clone was stimulated with 5 x 10^4 purified tumor cells from the primary, first recurrence, and second recurrence ascites samples and measured by IFN-γ ELISPOT assay. Autologous CD4 T cells were used as negative control target cells. **C**. The variant allele frequency (VAF) of HSDL1 was determined from targeted re-sequencing data for each of the three ascites sample time points.

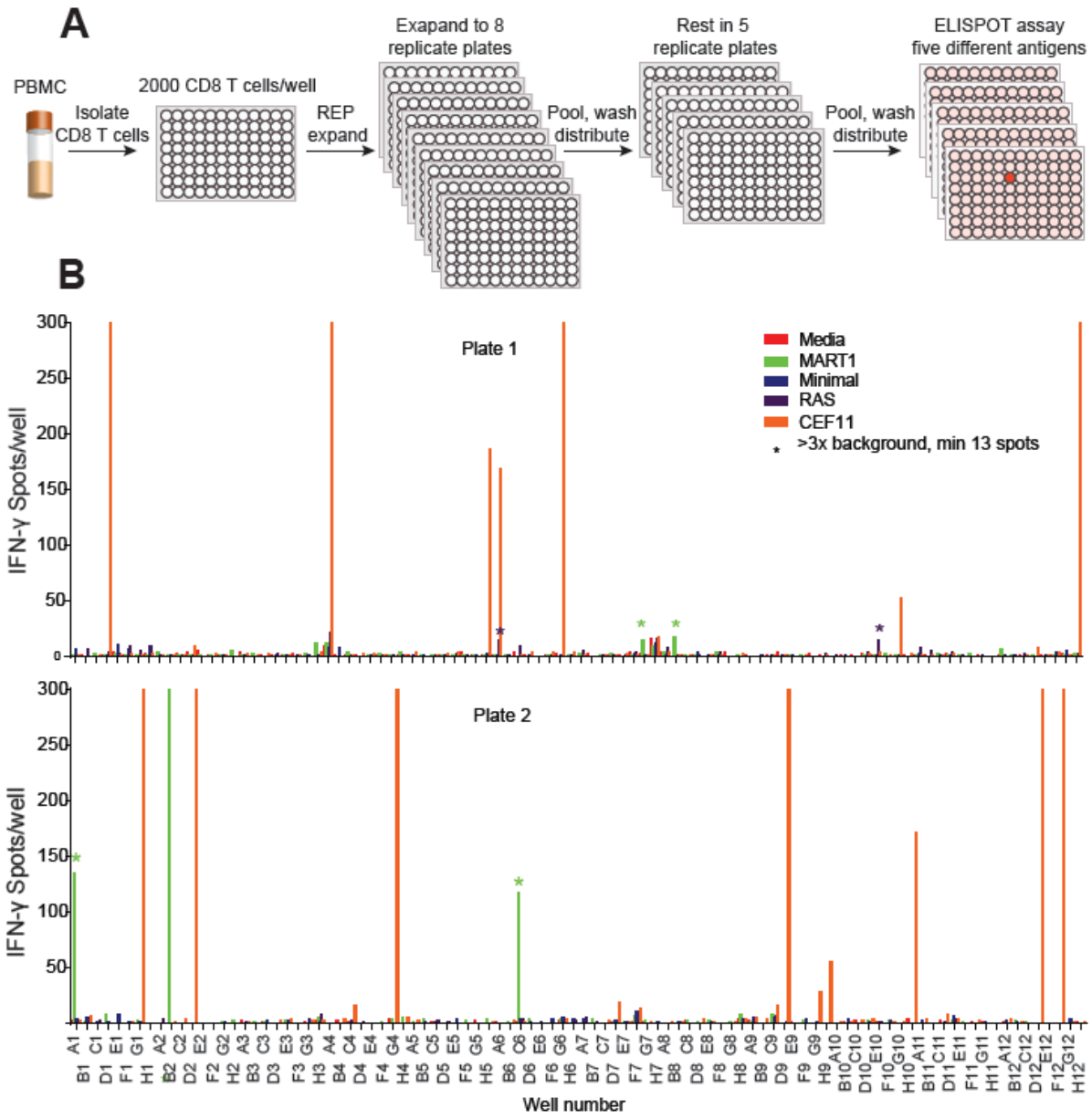

Figure 19. The miniline screen methodology and sample screen plates.
A. One vial of PBMC (10^7 cells) was thawed, CD8 T cells were isolated using magnetic columns and 2000 CD8 T cells were added to each well of a 96 well plate. Cells were stimulated with irradiated healthy donor PBMC (2 x 10^5), OKT3 antibody (30 ng/ml) and IL-2 (300 U/ml). Cells were expanded and split as necessary into eight replicate plates. Cells were then pooled, rested in low dose IL-2 (1 U/ml) and IL-7 (10 ng/ml) for 48 hours, pooled, and distributed to five ELISPOT plates. Each ELISPOT plate was stimulated with a different antigen. **B**. Example ELISPOT results from two miniline plates. Each plate was expanded and rested as in A and distributed into 5 ELISPOT plates/miniline plate. Each ELISPOT plate was stimulated with a different antigen as noted in the legend. Each point on the x axis represents the indicated well number from five ELISPOT plates, each stimulated with one of five antigens. Asterix represent positive wells (>13 spots and > 3-fold more spots than the average of other stimulation conditions for that well).

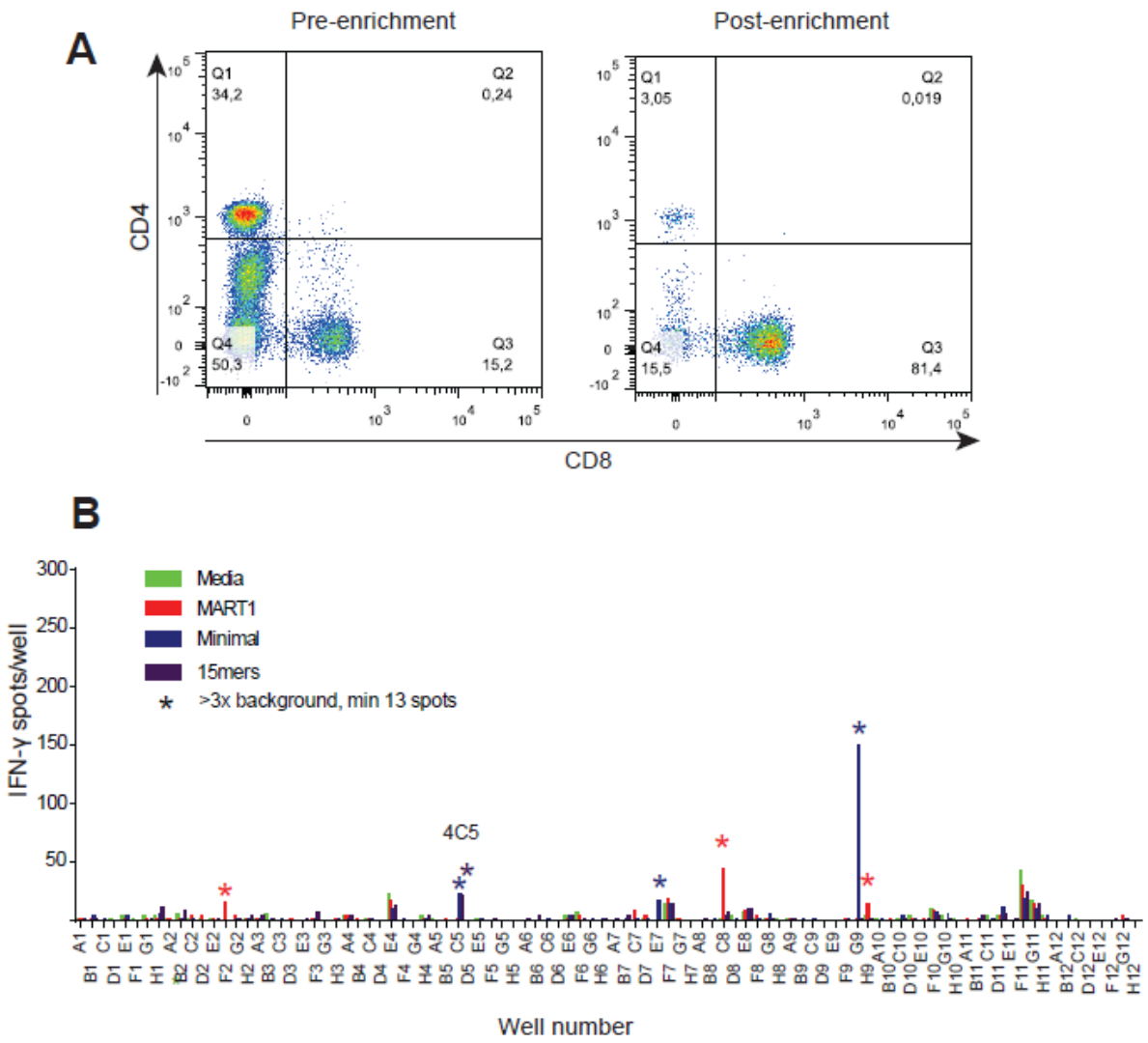

Figure 20. IROC024 miniline screen.
A. Representative flow cytometry plots for CD8 enrichment. CD8 T cells were enriched using magnetic purification, and pre- and post-enrichment cells were stained with viability dye, CD4 and CD8. **B**. Sample miniline screen of IROC024 T cells. Purified CD8 T cells were expanded using the miniline protocol and stimulated in separate ELISPOT plates with media alone, MART1 peptide, a peptide pool of all IROC024 predicted mutant minimal MHCI-binding peptides, and an overlapping 15mer pool encompassing each mutation. Asterix represent positive wells. 4C5 is highlighted and was considered positive towards both the minimal pool and the 15mer pool.

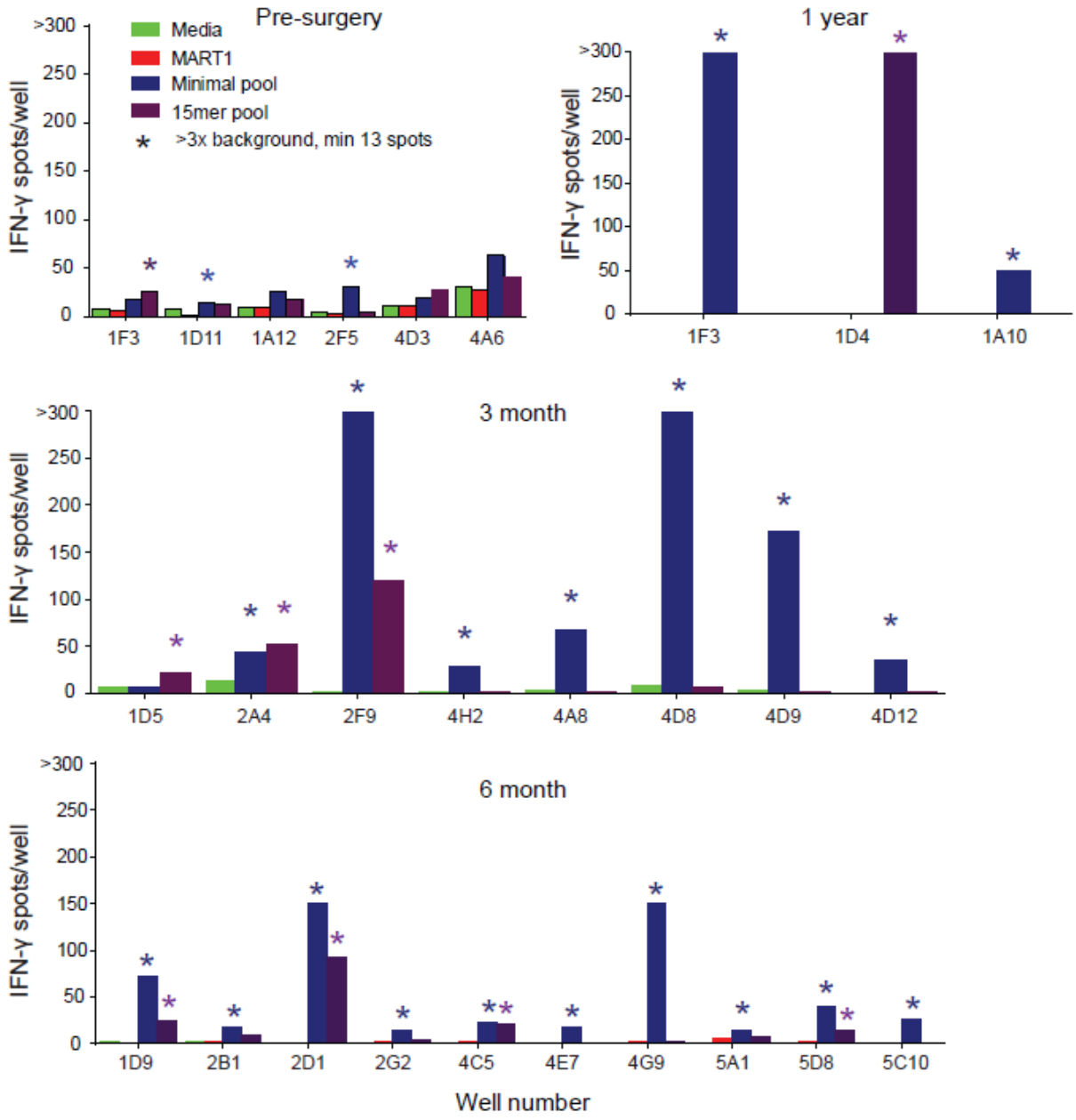

Figure 21. Positive T cell cultures from all miniline screens.
One vial of blood was thawed from each of the four blood donation time points and expanded using the miniline protocol (Figure 19a). Cells were stimulated in ELISPOT assays with media alone, MART1 minimal peptide, a pool of all predicted minimal mutant peptides, or an overlapping 15mer pool encompassing each mutation. Positivity was determined as > 13 spots and > 3-fold more than the average of the other stimulations for the well.

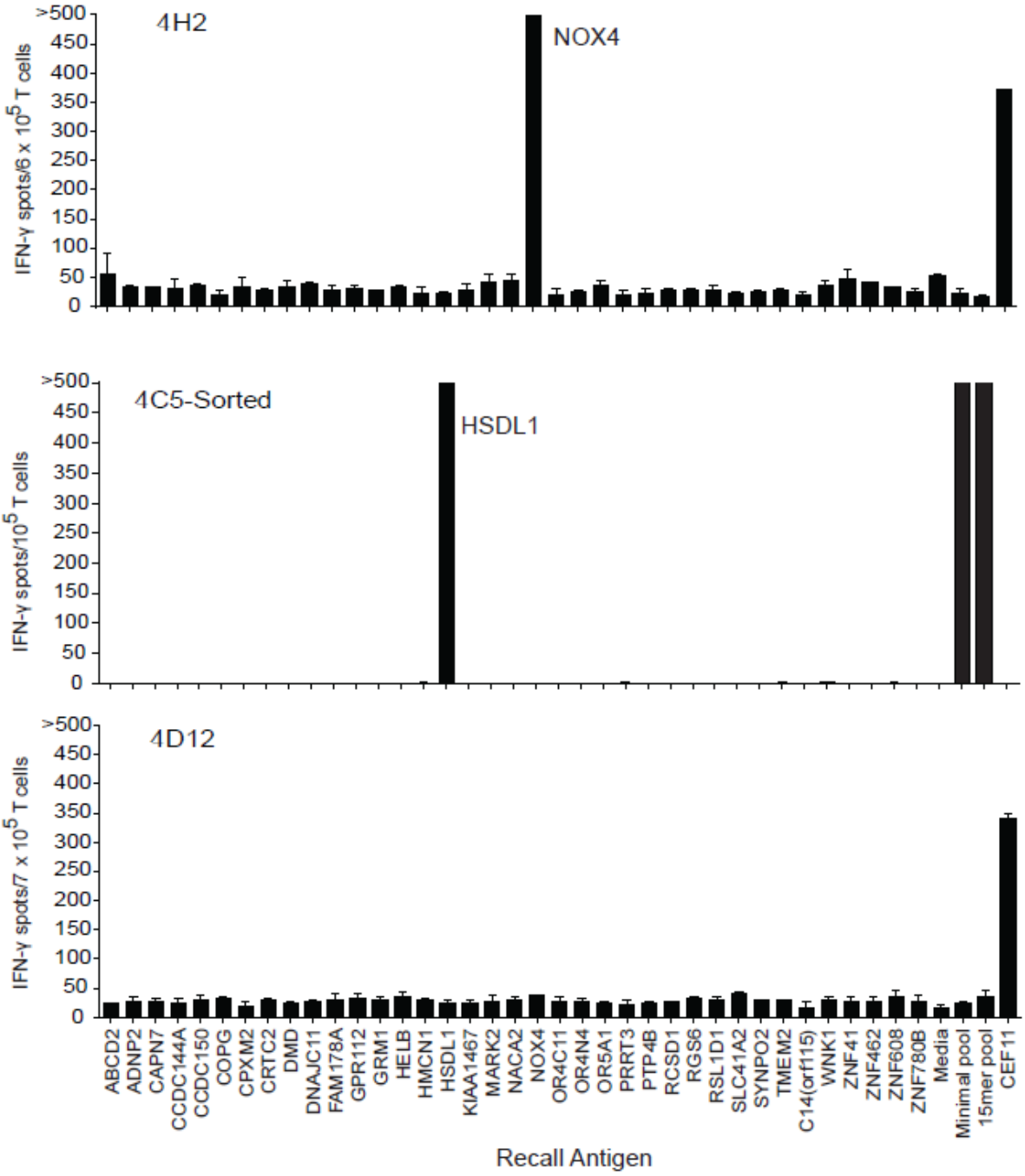

Figure 22. Deconvolution ELISPOT to determine mutation reactivity.
Each positive T cell culture from the screen was bulk-REP expanded (200/1 irradiated donor PBMC feeder cells/cultured T cell, 300 U/ml of IL-2, 30 ng/ml OKT3) and rested (1 U of IL-2, 10 ng/ml IL-7). Resultant T cells were stimulated with 37 mutated peptide pools encompassing all predicted mutant peptides for a single gene (in duplicate) in IFN-γ ELISPOT assays. Three examples are shown: Top, three month miniline screen well 4H2; middle, six month miniline well 4C5 (sorted and expanded); bottom, three month miniline well 4D12 (reactivity not confirmed). CEF11 was used as a positive control.

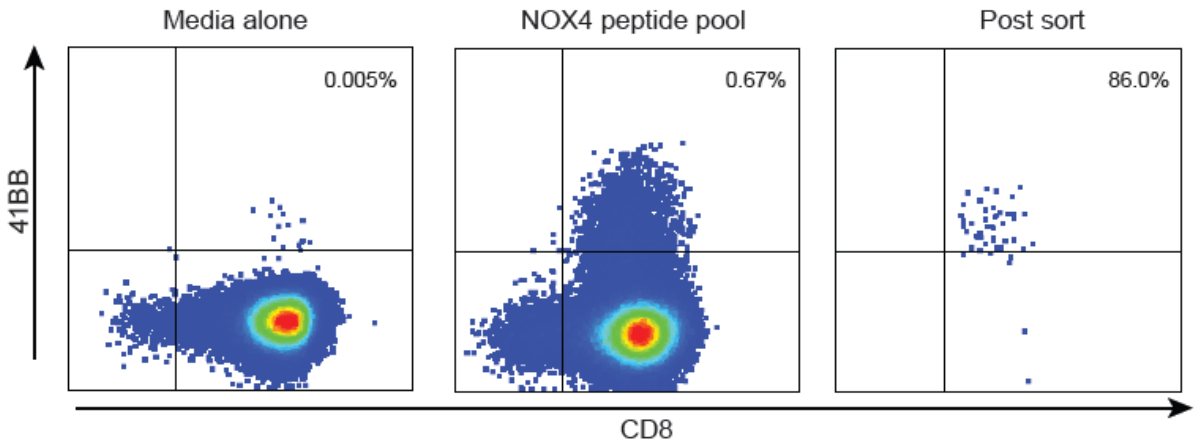

Figure 23. Sample sorting of mutation reactive T cells.
Bulk-REP expanded, mutation reactive T cells were thawed, rested in IL-2 (300 U/ml) for 24 hours then stimulated with minimal peptides encompassing the mutation towards which the cells were reactive or media alone. Cells were stained with viability dye, CD8 and 41BB antibodies and sorted using an Influx cell sorter. Shown is an example of well 4H2. Left: non-stimulated, Middle: stimulated with all peptides encompassing the NOX4 mutation, and Right: stimulated cells after sorting.

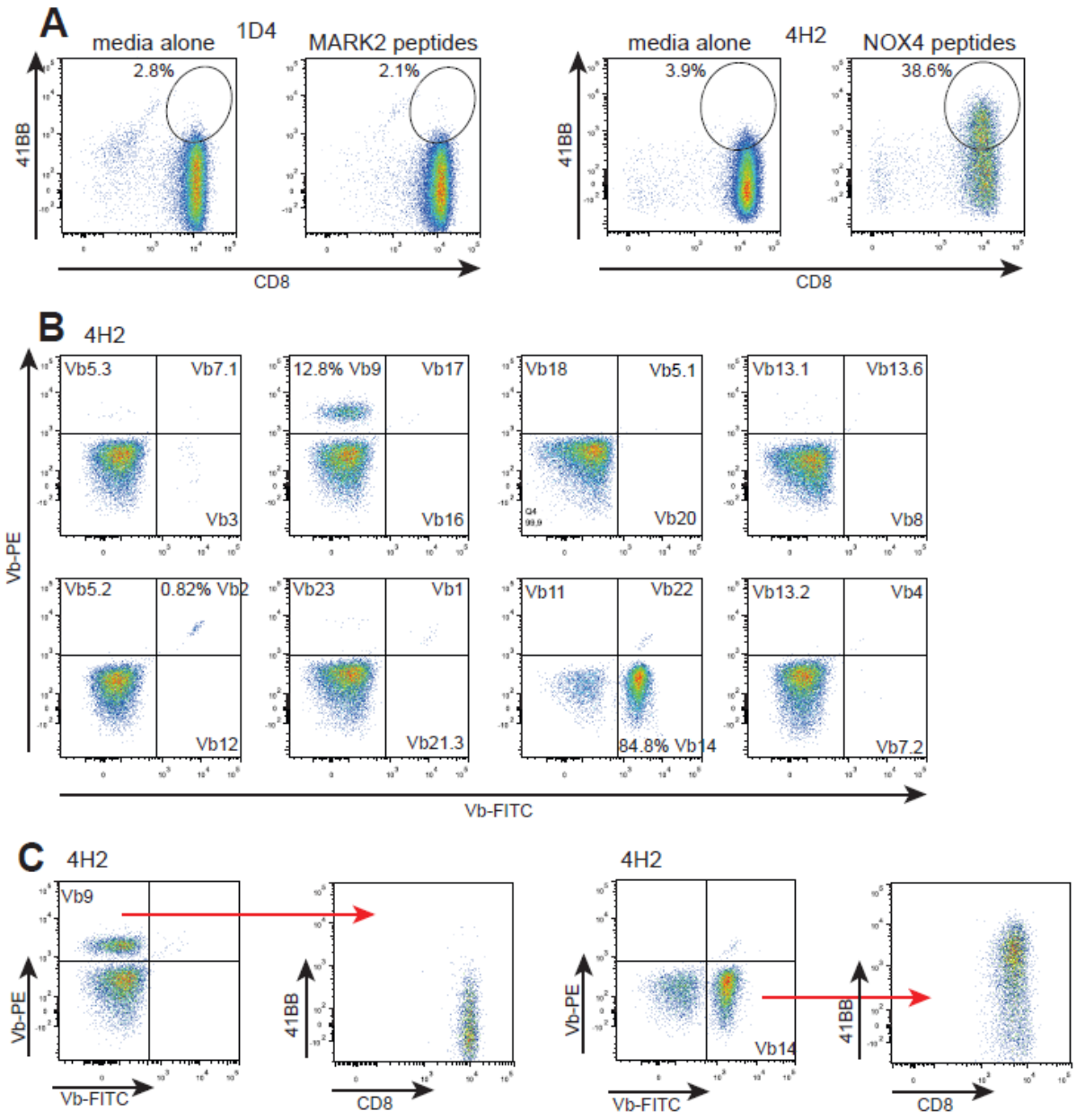

Figure 24. Clonality of sorted T cell lines.
A. Sorted T cell lines were thawed, rested in IL-2 (300 U/ml) for 24 hours and stimulated with cognate peptide. Wells 1D4 and 4H2 are shown as examples of a non-mutation reactive T cell line and a mutation reactive T cell line. Percentage of CD8 T cell that up-regulate 41BB in response to peptide is shown. **B.** Sample Vβ spectratyping for one T cell line (4H2). Cells were thawed and incubated with viability dye, CD8 antibody, and each of eight Vβ antibody cocktails. **C.** For T cell lines with more than one large Vβ population, cells were stimulated with cognate peptide and stained with viability dye, CD8 and 41BB antibodies, and each of the Vβ cocktails found to be enriched in the culture. Well 4H2 is shown as an example of a T cell line with two dominant Vβ.

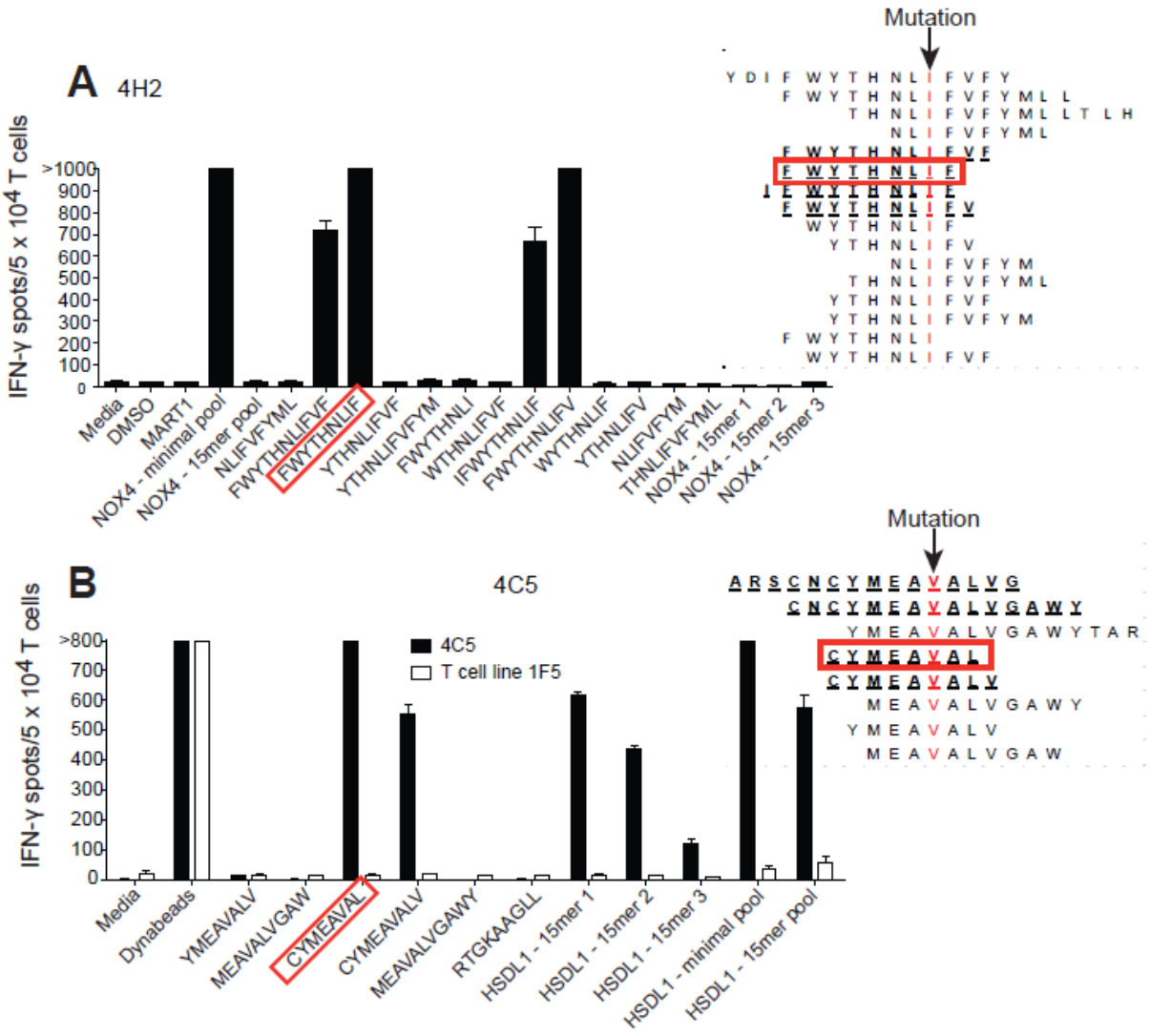

Figure 25. Deconvolution of minimal epitope for highly clonal T cell lines.
Each highly enriched mutation-recognizing T cell line was stimulated with each of the individual peptides that encompassed the mutation and assessed by IFN-γ ELISPOT. At the right is each peptide aligned and the shortest peptide that elicits a robust T cell response is boxed in red. Shown are two examples of mutation reactive T cell lines 4H2 and 4C5. Peptides that elicited a response are bolded and underlined, the mutation is red, and the minimal peptide encompassed by a red box. **A.** Well 4H2 (mutant NOX4 reactive). **B.** Well 4C5 (mutant HSDL1 reactive).

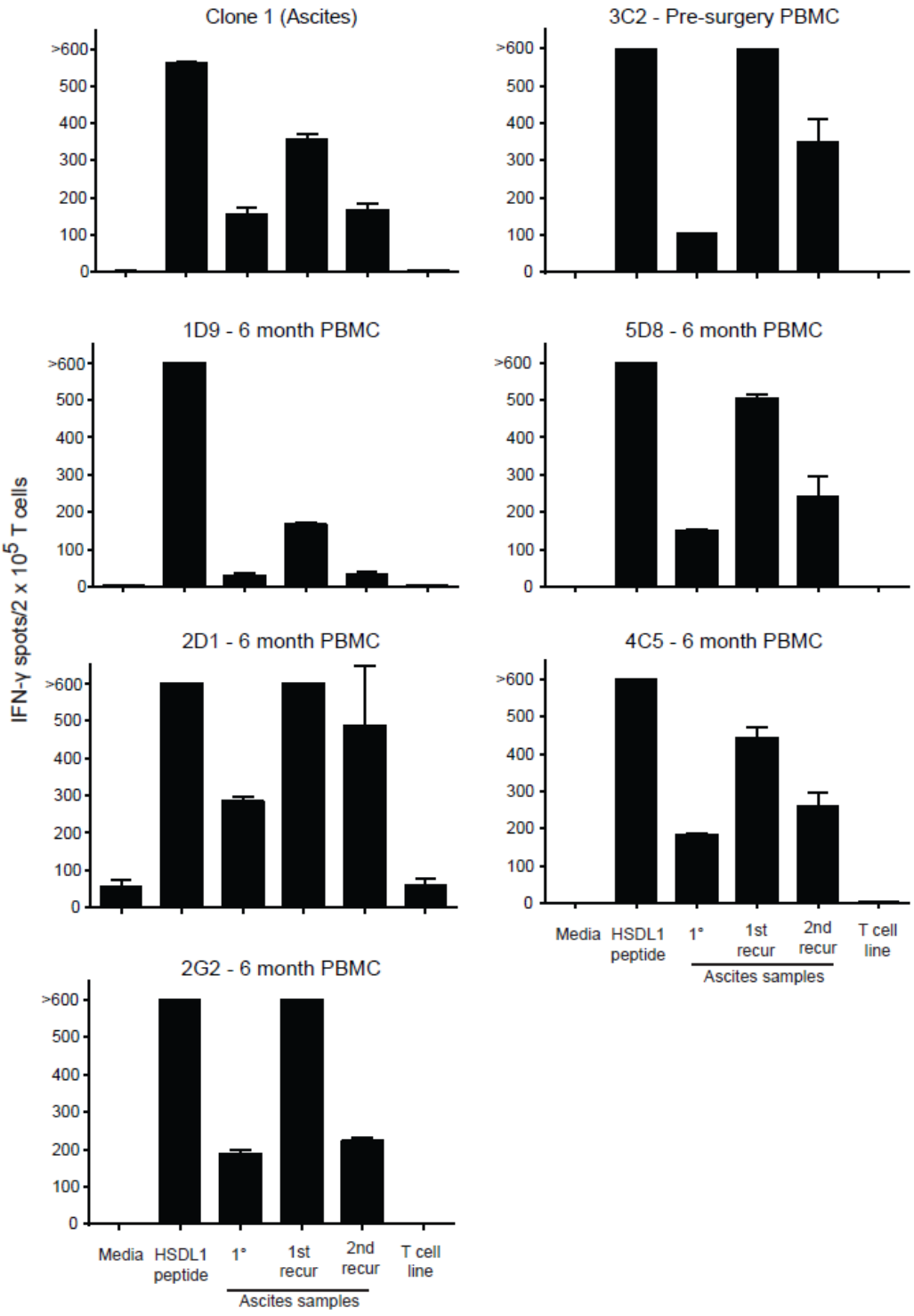

Figure 26. Mutant HSDL1-specific T cell reactivity to ascites
Each of the HSDL1 specific T cell lines were co-incubated in IFN-γ ELISPOT assays with media alone, minimal HSDL1 peptide (5 μg/ml), or bulk ascites cells (10^5) from the primary, first recurrence, or second recurrence. A non-reactive T cell line was used as a negative control target cell. The HSDL1 clone from the first recurrent ascites sample was used as a positive control T cell line.

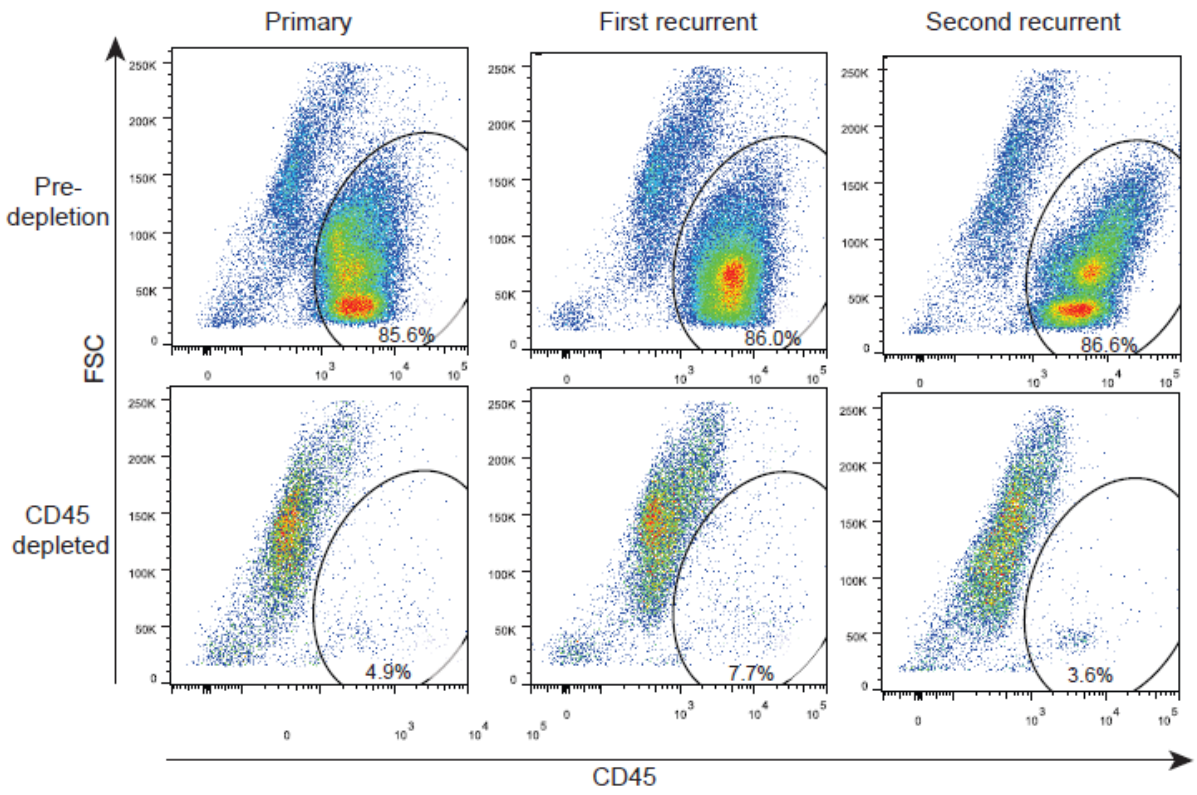

Figure 27. CD45 depletion of IROC024 ascites.
Ascites samples were thawed, filtered through 100 µm and 60 µm screens, and magnetically depleted of CD45 positive cells. Aliquots from each sample were taken from the pre-depletion samples and post-depletion samples and stained with viability dye, CD45 (using a different antibody clone than the depletion), CD3 and MHCII antibodies. Percentages shown are the percent of live cells that are CD45+.

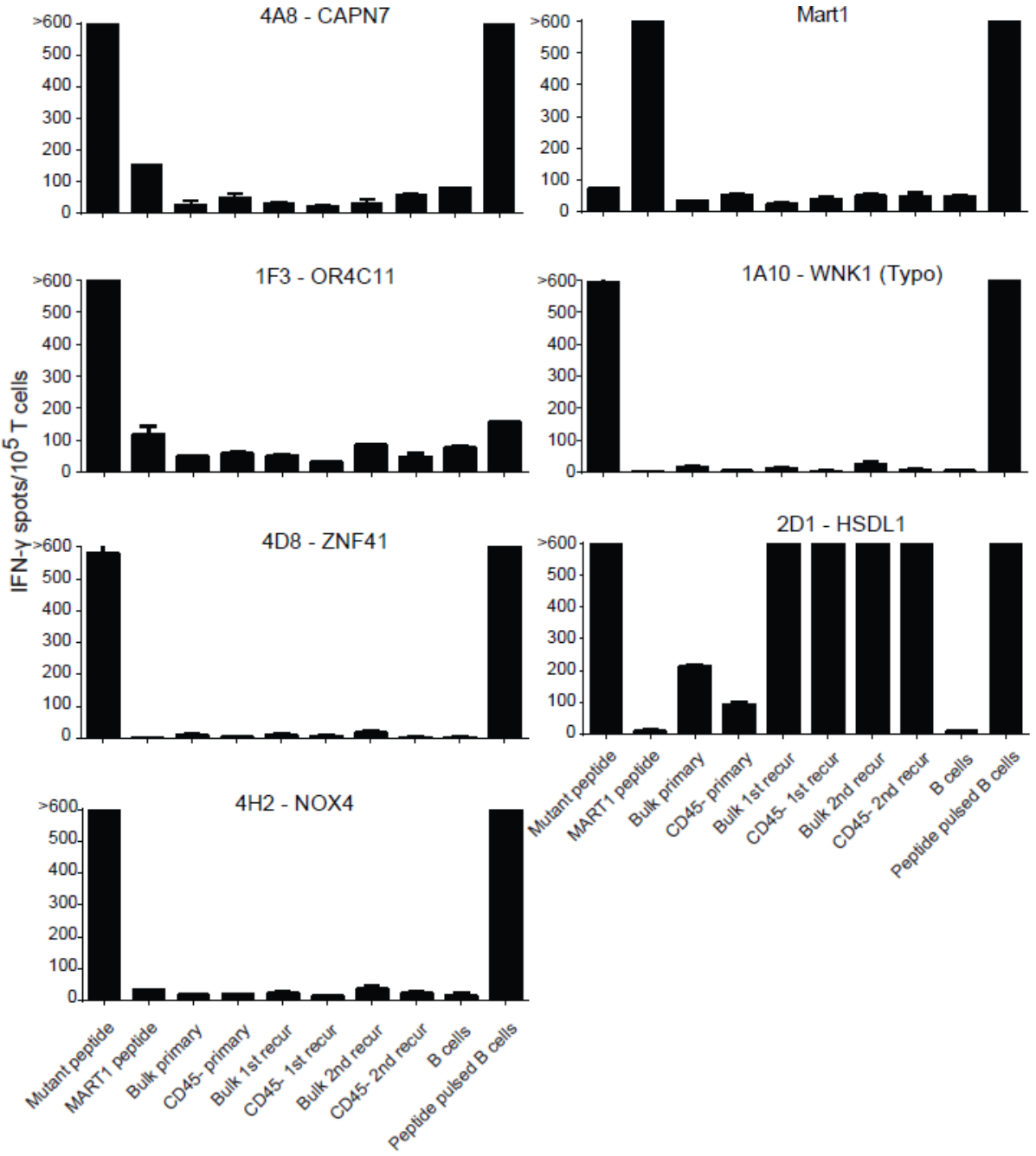

Figure 28. Mutation-specific T cells reactivities to ascites.
CD45 depletion was performed as in Figure 26. In IFN-γ ELISPOT assays, T cells (10^5) from each line were incubated with the cognate mutant peptide (5μg/ml), CD45 depleted ascites cells (2×10^4) from each time point, and bulk ascites cells (10^5) from each time point. T cell line 2D1 (HSDL1 reactive) was used as a positive control effector cell line, and a MART1 and WNK1-typo reactive T cell lines were used as a negative control effector cell lines. Autologous CD40L activated B cells were used as negative control target cells, and B cells pulsed with cognate peptide were used as positive control target cells. MART1 peptide was used as a negative control peptide for each T cell line.

4.6 Tables

Table 4.1. Minimal peptides ordered encompassing each mutation

Gene Name	Amino Acid Substitution	Minimal Peptide Tested	IC50 (nM)	HLA Restriction
ABCD2	E686Q	RFQQLDTAIRL	23.6	HLA-C14:03
		QQLDTAIRLTL	30.8	HLA-B39:01
		RFQQLDTAI	38.7	HLA-C14:03
		WRFQQLDTAI	39.0	HLA-B39:01
ADNP2	R792T	HSRNTHLGK	4.0	HLA-A30:01
		HSRNTHLGKK	5.0	HLA-A30:01
		HSRNTHLGKKK	12.0	HLA-A30:01
VRTN	C360S	LLGSGTSPAL	79.1	HLA-A02:01
CAPN7	n/a	FQETHLPI	35.6	HLA-B39:01
CCDC144B	R326T	LLDNSTTGTDV	200.2	HLA-A02:01
CCDC150	A905P	KTQIKLHLSPK	5.9	HLA-A30:01
		QIKLHLSPK	16.8	HLA-A30:01
COPG	N17S	GSSPFQHLEK	75.4	HLA-A30:01
CPXM2	N106S	SSKKVMRTK	8.4	HLA-A30:01
		HSSKKVMRTK	30.5	HLA-A30:01
CRTC2	A354S	SSLSSPQPQL	639.5	HLA-A30:01
DMD	n/a	KTLGPIWK	29.1	HLA-A30:01
		SELRKTLGPIW	32.6	HLA-B44:03
DNAJC11	V322L	QTRLKGSLK	7.2	HLA-A30:01
		FQDDDQTRL	44.6	HLA-B39:01
FAM178A	R357I	SMIPKAIESF	18.6	HLA-C14:03
		KAIESFLEK	22.3	HLA-A30:01
		SMIPKAIESFL	37.3	HLA-A02:01
GPR112	E363G	KMVEAMATGI	13.8	HLA-A02:01
GRM1	R684L	KTNRIALI	33.1	HLA-A30:01
		KTNRIALILA	39.8	HLA-A30:01
		RIALILAGSK	43.3	HLA-A30:01
HELB	P539R	RTGKAAGLL	144.0	HLA-A30:01
HMCN1	Q4859E	RPCPGDTTEV	3099.9	HLA-C14:03
HSDL1	L25V	CYMEAVAL	5.6	HLA-C14:03
		YMEAVALV	8.6	HLA-A02:01
		MEAVALVGAW	17.7	HLA-B44:03
		CYMEAVALV	22.6	HLA-C14:03
		MEAVALVGAWY	26.8	HLA-B44:03
KIAA1467	Q92E	EEKAASSLVSY	104.5	HLA-B44:03
MARK2	E13K	RGRNSATSADK	7.5	HLA-A30:01
NACA2	V184L	LLMSQANV	7.0	HLA-A02:01
		KLLMSQANV	34.6	HLA-A02:01
NOX4	F197I	FWYTHNLIFVF	4.4	HLA-C14:03
		FWYTHNLIF	4.6	HLA-C14:03
		YTHNLIFVF	10.5	HLA-C14:03
		YTHNLIFVFYM	18.5	HLA-C14:03
		FWYTHNLI	21.0	HLA-C14:03
		WYTHNLIFVF	25.7	HLA-C14:03
		IFWYTHNLIF	29.3	HLA-C14:03
		YTHNLIFV	29.4	HLA-A02:01
		FWYTHNLIFV	31.1	HLA-C14:03
		THNLIFVFYML	35.0	HLA-B39:01
		WYTHNLIF	38.2	HLA-C14:03
		NLIFVFYML	38.4	HLA-A02:01
		NLIFVFYM	46.1	HLA-A02:01
OR4C11	S154Y	IHYTAQIILAL	15.0	HLA-B39:01
		SLIHYTAQI	16.1	HLA-A02:01
		YTAQIILAL	21.2	HLA-C14:03
		HYTAQIILAL	23.1	HLA-C14:03
		IHYTAQIIL	23.9	HLA-B39:01
OR4N4	R182Q	FFCDVQQVIKL	269.2	HLA-C14:03
OR5A1	n/a	FWEQKTISF	15.0	HLA-C14:03
		WEQKTISF	48.6	HLA-B44:03
PRRT3	F61Y	SEPQAFDVY	432.9	HLA-B44:03
PTPRB	S943R	SFRQERTVPDK	40.9	HLA-A30:01
RCSD1	E347D	AVKDTPHSPPG	292.0	HLA-A30:01
RGS6	I429L	FEDAQEHLYKL	88.4	HLA-B39:01
RSL1D1	S400T	KSPNPTTPRGK	112.7	HLA-A30:01
SLC41A2	K223N	VIVGSKNTGI	4554.8	HLA-A02:01
SYNPO2	N461T	VTFDWDSGLV	164.0	HLA-A02:01
TMEM2	S294R	YRNERRRLQEF	118.4	HLA-C14:03
WNK1	S2395C	CSRSSSLGNK	7.4	HLA-A30:01
		KSKGSKCSR	33.7	HLA-A30:01
		RSRSSSLGNK	2.6	HLA-A30:01
		RSRSSSLG	73.7	HLA-A30:01
ZNF41	G67E	HLLSVEYQI	31.5	HLA-A02:01
ZNF462	R695K	RTKIDEIASNL	29.6	HLA-A30:01
ZNF608	S1158T	KAPTTPEPNK	92.9	HLA-A30:01
ZNF780B	Y124C	FYFRNDSEC	386.2	HLA-C14:03

Table 2. Minimal peptides encompassing each IROC024 mutation

Table 4.2. Work up of each putatively positive T cell line identified in miniline screen of IROC024 peripheral blood							
Clone Number	Blood Sample	Recognized mutation	Enriched line derived?	Minimal Epitope	Vβ	Clonality	Recognize tumor?
1F3	Pre-surgery	Not confirmed					
1D11	Pre-surgery	Not confirmed					
4D3	Pre-surgery	Not confirmed					
4A6	Pre-surgery	Not confirmed					
1A12	Pre-surgery	KIAA1467	No				
2F5	Pre-surgery	KIAA1467	No				
3C2	Pre-surgery	HSDL1	Yes	CYMEAVAL	1		Yes
2A4	3 month	Not confirmed					
2F9	3 month	Not confirmed					
4D12	3 month	Not confirmed					
1D5	3 month	Not confirmed					
4D9	3 month	HSDL1	Yes	CYMEAVAL	4	40	Undetermined
4H2	3 month	NOX4	Yes	FWYTHNLIF	14	85	No
4A8	3 month	CAPN7	Yes	FQETHLPI	14	65	No
4D8	3 month	ZNF41	Yes	HLLSVEYQI	13.6	88	No
5C10	6 month	Not confirmed					
4E7	6 month	Not confirmed					
5A1	6 month	Not confirmed					
2B1	6 month	Not confirmed					
4G9	6 month	NOX4	No				
1D9	6 month	HSDL1	Yes	CYMEAVAL	13.6	88	Yes
2D1	6 month	HSDL1	Yes	CYMEAVAL	13.6	94	Yes
2G2	6 month	HSDL1	Yes	CYMEAVAL	5.2	80	Yes
4C5	6 month	HSDL1	Yes	CYMEAVAL	1	91	Yes
5D8	6 month	HSDL1	Yes	CYMEAVAL	5.2	80	Yes
1D4	1 year	MARK2	No				
1F3	1 year	OR4C11	Yes	IHYTAQIIL	13.1	80	No
1A10	1 year	WNK1-Typo	Yes	RSRSSSLGNK	21.3	10	No

Table 3. Assessment of each mutation reactive line from miniline screen

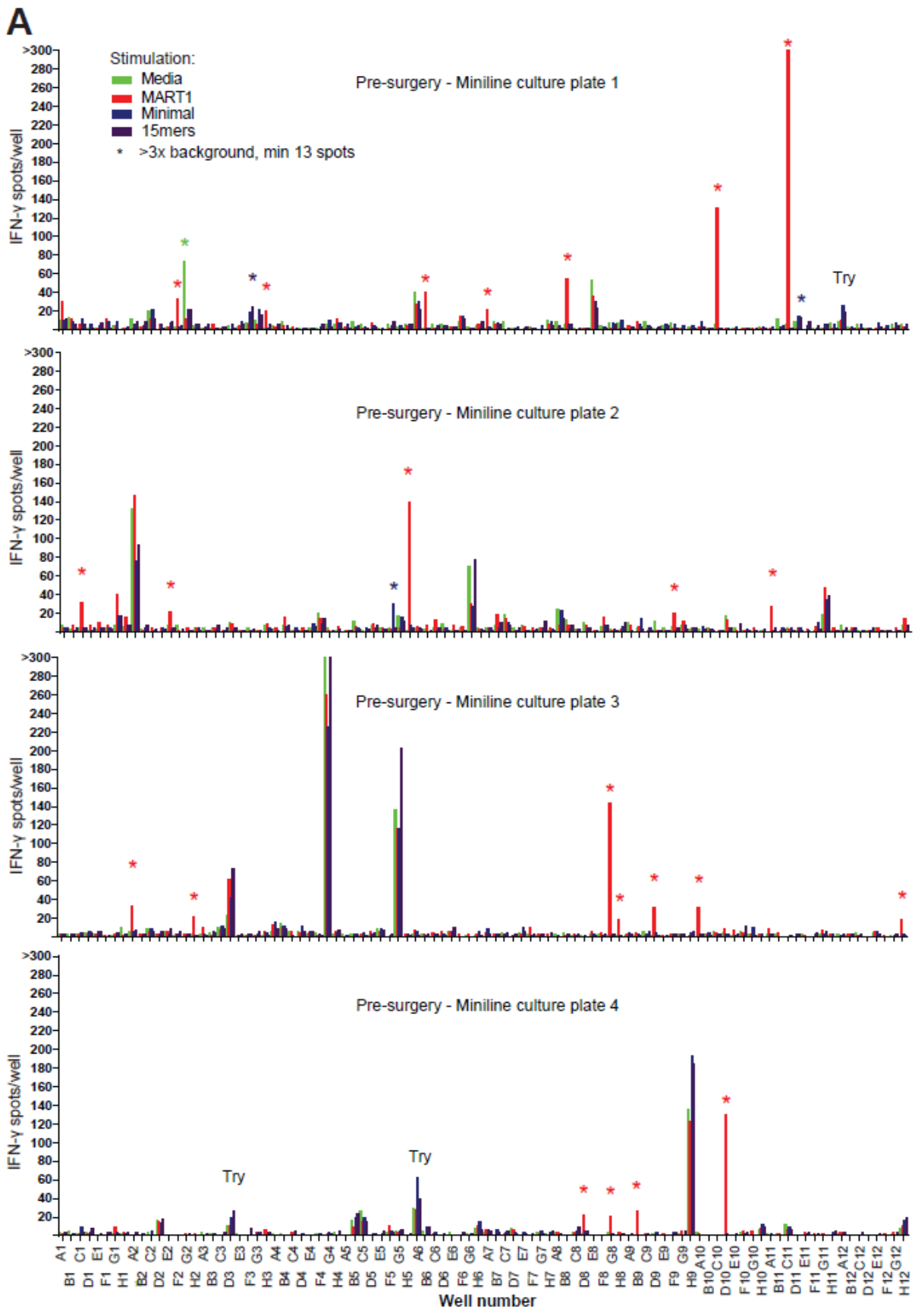
A
Stimulation:
Media
MART1
Minimal
15mers
* >3x background, min 13 spots
Pre-surgery - Miniline culture plate 1
Pre-surgery - Miniline culture plate 2
Pre-surgery - Miniline culture plate 3
Pre-surgery - Miniline culture plate 4
IFN-γ spots/well
Try
Well number

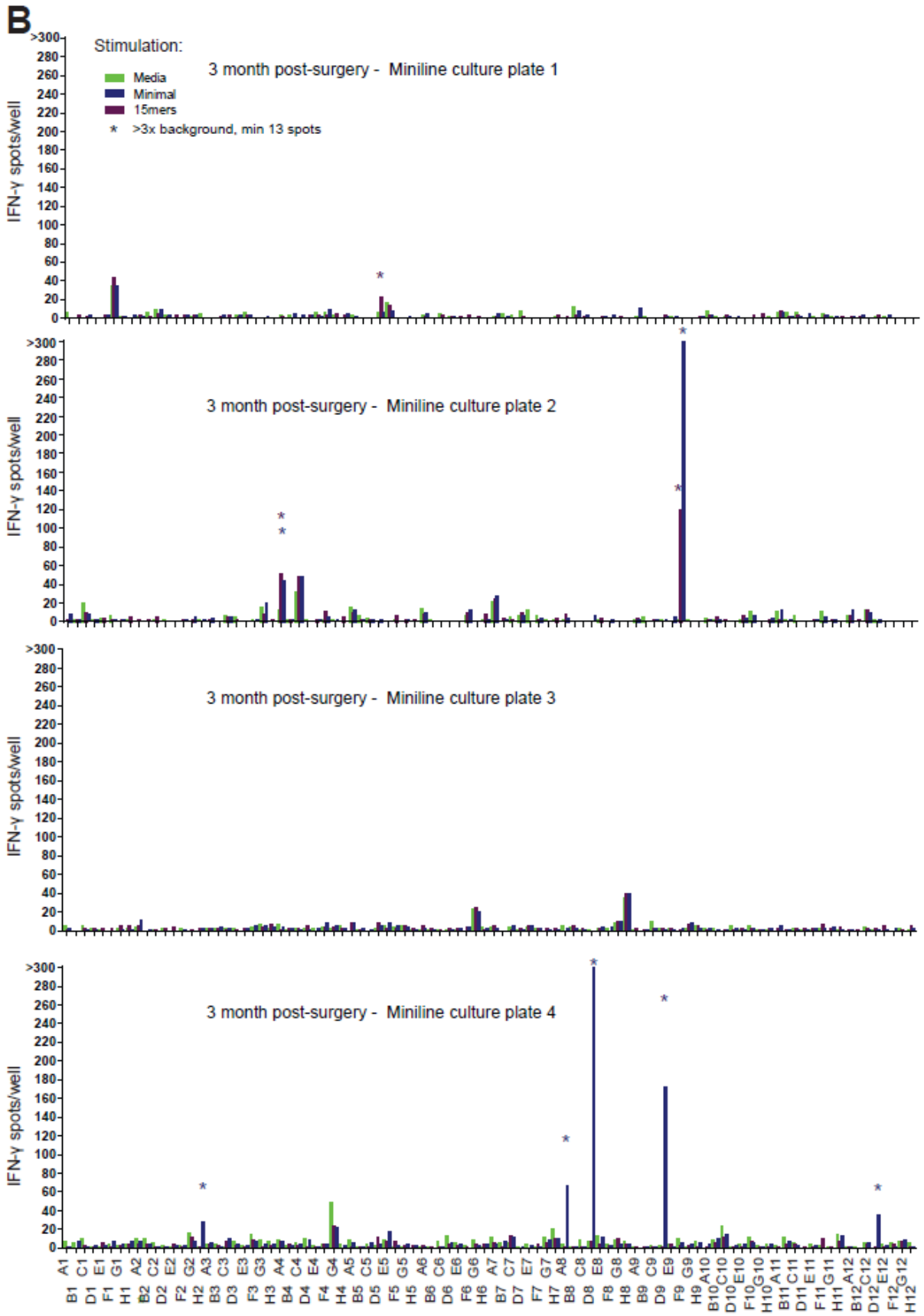
B
Stimulation:
Media
Minimal
15mers
* >3x background, min 13 spots
3 month post-surgery - Miniline culture plate 1
3 month post-surgery - Miniline culture plate 2
3 month post-surgery - Miniline culture plate 3
3 month post-surgery - Miniline culture plate 4
IFN-γ spots/well
>300
280
260
240
220
200
180
160
140
120
100
80
60
40
20
0
A1 C1 E1 G1 A2 C2 E2 G2 A3 C3 E3 G3 A4 C4 E4 G4 A5 C5 E5 G5 A6 C6 E6 G6 A7 C7 E7 G7 A8 C8 E8 G8 A9 C9 E9 G9 A10 C10 E10 G10 A11 C11 E11 G11 A12 C12 E12 G12
B1 D1 F1 H1 B2 D2 F2 H2 B3 D3 F3 H3 B4 D4 F4 H4 B5 D5 F5 H5 B6 D6 F6 H6 B7 D7 F7 H7 B8 D8 F8 H8 B9 D9 F9 H9 B10 D10 F10 H10 B11 D11 F11 H11 B12 D12 F12 H12

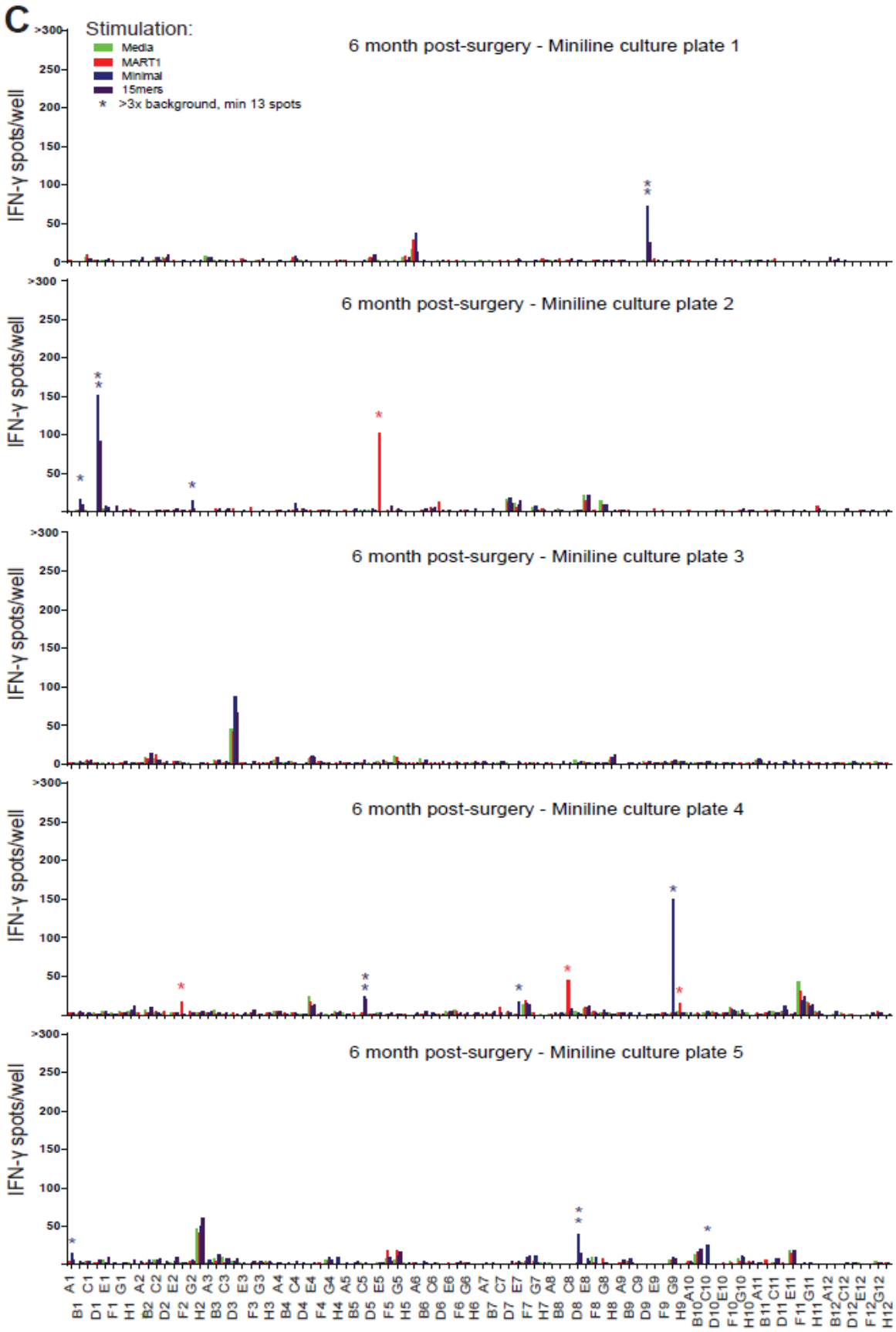
C
Stimulation:
Media
MART1
Minimal
15mers
* >3x background, min 13 spots
6 month post-surgery - Miniline culture plate 1
6 month post-surgery - Miniline culture plate 2
6 month post-surgery - Miniline culture plate 3
6 month post-surgery - Miniline culture plate 4
6 month post-surgery - Miniline culture plate 5
IFN-γ spots/well
>300
250
200
150
100
50
0
A1 B1 C1 D1 E1 F1 G1 H1 A2 B2 C2 D2 E2 F2 G2 H2 A3 B3 C3 D3 E3 F3 G3 H3 A4 B4 C4 D4 E4 F4 G4 H4 A5 B5 C5 D5 E5 F5 G5 H5 A6 B6 C6 D6 E6 F6 G6 H6 A7 B7 C7 D7 E7 F7 G7 H7 A8 B8 C8 D8 E8 F8 G8 H8 A9 B9 C9 D9 E9 F9 G9 H9 A10 B10 C10 D10 E10 F10 G10 H10 A11 B11 C11 D11 E11 F11 G11 H11 A12 B12 C12 D12 E12 F12 G12 H12

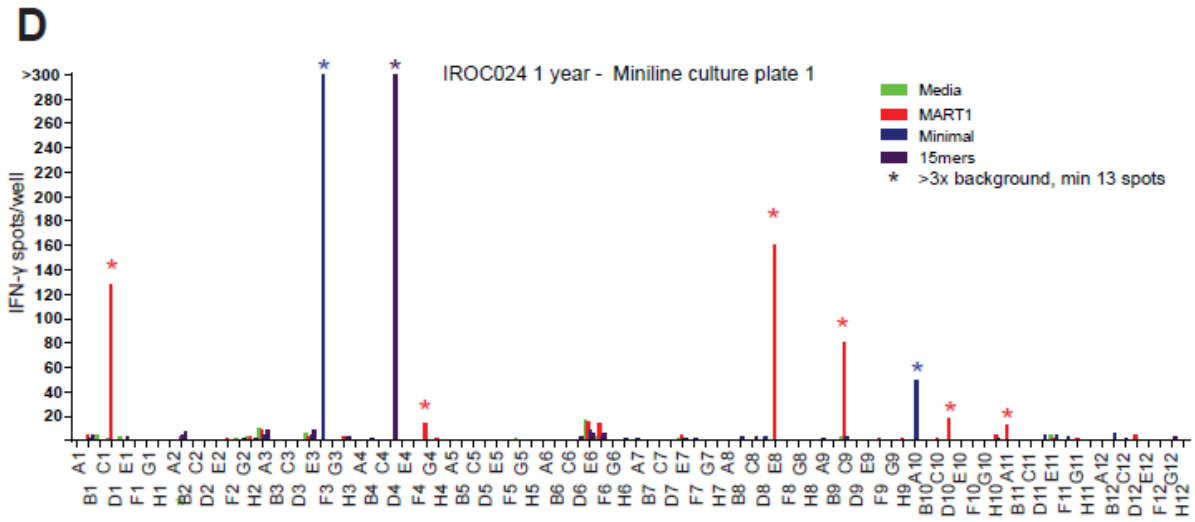

Figure 29-supplementary. Miniline culture ELISPOT screens.
Miniline cultures were generated from isolated CD8 T cells from each of four time point blood draws: **A**. Pre-surgery (4 plates of minilines), **B**. 3 month post-surgery (4 plates of minilines), **C**. 6 month post surgery (5 plates of minilines), and **D**. 1 year post-surgery (1 plate of minilines). Each miniline culture was distributed among 5 ELISPOT plates. Each ELISPOT plate was stimulated with one reagent: Media alone, MART1 peptide, minimal mutant peptide pool, 15mer mutant peptide pool, or CEF11 (not shown). Each graph represents one miniline culture split among 5 ELISPOT plates.

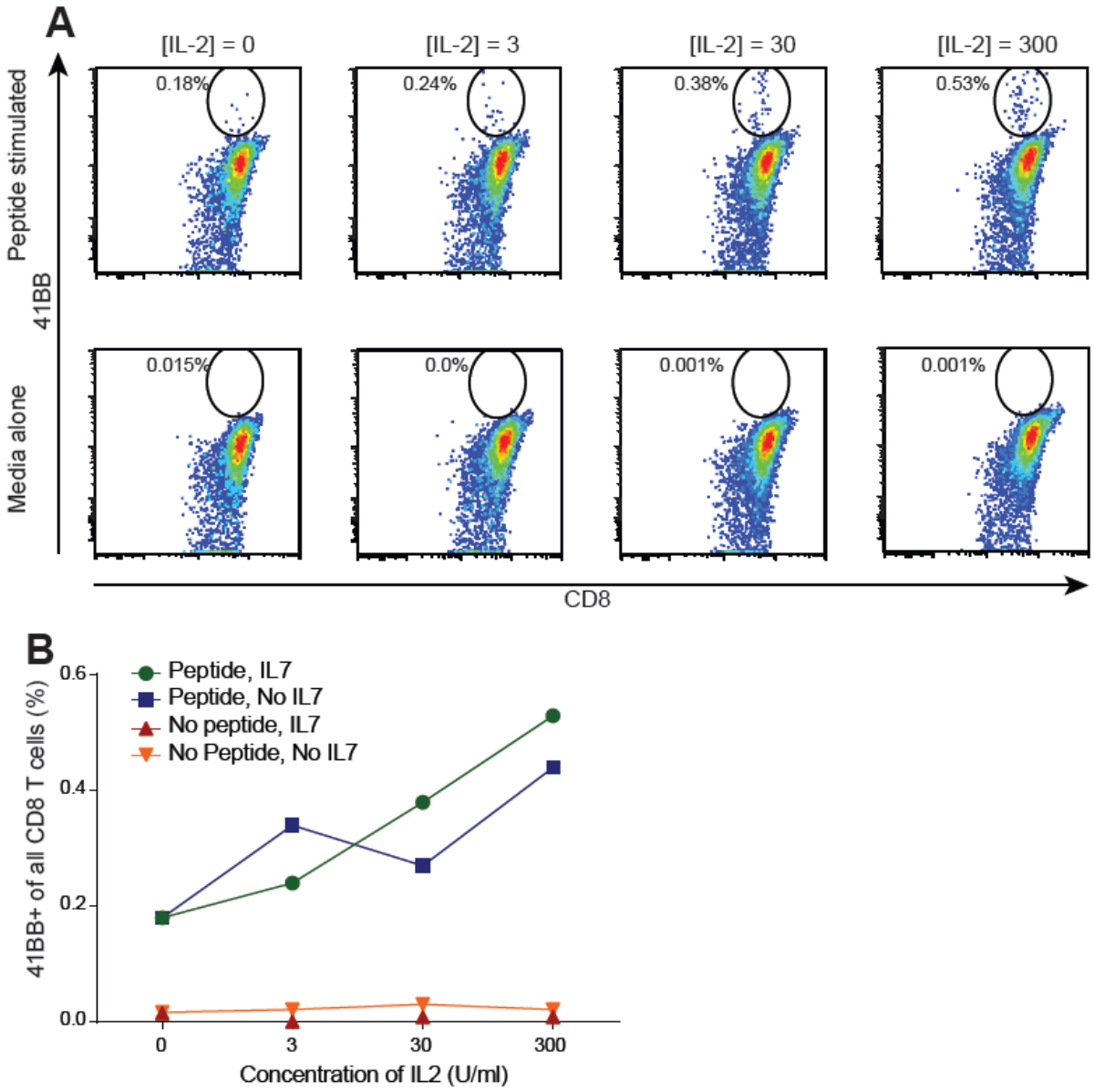

Figure 30-Supplementary. Improving 41BB detection by varying IL-2.
Bulk-REP expanded, mutation-reactive T cells were thawed and rested for 24 hours in media containing various concentrations of IL-2 either with or without 10 ng/ml IL-7. Cells were subsequently stimulated with mutant HSDL1 peptide for an additional 24 hours. Cells were stained with viability dye, CD8 and 41BB antibodies. Frequency of 41BB+ of all CD8 T cells is shown. **A**. Sample flow cytometry plots of T cells incubated in the indicated concentrations of IL-2 either plus or minus peptide stimulation. **B**. Graph of the percentage of CD8 T cells that up-regulate 41BB in the different resting conditions.

Supplementary Table 4.1 Example of 15mer and predicted minimal peptide pools for NOX4 mutation
4H2 - NOX4
15mers
Y D I F W Y T H N L I F V F Y
F W Y T H N L I F V F Y M L L
T H N L I F V F Y M L L T L H
Predicted minimal peptides
I F W Y T H N L I F
F W Y T H N L I
F W Y T H N L I F
F W Y T H N L I F V
F W Y T H N L I F V F
W Y T H N L I F
W Y T H N L I F V F
Y T H N L I F V
Y T H N L I F V F
Y T H N L I F V F Y M
T H N L I F V F Y M L
N L I F V F Y M
N L I F V F Y M L

Table 4-supplementary. Example of peptides used to assess a mutation in NOX4

Chapter Five: Conclusions

Overview

Several lines of evidence point to neoantigens as important immunogenic determinants underlying successful immunotherapies. Since they are tumor restricted, neoantigens may be recognized by T cells bearing high affinity TCR. Additionally, clinical studies have shown that increased mutation loads correlated with responses to checkpoint blockade in lung cancer and melanoma [331,342,385]. Moreover, neoantigen-specific T cells have been often found in melanoma patients who undergo successful ACT with TIL [345,346,348,349,445]. Furthermore, neoantigen vaccines have successfully treated mice harboring highly-mutated tumor models [238,314,343,358]. Almost all of the identified neoantigen-reactive T cells recognized mutations unique to a single tumor, meaning that treatments designed to activate these T cells need to be personalized. However, prior to this study, it was unknown the extent to which neoantigens are present, or targetable, in tumors with intermediate mutation burdens like ovarian cancer.

Anti-tumor vaccines seem a rational option to raise an immune response towards tumor antigens, and a few clinical trials have been initiated to target neoantigens [359,360,446]. However historically, therapeutic anti-cancer vaccines have elicited only sporadic clinical responses. Two main challenges have been that anti-tumor vaccines elicit weak T cell responses, and they have targeted antigens that were not tumor restricted. I investigated opportunities to overcome both of these challenges. I hypothesized that (1) modifications to vaccination schedules can lead to improved T cell responses to SLP vaccines, (2) neoantigen peptide vaccines can elicit therapeutic T cell responses towards murine ovarian cancer, and (3) naive or activated neoantigen-reactive T cells are present in ovarian cancer patient tumors and blood.

To test these hypotheses, I developed and adapted techniques for maximizing T cell responses to SLP vaccines, which I piloted on model antigens and applied to neoantigens. Various SLP vaccination schedules were tested, and daily inoculations for four consecutive days (dubbed “cluster vaccination”) elicited the highest frequencies of antigen-specific T cells and rejected established E.G7 tumors. Furthermore, inclusion of an Synthetic Long Peptide (SLP) encompassing a CD4 T cell epitope in the cluster vaccinations protocol failed

to augment the CD8 T cell response and failed to reject tumors. Moreover, cluster-boost 21 days after the cluster-prime elicited very high frequencies of antigen-specific T cells. I then targeted neoantigens in the ID8-G7 ovarian cancer model with these optimized vaccination protocols. WES and RNA-seq were used to identify 92 missense mutations, 44 of which were expressed, but none of the mutated epitopes were predicted bind with high-affinity to MHCI. SLP vaccines targeting intermediate affinity mutant epitopes elicited high frequencies of mutation-specific T cells, most of which were CD4 T cells; however, these T cells had no effect on tumor growth and failed to recognize tumor cells *in vitro.* Additionally, *in silico* analysis of TCGA data revealed that most HGSC patients were predicted to harbor no high affinity mutated epitopes.

To further investigate the potential of targeting neoantigens in human ovarian cancer, three ascites samples and four peripheral blood samples donated by a HGSC patient were interrogated for reactivity to autologous tumor mutations. A single T cell response to a neoantigen (mutated HSDL1) was identified in the first recurrent ascites, with no evidence of HSDL1-specific T cells in primary or second recurrent ascites. Furthermore, using a unique method to assess all naive and activated CD8 T cells in each vial of blood, I identified several additional HSDL1-specific T cell clones from three different blood donation time points, each of which was prior to the detection of tumor recurrence. Several other T cells reactive to other mutations also were detected and isolated, but these T cells failed to recognize tumor. Overall, studies of both the ID8-G7 tumor model and the human HGSC patient suggest that efforts to activate naive mutation-reactive T cells may elicit only irrelevant T cells that cannot recognize tumor cells. Thus, assessment of T cell recognition of authentic neoepitopes on the tumor cells is a critical step that should be incorporated when targeting neoantigens with personalized vaccines.

Cluster vaccination versus other vaccine strategies

The majority of therapeutic anti-cancer vaccine clinical trials have used minimal epitopes peptides from confirmed cancer antigens admixed in oil emulsions [447]. Though this seems like a rational choice of modalities and some clinical successes have been observed [247], minimal peptides in oil emulsions have several key drawbacks (as discussed in Chapter 1), and most clinical trials have failed to achieve responses [187]. The

shortcomings of minimal epitope peptide vaccines inspired development of SLP and inclusion of TLR agonists in contemporary vaccinations formulations [262,448]. One such clinical study in ovarian cancer showed that vaccinations targeting NY-ESO-1 with SLP plus poly(I:C) in oil emulsions elicited antigen specific T cell responses in 91% of patients [449]. Another study used SLP vaccines encompassing E6 and E7 proteins, which led to clinical responses in HPV positive vulvar intraepithelial neoplasias [278]. Clinical responses associated with higher frequencies of activated effector T cells [389], demonstrating the utility of anti-cancer SLP vaccines and providing rationale for further development of SLP vaccination methodologies.

Recognizing the need to improve SLP vaccine effectiveness, I modified the SLP vaccine schedules to maximize the primary antigen-specific T cell response. While delivering vaccines in oil emulsions releases antigen slowly and may result in T cell tolerance [253], delivering vaccines in soluble form may allow antigen presentation for too short of time and result in weak T cell expansion [391,392,394]. My studies demonstrate that daily vaccinations for four consecutive days (cluster vaccination) with soluble antigen and poly(I:C) resulted in greater primary CD8 T cell expansion compared to vaccinations for less than four days or vaccinations for eight consecutive days (Figure 1, 5). Cluster vaccination provided antigen and adjuvant for an ideal duration that resulted in immediate and robust T cell responses, superior to most peptide vaccination strategies to date. For example, some contemporary murine studies used variations of SLP vaccines and TLR agonists to reject model tumors. However, these studies required *in vitro* stimulation of vaccinated mouse splenocytes to detect vaccine induced T cells, indicating suboptimal T cell priming [252,387]. Alternatively, single prime-boost vaccinations with SLP encompassing an HPV-E7 epitope elicited antigen-specific T cells that comprised 7% of all CD8 T cells, but the peak response was delayed until 21 days after the first vaccination [269]. In contrast to these studies, cluster vaccination with poly(I:C) and an SLP encompassing SIINFEKL induced T cell responses easily detectable directly *ex vivo* seven days after vaccination, demonstrating the superiority of this vaccination schedule for eliciting robust primary T cell responses.

Why is cluster vaccination superior to other vaccine techniques?

A robust, sudden primary T cell response to vaccination may be required for tumor eradication, but a slowly evolving T cell response may allow tumors to evade immune pressure. In non-tumor bearing mice, the peak T cell responses elicited by cluster vaccination and single prime-boost vaccination were similar in magnitude but delayed for several days in the single prime-boost group (Figure 2c). However, cluster vaccination induced tumor rejection, whereas single prime-boost vaccination allowed continued tumor growth (Figure 3). Why did similar magnitude T cell responses result in dramatically different therapeutic results? One explanation for the failure of single prime-boost vaccinations to reject tumors could be that the delayed peak T cell response allowed increased tumor growth and the tumor became too large for T cells to eliminate. A related explanation provides some mechanistic insight into the differential tumor control of cluster vaccination versus single prime-boost. Effective anti-tumor immunity may require immediate and potent T cell responses that cluster vaccination achieves. For example a study showed that a slowly evolving T cell response induced a small wave of T cells that entered the tumor microenvironment five days after vaccination and caused the tumor to rapidly upregulate immune inhibiting molecules like PD-L1, PD-L2, Galectin-9, and TGF-β [388]. These immune dampening molecules prevented the subsequent flood of antigen-specific T cells from killing the tumor [388]. Further analysis found that the size of the initial wave of T cells predicted tumor regression, but the size of the peak T cell response was not associated with tumor regression; thus, the T cell expansion kinetics rather than the peak T cell response dictated tumor regression [388]. These results may help to explain the poor control of E.G7 tumors when a single prime-boost SLP vaccine was used: The initial small T cell response to the prime may have allowed the tumor to upregulate immune evasion molecules prior to the large wave of T cells in response to the boost. In contrast, cluster vaccination provides a massive primary attack that may control E.G7 tumor prior to induction of immune evasion molecules. Further research is warranted to investigate the immune inhibitory network expressed in the tumor microenvironment during cluster versus single prime-boost vaccinations to determine the mechanism for differential tumor control.

Applying cluster vaccination to human cancers

If the T cell kinetics prove to be responsible for improved efficacy of cluster vaccination, the results could help explain the lack of responses observed in most clinical vaccine trials [450], even when large T cell responses are eventually activated [249]. Clinical anti-cancer vaccine trials typically use weekly or monthly boosts, resulting in small primary T cell responses that slowly increase [412]. Thus, the small wave of T cells may prepare human tumors to evade the subsequent massive wave of T cells induced by the boost vaccinations. In contrast to slowly evolving T cell responses to long interval prime-boost vaccines, clinical TIL-ACT trials administer massive numbers of T cells all at once, and they achieve higher response rates than vaccines. Potentially, the immediacy of the large T cell attack from TIL-ACT could be partially responsible for superior responses. If proved correct, the immediate and potent T cell response induced by cluster vaccination could improve clinical anti-cancer vaccine trials. However, another challenge of clinical vaccine trials has been that most targeted self-proteins, which typically activate T cells with lower affinity TCR.

Neoantigen targeted therapies: mutation counts matter

Targeting neoantigens offers several advantages over targeting self-proteins (as discussed in Chapter 1), but the low frequency of mutations that give rise to authentic neoantigens and the lack of shared mutations among patients make identifying and targeting neoantigens challenging. In the ID8-G7 neoantigen vaccine study described in Chapter 3, the low mutation burden and corresponding weak predicted binding epitopes were probably major factors for the absence of authentic neoantigen-reactive T cells. However, the ID8-G7 neoantigen load was likely more representative of typical human tumors than the models targeted by other groups. For example, the thousands of mutations identified in published murine neoantigen vaccines studies [238,314,343,358] are orders of magnitude higher than the median of 44 in human tumors [303]. Moreover, most clinical studies that identified neoantigen specific T cells within TIL were conducted in highly-mutated melanomas [344,345,347,349]. In contrast, our group found that only 1 of 3 HGSC patients harbored neoantigen-reactive T cells, with the lone positive case further examined in Chapter 4 [439]. Furthermore, a study of non-small cell lung cancer patients treated with PD-1 blocking

antibodies determined that the number of mutations that best divided responders from non-responders was 178 [331], a mutation frequency that is rare in most cancer types. Thus, mutation burden has proved to be a critical factor determining whether a tumor will harbor authentic neoantigens. However, analysis in Chapter 3 of TCGA data found that the median number of predicted neoantigens in human ovarian tumors was 0.48, meaning that just over half of human HGSC tumors were predicted to have no targetable neoantigens. Therefore, my results suggest that, similar to failed tumor control in the ID8-G7 model, most HGSC patients would fail neoantigen targeted treatments.

In addition to considering *average* mutation burden in a tumor type, it is important to recognize that mutation burden can vary by several orders of magnitude within some tumor types [300]. An extreme example of this phenomenon is endometrial cancer (EC), where patients with mutations in *POLE*, encoding a DNA proofreading enzyme, have 105-fold more predicted neoantigens than POLE non-mutated EC [451]. These patients have very high levels of TIL and favorable prognosis [452,453]. Another example is colorectal cancer, where cases with microsatellite instability harbor dramatically more mutations than microsatellite stable tumors [304]. Interestingly, the highly mutated subset of colorectal tumors responded more favorably to checkpoint blockade than less mutated cases [454]. Unfortunately, HGSC exhibits a relatively narrow range of mutation burdens and lacks a hypermutated subtype [455]. Indeed, only 12% of HGSC cases have > 90% chance of harboring at least one authentic neoantigen compared to 51% of lung cancers (Figure 15). Therefore, neoantigen targeted vaccines may be suited for only a few HGSC patients.

The number of mutations in a tumor can be evaluated as higher or lower depending on the depth of sequencing. The initial founder cell that develops into a tumor harbors a distinct set of mutations that are found in all daughter cells. The VAF of these mutations is often close to 0.5 (assuming a pure tumor sample with heterozygous mutations in one of two alleles). However, tumors also develop additional mutations, mostly passengers, as they grow and divide [365]. When a tumor is sequenced, the VAF is lower for mutations generated in cells further from the founder cell. The mutation frequency follows an inverse power law with the allelic frequency: increasingly more mutations are found at lower VAF [456]. Interestingly, one group found that responses in lung cancer and melanoma patients to immune-checkpoint blockade were associated with higher mutation loads in founder clones,

but not with higher mutation loads in subclones (as determined by the VAF) [342]. These data suggest that tumors derived from founder cells exposed to a lifetime of mutagenic assaults (for example melanoma and lung cancers mutated by UV rays and smoking, respectively) would respond well to immune checkpoint blockade. However, tumors that acquire a mutator phenotype later during tumor progression would have fewer founder mutations and respond poorly to immune checkpoint blockade. Though these tumors may have many mutations, each mutation would have a low VAF. Indeed thousands of mutations would be identified in every tumor if it was sequenced extremely deeply, and some of these mutations would likely be immunogenic. However, targeting these subclonal mutations would probably be futile, as only a small proportion of the tumor cells would be recognized and killed. Therefore, neoantigen vaccine design should give higher priority to mutations in founder clones compared to mutations in subclones. On the other hand, there may be exceptions (as discussed below) where a T cell response to a minor subclone may prevent clonal outgrowth.

Clinical trials may have already demonstrated the challenges of targeting low VAF mutations. One study investigated gastrointestinal tumors and identified mutation reactive T cells in 9/10 patient TIL [351]. This study used a low VAF cutoff to call mutations, resulting in an average of 145 mutation-calls/patient. Lowering the mutation calling threshold had a similar effect to sequencing more deeply: more mutations are identified at lower VAF (though more false positive variants would also be identified). When neoantigen reactive TIL products recognizing these mutations were administered to patients, few clinical responses were observed (Tran E, Canadian Cancer Immunotherapy Consortium, Vancouver BC, May 2015). The reason for the low response rate is difficult to determine since T cell reactivity to autologous tumor was not assessed, but low VAF of target mutations may have contributed [351]. In contrast, in a second study, a patient derived T cell clone was isolated that recognized a putative driver mutation (in ERBB2IP) that was present in all assessed metastases, indicating the mutation was in a founder clone. The T cell recognized tumor cells, and ACT of a near clonal neoantigen specific T cell product led to tumor regression [351]. In summary, when targeting neoantigens with ACT or vaccines, mutations with high VAF should be prioritized to improve clinical responses.

Identification of neoantigen specific T cells prior to vaccination

In both the ID8-G7 and HGSC projects (Chapters 3 and 4), I activated and identified several mutation reactive T cell responses that were ultimately red herrings, unable to recognize autologous tumor. An alternative approach to neoantigen vaccine design is to first identify endogenously-activated neoantigen-specific T cells. For example, one group investigated neoantigen-specific T cells in TIL from a murine tumor [343]. T cells were identified that recognized two of the 62 predicted MHCI-binding mutant epitopes (IC50 < 30 nM) assessed. Tumor-bearing mice treated with SLP vaccines encoding the two confirmed neoantigens led to statistically significant improved survival [343]. By first identifying endogenously-activated neoantigen-reactive T cells, vaccines could be designed to target antigens known to be authentic. In my studies of IROC024 neoantigens (Chapter 4), T cells were identified in patient peripheral blood that recognized several mutations, including mutated HSDL1. However, the only authentic neoantigen was the HSDL1 mutation, and T cells recognizing this mutation were spontaneously activated and expanded in the ascites. If this patient had received a cocktail of predicted neoantigen peptides, several T cell responses may have been elicited, but only one would be biologically relevant. As discussed in Chapter 1, when two vaccine antigens are presented by the same APC, the T cell response to one antigen can inhibit the T cell response to a second antigen, a phenomenon known as immunodomination [16,115,119]. Therefore, a vaccine cocktail of predicted IROC024 neoantigens may have led to non-relevant mutation-specific T cells inhibiting the T cell responses to the authentic HSDL1 neoantigen. By first identifying authentic neoantigen reactive T cells in ascites or tumor, personalized vaccines can be designed to target only the biologically relevant antigen(s).

Often in clinical settings, TIL or TAL are unavailable for the identification of neoantigen reactive T cells, but the methods developed in Chapter 4 could be used to detect authentic neoantigen-reactive T cells from small quantities of blood. To generate TIL or TAL, live tumor or ascites are required, but these samples are often unavailable due to morbidities associated with surgical resection [440,441]. Additionally, in some cases TIL fail to expand *ex vivo* and are therefore unavailable to assess for neoantigen reactivity [457]. Patient peripheral blood is much more accessible than TIL or TAL, and neoantigen specific T cells have been identified in peripheral blood using tandem-minigene-transfected

autologous DCs [348]. However, DC generation required leukapheresis and large quantities of blood, which some cancer patients may be unable to supply. In contrast, the methods applied in Chapter 4 detected, isolated, and expanded endogenously-activated HSDL1-specific T cells from small quantities of blood. Using these methods, almost all cancer patients could be assessed for neoantigen reactivity, and an immunotherapy could be designed to target each patient's authentic neoantigens.

Proteomics to identify neoantigens

Proteomic analysis of peptides eluted from MHC molecules is another method to ensure that neoantigens are processed and presented [458]. One group assessed two mouse tumor models, MC-38 and TRAMP-C1, using a combination of exome sequencing, epitope prediction, and proteomics analysis. Exome sequencing identified 4285 and 949 non-synonymous mutations, epitope prediction identified 170 and 6 predicted neoepitopes (IC50 < 500 nM), and mass spectrometric (MS) analysis identified seven and zero mutated peptides from MC-38 and TRAMP-C1, respectively. T cells recognizing three neoantigens were identified in MC-38 TIL, and vaccines targeting these three neoantigens induced tumor rejection. The three authentic neoantigens in the MC-38 model bound to MHCI with predicted IC50 values of 8, 9, and 2 nM, highlighting the high affinity of authentic neoepitopes for MHCI. In contrast, this study identified very few mutated peptides that were predicted to bind MHCI in the TRAMP-C1 model, and similar to my findings on ID8-G7 described in Chapter 3, no authentic neoantigens were identified in the TRAMP-C1 model. By using MS, the authors avoided chasing predicted neoantigens that were not processed and presented in the TRAMP-C1 model. Similar approaches have identified SNP-derived peptides presented on MHCI in humans [202,459], demonstrating the feasibility of this technique in some cases. For these studies, billions of live cells were required for MS mediated discovery of epitopes; therefore, MS mediated neoantigen discovery would be limited to either tumor cell lines or tumor types with large quantities of available cells. However, MS technologies are constantly improving and sensitivities are increasing; therefore, MS techniques could soon allow identification of mutated peptides from patient tumor-cells.

Neoantigen specific T cell co-evolution with tumor

Although causal relationships cannot be determined through anecdotal observations, the HSDL1 neoantigen T cell response could demonstrate an interesting move/counter move between the tumor and anti-tumor T cells. The HSDL1 VAF was only 3.5% in the primary ascites sample, and the HSDL1 neoantigen was ignored by the immune system at this time point. However, in the first recurrence ascites the HSDL1 VAF became > 50%, and the immune system no longer ignored the HSDL1 mutation. Along with the sudden abundance of neoantigen came an HSDL1-mutation specific T cell attack that was detectable in the first recurrent ascites and was expanded in the blood. At second recurrence, the HSDL1 VAF was still > 50%, but the HSDL1 specific T cells had disappeared from the ascites and blood, indicating that the immune system had lost the battle. Thus, the tumor seemed to have counteracted the neoantigen specific T cell response, not by evolving into an antigen-loss variant, or so called "immune editing", but potentially, by eliminating the T cells that were attacking the tumor, or "tumor editing". Several mechanisms discussed in Chapter 1 could account for tumor editing. For example, high levels of PD-L1 expression on the tumor, TAM, MDSC, or Tregs may have caused HSDL1 specific T cell anergy and eventual T cell death [134]. Also, these immune inhibiting cells could secrete various factors like TGF-β, Arginase-1, and IL-10 that inhibit activated T cells [127-129]. Moreover, persistent antigen in a non-inflammatory microenvironment could induce T cell anergy [78]. By whatever mechanism, the HSDL1 mutation specific T cell response was no longer found in ascites or blood by second recurrence. Potentially, immune intervention could have potentiated the HSDL1-specific T cells and perpetuated the battle between the immune system versus cancer.

The study described in Chapter 4 was unique in that mutation-reactive T cells were assessed at multiple time points in both tumor and PBMC. A single HSDL1-mutant reactive T cell response was identified in the pre-surgery and three month blood draw time points. Given the low frequency of these clones ($1/8x10^5$), it is probable that these T cells were still naive. In contrast, five HSDL1 mutation specific T cells were identified in the six month blood draw, indicating that these T cells had become activated. However, at this time point, tumor recurrence had not been diagnosed. Therefore, the T cell expansion foretold of the impending tumor recurrence. Hypothetically, had we been monitoring the PBMC in real time

and identified the expanded HSDL1-specific T cell response, treatments could have been initiated prior to biochemical relapse (increased CA-125). Further, identification of expanded neoantigen-specific T cells would have provided rationale for immunotherapies once they proved to recognize autologous tumor. For example, the patient could have been treated with an ACT product composed of clonal HSDL1-specific T cells, immune checkpoint blockade to potentiate the T cell response, or an HSDL1 mutated peptide vaccine to amplify these T cells.

If the case described in Chapter 4 had been studied at only one time point, I may have arrived at dramatically different conclusions about the potential value of neoantigen-targeted vaccines. For example, had only the primary sample been analyzed, the HSDL1 response would have been undetectable in the ascites but detectable in blood. Thus, I would likely conclude that the blood harbors authentic neoantigen-reactive T cells that are absent from the ascites. Had only the first recurrent samples been analyzed, the HSDL1 response would have been detected in ascites and blood. Thus, I would likely conclude that T cells recognizing all authentic neoantigens are activated and can be found both in the blood and the ascites. However, had only the second recurrence been analyzed, the HSDL1 response would be undetectable in both ascites and blood. Thus, I would have likely concluded that this tumor was devoid of neoantigens. The diversity of these theoretical conclusions based on when the sample was analyzed demonstrates the plasticity of the immune response to tumors. It also demonstrates that large numbers of patients should be analyzed at multiple time points to draw firm conclusions about the true neoantigen repertoire of cancers and the utility of targeting neoantigens with vaccines.

Alternative neoantigen targets

To date, all NGS studies that identified neoantigens – including the present study – have evaluated only point mutations and small indels. However, like many cancers, HGSC is thought to be primarily driven by large genomic rearrangements and transcriptome aberrations rather than point mutations [367,460]. These aberrations can give rise to other classes of neoantigen involving gene fusions [327], intron retentions [461], and splice variants [462]. Some of these alterations can be highly immunogenic, as they deviate even further from the germ line sequence compared to point mutations. Typically, these types of

variants are identified using RNA-seq, which at present, is beset with high rates of false positive variant calls. Further improvement in the construction of RNA-seq libraries and bioinformatic analysis of RNA-seq data will create access to new classes of neoantigens for immunotherapeutic targeting in HGSC and other chromosomally unstable cancers. Thus, while the "point neoantigen repertoire" of HGSC may contain relatively few targets for immunotherapy, other classes of neoantigen await investigation. The strong prognostic significance of tumor-infiltrating T cells in HGSC [6,371] provides both impetus and optimism for these efforts.

Concluding remarks

Cancer immunotherapy has enjoyed a renaissance during the last five years. The successful use – and eventual FDA approval – of T cell activating antibodies to destroy human tumors has driven renewed ambition for developing new immunotherapies. Advances in NGS make it feasible to identify immune responses to private tumor mutations, and studies indicate that tumor mutations may be the underlying antigens targeted by successful immune therapies: (1) Tumors with higher mutation burdens respond better than tumors with low mutation burden to immune checkpoint blockade [331,340]; (2) neoantigen-targeted vaccines have cured mice of established tumors in several cancer model systems [238,314,343,358]; (3) neoantigen specific T cells are commonly identified in patients who observe clinical responses to TIL ACT [463]; and (4) neoantigens are not found in the germ line so TCR that bind to neoantigens may be exceptionally high affinity [21]. Thus, several lines of evidence indicate that neoantigens represent outstanding targets for successful immunotherapy.

The studies presented in this thesis demonstrate improved methods for activation and identification of neoantigen specific T cells, yet they also offer sober reflection on the broader applicability of targeting neoantigens in many tumor types. My studies demonstrate that tumors with low or intermediate mutation burdens may harbour no targetable neoantigens. This is in concordance with a study that showed that patients with less than 178 mutations were unlikely to respond to PD-1 blockade therapy [331]. Furthermore, the identification of a tumor neoantigen is only the first small step towards successfully targeting that mutation with a vaccine. For example, HPV E6 and E7 proteins seem to represent ideal

antigens that share many antigenic properties with neoantigens: (1) HPV proteins are present in most cervical cancer cases; (2) they are completely foreign; (3) epitopes are well described; (4) the proteins are ubiquitously expressed within tumor cells; and (5) they are driver proteins. Yet immunotherapies targeting HPV antigens continue to have only moderate clinical response rates [464]. Once neoantigens are readily identifiable in each tumor, will immunotherapies targeting neoantigens also suffer from moderate clinical response rates?

Methods to identify and target neoantigens with personalized therapies are in their infancy. As described in this thesis, I advanced development of these therapies by improving SLP vaccination protocols to elicit potent and immediate T cell responses and by developing a technique to identify antigen specific T cells from small amounts of peripheral blood. The improved vaccination protocols can be easily be applied for targeting confirmed neoantigens. Furthermore, the miniline approach detected rare, activated and naive neoantigen-reactive T cells, which could be used to direct or generate neoantigen-targeted immunotherapies. Though neoantigen-targeted immunotherapies are in their infancy, continued advancements could make these treatments a viable option for select cancer patients in the near future.

Bibliography

1. Coulie PG, Van den Eynde BJ, van der Bruggen P, Boon T (2014) Tumour antigens recognized by T lymphocytes: at the core of cancer immunotherapy. Nat Rev Cancer 14: 135-146.

2. Vigneron N, Stroobant V, Van den Eynde BJ, van der Bruggen P (2013) Database of T cell-defined human tumor antigens: the 2013 update. Cancer Immun 13: 15.

3. Melief CJ, van Hall T, Arens R, Ossendorp F, van der Burg SH (2015) Therapeutic cancer vaccines. J Clin Invest 125: 3401-3412.

4. LeBlanc VG, Marra MA (2015) Next-Generation Sequencing Approaches in Cancer: Where Have They Brought Us and Where Will They Take Us? Cancers (Basel) 7: 1925-1958.

5. Bowtell DD, Bohm S, Ahmed AA, Aspuria PJ, Bast RC, Jr., et al. (2015) Rethinking ovarian cancer II: reducing mortality from high-grade serous ovarian cancer. Nat Rev Cancer 15: 668-679.

6. Zhang L, Conejo-Garcia JR, Katsaros D, Gimotty PA, Massobrio M, et al. (2003) Intratumoral T cells, recurrence, and survival in epithelial ovarian cancer. N Engl J Med 348: 203-213.

7. Cascio P, Hilton C, Kisselev AF, Rock KL, Goldberg AL (2001) 26S proteasomes and immunoproteasomes produce mainly N-extended versions of an antigenic peptide. EMBO J 20: 2357-2366.

8. Neefjes J, Jongsma ML, Paul P, Bakke O (2011) Towards a systems understanding of MHC class I and MHC class II antigen presentation. Nat Rev Immunol 11: 823-836.

9. York IA, Chang SC, Saric T, Keys JA, Favreau JM, et al. (2002) The ER aminopeptidase ERAP1 enhances or limits antigen presentation by trimming epitopes to 8-9 residues. Nat Immunol 3: 1177-1184.

10. Koopmann JO, Albring J, Huter E, Bulbuc N, Spee P, et al. (2000) Export of antigenic peptides from the endoplasmic reticulum intersects with retrograde protein translocation through the Sec61p channel. Immunity 13: 117-127.

11. Vyas JM, Van der Veen AG, Ploegh HL (2008) The known unknowns of antigen processing and presentation. Nat Rev Immunol 8: 607-618.

12. Carbone FR, Bevan MJ (1990) Class I-restricted processing and presentation of exogenous cell-associated antigen in vivo. J Exp Med 171: 377-387.

13. Gutierrez-Martinez E, Planes R, Anselmi G, Reynolds M, Menezes S, et al. (2015) Cross-Presentation of Cell-Associated Antigens by MHC Class I in Dendritic Cell Subsets. Front Immunol 6: 363.

14. Assarsson E, Sidney J, Oseroff C, Pasquetto V, Bui HH, et al. (2007) A quantitative analysis of the variables affecting the repertoire of T cell specificities recognized after vaccinia virus infection. J Immunol 178: 7890-7901.

15. Sette A, Vitiello A, Reherman B, Fowler P, Nayersina R, et al. (1994) The relationship between class I binding affinity and immunogenicity of potential cytotoxic T cell epitopes. J Immunol 153: 5586-5592.

16. Yewdell JW, Bennink JR (1999) Immunodominance in major histocompatibility complex class I-restricted T lymphocyte responses. Annu Rev Immunol 17: 51-88.

17. Paul S, Weiskopf D, Angelo MA, Sidney J, Peters B, et al. (2013) HLA class I alleles are associated with peptide-binding repertoires of different size, affinity, and immunogenicity. J Immunol 191: 5831-5839.

18. Mungall AJ, Palmer SA, Sims SK, Edwards CA, Ashurst JL, et al. (2003) The DNA sequence and analysis of human chromosome 6. Nature 425: 805-811.

19. Robinson J, Halliwell JA, Hayhurst JD, Flicek P, Parham P, et al. (2015) The IPD and IMGT/HLA database: allele variant databases. Nucleic Acids Res 43: D423-431.

20. Engels B, Engelhard VH, Sidney J, Sette A, Binder DC, et al. (2013) Relapse or eradication of cancer is predicted by peptide-major histocompatibility complex affinity. Cancer Cell 23: 516-526.

21. Obenaus M, Leitao C, Leisegang M, Chen X, Gavvovidis I, et al. (2015) Identification of human T-cell receptors with optimal affinity to cancer antigens using antigen-negative humanized mice. Nat Biotechnol 33: 402-407.

22. Valmori D, Fonteneau JF, Lizana CM, Gervois N, Lienard D, et al. (1998) Enhanced generation of specific tumor-reactive CTL in vitro by selected Melan-A/MART-1 immunodominant peptide analogues. J Immunol 160: 1750-1758.

23. Harndahl M, Rasmussen M, Roder G, Dalgaard Pedersen I, Sorensen M, et al. (2012) Peptide-MHC class I stability is a better predictor than peptide affinity of CTL immunogenicity. Eur J Immunol 42: 1405-1416.

24. Vitiello A, Yuan L, Chesnut RW, Sidney J, Southwood S, et al. (1996) Immunodominance analysis of CTL responses to influenza PR8 virus reveals two new dominant and subdominant Kb-restricted epitopes. J Immunol 157: 5555-5562.

25. Masuko K, Wakita D, Togashi Y, Kita T, Kitamura H, et al. (2015) Artificially synthesized helper/killer-hybrid epitope long peptide (H/K-HELP): preparation and immunological analysis of vaccine efficacy. Immunol Lett 163: 102-112.

26. Wall EM, Milne K, Martin ML, Watson PH, Theiss P, et al. (2007) Spontaneous mammary tumors differ widely in their inherent sensitivity to adoptively transferred T cells. Cancer Res 67: 6442-6450.

27. Yang T, Wall EM, Milne K, Theiss P, Watson P, et al. (2007) CD8+ T cells induce complete regression of advanced ovarian cancers by an interleukin (IL)-2/IL-15 dependent mechanism. Clin Cancer Res 13: 7172-7180.

28. Hassan C, Chabrol E, Jahn L, Kester MG, de Ru AH, et al. (2015) Naturally processed non-canonical HLA-A*02:01 presented peptides. J Biol Chem 290: 2593-2603.

29. Dudley ME, Wunderlich J, Nishimura MI, Yu D, Yang JC, et al. (2001) Adoptive transfer of cloned melanoma-reactive T lymphocytes for the treatment of patients with metastatic melanoma. J Immunother 24: 363-373.

30. Zhang GL, Ansari HR, Bradley P, Cawley GC, Hertz T, et al. (2011) Machine learning competition in immunology - Prediction of HLA class I binding peptides. J Immunol Methods 374: 1-4.

31. Lundegaard C, Lund O, Nielsen M (2011) Prediction of epitopes using neural network based methods. J Immunol Methods 374: 26-34.

32. Hoof I, Peters B, Sidney J, Pedersen LE, Sette A, et al. (2009) NetMHCpan, a method for MHC class I binding prediction beyond humans. Immunogenetics 61: 1-13.

33. Nielsen M, Lundegaard C, Worning P, Lauemoller SL, Lamberth K, et al. (2003) Reliable prediction of T-cell epitopes using neural networks with novel sequence representations. Protein Sci 12: 1007-1017.

34. Peters B, Bui HH, Frankild S, Nielson M, Lundegaard C, et al. (2006) A community resource benchmarking predictions of peptide binding to MHC-I molecules. PLoS Comput Biol 2: e65.

35. Moutaftsi M, Peters B, Pasquetto V, Tscharke DC, Sidney J, et al. (2006) A consensus epitope prediction approach identifies the breadth of murine T(CD8+)-cell responses to vaccinia virus. Nat Biotechnol 24: 817-819.

36. Nielsen M, Lundegaard C, Lund O, Kesmir C (2005) The role of the proteasome in generating cytotoxic T-cell epitopes: insights obtained from improved predictions of proteasomal cleavage. Immunogenetics 57: 33-41.

37. Tenzer S, Peters B, Bulik S, Schoor O, Lemmel C, et al. (2005) Modeling the MHC class I pathway by combining predictions of proteasomal cleavage, TAP transport and MHC class I binding. Cell Mol Life Sci 62: 1025-1037.

38. Calis JJ, Reinink P, Keller C, Kloetzel PM, Kesmir C (2015) Role of peptide processing predictions in T cell epitope identification: contribution of different prediction programs. Immunogenetics 67: 85-93.

39. Backert L, Kohlbacher O (2015) Immunoinformatics and epitope prediction in the age of genomic medicine. Genome Med 7: 119.

40. Gowthaman U, Agrewala JN (2008) In silico tools for predicting peptides binding to HLA-class II molecules: more confusion than conclusion. J Proteome Res 7: 154-163.

41. Singh SP, Mishra BN (2016) Major histocompatibility complex linked databases and prediction tools for designing vaccines. Hum Immunol 77: 295-306.

42. Meydan C, Otu HH, Sezerman OU (2013) Prediction of peptides binding to MHC class I and II alleles by temporal motif mining. BMC Bioinformatics 14 Suppl 2: S13.

43. Davis MM, Bjorkman PJ (1988) T-cell antigen receptor genes and T-cell recognition. Nature 334: 395-402.

44. Bassing CH, Swat W, Alt FW (2002) The mechanism and regulation of chromosomal V(D)J recombination. Cell 109 Suppl: S45-55.

45. Arstila TP, Casrouge A, Baron V, Even J, Kanellopoulos J, et al. (1999) A direct estimate of the human alphabeta T cell receptor diversity. Science 286: 958-961.

46. Bains I, Antia R, Callard R, Yates AJ (2009) Quantifying the development of the peripheral naive CD4+ T-cell pool in humans. Blood 113: 5480-5487.

47. Klein L, Kyewski B, Allen PM, Hogquist KA (2014) Positive and negative selection of the T cell repertoire: what thymocytes see (and don't see). Nat Rev Immunol 14: 377-391.

48. Germain RN (2002) T-cell development and the CD4-CD8 lineage decision. Nat Rev Immunol 2: 309-322.

49. Kwan J, Killeen N (2004) CCR7 directs the migration of thymocytes into the thymic medulla. J Immunol 172: 3999-4007.

50. Wang L, Xiong Y, Bosselut R (2010) Tenuous paths in unexplored territory: From T cell receptor signaling to effector gene expression during thymocyte selection. Semin Immunol 22: 294-302.

51. Anderson MS, Venanzi ES, Klein L, Chen Z, Berzins SP, et al. (2002) Projection of an immunological self shadow within the thymus by the aire protein. Science 298: 1395-1401.

52. Abramson J, Goldfarb Y (2016) AIRE: From promiscuous molecular partnerships to promiscuous gene expression. Eur J Immunol 46: 22-33.

53. Morgan DJ, Kreuwel HT, Fleck S, Levitsky HI, Pardoll DM, et al. (1998) Activation of low avidity CTL specific for a self epitope results in tumor rejection but not autoimmunity. J Immunol 160: 643-651.

54. Ohashi PS, Oehen S, Buerki K, Pircher H, Ohashi CT, et al. (1991) Ablation of "tolerance" and induction of diabetes by virus infection in viral antigen transgenic mice. Cell 65: 305-317.

55. Legoux FP, Lim JB, Cauley AW, Dikiy S, Ertelt J, et al. (2015) CD4(+) T Cell Tolerance to Tissue-Restricted Self Antigens Is Mediated by Antigen-Specific Regulatory T Cells Rather Than Deletion. Immunity 43: 896-908.

56. Richards DM, Kyewski B, Feuerer M (2016) Re-examining the Nature and Function of Self-Reactive T cells. Trends Immunol 37: 114-125.

57. Jung S, Unutmaz D, Wong P, Sano G, De los Santos K, et al. (2002) In vivo depletion of CD11c+ dendritic cells abrogates priming of CD8+ T cells by exogenous cell-associated antigens. Immunity 17: 211-220.

58. Goulopoulou S, McCarthy CG, Webb RC (2016) Toll-like Receptors in the Vascular System: Sensing the Dangers Within. Pharmacol Rev 68: 142-167.

59. Redmond WL, Sherman LA (2005) Peripheral tolerance of CD8 T lymphocytes. Immunity 22: 275-284.

60. den Haan JM, Arens R, van Zelm MC (2014) The activation of the adaptive immune system: cross-talk between antigen-presenting cells, T cells and B cells. Immunol Lett 162: 103-112.

61. Mueller SN, Gebhardt T, Carbone FR, Heath WR (2013) Memory T cell subsets, migration patterns, and tissue residence. Annu Rev Immunol 31: 137-161.

62. Bromley SK, Thomas SY, Luster AD (2005) Chemokine receptor CCR7 guides T cell exit from peripheral tissues and entry into afferent lymphatics. Nat Immunol 6: 895-901.

63. Mandl JN, Liou R, Klauschen F, Vrisekoop N, Monteiro JP, et al. (2012) Quantification of lymph node transit times reveals differences in antigen surveillance strategies of naive CD4+ and CD8+ T cells. Proc Natl Acad Sci U S A 109: 18036-18041.

64. van Heijst JW, Gerlach C, Swart E, Sie D, Nunes-Alves C, et al. (2009) Recruitment of antigen-specific CD8+ T cells in response to infection is markedly efficient. Science 325: 1265-1269.

65. Zehn D, Lee SY, Bevan MJ (2009) Complete but curtailed T-cell response to very low-affinity antigen. Nature 458: 211-214.

66. Alexander-Miller MA, Leggatt GR, Berzofsky JA (1996) Selective expansion of high- or low-avidity cytotoxic T lymphocytes and efficacy for adoptive immunotherapy. Proc Natl Acad Sci U S A 93: 4102-4107.

67. Yee C, Savage PA, Lee PP, Davis MM, Greenberg PD (1999) Isolation of high avidity melanoma-reactive CTL from heterogeneous populations using peptide-MHC tetramers. J Immunol 162: 2227-2234.

68. Smith-Garvin JE, Koretzky GA, Jordan MS (2009) T cell activation. Annu Rev Immunol 27: 591-619.

69. Watts TH (2005) TNF/TNFR family members in costimulation of T cell responses. Annu Rev Immunol 23: 23-68.

70. Blanco P, Palucka AK, Pascual V, Banchereau J (2008) Dendritic cells and cytokines in human inflammatory and autoimmune diseases. Cytokine Growth Factor Rev 19: 41-52.

71. Blattman JN, Antia R, Sourdive DJ, Wang X, Kaech SM, et al. (2002) Estimating the precursor frequency of naive antigen-specific CD8 T cells. J Exp Med 195: 657-664.

72. Bennett SR, Carbone FR, Karamalis F, Flavell RA, Miller JF, et al. (1998) Help for cytotoxic-T-cell responses is mediated by CD40 signalling. Nature 393: 478-480.

73. Schoenberger SP, Toes RE, van der Voort EI, Offringa R, Melief CJ (1998) T-cell help for cytotoxic T lymphocytes is mediated by CD40-CD40L interactions. Nature 393: 480-483.

74. Smith CM, Wilson NS, Waithman J, Villadangos JA, Carbone FR, et al. (2004) Cognate CD4(+) T cell licensing of dendritic cells in CD8(+) T cell immunity. Nat Immunol 5: 1143-1148.

75. Castellino F, Huang AY, Altan-Bonnet G, Stoll S, Scheinecker C, et al. (2006) Chemokines enhance immunity by guiding naive CD8+ T cells to sites of CD4+ T cell-dendritic cell interaction. Nature 440: 890-895.

76. Steinman RM, Hawiger D, Nussenzweig MC (2003) Tolerogenic dendritic cells. Annu Rev Immunol 21: 685-711.

77. Osorio F, Fuentes C, Lopez MN, Salazar-Onfray F, Gonzalez FE (2015) Role of Dendritic Cells in the Induction of Lymphocyte Tolerance. Front Immunol 6: 535.

78. Willimsky G, Blankenstein T (2005) Sporadic immunogenic tumours avoid destruction by inducing T-cell tolerance. Nature 437: 141-146.

79. Dwyer JM, Johnson C (1981) The use of concanavalin A to study the immunoregulation of human T cells. Clin Exp Immunol 46: 237-249.

80. Dudley ME, Wunderlich JR, Shelton TE, Even J, Rosenberg SA (2003) Generation of tumor-infiltrating lymphocyte cultures for use in adoptive transfer therapy for melanoma patients. J Immunother 26: 332-342.

81. Suhoski MM, Golovina TN, Aqui NA, Tai VC, Varela-Rohena A, et al. (2007) Engineering artificial antigen-presenting cells to express a diverse array of co-stimulatory molecules. Mol Ther 15: 981-988.

82. Forget MA, Malu S, Liu H, Toth C, Maiti S, et al. (2014) Activation and propagation of tumor-infiltrating lymphocytes on clinical-grade designer artificial antigen-presenting cells for adoptive immunotherapy of melanoma. J Immunother 37: 448-460.

83. Nayar S, Dasgupta P, Galustian C (2015) Extending the lifespan and efficacies of immune cells used in adoptive transfer for cancer immunotherapies-A review. Oncoimmunology 4: e1002720.

84. Ho WY, Nguyen HN, Wolfl M, Kuball J, Greenberg PD (2006) In vitro methods for generating CD8+ T-cell clones for immunotherapy from the naive repertoire. J Immunol Methods 310: 40-52.

85. Kotturi MF, Scott I, Wolfe T, Peters B, Sidney J, et al. (2008) Naive precursor frequencies and MHC binding rather than the degree of epitope diversity shape CD8+ T cell immunodominance. J Immunol 181: 2124-2133.

86. Prlic M, Hernandez-Hoyos G, Bevan MJ (2006) Duration of the initial TCR stimulus controls the magnitude but not functionality of the CD8+ T cell response. J Exp Med 203: 2135-2143.

87. Gett AV, Sallusto F, Lanzavecchia A, Geginat J (2003) T cell fitness determined by signal strength. Nat Immunol 4: 355-360.

88. Lefrancois L, Altman JD, Williams K, Olson S (2000) Soluble antigen and CD40 triggering are sufficient to induce primary and memory cytotoxic T cells. J Immunol 164: 725-732.

89. Zinkernagel RM (2000) Localization dose and time of antigens determine immune reactivity. Semin Immunol 12: 163-171; discussion 257-344.

90. Butz EA, Bevan MJ (1998) Massive expansion of antigen-specific CD8+ T cells during an acute virus infection. Immunity 8: 167-175.

91. Saeidi A, Buggert M, Che KF, Kong YY, Velu V, et al. (2015) Regulation of CD8+ T-cell cytotoxicity in HIV-1 infection. Cell Immunol 298: 126-133.

92. Jenner RG, Townsend MJ, Jackson I, Sun K, Bouwman RD, et al. (2009) The transcription factors T-bet and GATA-3 control alternative pathways of T-cell differentiation through a shared set of target genes. Proc Natl Acad Sci U S A 106: 17876-17881.

93. Voskoboinik I, Smyth MJ, Trapani JA (2006) Perforin-mediated target-cell death and immune homeostasis. Nat Rev Immunol 6: 940-952.

94. Rao RR, Li Q, Gubbels Bupp MR, Shrikant PA (2012) Transcription factor Foxo1 represses T-bet-mediated effector functions and promotes memory CD8(+) T cell differentiation. Immunity 36: 374-387.

95. Wong P, Lara-Tejero M, Ploss A, Leiner I, Pamer EG (2004) Rapid development of T cell memory. J Immunol 172: 7239-7245.

96. Badovinac VP, Harty JT (2007) Manipulating the rate of memory CD8+ T cell generation after acute infection. J Immunol 179: 53-63.

97. Huang RY, Eppolito C, Lele S, Shrikant P, Matsuzaki J, et al. (2015) LAG3 and PD1 co-inhibitory molecules collaborate to limit CD8+ T cell signaling and dampen antitumor immunity in a murine ovarian cancer model. Oncotarget 6: 27359-27377.

98. Kim PS, Ahmed R (2010) Features of responding T cells in cancer and chronic infection. Curr Opin Immunol 22: 223-230.

99. Nakanishi Y, Lu B, Gerard C, Iwasaki A (2009) CD8(+) T lymphocyte mobilization to virus-infected tissue requires CD4(+) T-cell help. Nature 462: 510-513.

100. Seledtsov VI, Seledtsova GV (2012) A balance between tissue-destructive and tissue-protective immunities: a role of toll-like receptors in regulation of adaptive immunity. Immunobiology 217: 430-435.

101. Tran E, Turcotte S, Gros A, Robbins PF, Lu YC, et al. (2014) Cancer immunotherapy based on mutation-specific CD4+ T cells in a patient with epithelial cancer. Science 344: 641-645.

102. Braumuller H, Wieder T, Brenner E, Assmann S, Hahn M, et al. (2013) T-helper-1-cell cytokines drive cancer into senescence. Nature 494: 361-365.

103. Brunkow ME, Jeffery EW, Hjerrild KA, Paeper B, Clark LB, et al. (2001) Disruption of a new forkhead/winged-helix protein, scurfin, results in the fatal lymphoproliferative disorder of the scurfy mouse. Nat Genet 27: 68-73.

104. Bennett CL, Christie J, Ramsdell F, Brunkow ME, Ferguson PJ, et al. (2001) The immune dysregulation, polyendocrinopathy, enteropathy, X-linked syndrome (IPEX) is caused by mutations of FOXP3. Nat Genet 27: 20-21.

105. Chen W, Jin W, Hardegen N, Lei KJ, Li L, et al. (2003) Conversion of peripheral CD4+CD25- naive T cells to CD4+CD25+ regulatory T cells by TGF-beta induction of transcription factor Foxp3. J Exp Med 198: 1875-1886.

106. Li MO, Wan YY, Flavell RA (2007) T cell-produced transforming growth factor-beta1 controls T cell tolerance and regulates Th1- and Th17-cell differentiation. Immunity 26: 579-591.

107. Rubtsov YP, Rasmussen JP, Chi EY, Fontenot J, Castelli L, et al. (2008) Regulatory T cell-derived interleukin-10 limits inflammation at environmental interfaces. Immunity 28: 546-558.

108. Friedline RH, Brown DS, Nguyen H, Kornfeld H, Lee J, et al. (2009) CD4+ regulatory T cells require CTLA-4 for the maintenance of systemic tolerance. J Exp Med 206: 421-434.

109. Kobie JJ, Shah PR, Yang L, Rebhahn JA, Fowell DJ, et al. (2006) T regulatory and primed uncommitted CD4 T cells express CD73, which suppresses effector CD4 T cells by converting 5'-adenosine monophosphate to adenosine. J Immunol 177: 6780-6786.

110. Borsellino G, Kleinewietfeld M, Di Mitri D, Sternjak A, Diamantini A, et al. (2007) Expression of ectonucleotidase CD39 by Foxp3+ Treg cells: hydrolysis of extracellular ATP and immune suppression. Blood 110: 1225-1232.

111. Pandiyan P, Zheng L, Ishihara S, Reed J, Lenardo MJ (2007) CD4+CD25+Foxp3+ regulatory T cells induce cytokine deprivation-mediated apoptosis of effector CD4+ T cells. Nat Immunol 8: 1353-1362.

112. Zou W (2006) Regulatory T cells, tumour immunity and immunotherapy. Nat Rev Immunol 6: 295-307.

113. Akram A, Inman RD (2012) Immunodominance: a pivotal principle in host response to viral infections. Clin Immunol 143: 99-115.

114. Moon JJ, Chu HH, Pepper M, McSorley SJ, Jameson SC, et al. (2007) Naive CD4(+) T cell frequency varies for different epitopes and predicts repertoire diversity and response magnitude. Immunity 27: 203-213.

115. Weaver JM, Chaves FA, Sant AJ (2009) Abortive activation of CD4 T cell responses during competitive priming in vivo. Proc Natl Acad Sci U S A 106: 8647-8652.

116. Liu F, Whitton JL, Slifka MK (2004) The rapidity with which virus-specific CD8+ T cells initiate IFN-gamma synthesis increases markedly over the course of infection and correlates with immunodominance. J Immunol 173: 456-462.

117. Tung J, Sant AJ (2013) Orchestration of CD4 T cell epitope preferences after multipeptide immunization. J Immunol 191: 764-772.

118. Kedl RM, Rees WA, Hildeman DA, Schaefer B, Mitchell T, et al. (2000) T cells compete for access to antigen-bearing antigen-presenting cells. J Exp Med 192: 1105-1113.

119. Galea I, Stasakova J, Dunscombe MS, Ottensmeier CH, Elliott T, et al. (2012) CD8+ T-cell cross-competition is governed by peptide-MHC class I stability. Eur J Immunol 42: 256-263.

120. Slaney CY, Kershaw MH, Darcy PK (2014) Trafficking of T cells into tumors. Cancer Res 74: 7168-7174.

121. Chen DS, Mellman I (2013) Oncology meets immunology: the cancer-immunity cycle. Immunity 39: 1-10.

122. Dunn GP, Old LJ, Schreiber RD (2004) The three Es of cancer immunoediting. Annu Rev Immunol 22: 329-360.

123. Curiel TJ, Coukos G, Zou L, Alvarez X, Cheng P, et al. (2004) Specific recruitment of regulatory T cells in ovarian carcinoma fosters immune privilege and predicts reduced survival. Nat Med 10: 942-949.

124. Quezada SA, Peggs KS, Curran MA, Allison JP (2006) CTLA4 blockade and GM-CSF combination immunotherapy alters the intratumor balance of effector and regulatory T cells. J Clin Invest 116: 1935-1945.

125. Gao Q, Qiu SJ, Fan J, Zhou J, Wang XY, et al. (2007) Intratumoral balance of regulatory and cytotoxic T cells is associated with prognosis of hepatocellular carcinoma after resection. J Clin Oncol 25: 2586-2593.

126. Sato E, Olson SH, Ahn J, Bundy B, Nishikawa H, et al. (2005) Intraepithelial CD8+ tumor-infiltrating lymphocytes and a high CD8+/regulatory T cell ratio are associated with favorable prognosis in ovarian cancer. Proc Natl Acad Sci U S A 102: 18538-18543.

127. Brady NJ, Chuntova P, Schwertfeger KL (2016) Macrophages: Regulators of the Inflammatory Microenvironment during Mammary Gland Development and Breast Cancer. Mediators Inflamm 2016: 4549676.

128. Marvel D, Gabrilovich DI (2015) Myeloid-derived suppressor cells in the tumor microenvironment: expect the unexpected. J Clin Invest 125: 3356-3364.

129. Kokubu Y, Tabu K, Muramatsu N, Wang W, Murota Y, et al. (2016) Induction of protumoral CD11c(high) macrophages by glioma cancer stem cells through GM-CSF. Genes Cells 21: 241-251.

130. Movahedi K, Guilliams M, Van den Bossche J, Van den Bergh R, Gysemans C, et al. (2008) Identification of discrete tumor-induced myeloid-derived suppressor cell subpopulations with distinct T cell-suppressive activity. Blood 111: 4233-4244.

131. Comber JD, Philip R (2014) MHC class I antigen presentation and implications for developing a new generation of therapeutic vaccines. Ther Adv Vaccines 2: 77-89.

132. Yee C, Thompson JA, Byrd D, Riddell SR, Roche P, et al. (2002) Adoptive T cell therapy using antigen-specific CD8+ T cell clones for the treatment of patients with metastatic melanoma: in vivo persistence, migration, and antitumor effect of transferred T cells. Proc Natl Acad Sci U S A 99: 16168-16173.

133. Vinay DS, Ryan EP, Pawelec G, Talib WH, Stagg J, et al. (2015) Immune evasion in cancer: Mechanistic basis and therapeutic strategies. Semin Cancer Biol 35 Suppl: S185-198.

134. Shin DS, Ribas A (2015) The evolution of checkpoint blockade as a cancer therapy: what's here, what's next? Curr Opin Immunol 33: 23-35.

135. Hall SS (1997) A commotion in the blood : life, death, and the immune system. New York: Henry Holt. xiv, 544 p. p.

136. Sylvester RJ, van der MA, Lamm DL (2002) Intravesical bacillus Calmette-Guerin reduces the risk of progression in patients with superficial bladder cancer: a meta-analysis of the published results of randomized clinical trials. J Urol 168: 1964-1970.

137. Sapre N, Corcoran NM (2013) Modulating the immune response to Bacillus Calmette-Guerin (BCG): a novel way to increase the immunotherapeutic effect of BCG for treatment of bladder cancer? BJU Int 112: 852-853.

138. van der Meijden AP, Sylvester RJ, Oosterlinck W, Hoeltl W, Bono AV, et al. (2003) Maintenance Bacillus Calmette-Guerin for Ta T1 bladder tumors is not associated with increased toxicity: results from a European Organisation for Research and Treatment of Cancer Genito-Urinary Group Phase III Trial. Eur Urol 44: 429-434.

139. Brausi M, Oddens J, Sylvester R, Bono A, van de Beek C, et al. (2014) Side effects of Bacillus Calmette-Guerin (BCG) in the treatment of intermediate- and high-risk Ta, T1 papillary carcinoma of the bladder: results of the EORTC genito-urinary cancers

group randomised phase 3 study comparing one-third dose with full dose and 1 year with 3 years of maintenance BCG. Eur Urol 65: 69-76.

140. Kirkwood JM, Strawderman MH, Ernstoff MS, Smith TJ, Borden EC, et al. (1996) Interferon alfa-2b adjuvant therapy of high-risk resected cutaneous melanoma: the Eastern Cooperative Oncology Group Trial EST 1684. J Clin Oncol 14: 7-17.

141. Gogas H, Ioannovich J, Dafni U, Stavropoulou-Giokas C, Frangia K, et al. (2006) Prognostic significance of autoimmunity during treatment of melanoma with interferon. N Engl J Med 354: 709-718.

142. Atkins MB, Lotze MT, Dutcher JP, Fisher RI, Weiss G, et al. (1999) High-dose recombinant interleukin 2 therapy for patients with metastatic melanoma: analysis of 270 patients treated between 1985 and 1993. J Clin Oncol 17: 2105-2116.

143. Dutcher J (2002) Current status of interleukin-2 therapy for metastatic renal cell carcinoma and metastatic melanoma. Oncology (Williston Park) 16: 4-10.

144. Hughes T, Klairmont M, Sharfman WH, Kaufman HL (2015) Interleukin-2, Ipilimumab, and Anti-PD-1: Clinical Management and the Evolving Role of Immunotherapy for the Treatment of Patients With Metastatic Melanoma. Cancer Biol Ther: 0.

145. Li Y, Zhou L, Sun B, Li X, Duan K, et al. (2015) Interleukin-2 administration after modified radical mastectomy in breast cancer therapy increases peripheral regulatory T cells. Int J Clin Exp Med 8: 7816-7822.

146. Cesana GC, DeRaffele G, Cohen S, Moroziewicz D, Mitcham J, et al. (2006) Characterization of CD4+CD25+ regulatory T cells in patients treated with high-dose interleukin-2 for metastatic melanoma or renal cell carcinoma. J Clin Oncol 24: 1169-1177.

147. Weiden PL, Sullivan KM, Flournoy N, Storb R, Thomas ED (1981) Antileukemic effect of chronic graft-versus-host disease: contribution to improved survival after allogeneic marrow transplantation. N Engl J Med 304: 1529-1533.

148. Itonaga H, Iwanaga M, Aoki K, Aoki J, Ishiyama K, et al. (2016) Impacts of graft-versus-host disease on outcomes after allogeneic hematopoietic stem cell transplantation for chronic myelomonocytic leukemia: A nationwide retrospective study. Leuk Res 41: 48-55.

149. Horowitz MM, Gale RP, Sondel PM, Goldman JM, Kersey J, et al. (1990) Graft-versus-leukemia reactions after bone marrow transplantation. Blood 75: 555-562.

150. AlJohani NI, Thompson K, Hasegawa W, White D, Kew A, et al. (2014) Non-myeloablative allogeneic hematopoietic transplantation for patients with hematologic malignancies: 9-year single-centre experience. Curr Oncol 21: e434-440.

151. Davies JK, Taussig D, Oakervee H, Smith M, Agrawal S, et al. (2013) Long-term survival with low toxicity after allogeneic transplantation for acute myeloid leukaemia and myelodysplasia using non-myeloablative conditioning without T cell depletion. Br J Haematol 162: 525-529.

152. Robin M, Porcher R, Ades L, Boissel N, Raffoux E, et al. (2013) Matched unrelated or matched sibling donors result in comparable outcomes after non-myeloablative HSCT in patients with AML or MDS. Bone Marrow Transplant 48: 1296-1301.

153. Hambach L, Vermeij M, Buser A, Aghai Z, van der Kwast T, et al. (2008) Targeting a single mismatched minor histocompatibility antigen with tumor-restricted expression eradicates human solid tumors. Blood 112: 1844-1852.

154. Warren EH, Fujii N, Akatsuka Y, Chaney CN, Mito JK, et al. (2010) Therapy of relapsed leukemia after allogeneic hematopoietic cell transplantation with T cells specific for minor histocompatibility antigens. Blood 115: 3869-3878.

155. Gros A, Robbins PF, Yao X, Li YF, Turcotte S, et al. (2014) PD-1 identifies the patient-specific CD8(+) tumor-reactive repertoire infiltrating human tumors. J Clin Invest 124: 2246-2259.

156. Hinrichs CS, Rosenberg SA (2014) Exploiting the curative potential of adoptive T-cell therapy for cancer. Immunol Rev 257: 56-71.

157. Rosenberg SA, Yang JC, Sherry RM, Kammula US, Hughes MS, et al. (2011) Durable complete responses in heavily pretreated patients with metastatic melanoma using T-cell transfer immunotherapy. Clin Cancer Res 17: 4550-4557.

158. Radvanyi LG, Bernatchez C, Zhang M, Fox PS, Miller P, et al. (2012) Specific lymphocyte subsets predict response to adoptive cell therapy using expanded autologous tumor-infiltrating lymphocytes in metastatic melanoma patients. Clin Cancer Res 18: 6758-6770.

159. Dudley ME, Yang JC, Sherry R, Hughes MS, Royal R, et al. (2008) Adoptive cell therapy for patients with metastatic melanoma: evaluation of intensive myeloablative chemoradiation preparative regimens. J Clin Oncol 26: 5233-5239.

160. Fujita K, Ikarashi H, Takakuwa K, Kodama S, Tokunaga A, et al. (1995) Prolonged disease-free period in patients with advanced epithelial ovarian cancer after adoptive transfer of tumor-infiltrating lymphocytes. Clin Cancer Res 1: 501-507.

161. Li J, Chen QY, He J, Li ZL, Tang XF, et al. (2015) Phase I trial of adoptively transferred tumor-infiltrating lymphocyte immunotherapy following concurrent chemoradiotherapy in patients with locoregionally advanced nasopharyngeal carcinoma. Oncoimmunology 4: e976507.

162. Gill S, June CH (2015) Going viral: chimeric antigen receptor T-cell therapy for hematological malignancies. Immunol Rev 263: 68-89.

163. Maus MV, Grupp SA, Porter DL, June CH (2014) Antibody-modified T cells: CARs take the front seat for hematologic malignancies. Blood 123: 2625-2635.

164. Davila ML, Riviere I, Wang X, Bartido S, Park J, et al. (2014) Efficacy and toxicity management of 19-28z CAR T cell therapy in B cell acute lymphoblastic leukemia. Sci Transl Med 6: 224ra225.

165. Dai H, Wang Y, Lu X, Han W (2016) Chimeric Antigen Receptors Modified T-Cells for Cancer Therapy. J Natl Cancer Inst 108.

166. Ahmed N, Brawley VS, Hegde M, Robertson C, Ghazi A, et al. (2015) Human Epidermal Growth Factor Receptor 2 (HER2) -Specific Chimeric Antigen Receptor-Modified T Cells for the Immunotherapy of HER2-Positive Sarcoma. J Clin Oncol 33: 1688-1696.

167. Couzin-Frankel J (2013) Breakthrough of the year 2013. Cancer immunotherapy. Science 342: 1432-1433.

168. US Food and Drug Administration (2014) FDA.gov.

169. Hodi FS, O'Day SJ, McDermott DF, Weber RW, Sosman JA, et al. (2010) Improved survival with ipilimumab in patients with metastatic melanoma. N Engl J Med 363: 711-723.

170. Robert C, Long GV, Brady B, Dutriaux C, Maio M, et al. (2015) Nivolumab in previously untreated melanoma without BRAF mutation. N Engl J Med 372: 320-330.

171. US Food and Drug Administration (2015) FDA.gov.

172. Krummel MF, Allison JP (1995) CD28 and CTLA-4 have opposing effects on the response of T cells to stimulation. J Exp Med 182: 459-465.

173. Freeman GJ, Long AJ, Iwai Y, Bourque K, Chernova T, et al. (2000) Engagement of the PD-1 immunoinhibitory receptor by a novel B7 family member leads to negative regulation of lymphocyte activation. J Exp Med 192: 1027-1034.

174. Motzer RJ, Escudier B, McDermott DF, George S, Hammers HJ, et al. (2015) Nivolumab versus Everolimus in Advanced Renal-Cell Carcinoma. N Engl J Med 373: 1803-1813.

175. Brahmer J, Reckamp KL, Baas P, Crino L, Eberhardt WE, et al. (2015) Nivolumab versus Docetaxel in Advanced Squamous-Cell Non-Small-Cell Lung Cancer. N Engl J Med 373: 123-135.

176. Borghaei H, Paz-Ares L, Horn L, Spigel DR, Steins M, et al. (2015) Nivolumab versus Docetaxel in Advanced Nonsquamous Non-Small-Cell Lung Cancer. N Engl J Med 373: 1627-1639.

177. Wolach O, Stone RM (2015) Blinatumomab for the Treatment of Philadelphia Chromosome-Negative, Precursor B-cell Acute Lymphoblastic Leukemia. Clin Cancer Res 21: 4262-4269.

178. Przepiorka D, Ko CW, Deisseroth A, Yancey CL, Candau-Chacon R, et al. (2015) FDA Approval: Blinatumomab. Clin Cancer Res 21: 4035-4039.

179. Baksh K, Weber J (2015) Immune checkpoint protein inhibition for cancer: preclinical justification for CTLA-4 and PD-1 blockade and new combinations. Semin Oncol 42: 363-377.

180. Curti BD, Kovacsovics-Bankowski M, Morris N, Walker E, Chisholm L, et al. (2013) OX40 is a potent immune-stimulating target in late-stage cancer patients. Cancer Res 73: 7189-7198.

181. Sanmamed MF, Pastor F, Rodriguez A, Perez-Gracia JL, Rodriguez-Ruiz ME, et al. (2015) Agonists of Co-stimulation in Cancer Immunotherapy Directed Against CD137, OX40, GITR, CD27, CD28, and ICOS. Semin Oncol 42: 640-655.

182. Ascierto PA, Simeone E, Sznol M, Fu YX, Melero I (2010) Clinical experiences with anti-CD137 and anti-PD1 therapeutic antibodies. Semin Oncol 37: 508-516.

183. Larkin J, Chiarion-Sileni V, Gonzalez R, Grob JJ, Cowey CL, et al. (2015) Combined Nivolumab and Ipilimumab or Monotherapy in Untreated Melanoma. N Engl J Med 373: 23-34.

184. Wolchok JD, Kluger H, Callahan MK, Postow MA, Rizvi NA, et al. (2013) Nivolumab plus ipilimumab in advanced melanoma. N Engl J Med 369: 122-133.

185. Postow MA, Chesney J, Pavlick AC, Robert C, Grossmann K, et al. (2015) Nivolumab and ipilimumab versus ipilimumab in untreated melanoma. N Engl J Med 372: 2006-2017.

186. Group FIS (2007) Quadrivalent vaccine against human papillomavirus to prevent high-grade cervical lesions. N Engl J Med 356: 1915-1927.

187. Klebanoff CA, Acquavella N, Yu Z, Restifo NP (2011) Therapeutic cancer vaccines: are we there yet? Immunol Rev 239: 27-44.

188. Kantoff PW, Schuetz TJ, Blumenstein BA, Glode LM, Bilhartz DL, et al. (2010) Overall survival analysis of a phase II randomized controlled trial of a Poxviral-based PSA-targeted immunotherapy in metastatic castration-resistant prostate cancer. J Clin Oncol 28: 1099-1105.

189. Mittendorf EA, Clifton GT, Holmes JP, Clive KS, Patil R, et al. (2012) Clinical trial results of the HER-2/neu (E75) vaccine to prevent breast cancer recurrence in high-risk patients: from US Military Cancer Institute Clinical Trials Group Study I-01 and I-02. Cancer 118: 2594-2602.

190. Brunsvig PF, Kyte JA, Kersten C, Sundstrom S, Moller M, et al. (2011) Telomerase peptide vaccination in NSCLC: a phase II trial in stage III patients vaccinated after chemoradiotherapy and an 8-year update on a phase I/II trial. Clin Cancer Res 17: 6847-6857.

191. US National Library of Medicine (2014) clinicaltrials.gov/show/NCT01322490.

192. US National Library of Medicine (2012) clinicaltrials.gov/show/NCT01579188.

193. Kantoff PW, Higano CS, Shore ND, Berger ER, Small EJ, et al. (2010) Sipuleucel-T immunotherapy for castration-resistant prostate cancer. N Engl J Med 363: 411-422.

194. Gross L (1943) Intradermal immunization of C3H mice against a sarcoma that originated in an animal of the same line. Cancer Research 3: 326-333.

195. De Plaen E, Lurquin C, Van Pel A, Mariame B, Szikora JP, et al. (1988) Immunogenic (tum-) variants of mouse tumor P815: cloning of the gene of tum- antigen P91A and identification of the tum- mutation. Proc Natl Acad Sci U S A 85: 2274-2278.

196. van der Bruggen P, Traversari C, Chomez P, Lurquin C, De Plaen E, et al. (1991) A gene encoding an antigen recognized by cytolytic T lymphocytes on a human melanoma. Science 254: 1643-1647.

197. Mendoza LM, Malarkannan S, Shastri N (2001) Identification of CD8+ T-cell-stimulating antigen genes in cDNA libraries. Methods Mol Biol 156: 255-263.

198. Viatte S, Alves PM, Romero P (2006) Reverse immunology approach for the identification of CD8 T-cell-defined antigens: advantages and hurdles. Immunol Cell Biol 84: 318-330.

199. Sahin U, Tureci O, Schmitt H, Cochlovius B, Johannes T, et al. (1995) Human neoplasms elicit multiple specific immune responses in the autologous host. Proc Natl Acad Sci U S A 92: 11810-11813.

200. Sahin U, Tureci O (2013) Antigen identification using SEREX. Methods Mol Biol 1061: 59-77.

201. Hunt DF, Henderson RA, Shabanowitz J, Sakaguchi K, Michel H, et al. (1992) Characterization of peptides bound to the class I MHC molecule HLA-A2.1 by mass spectrometry. Science 255: 1261-1263.

202. Granados DP, Sriranganadane D, Daouda T, Zieger A, Laumont CM, et al. (2014) Impact of genomic polymorphisms on the repertoire of human MHC class I-associated peptides. Nat Commun 5: 3600.

203. Wick DA, Webb JR (2011) A novel, broad spectrum therapeutic HPV vaccine targeting the E7 proteins of HPV16, 18, 31, 45 and 52 that elicits potent E7-specific CD8T cell immunity and regression of large, established, E7-expressing TC-1 tumors. Vaccine 29: 7857-7866.

204. Sivars L, Tani E, Nasman A, Ramqvist T, Munck-Wikland E, et al. (2016) Human Papillomavirus as a Diagnostic and Prognostic Tool in Cancer of Unknown Primary in the Head and Neck Region. Anticancer Res 36: 487-493.

205. De Flora S, La Maestra S (2015) Epidemiology of cancers of infectious origin and prevention strategies. J Prev Med Hyg 56: E15-20.

206. Ang KK, Harris J, Wheeler R, Weber R, Rosenthal DI, et al. (2010) Human papillomavirus and survival of patients with oropharyngeal cancer. N Engl J Med 363: 24-35.

207. zur Hausen H (1991) Viruses in human cancers. Science 254: 1167-1173.

208. Fisk B, Blevins TL, Wharton JT, Ioannides CG (1995) Identification of an immunodominant peptide of HER-2/neu protooncogene recognized by ovarian tumor-specific cytotoxic T lymphocyte lines. J Exp Med 181: 2109-2117.

209. Zsiros E, Duttagupta P, Dangaj D, Li H, Frank R, et al. (2015) The Ovarian Cancer Chemokine Landscape Is Conducive to Homing of Vaccine-Primed and CD3/CD28-Costimulated T Cells Prepared for Adoptive Therapy. Clin Cancer Res 21: 2840-2850.

210. Mittendorf EA, Clifton GT, Holmes JP, Schneble E, van Echo D, et al. (2014) Final report of the phase I/II clinical trial of the E75 (nelipepimut-S) vaccine with booster inoculations to prevent disease recurrence in high-risk breast cancer patients. Ann Oncol 25: 1735-1742.

211. Bendle GM, Holler A, Downs AM, Xue SA, Stauss HJ (2005) Broadly expressed tumour-associated proteins as targets for cytotoxic T lymphocyte-based cancer immunotherapy. Expert Opin Biol Ther 5: 1183-1192.

212. Kawakami Y, Eliyahu S, Sakaguchi K, Robbins PF, Rivoltini L, et al. (1994) Identification of the immunodominant peptides of the MART-1 human melanoma antigen recognized by the majority of HLA-A2-restricted tumor infiltrating lymphocytes. J Exp Med 180: 347-352.

213. Wolfel T, Van Pel A, Brichard V, Schneider J, Seliger B, et al. (1994) Two tyrosinase nonapeptides recognized on HLA-A2 melanomas by autologous cytolytic T lymphocytes. Eur J Immunol 24: 759-764.

214. Rolla S, Nicolo C, Malinarich S, Orsini M, Forni G, et al. (2006) Distinct and non-overlapping T cell receptor repertoires expanded by DNA vaccination in wild-type and HER-2 transgenic BALB/c mice. J Immunol 177: 7626-7633.

215. Aleksic M, Liddy N, Molloy PE, Pumphrey N, Vuidepot A, et al. (2012) Different affinity windows for virus and cancer-specific T-cell receptors: implications for therapeutic strategies. Eur J Immunol 42: 3174-3179.

216. Morgan RA, Chinnasamy N, Abate-Daga D, Gros A, Robbins PF, et al. (2013) Cancer regression and neurological toxicity following anti-MAGE-A3 TCR gene therapy. J Immunother 36: 133-151.

217. Whitehurst AW (2014) Cause and consequence of cancer/testis antigen activation in cancer. Annu Rev Pharmacol Toxicol 54: 251-272.

218. Jungbluth AA, Stockert E, Chen YT, Kolb D, Iversen K, et al. (2000) Monoclonal antibody MA454 reveals a heterogeneous expression pattern of MAGE-1 antigen in formalin-fixed paraffin embedded lung tumours. Br J Cancer 83: 493-497.

219. Huijbers IJ, Soudja SM, Uyttenhove C, Buferne M, Inderberg-Suso EM, et al. (2012) Minimal tolerance to a tumor antigen encoded by a cancer-germline gene. J Immunol 188: 111-121.

220. Ward JE, McNeel DG (2007) GVAX: an allogeneic, whole-cell, GM-CSF-secreting cellular immunotherapy for the treatment of prostate cancer. Expert Opin Biol Ther 7: 1893-1902.

221. Lipson EJ, Sharfman WH, Chen S, McMiller TL, Pritchard TS, et al. (2015) Safety and immunologic correlates of Melanoma GVAX, a GM-CSF secreting allogeneic melanoma cell vaccine administered in the adjuvant setting. J Transl Med 13: 214.

222. Guo X, Zhou Y, Wu T, Zhu X, Lai W, et al. (2016) Generation of mouse and human dendritic cells in vitro. J Immunol Methods 432: 24-29.

223. Mellman I, Coukos G, Dranoff G (2011) Cancer immunotherapy comes of age. Nature 480: 480-489.

224. Murphy KA, Lechner MG, Popescu FE, Bedi J, Decker SA, et al. (2012) An in vivo immunotherapy screen of costimulatory molecules identifies Fc-OX40L as a potent reagent for the treatment of established murine gliomas. Clin Cancer Res 18: 4657-4668.

225. Lin B, Zhao H, Fan J, Xie F, Wang W, et al. (2014) B16 cell lysates plus polyinosinic-cytidylic acid effectively eradicate melanoma in a mouse model by acting as a prophylactic vaccine. Mol Med Rep 10: 911-916.

226. Chiang CL, Coukos G, Kandalaft LE (2015) Whole Tumor Antigen Vaccines: Where Are We? Vaccines (Basel) 3: 344-372.

227. Vandenberk L, Belmans J, Van Woensel M, Riva M, Van Gool SW (2015) Exploiting the Immunogenic Potential of Cancer Cells for Improved Dendritic Cell Vaccines. Front Immunol 6: 663.

228. Pan K, Zhao JJ, Wang H, Li JJ, Liang XT, et al. (2010) Comparative analysis of cytotoxic T lymphocyte response induced by dendritic cells loaded with hepatocellular carcinoma -derived RNA or cell lysate. Int J Biol Sci 6: 639-648.

229. Koido S, Homma S, Okamoto M, Namiki Y, Takakura K, et al. (2013) Fusions between dendritic cells and whole tumor cells as anticancer vaccines. Oncoimmunology 2: e24437.

230. Philip R, Alters SE, Brunette E, Ashton J, Gadea J, et al. (2000) Dendritic cells loaded with MART-1 peptide or infected with adenoviral construct are functionally equivalent in the induction of tumor-specific cytotoxic T lymphocyte responses in patients with melanoma. J Immunother 23: 168-176.

231. Chiang CL, Kandalaft LE, Tanyi J, Hagemann AR, Motz GT, et al. (2013) A dendritic cell vaccine pulsed with autologous hypochlorous acid-oxidized ovarian cancer lysate primes effective broad antitumor immunity: from bench to bedside. Clin Cancer Res 19: 4801-4815.

232. de Vries IJ, Lesterhuis WJ, Scharenborg NM, Engelen LP, Ruiter DJ, et al. (2003) Maturation of dendritic cells is a prerequisite for inducing immune responses in advanced melanoma patients. Clin Cancer Res 9: 5091-5100.

233. Zobywalski A, Javorovic M, Frankenberger B, Pohla H, Kremmer E, et al. (2007) Generation of clinical grade dendritic cells with capacity to produce biologically active IL-12p70. J Transl Med 5: 18.

234. Gurunathan S, Klinman DM, Seder RA (2000) DNA vaccines: immunology, application, and optimization*. Annu Rev Immunol 18: 927-974.

235. Greenland JR, Letvin NL (2007) Chemical adjuvants for plasmid DNA vaccines. Vaccine 25: 3731-3741.

236. Rice J, Ottensmeier CH, Stevenson FK (2008) DNA vaccines: precision tools for activating effective immunity against cancer. Nat Rev Cancer 8: 108-120.

237. Kreiter S, Selmi A, Diken M, Koslowski M, Britten CM, et al. (2010) Intranodal vaccination with naked antigen-encoding RNA elicits potent prophylactic and therapeutic antitumoral immunity. Cancer Res 70: 9031-9040.

238. Kreiter S, Vormehr M, van de Roemer N, Diken M, Lower M, et al. (2015) Mutant MHC class II epitopes drive therapeutic immune responses to cancer. Nature 520: 692-696.

239. Kreiter S, Diken M, Selmi A, Tureci O, Sahin U (2011) Tumor vaccination using messenger RNA: prospects of a future therapy. Curr Opin Immunol 23: 399-406.

240. Houseley J, Tollervey D (2009) The many pathways of RNA degradation. Cell 136: 763-776.

241. Scheel B, Teufel R, Probst J, Carralot JP, Geginat J, et al. (2005) Toll-like receptor-dependent activation of several human blood cell types by protamine-condensed mRNA. Eur J Immunol 35: 1557-1566.

242. Wasungu L, Hoekstra D (2006) Cationic lipids, lipoplexes and intracellular delivery of genes. J Control Release 116: 255-264.

243. Gulley JL, Madan RA, Tsang KY, Jochems C, Marte JL, et al. (2014) Immune impact induced by PROSTVAC (PSA-TRICOM), a therapeutic vaccine for prostate cancer. Cancer Immunol Res 2: 133-141.

244. Lin IY, Van TT, Smooker PM (2015) Live-Attenuated Bacterial Vectors: Tools for Vaccine and Therapeutic Agent Delivery. Vaccines (Basel) 3: 940-972.

245. Li LL, Wang HR, Zhou ZY, Luo J, Xiao XQ, et al. (2016) One-prime multi-boost strategy immunization with recombinant DNA, adenovirus, and MVA vector vaccines expressing HPV16 L1 induces potent, sustained, and specific immune response in mice. Antiviral Res 128: 20-27.

246. Kim SB, Ahn JH, Kim J, Jung KH (2015) A phase 1 study of a heterologous prime-boost vaccination involving a truncated HER2 sequence in patients with HER2-expressing breast cancer. Mol Ther Methods Clin Dev 2: 15031.

247. Schwartzentruber DJ, Lawson DH, Richards JM, Conry RM, Miller DM, et al. (2011) gp100 peptide vaccine and interleukin-2 in patients with advanced melanoma. N Engl J Med 364: 2119-2127.

248. Hailemichael Y, Overwijk WW (2014) Cancer vaccines: Trafficking of tumor-specific T cells to tumor after therapeutic vaccination. Int J Biochem Cell Biol 53: 46-50.

249. Rosenberg SA, Sherry RM, Morton KE, Scharfman WJ, Yang JC, et al. (2005) Tumor progression can occur despite the induction of very high levels of self/tumor antigen-specific CD8+ T cells in patients with melanoma. J Immunol 175: 6169-6176.

250. Rezvani K, Yong AS, Mielke S, Jafarpour B, Savani BN, et al. (2011) Repeated PR1 and WT1 peptide vaccination in Montanide-adjuvant fails to induce sustained high-avidity, epitope-specific CD8+ T cells in myeloid malignancies. Haematologica 96: 432-440.

251. Hailemichael Y, Dai Z, Jaffarzad N, Ye Y, Medina MA, et al. (2013) Persistent antigen at vaccination sites induces tumor-specific CD8(+) T cell sequestration, dysfunction and deletion. Nat Med 19: 465-472.

252. Bijker MS, van den Eeden SJ, Franken KL, Melief CJ, van der Burg SH, et al. (2008) Superior induction of anti-tumor CTL immunity by extended peptide vaccines involves prolonged, DC-focused antigen presentation. Eur J Immunol 38: 1033-1042.

253. Toes RE, Offringa R, Blom RJ, Melief CJ, Kast WM (1996) Peptide vaccination can lead to enhanced tumor growth through specific T-cell tolerance induction. Proc Natl Acad Sci U S A 93: 7855-7860.

254. Bijker MS, van den Eeden SJ, Franken KL, Melief CJ, Offringa R, et al. (2007) CD8+ CTL priming by exact peptide epitopes in incomplete Freund's adjuvant induces a vanishing CTL response, whereas long peptides induce sustained CTL reactivity. J Immunol 179: 5033-5040.

255. Clancy-Thompson E, King LK, Nunnley LD, Mullins IM, Slingluff CL, Jr., et al. (2013) Peptide vaccination in Montanide adjuvant induces and GM-CSF increases CXCR3 and cutaneous lymphocyte antigen expression by tumor antigen-specific CD8 T cells. Cancer Immunol Res 1: 332-339.

256. Slingluff CL, Jr., Lee S, Zhao F, Chianese-Bullock KA, Olson WC, et al. (2013) A randomized phase II trial of multiepitope vaccination with melanoma peptides for cytotoxic T cells and helper T cells for patients with metastatic melanoma (E1602). Clin Cancer Res 19: 4228-4238.

257. Metcalf D, Begley CG, Williamson DJ, Nice EC, De Lamarter J, et al. (1987) Hemopoietic responses in mice injected with purified recombinant murine GM-CSF. Exp Hematol 15: 1-9.

258. Wicks IP, Roberts AW (2016) Targeting GM-CSF in inflammatory diseases. Nat Rev Rheumatol 12: 37-48.

259. Filipazzi P, Valenti R, Huber V, Pilla L, Canese P, et al. (2007) Identification of a new subset of myeloid suppressor cells in peripheral blood of melanoma patients with modulation by a granulocyte-macrophage colony-stimulation factor-based antitumor vaccine. J Clin Oncol 25: 2546-2553.

260. Serafini P, Carbley R, Noonan KA, Tan G, Bronte V, et al. (2004) High-dose granulocyte-macrophage colony-stimulating factor-producing vaccines impair the immune response through the recruitment of myeloid suppressor cells. Cancer Res 64: 6337-6343.

261. Slingluff CL, Jr., Petroni GR, Olson WC, Smolkin ME, Ross MI, et al. (2009) Effect of granulocyte/macrophage colony-stimulating factor on circulating CD8+ and CD4+ T-cell responses to a multipeptide melanoma vaccine: outcome of a multicenter randomized trial. Clin Cancer Res 15: 7036-7044.

262. Ahonen CL, Wasiuk A, Fuse S, Turk MJ, Ernstoff MS, et al. (2008) Enhanced efficacy and reduced toxicity of multifactorial adjuvants compared with unitary adjuvants as cancer vaccines. Blood 111: 3116-3125.

263. Fujimoto C, Nakagawa Y, Ohara K, Takahashi H (2004) Polyriboinosinic polyribocytidylic acid [poly(I:C)]/TLR3 signaling allows class I processing of exogenous protein and induction of HIV-specific CD8+ cytotoxic T lymphocytes. Int Immunol 16: 55-63.

264. Poltorak A, He X, Smirnova I, Liu MY, Van Huffel C, et al. (1998) Defective LPS signaling in C3H/HeJ and C57BL/10ScCr mice: mutations in Tlr4 gene. Science 282: 2085-2088.

265. Alexopoulou L, Holt AC, Medzhitov R, Flavell RA (2001) Recognition of double-stranded RNA and activation of NF-kappaB by Toll-like receptor 3. Nature 413: 732-738.

266. Hemmi H, Takeuchi O, Kawai T, Kaisho T, Sato S, et al. (2000) A Toll-like receptor recognizes bacterial DNA. Nature 408: 740-745.

267. Hemmi H, Kaisho T, Takeuchi O, Sato S, Sanjo H, et al. (2002) Small anti-viral compounds activate immune cells via the TLR7 MyD88-dependent signaling pathway. Nat Immunol 3: 196-200.

268. Schwarz K, Storni T, Manolova V, Didierlaurent A, Sirard JC, et al. (2003) Role of Toll-like receptors in costimulating cytotoxic T cell responses. Eur J Immunol 33: 1465-1470.

269. van Duikeren S, Fransen MF, Redeker A, Wieles B, Platenburg G, et al. (2012) Vaccine-induced effector-memory CD8+ T cell responses predict therapeutic efficacy against tumors. J Immunol 189: 3397-3403.

270. Pol J, Bloy N, Buque A, Eggermont A, Cremer I, et al. (2015) Trial Watch: Peptide-based anticancer vaccines. Oncoimmunology 4: e974411.

271. Hailemichael Y, Overwijk WW (2013) Peptide-based anticancer vaccines: The making and unmaking of a T-cell graveyard. Oncoimmunology 2: e24743.

272. Melief CJ, van der Burg SH (2008) Immunotherapy of established (pre)malignant disease by synthetic long peptide vaccines. Nat Rev Cancer 8: 351-360.

273. Rosalia RA, Quakkelaar ED, Redeker A, Khan S, Camps M, et al. (2013) Dendritic cells process synthetic long peptides better than whole protein, improving antigen presentation and T-cell activation. Eur J Immunol 43: 2554-2565.

274. van der Sluis TC, Sluijter M, van Duikeren S, West BL, Melief CJ, et al. (2015) Therapeutic Peptide Vaccine-Induced CD8 T Cells Strongly Modulate Intratumoral Macrophages Required for Tumor Regression. Cancer Immunol Res 3: 1042-1051.

275. van der Sluis TC, van Duikeren S, Huppelschoten S, Jordanova ES, Beyranvand Nejad E, et al. (2015) Vaccine-induced tumor necrosis factor-producing T cells synergize with cisplatin to promote tumor cell death. Clin Cancer Res 21: 781-794.

276. Zhang L, Chen J, Song X, Wen W, Li Y, et al. (2013) Cancer/testis antigen HCA587-derived long peptide vaccine generates potent immunologic responses and antitumor effects in mouse model. Oncol Res 21: 193-200.

277. van Poelgeest MI, Welters MJ, Vermeij R, Stynenbosch LF, Loof NM, et al. (2016) Vaccination against Oncoproteins of HPV16 for Noninvasive Vulvar/Vaginal Lesions: Lesion Clearance Is Related to the Strength of the T-Cell Response. Clin Cancer Res 22: 2342-2350.

278. Kenter GG, Welters MJ, Valentijn AR, Lowik MJ, Berends-van der Meer DM, et al. (2009) Vaccination against HPV-16 oncoproteins for vulvar intraepithelial neoplasia. N Engl J Med 361: 1838-1847.

279. Corradin G, Kajava AV, Verdini A (2010) Long synthetic peptides for the production of vaccines and drugs: a technological platform coming of age. Sci Transl Med 2: 50rv53.

280. Wick DA, Martin SD, Nelson BH, Webb JR (2011) Profound CD8+ T cell immunity elicited by sequential daily immunization with exogenous antigen plus the TLR3 agonist poly(I:C). Vaccine 29: 984-993.

281. Sanger F, Nicklen S, Coulson AR (1977) DNA sequencing with chain-terminating inhibitors. Proc Natl Acad Sci U S A 74: 5463-5467.

282. Smith LM, Sanders JZ, Kaiser RJ, Hughes P, Dodd C, et al. (1986) Fluorescence detection in automated DNA sequence analysis. Nature 321: 674-679.

283. Prober JM, Trainor GL, Dam RJ, Hobbs FW, Robertson CW, et al. (1987) A system for rapid DNA sequencing with fluorescent chain-terminating dideoxynucleotides. Science 238: 336-341.

284. Saiki RK, Scharf S, Faloona F, Mullis KB, Horn GT, et al. (1985) Enzymatic amplification of beta-globin genomic sequences and restriction site analysis for diagnosis of sickle cell anemia. Science 230: 1350-1354.

285. Marsh M, Tu O, Dolnik V, Roach D, Solomon N, et al. (1997) High-throughput DNA sequencing on a capillary array electrophoresis system. J Capillary Electrophor 4: 83-89.

286. Venter JC, Adams MD, Myers EW, Li PW, Mural RJ, et al. (2001) The sequence of the human genome. Science 291: 1304-1351.

287. Lander ES, Linton LM, Birren B, Nusbaum C, Zody MC, et al. (2001) Initial sequencing and analysis of the human genome. Nature 409: 860-921.

288. Bentley DR, Balasubramanian S, Swerdlow HP, Smith GP, Milton J, et al. (2008) Accurate whole human genome sequencing using reversible terminator chemistry. Nature 456: 53-59.

289. Brockman W, Alvarez P, Young S, Garber M, Giannoukos G, et al. (2008) Quality scores and SNP detection in sequencing-by-synthesis systems. Genome Res 18: 763-770.

290. Ewing B, Green P (1998) Base-calling of automated sequencer traces using phred. II. Error probabilities. Genome Res 8: 186-194.

291. Menzel P, Frellsen J, Plass M, Rasmussen SH, Krogh A (2013) On the accuracy of short read mapping. Methods Mol Biol 1038: 39-59.

292. Shyr D, Liu Q (2013) Next generation sequencing in cancer research and clinical application. Biol Proced Online 15: 4.

293. Gnirke A, Melnikov A, Maguire J, Rogov P, LeProust EM, et al. (2009) Solution hybrid selection with ultra-long oligonucleotides for massively parallel targeted sequencing. Nat Biotechnol 27: 182-189.

294. Han Y, Gao S, Muegge K, Zhang W, Zhou B (2015) Advanced Applications of RNA Sequencing and Challenges. Bioinform Biol Insights 9: 29-46.

295. Stransky N, Cerami E, Schalm S, Kim JL, Lengauer C (2014) The landscape of kinase fusions in cancer. Nat Commun 5: 4846.

296. Goya R, Sun MG, Morin RD, Leung G, Ha G, et al. (2010) SNVMix: predicting single nucleotide variants from next-generation sequencing of tumors. Bioinformatics 26: 730-736.

297. Sultan M, Schulz MH, Richard H, Magen A, Klingenhoff A, et al. (2008) A global view of gene activity and alternative splicing by deep sequencing of the human transcriptome. Science 321: 956-960.

298. Mortazavi A, Williams BA, McCue K, Schaeffer L, Wold B (2008) Mapping and quantifying mammalian transcriptomes by RNA-Seq. Nat Methods 5: 621-628.

299. Adiconis X, Borges-Rivera D, Satija R, DeLuca DS, Busby MA, et al. (2013) Comparative analysis of RNA sequencing methods for degraded or low-input samples. Nat Methods 10: 623-629.

300. Lawrence MS, Stojanov P, Mermel CH, Robinson JT, Garraway LA, et al. (2014) Discovery and saturation analysis of cancer genes across 21 tumour types. Nature 505: 495-501.

301. Cancer Genome Atlas Research N (2014) Comprehensive molecular characterization of urothelial bladder carcinoma. Nature 507: 315-322.

302. Tamborero D, Gonzalez-Perez A, Perez-Llamas C, Deu-Pons J, Kandoth C, et al. (2013) Comprehensive identification of mutational cancer driver genes across 12 tumor types. Sci Rep 3: 2650.

303. Lawrence MS, Stojanov P, Polak P, Kryukov GV, Cibulskis K, et al. (2013) Mutational heterogeneity in cancer and the search for new cancer-associated genes. Nature 499: 214-218.

304. Kandoth C, McLellan MD, Vandin F, Ye K, Niu B, et al. (2013) Mutational landscape and significance across 12 major cancer types. Nature 502: 333-339.

305. Jones SJ, Laskin J, Li YY, Griffith OL, An J, et al. (2010) Evolution of an adenocarcinoma in response to selection by targeted kinase inhibitors. Genome Biol 11: R82.

306. Wagle N, Grabiner BC, Van Allen EM, Amin-Mansour A, Taylor-Weiner A, et al. (2014) Response and acquired resistance to everolimus in anaplastic thyroid cancer. N Engl J Med 371: 1426-1433.

307. Schwaederle M, Parker BA, Schwab RB, Fanta PT, Boles SG, et al. (2014) Molecular tumor board: the University of California-San Diego Moores Cancer Center experience. Oncologist 19: 631-636.

308. Tran B, Brown AM, Bedard PL, Winquist E, Goss GD, et al. (2013) Feasibility of real time next generation sequencing of cancer genes linked to drug response: results from a clinical trial. Int J Cancer 132: 1547-1555.

309. Arnedos M, Andre F, Farace F, Lacroix L, Besse B, et al. (2012) The challenge to bring personalized cancer medicine from clinical trials into routine clinical practice: the case of the Institut Gustave Roussy. Mol Oncol 6: 204-210.

310. Goncalves R, Warner WA, Luo J, Ellis MJ (2014) New concepts in breast cancer genomics and genetics. Breast Cancer Res 16: 460.

311. Chen Y, McGee J, Chen X, Doman TN, Gong X, et al. (2014) Identification of druggable cancer driver genes amplified across TCGA datasets. PLoS One 9: e98293.

312. Klausz K, Berger S, Lammerts van Bueren JJ, Derer S, Lohse S, et al. (2011) Complement-mediated tumor-specific cell lysis by antibody combinations targeting epidermal growth factor receptor (EGFR) and its variant III (EGFRvIII). Cancer Sci 102: 1761-1768.

313. Morgan RA, Johnson LA, Davis JL, Zheng Z, Woolard KD, et al. (2012) Recognition of glioma stem cells by genetically modified T cells targeting EGFRvIII and development of adoptive cell therapy for glioma. Hum Gene Ther 23: 1043-1053.

314. Yadav M, Jhunjhunwala S, Phung QT, Lupardus P, Tanguay J, et al. (2014) Predicting immunogenic tumour mutations by combining mass spectrometry and exome sequencing. Nature 515: 572-576.

315. Duan F, Duitama J, Al Seesi S, Ayres CM, Corcelli SA, et al. (2014) Genomic and bioinformatic profiling of mutational neoepitopes reveals new rules to predict anticancer immunogenicity. J Exp Med 211: 2231-2248.

316. Sharma G, Holt RA (2014) T-cell epitope discovery technologies. Hum Immunol 75: 514-519.

317. Cancer Immunity (2013) CancerImmunity.org.

318. Mandruzzato S, Brasseur F, Andry G, Boon T, van der Bruggen P (1997) A CASP-8 mutation recognized by cytolytic T lymphocytes on a human head and neck carcinoma. J Exp Med 186: 785-793.

319. Robbins PF, El-Gamil M, Li YF, Kawakami Y, Loftus D, et al. (1996) A mutated beta-catenin gene encodes a melanoma-specific antigen recognized by tumor infiltrating lymphocytes. J Exp Med 183: 1185-1192.

320. Wolfel T, Hauer M, Schneider J, Serrano M, Wolfel C, et al. (1995) A p16INK4a-insensitive CDK4 mutant targeted by cytolytic T lymphocytes in a human melanoma. Science 269: 1281-1284.

321. Echchakir H, Mami-Chouaib F, Vergnon I, Baurain JF, Karanikas V, et al. (2001) A point mutation in the alpha-actinin-4 gene generates an antigenic peptide recognized by autologous cytolytic T lymphocytes on a human lung carcinoma. Cancer Res 61: 4078-4083.

322. Chiari R, Foury F, De Plaen E, Baurain JF, Thonnard J, et al. (1999) Two antigens recognized by autologous cytolytic T lymphocytes on a melanoma result from a single point mutation in an essential housekeeping gene. Cancer Res 59: 5785-5792.

323. Sharkey MS, Lizee G, Gonzales MI, Patel S, Topalian SL (2004) CD4(+) T-cell recognition of mutated B-RAF in melanoma patients harboring the V599E mutation. Cancer Res 64: 1595-1599.

324. Gaudin C, Kremer F, Angevin E, Scott V, Triebel F (1999) A hsp70-2 mutation recognized by CTL on a human renal cell carcinoma. J Immunol 162: 1730-1738.

325. Linnebacher M, Gebert J, Rudy W, Woerner S, Yuan YP, et al. (2001) Frameshift peptide-derived T-cell epitopes: a source of novel tumor-specific antigens. Int J Cancer 93: 6-11.

326. Karanikas V, Colau D, Baurain JF, Chiari R, Thonnard J, et al. (2001) High frequency of cytolytic T lymphocytes directed against a tumor-specific mutated antigen detectable with HLA tetramers in the blood of a lung carcinoma patient with long survival. Cancer Res 61: 3718-3724.

327. Yotnda P, Firat H, Garcia-Pons F, Garcia Z, Gourru G, et al. (1998) Cytotoxic T cell response against the chimeric p210 BCR-ABL protein in patients with chronic myelogenous leukemia. J Clin Invest 101: 2290-2296.

328. Lennerz V, Fatho M, Gentilini C, Frye RA, Lifke A, et al. (2005) The response of autologous T cells to a human melanoma is dominated by mutated neoantigens. Proc Natl Acad Sci U S A 102: 16013-16018.

329. Corbiere V, Chapiro J, Stroobant V, Ma W, Lurquin C, et al. (2011) Antigen spreading contributes to MAGE vaccination-induced regression of melanoma metastases. Cancer Res 71: 1253-1262.

330. Fritsch EF, Rajasagi M, Ott PA, Brusic V, Hacohen N, et al. (2014) HLA-binding properties of tumor neoepitopes in humans. Cancer Immunol Res 2: 522-529.

331. Rizvi NA, Hellmann MD, Snyder A, Kvistborg P, Makarov V, et al. (2015) Cancer immunology. Mutational landscape determines sensitivity to PD-1 blockade in non-small cell lung cancer. Science 348: 124-128.

332. Snyder A, Makarov V, Merghoub T, Yuan J, Zaretsky JM, et al. (2014) Genetic basis for clinical response to CTLA-4 blockade in melanoma. N Engl J Med 371: 2189-2199.

333. Kessels HW, de Visser KE, Tirion FH, Coccoris M, Kruisbeek AM, et al. (2004) The impact of self-tolerance on the polyclonal CD8+ T cell repertoire. J Immunol 172: 2324-2331.

334. Bos R, Marquardt KL, Cheung J, Sherman LA (2012) Functional differences between low- and high-affinity CD8(+) T cells in the tumor environment. Oncoimmunology 1: 1239-1247.

335. Warren RL, Choe G, Freeman DJ, Castellarin M, Munro S, et al. (2012) Derivation of HLA types from shotgun sequence datasets. Genome Med 4: 95.

336. Brown SD, Warren RL, Gibb EA, Martin SD, Spinelli JJ, et al. (2014) Neo-antigens predicted by tumor genome meta-analysis correlate with increased patient survival. Genome Res 24: 743-750.

337. van Gool IC, Eggink FA, Freeman-Mills L, Stelloo E, Marchi E, et al. (2015) POLE Proofreading Mutations Elicit an Antitumor Immune Response in Endometrial Cancer. Clin Cancer Res 21: 3347-3355.

338. Rooney MS, Shukla SA, Wu CJ, Getz G, Hacohen N (2015) Molecular and genetic properties of tumors associated with local immune cytolytic activity. Cell 160: 48-61.

339. van Buuren MM, Calis JJ, Schumacher TN (2014) High sensitivity of cancer exome-based CD8 T cell neo-antigen identification. Oncoimmunology 3: e28836.

340. Champiat S, Ferte C, Lebel-Binay S, Eggermont A, Soria JC (2014) Exomics and immunogenics: Bridging mutational load and immune checkpoints efficacy. Oncoimmunology 3: e27817.

341. Le DT, Uram JN, Wang H, Bartlett BR, Kemberling H, et al. (2015) PD-1 Blockade in Tumors with Mismatch-Repair Deficiency. N Engl J Med 372: 2509-2520.

342. McGranahan N, Furness AJ, Rosenthal R, Ramskov S, Lyngaa R, et al. (2016) Clonal neoantigens elicit T cell immunoreactivity and sensitivity to immune checkpoint blockade. Science 351: 1463-1469.

343. Gubin MM, Zhang X, Schuster H, Caron E, Ward JP, et al. (2014) Checkpoint blockade cancer immunotherapy targets tumour-specific mutant antigens. Nature 515: 577-581.

344. van Rooij N, van Buuren MM, Philips D, Velds A, Toebes M, et al. (2013) Tumor exome analysis reveals neoantigen-specific T-cell reactivity in an ipilimumab-responsive melanoma. J Clin Oncol 31: e439-442.

345. Robbins PF, Lu YC, El-Gamil M, Li YF, Gross C, et al. (2013) Mining exomic sequencing data to identify mutated antigens recognized by adoptively transferred tumor-reactive T cells. Nat Med 19: 747-752.

346. Lu YC, Yao X, Crystal JS, Li YF, El-Gamil M, et al. (2014) Efficient identification of mutated cancer antigens recognized by T cells associated with durable tumor regressions. Clin Cancer Res 20: 3401-3410.

347. Linnemann C, van Buuren MM, Bies L, Verdegaal EM, Schotte R, et al. (2015) High-throughput epitope discovery reveals frequent recognition of neo-antigens by CD4+ T cells in human melanoma. Nat Med 21: 81-85.

348. Gros A, Parkhurst MR, Tran E, Pasetto A, Robbins PF, et al. (2016) Prospective identification of neoantigen-specific lymphocytes in the peripheral blood of melanoma patients. Nat Med 22: 433-438.

349. Cohen CJ, Gartner JJ, Horovitz-Fried M, Shamalov K, Trebska-McGowan K, et al. (2015) Isolation of neoantigen-specific T cells from tumor and peripheral lymphocytes. J Clin Invest 125: 3981-3991.

350. Rajasagi M, Shukla SA, Fritsch EF, Keskin DB, DeLuca D, et al. (2014) Systematic identification of personal tumor-specific neoantigens in chronic lymphocytic leukemia. Blood 124: 453-462.

351. Tran E, Ahmadzadeh M, Lu YC, Gros A, Turcotte S, et al. (2015) Immunogenicity of somatic mutations in human gastrointestinal cancers. Science 350: 1387-1390.

352. Ito D, Visus C, Hoffmann TK, Balz V, Bier H, et al. (2007) Immunological characterization of missense mutations occurring within cytotoxic T cell-defined p53 epitopes in HLA-A*0201+ squamous cell carcinomas of the head and neck. Int J Cancer 120: 2618-2624.

353. Gjertsen MK, Bjorheim J, Saeterdal I, Myklebust J, Gaudernack G (1997) Cytotoxic CD4+ and CD8+ T lymphocytes, generated by mutant p21-ras (12Val) peptide vaccination of a patient, recognize 12Val-dependent nested epitopes present within the vaccine peptide and kill autologous tumour cells carrying this mutation. Int J Cancer 72: 784-790.

354. Carreno BM, Magrini V, Becker-Hapak M, Kaabinejadian S, Hundal J, et al. (2015) Cancer immunotherapy. A dendritic cell vaccine increases the breadth and diversity of melanoma neoantigen-specific T cells. Science 348: 803-808.

355. Rahma OE, Hamilton JM, Wojtowicz M, Dakheel O, Bernstein S, et al. (2014) The immunological and clinical effects of mutated ras peptide vaccine in combination with IL-2, GM-CSF, or both in patients with solid tumors. J Transl Med 12: 55.

356. Carbone DP, Ciernik IF, Kelley MJ, Smith MC, Nadaf S, et al. (2005) Immunization with mutant p53- and K-ras-derived peptides in cancer patients: immune response and clinical outcome. J Clin Oncol 23: 5099-5107.

357. Jain N, Reuben JM, Kantarjian H, Li C, Gao H, et al. (2009) Synthetic tumor-specific breakpoint peptide vaccine in patients with chronic myeloid leukemia and minimal residual disease: a phase 2 trial. Cancer 115: 3924-3934.

358. Castle JC, Kreiter S, Diekmann J, Lower M, van de Roemer N, et al. (2012) Exploiting the mutanome for tumor vaccination. Cancer Res 72: 1081-1091.

359. US National Library of Medicine (2014) clinicaltrials.gov/show/NCT02035956.

360. US National Library of Medicine (2014) clinicaltrials.gov/ct2/show/NCT01970358.

361. Stewart BW, Kleihues P, International Agency for Research on Cancer. (2003) World cancer report. Lyon: IARC Press. 351 p. p.

362. Piek JM, van Diest PJ, Zweemer RP, Jansen JW, Poort-Keesom RJ, et al. (2001) Dysplastic changes in prophylactically removed Fallopian tubes of women predisposed to developing ovarian cancer. J Pathol 195: 451-456.

363. Kim J, Coffey DM, Ma L, Matzuk MM (2015) The ovary is an alternative site of origin for high-grade serous ovarian cancer in mice. Endocrinology 156: 1975-1981.

364. Ahmed N, Stenvers KL (2013) Getting to know ovarian cancer ascites: opportunities for targeted therapy-based translational research. Front Oncol 3: 256.

365. Vogelstein B, Papadopoulos N, Velculescu VE, Zhou S, Diaz LA, Jr., et al. (2013) Cancer genome landscapes. Science 339: 1546-1558.

366. Cancer Genome Atlas Research N (2011) Integrated genomic analyses of ovarian carcinoma. Nature 474: 609-615.

367. Ciriello G, Miller ML, Aksoy BA, Senbabaoglu Y, Schultz N, et al. (2013) Emerging landscape of oncogenic signatures across human cancers. Nat Genet 45: 1127-1133.

368. Mukhopadhyay A, Plummer ER, Elattar A, Soohoo S, Uzir B, et al. (2012) Clinicopathological features of homologous recombination-deficient epithelial ovarian cancers: sensitivity to PARP inhibitors, platinum, and survival. Cancer Res 72: 5675-5682.

369. Bashashati A, Ha G, Tone A, Ding J, Prentice LM, et al. (2013) Distinct evolutionary trajectories of primary high-grade serous ovarian cancers revealed through spatial mutational profiling. J Pathol 231: 21-34.

370. Tothill RW, Tinker AV, George J, Brown R, Fox SB, et al. (2008) Novel molecular subtypes of serous and endometrioid ovarian cancer linked to clinical outcome. Clin Cancer Res 14: 5198-5208.

371. Webb JR, Milne K, Watson P, Deleeuw RJ, Nelson BH (2014) Tumor-infiltrating lymphocytes expressing the tissue resident memory marker CD103 are associated with increased survival in high-grade serous ovarian cancer. Clin Cancer Res 20: 434-444.

372. Zsiros E, Tanyi J, Balint K, Kandalaft LE (2014) Immunotherapy for ovarian cancer: recent advances and perspectives. Curr Opin Oncol 26: 492-500.

373. Hamanishi J, Mandai M, Ikeda T, Minami M, Kawaguchi A, et al. (2015) Safety and Antitumor Activity of Anti-PD-1 Antibody, Nivolumab, in Patients With Platinum-Resistant Ovarian Cancer. J Clin Oncol 33: 4015-4022.

374. Chapman PB, Hauschild A, Robert C, Haanen JB, Ascierto P, et al. (2011) Improved survival with vemurafenib in melanoma with BRAF V600E mutation. N Engl J Med 364: 2507-2516.

375. Menderes G, Schwab CL, Black J, Santin AD (2016) The Role of the Immune System in Ovarian Cancer and Implications on Therapy. Expert Rev Clin Immunol: 1-15.

376. Rahma OE, Ashtar E, Czystowska M, Szajnik ME, Wieckowski E, et al. (2012) A gynecologic oncology group phase II trial of two p53 peptide vaccine approaches: subcutaneous injection and intravenous pulsed dendritic cells in high recurrence risk ovarian cancer patients. Cancer Immunol Immunother 61: 373-384.

377. Ohno S, Kyo S, Myojo S, Dohi S, Ishizaki J, et al. (2009) Wilms' tumor 1 (WT1) peptide immunotherapy for gynecological malignancy. Anticancer Res 29: 4779-4784.

378. Odunsi K, Matsuzaki J, Karbach J, Neumann A, Mhawech-Fauceglia P, et al. (2012) Efficacy of vaccination with recombinant vaccinia and fowlpox vectors expressing NY-ESO-1 antigen in ovarian cancer and melanoma patients. Proc Natl Acad Sci U S A 109: 5797-5802.

379. Ayyoub M, Pignon P, Classe JM, Odunsi K, Valmori D (2013) CD4+ T effectors specific for the tumor antigen NY-ESO-1 are highly enriched at ovarian cancer sites and coexist with, but are distinct from, tumor-associated Treg. Cancer Immunol Res 1: 303-308.

380. Yokokawa J, Palena C, Arlen P, Hassan R, Ho M, et al. (2005) Identification of novel human CTL epitopes and their agonist epitopes of mesothelin. Clin Cancer Res 11: 6342-6351.

381. Bagnoli M, Canevari S, Figini M, Mezzanzanica D, Raspagliesi F, et al. (2003) A step further in understanding the biology of the folate receptor in ovarian carcinoma. Gynecol Oncol 88: S140-144.

382. Odunsi K, Jungbluth AA, Stockert E, Qian F, Gnjatic S, et al. (2003) NY-ESO-1 and LAGE-1 cancer-testis antigens are potential targets for immunotherapy in epithelial ovarian cancer. Cancer Res 63: 6076-6083.

383. Odunsi K, Qian F, Matsuzaki J, Mhawech-Fauceglia P, Andrews C, et al. (2007) Vaccination with an NY-ESO-1 peptide of HLA class I/II specificities induces integrated humoral and T cell responses in ovarian cancer. Proc Natl Acad Sci U S A 104: 12837-12842.

384. Odunsi K, Matsuzaki J, James SR, Mhawech-Fauceglia P, Tsuji T, et al. (2014) Epigenetic potentiation of NY-ESO-1 vaccine therapy in human ovarian cancer. Cancer Immunol Res 2: 37-49.

385. Van Allen EM, Miao D, Schilling B, Shukla SA, Blank C, et al. (2015) Genomic correlates of response to CTLA-4 blockade in metastatic melanoma. Science 350: 207-211.

386. Martin SD, Coukos G, Holt RA, Nelson BH (2015) Targeting the undruggable: immunotherapy meets personalized oncology in the genomic era. Ann Oncol 26: 2367-2374.

387. Zom GG, Khan S, Britten CM, Sommandas V, Camps MG, et al. (2014) Efficient induction of antitumor immunity by synthetic toll-like receptor ligand-peptide conjugates. Cancer Immunol Res 2: 756-764.

388. McGray AJ, Hallett R, Bernard D, Swift SL, Zhu Z, et al. (2014) Immunotherapy-induced CD8+ T cells instigate immune suppression in the tumor. Mol Ther 22: 206-218.

389. Welters MJ, Kenter GG, de Vos van Steenwijk PJ, Lowik MJ, Berends-van der Meer DM, et al. (2010) Success or failure of vaccination for HPV16-positive vulvar lesions correlates with kinetics and phenotype of induced T-cell responses. Proc Natl Acad Sci U S A 107: 11895-11899.

390. Holmes JP, Gates JD, Benavides LC, Hueman MT, Carmichael MG, et al. (2008) Optimal dose and schedule of an HER-2/neu (E75) peptide vaccine to prevent breast cancer recurrence: from US Military Cancer Institute Clinical Trials Group Study I-01 and I-02. Cancer 113: 1666-1675.

391. Curtsinger JM, Johnson CM, Mescher MF (2003) CD8 T cell clonal expansion and development of effector function require prolonged exposure to antigen, costimulation, and signal 3 cytokine. J Immunol 171: 5165-5171.

392. Tseng KE, Chung CY, H'Ng W S, Wang SL (2009) Early infection termination affects number of CD8+ memory T cells and protective capacities in listeria monocytogenes-infected mice upon rechallenge. J Immunol 182: 4590-4600.

393. Blair DA, Turner DL, Bose TO, Pham QM, Bouchard KR, et al. (2011) Duration of antigen availability influences the expansion and memory differentiation of T cells. J Immunol 187: 2310-2321.

394. Shaulov A, Murali-Krishna K (2008) CD8 T cell expansion and memory differentiation are facilitated by simultaneous and sustained exposure to antigenic and inflammatory milieu. J Immunol 180: 1131-1138.

395. Storni T, Ruedl C, Renner WA, Bachmann MF (2003) Innate immunity together with duration of antigen persistence regulate effector T cell induction. J Immunol 171: 795-801.

396. Janssen EM, Lemmens EE, Wolfe T, Christen U, von Herrath MG, et al. (2003) CD4+ T cells are required for secondary expansion and memory in CD8+ T lymphocytes. Nature 421: 852-856.

397. Ghaffari-Nazari H, Tavakkol-Afshari J, Jaafari MR, Tahaghoghi-Hajghorbani S, Masoumi E, et al. (2015) Improving Multi-Epitope Long Peptide Vaccine Potency by Using a Strategy that Enhances CD4+ T Help in BALB/c Mice. PLoS One 10: e0142563.

398. Wu CY, Monie A, Pang X, Hung CF, Wu TC (2010) Improving therapeutic HPV peptide-based vaccine potency by enhancing CD4+ T help and dendritic cell activation. J Biomed Sci 17: 88.

399. Jemon K, Young V, Wilson M, McKee S, Ward V, et al. (2013) An enhanced heterologous virus-like particle for human papillomavirus type 16 tumour immunotherapy. PLoS One 8: e66866.

400. Janetzki S, Britten CM, Kalos M, Levitsky HI, Maecker HT, et al. (2009) "MIATA"-minimal information about T cell assays. Immunity 31: 527-528.

401. Fasso M, Waitz R, Hou Y, Rim T, Greenberg NM, et al. (2008) SPAS-1 (stimulator of prostatic adenocarcinoma-specific T cells)/SH3GLB2: A prostate tumor antigen identified by CTLA-4 blockade. Proc Natl Acad Sci U S A 105: 3509-3514.

402. Wherry EJ, Ha SJ, Kaech SM, Haining WN, Sarkar S, et al. (2007) Molecular signature of CD8+ T cell exhaustion during chronic viral infection. Immunity 27: 670-684.

403. Monsurro V, Nielsen MB, Perez-Diez A, Dudley ME, Wang E, et al. (2001) Kinetics of TCR use in response to repeated epitope-specific immunization. J Immunol 166: 5817-5825.

404. Johansen P, Storni T, Rettig L, Qiu Z, Der-Sarkissian A, et al. (2008) Antigen kinetics determines immune reactivity. Proc Natl Acad Sci U S A 105: 5189-5194.

405. DeMuth PC, Min Y, Irvine DJ, Hammond PT (2014) Implantable silk composite microneedles for programmable vaccine release kinetics and enhanced immunogenicity in transcutaneous immunization. Adv Healthc Mater 3: 47-58.

406. Badovinac VP, Messingham KA, Jabbari A, Haring JS, Harty JT (2005) Accelerated CD8+ T-cell memory and prime-boost response after dendritic-cell vaccination. Nat Med 11: 748-756.

407. Pham NL, Pewe LL, Fleenor CJ, Langlois RA, Legge KL, et al. (2010) Exploiting cross-priming to generate protective CD8 T-cell immunity rapidly. Proc Natl Acad Sci U S A 107: 12198-12203.

408. Surman DR, Dudley ME, Overwijk WW, Restifo NP (2000) Cutting edge: CD4+ T cell control of CD8+ T cell reactivity to a model tumor antigen. J Immunol 164: 562-565.

409. Antony PA, Piccirillo CA, Akpinarli A, Finkelstein SE, Speiss PJ, et al. (2005) CD8+ T cell immunity against a tumor/self-antigen is augmented by CD4+ T helper cells and hindered by naturally occurring T regulatory cells. J Immunol 174: 2591-2601.

410. Sun JC, Bevan MJ (2003) Defective CD8 T cell memory following acute infection without CD4 T cell help. Science 300: 339-342.

411. Slingluff CL, Jr., Petroni GR, Chianese-Bullock KA, Smolkin ME, Ross MI, et al. (2011) Randomized multicenter trial of the effects of melanoma-associated helper peptides and cyclophosphamide on the immunogenicity of a multipeptide melanoma vaccine. J Clin Oncol 29: 2924-2932.

412. Schaefer JT, Patterson JW, Deacon DH, Smolkin ME, Petroni GR, et al. (2010) Dynamic changes in cellular infiltrates with repeated cutaneous vaccination: a histologic and immunophenotypic analysis. J Transl Med 8: 79.

413. Cho S, Sun Y, Soisson AP, Dodson MK, Peterson CM, et al. (2013) Characterization and evaluation of pre-clinical suitability of a syngeneic orthotopic mouse ovarian cancer model. Anticancer Res 33: 1317-1324.

414. Krempski J, Karyampudi L, Behrens MD, Erskine CL, Hartmann L, et al. (2011) Tumor-infiltrating programmed death receptor-1+ dendritic cells mediate immune suppression in ovarian cancer. J Immunol 186: 6905-6913.

415. Duraiswamy J, Kaluza KM, Freeman GJ, Coukos G (2013) Dual blockade of PD-1 and CTLA-4 combined with tumor vaccine effectively restores T-cell rejection function in tumors. Cancer Res 73: 3591-3603.

416. Chiriva-Internati M, Yu Y, Mirandola L, Jenkins MR, Chapman C, et al. (2010) Cancer testis antigen vaccination affords long-term protection in a murine model of ovarian cancer. PLoS One 5: e10471.

417. Roby KF, Taylor CC, Sweetwood JP, Cheng Y, Pace JL, et al. (2000) Development of a syngeneic mouse model for events related to ovarian cancer. Carcinogenesis 21: 585-591.

418. Li H, Durbin R (2009) Fast and accurate short read alignment with Burrows-Wheeler transform. Bioinformatics 25: 1754-1760.

419. Li H, Handsaker B, Wysoker A, Fennell T, Ruan J, et al. (2009) The Sequence Alignment/Map format and SAMtools. Bioinformatics 25: 2078-2079.

420. Wang K, Li M, Hakonarson H (2010) ANNOVAR: functional annotation of genetic variants from high-throughput sequencing data. Nucleic Acids Res 38: e164.

421. Robinson JT, Thorvaldsdottir H, Winckler W, Guttman M, Lander ES, et al. (2011) Integrative genomics viewer. Nat Biotechnol 29: 24-26.

422. Hogquist KA, Jameson SC, Heath WR, Howard JL, Bevan MJ, et al. (1994) T cell receptor antagonist peptides induce positive selection. Cell 76: 17-27.

423. Kammertoens T, Blankenstein T (2013) It's the peptide-MHC affinity, stupid. Cancer Cell 23: 429-431.

424. Matsushita H, Vesely MD, Koboldt DC, Rickert CG, Uppaluri R, et al. (2012) Cancer exome analysis reveals a T-cell-dependent mechanism of cancer immunoediting. Nature 482: 400-404.

425. Lanitis E, Irving M, Coukos G (2015) Targeting the tumor vasculature to enhance T cell activity. Curr Opin Immunol 33: 55-63.

426. Munn DH, Bronte V (2015) Immune suppressive mechanisms in the tumor microenvironment. Curr Opin Immunol 39: 1-6.

427. Burkholder B, Huang RY, Burgess R, Luo S, Jones VS, et al. (2014) Tumor-induced perturbations of cytokines and immune cell networks. Biochim Biophys Acta 1845: 182-201.

428. Castellarin M, Milne K, Zeng T, Tse K, Mayo M, et al. (2013) Clonal evolution of high-grade serous ovarian carcinoma from primary to recurrent disease. J Pathol 229: 515-524.

429. Alanio C, Lemaitre F, Law HK, Hasan M, Albert ML (2010) Enumeration of human antigen-specific naive CD8+ T cells reveals conserved precursor frequencies. Blood 115: 3718-3725.

430. Hombrink P, Raz Y, Kester MG, de Boer R, Weissbrich B, et al. (2013) Mixed functional characteristics correlating with TCR-ligand koff -rate of MHC-tetramer reactive T cells within the naive T-cell repertoire. Eur J Immunol 43: 3038-3050.

431. Nielsen JS, Sedgwick CG, Shahid A, Zong Z, Brumme ZL, et al. (2016) Toward Personalized Lymphoma Immunotherapy: Identification of Common Driver Mutations Recognized by Patient CD8+ T Cells. Clin Cancer Res 22: 2226-2236.

432. Tavakoli S, Mederacke I, Herzog-Hauff S, Glebe D, Grun S, et al. (2008) Peripheral blood dendritic cells are phenotypically and functionally intact in chronic hepatitis B virus (HBV) infection. Clin Exp Immunol 151: 61-70.

433. Geiger R, Duhen T, Lanzavecchia A, Sallusto F (2009) Human naive and memory CD4+ T cell repertoires specific for naturally processed antigens analyzed using libraries of amplified T cells. J Exp Med 206: 1525-1534.

434. English D, Andersen BR (1974) Single-step separation of red blood cells. Granulocytes and mononuclear leukocytes on discontinuous density gradients of Ficoll-Hypaque. J Immunol Methods 5: 249-252.

435. Chevalier MF, Bobisse S, Costa-Nunes C, Cesson V, Jichlinski P, et al. (2015) High-throughput monitoring of human tumor-specific T-cell responses with large peptide pools. Oncoimmunology 4: e1029702.

436. Soletormos G, Duffy MJ, Othman Abu Hassan S, Verheijen RH, Tholander B, et al. (2016) Clinical Use of Cancer Biomarkers in Epithelial Ovarian Cancer: Updated Guidelines From the European Group on Tumor Markers. Int J Gynecol Cancer 26: 43-51.

437. Pittet MJ, Valmori D, Dunbar PR, Speiser DE, Lienard D, et al. (1999) High frequencies of naive Melan-A/MART-1-specific CD8(+) T cells in a large proportion of human histocompatibility leukocyte antigen (HLA)-A2 individuals. J Exp Med 190: 705-715.

438. Hodges E, Krishna MT, Pickard C, Smith JL (2003) Diagnostic role of tests for T cell receptor (TCR) genes. J Clin Pathol 56: 1-11.

439. Wick DA, Webb JR, Nielsen JS, Martin SD, Kroeger DR, et al. (2014) Surveillance of the tumor mutanome by T cells during progression from primary to recurrent ovarian cancer. Clin Cancer Res 20: 1125-1134.

440. Svane IM, Verdegaal EM (2014) Achievements and challenges of adoptive T cell therapy with tumor-infiltrating or blood-derived lymphocytes for metastatic melanoma: what is needed to achieve standard of care? Cancer Immunol Immunother 63: 1081-1091.

441. Hou JY, Kelly MG, Yu H, McAlpine JN, Azodi M, et al. (2007) Neoadjuvant chemotherapy lessens surgical morbidity in advanced ovarian cancer and leads to improved survival in stage IV disease. Gynecol Oncol 105: 211-217.

442. Verdegaal EM, Visser M, Ramwadhdoebe TH, van der Minne CE, van Steijn JA, et al. (2011) Successful treatment of metastatic melanoma by adoptive transfer of blood-derived polyclonal tumor-specific CD4+ and CD8+ T cells in combination with low-dose interferon-alpha. Cancer Immunol Immunother 60: 953-963.

443. Altman JD, Moss PA, Goulder PJ, Barouch DH, McHeyzer-Williams MG, et al. (1996) Phenotypic analysis of antigen-specific T lymphocytes. Science 274: 94-96.

444. Datta S, Sarvetnick N (2009) Lymphocyte proliferation in immune-mediated diseases. Trends Immunol 30: 430-438.

445. Gros A, Parkhurst MR, Tran E, Pasetto A, Robbins PF, et al. (2016) Prospective identification of neoantigen-specific lymphocytes in the peripheral blood of melanoma patients. Nat Med.

446. US National Library of Medicine (2015) Clinicaltrials.gov/show/NCT02287428.

447. Obeid J, Hu Y, Slingluff CL, Jr. (2015) Vaccines, Adjuvants, and Dendritic Cell Activators--Current Status and Future Challenges. Semin Oncol 42: 549-561.

448. Zwaveling S, Ferreira Mota SC, Nouta J, Johnson M, Lipford GB, et al. (2002) Established human papillomavirus type 16-expressing tumors are effectively eradicated following vaccination with long peptides. J Immunol 169: 350-358.

449. Sabbatini P, Tsuji T, Ferran L, Ritter E, Sedrak C, et al. (2012) Phase I trial of overlapping long peptides from a tumor self-antigen and poly-ICLC shows rapid induction of integrated immune response in ovarian cancer patients. Clin Cancer Res 18: 6497-6508.

450. Hanna MG, Jr. (2012) Cancer vaccines: are we there yet? Hum Vaccin Immunother 8: 1161-1165.

451. Howitt BE, Shukla SA, Sholl LM, Ritterhouse LL, Watkins JC, et al. (2015) Association of Polymerase e-Mutated and Microsatellite-Instable Endometrial Cancers With Neoantigen Load, Number of Tumor-Infiltrating Lymphocytes, and Expression of PD-1 and PD-L1. JAMA Oncol 1: 1319-1323.

452. McConechy MK, Talhouk A, Leung S, Chiu D, Yang W, et al. (2016) Endometrial Carcinomas with POLE Exonuclease Domain Mutations Have a Favorable Prognosis. Clin Cancer Res.

453. van Gool IC, Eggink FA, Freeman-Mills L, Stelloo E, Marchi E, et al. (2015) POLE proofreading mutations elicit an anti-tumor immune response in endometrial cancer. Clin Cancer Res.

454. Maby P, Tougeron D, Hamieh M, Mlecnik B, Kora H, et al. (2015) Correlation between Density of CD8+ T-cell Infiltrate in Microsatellite Unstable Colorectal Cancers and Frameshift Mutations: A Rationale for Personalized Immunotherapy. Cancer Res 75: 3446-3455.

455. Alexandrov LB, Nik-Zainal S, Wedge DC, Aparicio SA, Behjati S, et al. (2013) Signatures of mutational processes in human cancer. Nature 500: 415-421.

456. Williams MJ, Werner B, Barnes CP, Graham TA, Sottoriva A (2016) Identification of neutral tumor evolution across cancer types. Nat Genet 48: 238-244.

457. Karagiannis P, Iriguchi S, Kaneko S (2016) Reprogramming away from the exhausted T cell state. Semin Immunol 28: 35-44.

458. Rotzschke O, Falk K, Deres K, Schild H, Norda M, et al. (1990) Isolation and analysis of naturally processed viral peptides as recognized by cytotoxic T cells. Nature 348: 252-254.

459. Granados DP, Rodenbrock A, Laverdure JP, Cote C, Caron-Lizotte O, et al. (2016) Proteogenomic-based discovery of minor histocompatibility antigens with suitable features for immunotherapy of hematologic cancers. Leukemia 30: 1344-1354.

460. Patch AM, Christie EL, Etemadmoghadam D, Garsed DW, George J, et al. (2015) Whole-genome characterization of chemoresistant ovarian cancer. Nature 521: 489-494.

461. Lupetti R, Pisarra P, Verrecchia A, Farina C, Nicolini G, et al. (1998) Translation of a retained intron in tyrosinase-related protein (TRP) 2 mRNA generates a new cytotoxic T lymphocyte (CTL)-defined and shared human melanoma antigen not expressed in normal cells of the melanocytic lineage. J Exp Med 188: 1005-1016.

462. Kawase T, Akatsuka Y, Torikai H, Morishima S, Oka A, et al. (2007) Alternative splicing due to an intronic SNP in HMSD generates a novel minor histocompatibility antigen. Blood 110: 1055-1063.

463. Lu YC, Robbins PF (2016) Cancer immunotherapy targeting neoantigens. Semin Immunol 28: 22-27.

464. Skeate JG, Woodham AW, Einstein MH, Da Silva DM, Kast WM (2016) Current therapeutic vaccination and immunotherapy strategies for HPV-related diseases. Hum Vaccin Immunother: 1-12.